Development and chemical synthesis of natural product-derived and rationally designed small molecule probes for plant biology research

Dissertation

zur Erlangung des akademischen Grades eines
Doktors der Naturwissenschaften
– Dr. rer. nat. –

vorgelegt von

Julian Oeljeklaus, M. Sc.

geboren in Essen

Zentrum für Medizinische Biotechnologie
der
Universität Duisburg-Essen

2013

Die vorliegende Arbeit wurde im Zeitraum von November 2009 bis Juni 2011 am Chemical Genomics Centre der Max-Planck-Gesellschaft in Dortmund und in der Zeit von Juni 2011 bis November 2013 am Zentrum für Medizinische Biotechnologie im Arbeitskreis von Prof. Dr. Markus Kaiser an der Universität Duisburg-Essen angefertigt.

Gutachter: 1. Prof. Dr. Markus Kaiser
2. Prof. Dr. Carsten Schmuck

Datum der mündlichen Prüfung: 11.02. 2014

Prüfungsvorsitzender: Prof. Dr. Stefan Rumann

Während dieser Arbeit sind folgende Publikationen erschienen, die teilweise Inhalte dieser Dissertation enthalten:

Villamor, J. G., Kaschani, F., Colby, T., Oeljeklaus, J., Zhao, D., Kaiser, M., Patricelli, M. P. & van der Hoorn, R. A. (**2013**). Profiling protein kinases and other ATP binding proteins in Arabidopsis using acyl-ATP probes. *Molecular & Cellular Proteomics*, **12**(9), 2481-2496

Oeljeklaus, J., Kaschani, F. & Kaiser, M. (**2013**). Streamlining chemical probe discovery: libraries of "fully functionalized" small molecules for phenotypic screening. *Angewandte Chemie International Edition*, **52**, 1368-1370.

Lu, H., Wang, Z., Shabab, M., Oeljeklaus, J., Verhelst, S. H., Kaschani, F., Kaiser, M., Bogyo, M. & van der Hoorn, R. A. (**2013**). A substrate-inspired probe monitors translocation, activation, and subcellular targeting of bacterial type III effector protease AvrPphB. *Chemistry and Biology*, **20**, 168-176.

Weski, J., Meltzer, M., Spaan, L., Monig, T., Oeljeklaus, J., Hauske, P., Vouilleme, L., Volkmer, R., Boisguerin, P., Boyd, D., Huber, R., Kaiser, M. & Ehrmann, M. (**2012**). Chemical biology approaches reveal conserved features of a C-terminal processing PDZ protease. *Chembiochem*, **13**, 402-408.

Table of contents

1. INTRODUCTION 1

2. THEORETICAL BACKGROUND 2

2.1 *Arabidopsis thaliana* as a model plant in plant biology research 2
2.2 Small molecules at the interface of Chemistry and Biology 3
2.2.1 Natural products as starting points for chemical biology approaches 4
2.3 Chemical biological approaches in plant biology research 6
2.3.1 Traditional genetics vs. chemical genetics 6
2.3.2 Examples for chemical genetics applications in plants 8
2.4 Activity based protein profiling (ABPP) for functional proteomics in plants 13
2.4.1 Basic principle of ABPP 13
2.4.2 Composition and design of activity-based probes (ABP) 14
2.4.3 Classes of ABPs 16
2.4.3.1 Directed probes 16
2.4.3.2 Non-directed probes 17
2.4.4 Two-step ABPP 20
2.4.5 Analytical platforms for ABPP 21
2.4.5.1 Gel-based approaches 21
2.4.5.2 Gel-free approaches 21
2.4.6 Comparative ABPP 23
2.4.7 Competitive ABPP 24
2.4.8 ABPP with natural product-derived probes 24
2.5 Solid phase supported synthesis 26
2.5.1 Peptide bond formation 27
2.5.2 Protecting group strategies 29
2.5.2.1 The *tert*-Butoxycarbonyl protecting group 30
2.5.2.2 The 9-Fluorenylmethoxycarbonyl group 31
2.5.2.3 The *N*-allyloxycarbonyl group 32
2.5.3 The principle of solid phase supported peptide synthesis (SPPS) 33

3. AIMS OF THE PHD THESIS 36

4. RESULTS AND DISCUSSION 39

4.1 Studies on Rotihibin A, a plant growth regulator from *Streptomyces graminofaciens* 39
4.1.1 Synthetic considerations towards Rotihibin A 40
4.1.2 Synthesis of required building blocks 43
4.1.3 Total synthesis of Rotihibin A 50
4.1.4 Synthesis of Rotihibin A derivatives for SAR studies 53
4.1.5 Biological evaluation of Rotihibin A and derivatives thereof 55
4.1.5.1 Growth inhibitions studies with *Arabidopsis* seedlings 55
4.1.5.2 Cell proliferation studies with *Arabidopsis* cell cultures 60
4.1.5.3 Evaluation of Rotihibin A and derivatives in a cyclin B-reporter plant assays 61
4.2 Studies towards plant growth regulators Brevicompanine A, B & C 66
4.2.1 Biological evaluation of Brevicompanines and derivatives thereof 72
4.2.2 ABPP experiments for cellular target elucidation 75
4.3 Synthesis of acyl-ATP probes for profiling of ATP binding proteins in *A. thaliana* 76

5. SUMMARY AND OUTLOOK 84

6. ZUSAMMENFASSUNG UND AUSBLICK 86

7. EXPERIMENTAL PART 89

7.1 General methods and instruments 89
7.2 Synthesis of Rotihibin A and derivatives 92
7.2.1 Syntheses of building blocks 92
7.2.2 Solid phase synthesis of Rotihibin A 104
7.2.3 Solid phase synthesis of Rotihibin A-derivatives 108
7.3 Synthesis of Brevicompanines 117
7.4 Synthesis of acyl-ATP probes 141
7.5 Biological Procedures 147

8. REFERENCES 150

9. APPENDIX 161

9.1 Abbreviations 161
9.2 List of publications 165
9.3 Curriculum Vitae 166
9.4 Erklärungen 170
9.5 Acknowledgements/Danksagungen 171

1. INTRODUCTION

Plants are living multicellular eukaryotic organisms that constitute one of the five kingdoms of life which includes thousands of different species prospering on land, in oceans and fresh water. They are capable to produce self-generated energy through photosynthesis, using sunlight to biosynthesize carbohydrates from water and carbon dioxide and releasing oxygen as a by-product. Due to this unique ability, plants or plant-derived products such as grains, fruits and vegetables represent the basis of the food chain for animals and humans. Especially cereals such as maize (or corn), wheat and rice have been domesticated by mankind for millennia and are forming the major energy source in human nutrition.

In contrast to organisms such as animals or bacteria, higher plants are however sessile and cannot simply escape from environmental stresses; consequently, they are steadily exposed to adverse environmental influences. Thus, plants have evolved many different and highly complex regulatory systems that allow them to still survive and even prosper in swiftly changing environmental conditions. A better understanding of these regulatory processes is therefore not only of scientific interest but due to their role in basic nutrition also of socioeconomic importance. The study of cellular processes in living plants therefore not only increases our basic scientific knowledge but may also open up new strategies for crop improvement.

Fostered by recent developments in chemistry, biochemistry, genomics, and molecular biology, chemical biology approaches have recently emerged that allow an alternative approach to study plant biology. The present thesis reports on such a chemical biology approach which was used to investigate the molecular mechanisms of plant growth.

2. THEORETICAL BACKGROUND

2.1 *Arabidopsis thaliana* as a model plant in plant biology research

Most of the basic classical and molecular genetic studies in plant biology have focused on crop species, such as corn, pea, tobacco, wheat and tomato. These plants are typically large in size, require a large growing area and have a long generation time (allowing only 2-3 generations per year), and thus are inconvenient for some types of molecular genetic experiments. In fact, an ideal plant for molecular biological studies should feature a small size (for facile cultivation of large numbers in the lab), a short generation time and a small genome size. Such a plant was found in *Arabidopsis thaliana* which therefore rapidly became the most important model plant in plant biology.

Arabidopsis thaliana (or thale cress) is a member of the mustard family (*Cruciferae or Brassicaceae*) with a broad natural distribution throughout Europe, Asia, and North America. Many different ecotypes have been collected from natural populations and are available for experimental analysis. Of them, the Columbia and Landsberg ecotypes have become the gold standards for genetic and molecular studies. *Arabidopsis* has no direct importance in agriculture but meets all the requirements for a viable model plant and is used since the 1940s as the major model organism in plant science.[1] Along these lines, *Arabidopsis* was therefore also the first plant with a completely sequenced genome.[2] The *Arabidopsis* genome consists of ca. 120 mega base pairs; therefore, *Arabidopsis* has one of the smallest plant genomes which significantly facilitates all kinds of biological and in particular genetic studies.

Several other advantages account for the role of *Arabidopsis* as the major plant biology model organism. For example, *Arabidopsis* possesses a relatively short generation cycle of only six weeks and generally produces many seeds that can be easily stored for long terms and still maintain their ability to germinate.[3] The small growth size of the plant is also beneficial for cultivation in laboratories and allows nurturing thousands of mature *Arabidospis* plants in a normal lab space without special facilities. Moreover, young *Arabidopsis* seedlings and cells from cell culture are relative translucent and are thus well suited for (fluorescence) microscopy studies. Physiologically, *Arabidopsis thaliana* represents

a suitable model for the economically and scientifically most interesting higher plant species. Finally, *Arabidopsis* can be efficiently manipulated by genetics, using well-established methodologies. For example, plant transformation can be achieved with *Agrobacterium tumefaciens*, a bacterial vector that allows to insert DNA sequences into the plant genome.[4]

Due to its major role in plant biology, much work has been done to assign functions to the ca. 27.000 genes and its corresponding gene products that are encoded in the *Arabidopsis* genome.[5] To this puropose, genetic methods have mostly been used. Recently, post-genomic approaches such as chemical biology methodologies have however proven to be complementary and useful techniques that may provide novel and meaningful insights into the biology of living plants.[6; 7]

2.2 Small molecules at the interface of Chemistry and Biology

Chemical biology may broadly be defined as the application of chemical methods for studying biological phenomena. Therefore, chemical biology consists of the use of small molecules to both interrogate and manipulate biology for investigating the behavior of biological systems, from the protein to the organismal and thus physiologically relevant level.

By definition, small molecules are organic molecules of low molecular weight (< 1000 Da).[8] Furthermore, they should harbor a biological activity resulting from their binding to a protein or in rare cases other biomolecules, commonly called as the "target", which could for example be involved in distinct signaling or metabolic pathways. To exert bioactivity, the binding event is accompanied by a modulation of the protein's function. In some cases, small molecules modulate the protein's function by inactivating it which defines the molecule as an inhibitor.[9] In other cases, it activates the function of a protein or increases the activity of a certain enzyme. These compounds are then referred to as activators. There are many other ways of modulating the function of a protein, for example binding of a small molecule inhibitor to its target can also hinder a substrate from entering the enzyme's active site or hamper the enzyme from catalyzing its reaction.

The binding event can either be reversible or irreversible. Molecules that bind irreversible to their targets usually react with the protein, thereby changing it chemically. This mode-of-action is most often seen for enzymes. Such irreversible inhibitors modify catalytic key amino acid residues required for enzymatic turnover in a covalent manner which finally leads to a deactivation of the enzyme's function. In contrast, reversible inhibitors bind non-

covalently to their targets. For enzymes, different types of reversible inhibition are known. For example, reversible inhibitors can bind to the enzyme in a substrate competitive way (competitive inhibition)[9] or in a non-competitive fashion, which can for example come along with deactivating conformational changes (allosteric inhibition)[9].

In contrast to unbiased screening methods and thus a more-or-less serendipity-based approach for identifiying bioactive small molecules, also rational, i.e. knowledge-based, approaches have been developed. For the rational design of small molecules the determination of the X-ray structure of the biological target which is feasible since the late 1950's is greatly helpful.[10] With this information in hands, scientists are able to adjust the chemical structure of a molecule to the structural information of a biological target to affect its activity.

Hence, the use of bioactive small molecules as biological probes with high affinity and specificity is clearly beneficial for studying biologically relevant processes. Despite these evident advantages, the widespread use of small molecules in chemical biological approaches to probe cellular signaling has however some inherent limitations: Such approaches require the availability of appropriate small molecules that target a certain enzyme or protein with high selectivity and affinity to trigger a desired phenotypic effect. To date, the number of proper small molecules still represents the bottle-neck of chemical biology approaches. To expand the scope of bioactive small molecules, synthetic efforts have focused on generating novel compound libraries.[11] This chemical toolboxes consists for example of collections derived from diversity-oriented synthesis (DOS), target-guided ligand assembly, (dynamic) combinatorial libraries or annotated chemical libraries.[12] The goal of these strategies is to get a quick and efficient access to a large number of small molecules for screening and subsequent identification of those with interesting bioactivities.

2.2.1 Natural products as starting points for chemical biology approaches

A natural product is a chemical compound produced by a metabolizing, living organism. Many of these compounds feature a defined bioactivity to accomplish a distinct biological function. Such natural products are biosynthesized by living organisms for example to provide the organism with a natural selective advantage towards other competitive organisms. These bioactive natural products can therefore be considered as chemical scaffolds that were evolutionarily selected and approved for binding to particular target-proteins.

Their underlying chemical scaffolds are often chemically highly diverse. Because of their broad spectrum of chemical and functional diversity, natural products have consequently seen a great impact upon drug discovery (*Fig. 1*).[13] Moreover, natural product-derived compound libraries have demonstrated enhanced hit rates in biological screens.

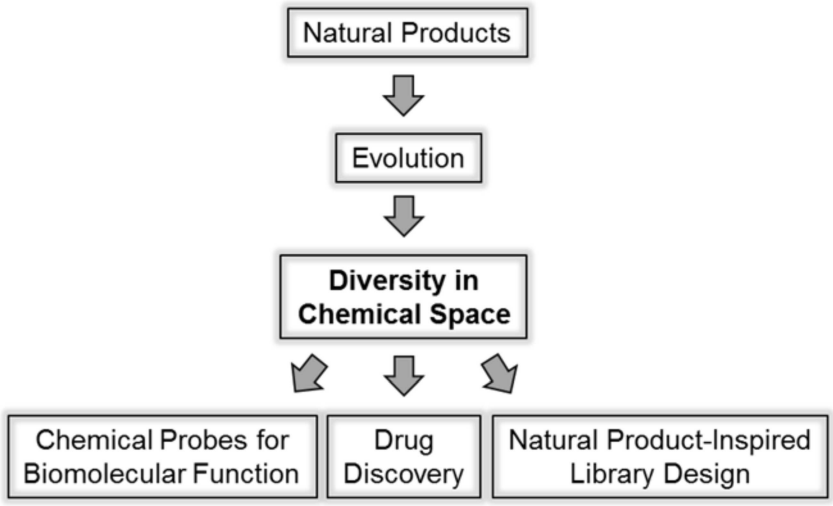

Figure 1: Natural product diversity (Adapted and modified from Hong *et al*.[14])

To benefit from the evolutionary pre-selected structure of natural products and their enhanced hit rates, strategies like biology-oriented synthesis (BIOS) were developed.[15] Here, natural product scaffolds are used as a blueprint to generate structurally simplified natural product-derived compound collections.[16] Another approach is the rational derivatization of natural compounds that allows detailed structure-activity mapping and can result in derivatives that possess even an enhanced bioactivity.[17] In this approach, the bottleneck is however the synthetic access to such a natural product but once it is established, this rational derivatization can even result in compounds with higher hit rates in screens (i.e. displaying a better ratio between hits and the number of screened compounds).

Beyond all doubt, besides the rational or combinatorial creation of small molecules, the use of natural products for interrogation of biological systems had and still has a big impact, not only for the development of new chemotherapies (currently, more than 50% of all FDA-approved drugs are natural products or natural product derivatives) or of additives for agriculture, but also as chemical probes in scientific chemical biology studies.[18]

2.3 Chemical biological approaches in plant biology research

2.3.1 Traditional genetics vs. chemical genetics

Genetic approaches have played and still play a major role for elucidating the biology of living organisms, including plants. To this end, gene knock-outs or mutation strategies are used to silence gene-products. Two approaches are usually distinguished: In the classical *forward genetic* approach, random mutagenesis is used to produce a phenotype of interest (*Fig. 2*). This often requires a generation of a huge number of mutants followed by an extensive screening for mutants with an either gain- or loss-of-function phenotype. In order to analyze the phenotypic response of distinct genes, *reverse genetics* is used (*Fig. 2*). Here, mutations or knock-outs are targeted to a particular gene and the role of the gene product is studied from the phenotype of the resulting mutant.

The advantage of such "traditional" genetic approaches is that they are highly specific as a single point mutation can be engendered by a single nucleotide change within 3 billion base pairs. Moreover, this approach is highly transferable as in principle any organism can be genetically modified. Nonetheless, there are also some general drawbacks of traditional genetics. Some gene knock-outs or loss-of-function mutations are lethal; consequently, genetic studies of such genes cannot be performed. Moreover, non-essential knock-outs can often be masked by gene redundancy. This issue is of particular importance in plant genetics because extensive genome duplications have occurred multiple times in the evolutionary history of most plants. Therefore, most plant genes are part of gene families and single knock-out plants consequently often lack a clear phenotypic response because the missing knocked-out enzyme activity is compensated by other members of the related gene family. Thus, classical genetic approaches may fail to identify certain gene products that exist in gene families.[19]

To overcome these limitations, a complementary approach commonly known as chemical genetics (thereby pronouncing its similarities to traditional genetics) has been established in the last decade. In this approach, small molecules are used to mimic mutagenesis and to elicit phenotypes of interests (*Fig. 2*).[12] To this end, chemical libraries of small molecules are screened on living systems. Suitable bioactive small molecules then interfere in the cellular function of their target proteins resulting in an observable phenotypic effect that often resembles a mutant (e.g. knock-out) phenotype, thereby justifying the term

chemical genetics. This concept is called *forward chemical genetics* (*Fig. 2*). After identification of an interesting phenotype, the target of the small molecule is elucidated, thereby allowing correlation of the phenotype with a molecular mechanism. In the second approach, commonly referred to as *reverse chemical genetics,* small molecule modulators of proteins of interest (for example from a previous target-oriented drug discovery campaign) are used to disturb the function of the target protein of the small molecule probe in a living system. The analysis of the resulting phenotype then allows to gain insights into the function of the target protein in an in vivo system.[20]

Chemical genetics offers many advantages to 'traditional' genetics: For example, small molecule modulators are able to distinguish between different protein forms produced by the same gene, e.g. zymogens or post-translational modifications.[21] Moreover, small molecules have the capacity to overcome the problems associated with gene redundancy because the proteins encoded by one gene family often share conserved binding sites susceptible to the same small molecule inhibitor. Thus, the activity of a whole gene family can be shut down with one small molecule probe, thereby causing a clear phenotypic response that single gene knockouts might miss. Furthermore, the biological effect from a delivered small molecule is principally tunable. This enables graded phenotypes by varying the concentration of the bioactive small molecule. Furthermore, small molecule phenotypes are often reversible because small molecules can be removed from living organisms. Finally, small molecule modulation is conditional and can be spatially and temporally controlled and induced at any developmental stage of the studied biological system.

Unfortunately, chemical genetics however also displays several disadvatages: First, the identification and availability of a bioactive small molecule that induces a phenotype of interest is a prerequisite for further investigations. To this end, either screening of large compound libraries are required which is time and cost-intensive and sometimes fails to deliver potent small molecule probes. Moreover, the subsequent identification of cellular targets of bioactive small molecules is still a major challenge. Although several proteomic-based methods such as affinity purification[22], protein microarrays[23], yeast-three-hybrid systems[24], phage display[25] and the activity based protein profiling approach[26]are nowadays available, none of them represents a generic approach, turning target identification into the bottleneck of forward chemical genetics approaches.

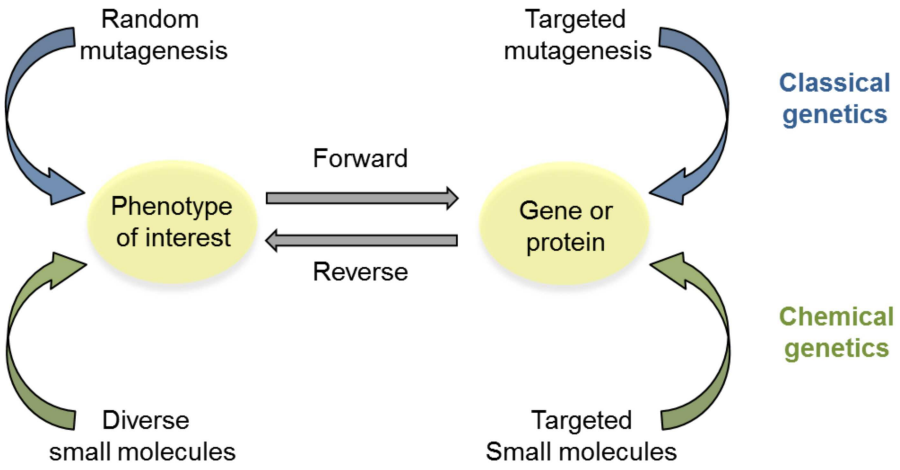

Figure 2: Schematic depiction of classical genetics versus chemical genetics. Classical genetics employs (random) mutagenesis strategies, like knock-outs, to target a (particular) gene and the role of the gene product is studied from the phenotype of the resulting mutant for elucidating the correlation between genes and observed phenotypes. In contrast, chemical genetics uses small-molecules to achieve this goal. A forward genetic study is a hypothesis-generating approach in which phenotypes of interest are provoked by small molecules, followed by elucidation of the gene/protein causing the phenotype. A reverse genetic study is a hypothesis-based approach in which genes or proteins are directly targeted by pre-selected small molecules to analyze their role via studying the resulting phenotype (adapted and modified from Kawasumi *et al.*[27]).

Beside the screening approach of chemical genetics, one can also employ pre-selected small molecules, such as natural products derived for example from plant pathogens that display a known plant specific phenotypic response, to investigate biological processes such as plant-pathogen interactions or to get more insights into regulatory processes underlying the caused phenotype.

2.3.2 Examples for chemical genetics applications in plants

Plants offer an attractive platform for phenotypic screening in chemical genetics. Since all natural occurring known plant growth regulators are small molecules, the experimental protocols for analyzing chemical compounds can easily be adapted to unbiased chemical genetic srceens (*Fig. 3*).[19] Furthermore, the genome of the major model organism in plant biology, *Arabidopsis thaliana*, is already fully sequenced and a variety of classical genetic tools are available to the scientific community (c.f. *Chapter 2.1*).[5] Such a tractable genetic system therefore greatly facilitates the target identification process for the identified

compounds. Moreover, plant roots conveniently take-up small molecules, avoiding many of the permeability and transport issues in traditional chemical genetic systems. In fact, plants respond to, metabolize and produce a diverse range of small molecules. Examples are plant hormones, such as auxin, gibberellic acid, abscisic acid (ABA) and salicylic acid.[28] These compounds are a structurally unrelated collection of endogenous small molecules derived from essential metabolic pathways and are important regulators of plant growth as well as mediate additionally almost every aspect of plant life, from pattern formation during development to responses to both biotic and abiotic stresses. Besides, exogenous small molecules like herbicides, plant growth regulators from (pathogenic) microbial sources or other bioactive compounds identified from screening chemical libraries are examples of the suitability of plants to respond to small molecule treatments.

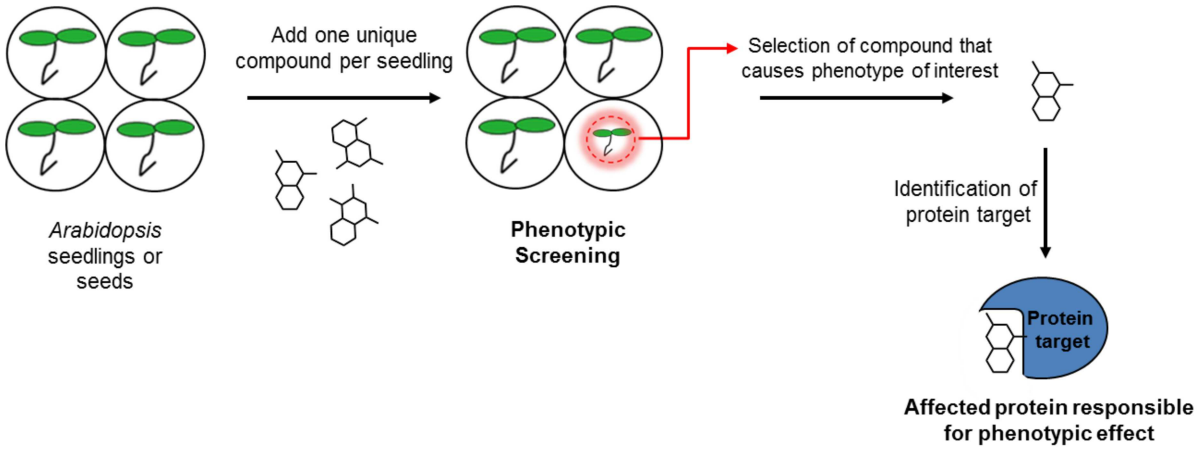

Figure 3: A typical forward chemical genetics screening approach in plants. Multiple seedlings are grown in well-plates and incubated with a set of compounds. Plants demonstrating a phenotype of interest are selected. The very last step is the identification of the protein causing the phenotypic effect.

Therefore, chemical genetics approaches in plant biology are highly rewarding and have led to the identification of innumerous bioactive small molecules. In addition to their importance as essential agrochemicals, such elucidated small molecules may serve as powerful research tools to address questions at all levels of biological complexity from protein function to plant biotic interactions. In certain contexts, such chemical tools are complementary or even preferred to genetic analysis, since not all experimental systems are accessible for genetic dissection in plants. For example, plant mutants impaired in oxygen sensing cannot easily be recovered.[29] Pharmacological and chemical genetics approaches therefore represent rewarding methodologies to study such genetically intractable systems.[19] In Figure 4 are depicted some

examples of exogenous small molecules identified from either screening campaigns or by pre-selection due to their plant-specific activity. These compounds are examples of chemical probes nowadays used in plant biology research.

Pyrabactin (*Fig. 4*) was identified in a chemical genetic screen aiming at identifying germination inhibitors.[30] Pyrabactin has received high attention as it served as the major chemical tool for investigating the ABA signaling pathway in plants. In fact, a screen for Pyrabactin-insensitive mutants allowed the identification of insensitive alleles of PYR1 (Pyrabactin Resistance 1), a member of a novel 14-member gene family of previously unknown function. In the presence of Pyrabactin, PYR1 interacts with protein phosphatase HAB1, a key negative regulator of abscisic acid (ABA) responses. In contrast to pyrabactin, which is selective for PYR1 in seeds, ABA interacts with all PYR1-like homologs, which causes redundancy in the ABA signalling pathway, thereby hampering its investigation by traditional genetics methods. Thus, the application of a chemical compound that shows selectivity to some genes of the ABA signalling cascade enabled the identification of key signalling components which was not possible by classical forward genetics.[30]

Morlin (*Fig. 4*) was discovered in a phenotypic chemical genetic screen of 20,000 compounds.[33] Morlin stimulated morphological defects in *Arabidopsis*, such as right handed helical root growth at low concentrations and radial swelling in elongating roots, and hypocotyls at high concentrations (>5 μM). Live-cell imaging of fluorescently labeled cellulose synthase (CESA) and microtubules showed that Morlin acts on cortical microtubules and alters the movement of CESA. Morlin caused a novel syndrome of cytoskeletal defects, characterized by cortical array reorientation and compromised rates of both microtubule elongation and shrinking.[33]

In a phenotype-based chemical genetic screen using *Arabidopsis* seedlings, the small molecule Bikinin (*Fig. 4*) was identified as it caused an increase in hypocotyl length, the formation of long and bending petioles, and the emergence of blade-shaped, pale-green leaves.[34] It was shown that Bikinin activates brassinosteroid (BR) signaling downstream of the BR receptor via direct binding to glycogen synthase kinase 3 (GSK3) BIN2 as well as inhibiting the activity of six other *Arabidopsis* GSK3s.

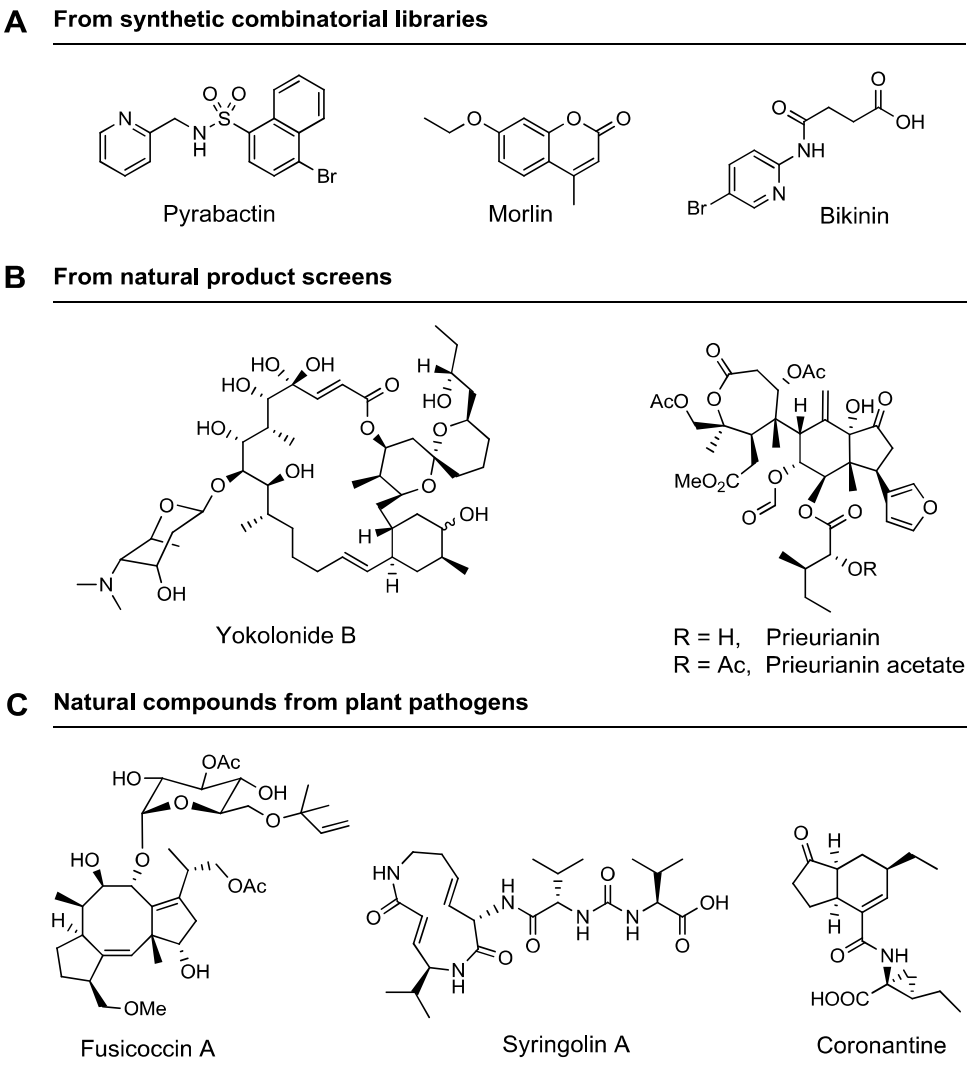

Figure 4: Examples of bioactive small molecules nowadays used in plant research and identified through different approaches. (A) Compounds identified from chemical genetic screens using combinatorial libraries. (B) Compounds identified from chemical genetic screens using natural product-based screens. (C) Natural compounds from plant pathogens. For more examples see Ref. [31] and [32].

Yokonolide B (YkB; also known as A82548A), a spiroketal-macrolide (*Fig. 4*), was isolated from *Streptomyces diastatochromogenes* B59 in a screen for inhibitors of auxin responses in Arabidopsis.[35] YkB was shown to inhibit the expression of auxin-inducible genes after stimulation with native and synthetic auxin promoters. YkB-treated *Arabidopsis* seedlings thereby displayed similar phenotypes as dominant AUX/IAA mutants. Further studies on the underlying molecular mechanism have however not yet been reported.

To identify circadian clock effectors *in planta*, a natural product library was screened in the model plant *Arabidopsis thaliana*. Two compounds, Prieurianin and Prieurianin acetate (*Fig. 4*), were identified as causing a shorter circadian period. It was shown that Prieurianin

primarily affects actin filament flexibility in vivo, resulting in reduced severing and filament depolymerization. This stabilization of the actin cytoskeleton is accompanied by impaired vesicle trafficking. Again, the underlying molecular mechanism is however unknown so far.

Fusicoccin A (*Fig. 4*) is produced by the fungus *Fusicoccum amygdali* which is a plant pathogen of mainly almond and peach trees. Application of Fusicoccin A on plants causes wilting of the leafs due to a uncontrolled loss of water through the stomatal pores which are localized in the leaf epidermis.[36] Several biological studies have discovered that this effect is based on the binding of Fusicoccin A to a protein complex consisting of the (plasma membrane-) H^+-ATPase (PMA) and 14-3-3 proteins.[37] The (plasma membrane) H^+-ATPase is an integral membrane protein that transfers protons (H^+) from the cytoplasm into the extracellular space. Activation of the H^+-ATPase results in an opening of the stomata, while deactivation leads to its closing. Fusicoccin A has been shown to enforce stomatal pore opening by binding to the edge of the interface of the activated H^+-ATPase/14-3-3 complex, thereby stabilizing the interaction between H^+-ATPase and 14-3-3 proteins. This stabilization then causes a permanent activation of the H^+-ATPase and thus irreversible opening of the stomata, thereby causing wilting of the plant due to the high transpirational water loss.

Syringolin A (*Fig. 4*) is a potent and selective inhibitor of the eukaryotic 20S proteasome of plants.[38; 39] It acts by irreversible modification of the active site residue, an *N*-terminal threonine moiety located at the catalytically active subunits β1, β2 or β5. Inhibition of the plant proteasome leads to an impairment of the plant immune system. Thereby, Syringolin A is an important virulence factor for certain phyto-pathogenic *Pseudomonas syringae* strains.[40]

Coronatine (*Fig. 4*) is a phytotoxin also produced by the plant pathogen *Pseudomonas syringae*. Coronatine mimics the endogenous small molecule phytohormone JA-Ile and promotes opening of stomata for bacterial entry and disease symptoms in plants.[41] It was shown that Coronatine stabilizes the interaction between the F-box protein COI1 and JAZ proteins. Thereby, direct recognition of coronatine by COI1 is coupled to ubiquitin-mediated degradation of JAZ proteins and leads subsequently to depression of primary response genes.[42]

2.4 Activity based protein profiling (ABPP) for functional proteomics in plants

The application of activity based protein profiling (ABPP) is a relatively new approach in plant science as the active plant proteome has so far been mined with only a limited number of probes. However, several initial ABPP studies on plants, mainly launched by van der Hoorn and coworkers, demonstrated the versatility and robustness of ABPP to study plant enzymes. These studies illustrated the potential of ABPP as a discovery tool to detect differential protein activities and inhibitors also in plant species.

2.4.1 Basic principle of ABPP

The elucidation of the proteome, i.e. the entire inventory of all proteins including their posttranslational modifications, at a given time point in an organism is challenging and often referred to as "proteomics".[43; 44] Consequently, many different proteomic techniques have been developed in the last years to quantitatively determine protein levels on a proteomic scale.[45] For enzymes, the determination of protein level is however not always correlating with its proper activity as the activity state of enzymes are regulated by various post-translational and other mechanisms e.g. by regulated proteolysis of inactive protease precursors (zymogenes). Therefore, it is important to have a proteomic technology available that is able to distinguish between enzyme abundance and activity.[46] Activity based protein profiling (ABPP) has emerged as such a methodology and is based on the application of target-based small molecules to characterize enzyme activities directly in native biological systems which may even be whole living organisms.[47]

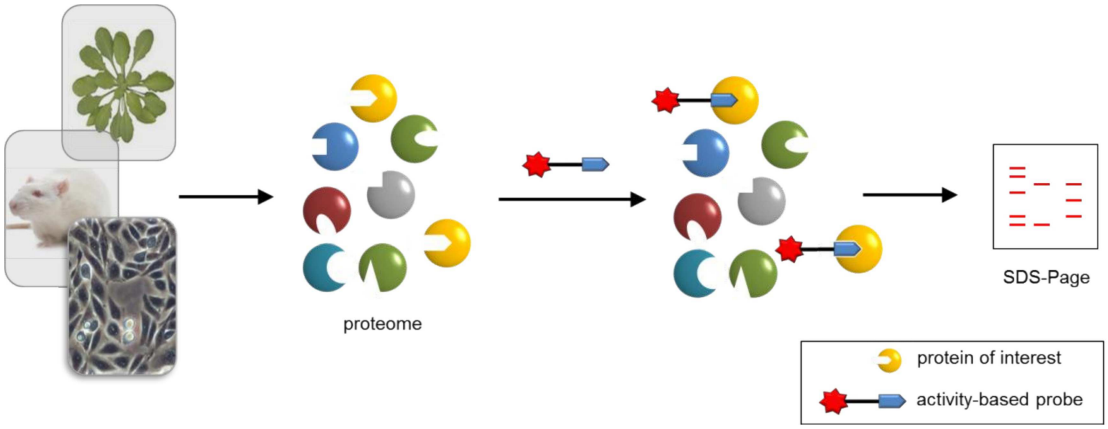

Figure 5: Concept of activity-based protein profiling (ABPP). Proteomes are incubated with activity-based probes, which address distinct active enzymes. The probe-labeled proteome is resolved and enzyme activities are visualized, for example by fluorescence or blotting.

In a typically ABBP experiment, proteomes are exposed to a certain type of an activity-based probe either in vitro or in vivo resulting in a covalent modification of active enzymes at their active-site residues by the activity-based probes (*Fig. 5*). As the activity-based probes react with the catalytic amino acid residue in the active site of the enzyme, only active forms and not the inactive precursor-enzyme or even inhibited enzymes are addressed.[21] In the most classical approach, the probe-labeled proteome is then resolved by gel-electrophoresis, followed by visualization of probe-labeled by either in-gel fluorescence scanning (for fluorescent probes) or by Western-blots (for biotinylated probes). By the use of active site-directed chemical probes it is possible to visualize distinct activities of anticipated enzymes or enzyme subclasses and thus to obtain a direct correlation or distinction of the visualized activity and the proper abundance of certain enzymes.[48]

2.4.2 Composition and design of activity-based probes (ABP)

ABPP is based on the use of active-site-directed activity based probes (ABPs) which depict enzyme functions of specific subsets of enzymes in complex proteomes. For a quantitative readout of the functional state of probe-targeted enzymes, a covalent and irreversible bond between the active-site directed probe and the enzyme has to form. Activity-based probes thereby often target a large, but workable subset of the proteome, regularly defined by shared

homological features of the targeted enzymes. An ABP consists of three general core elements (*Fig. 6*):

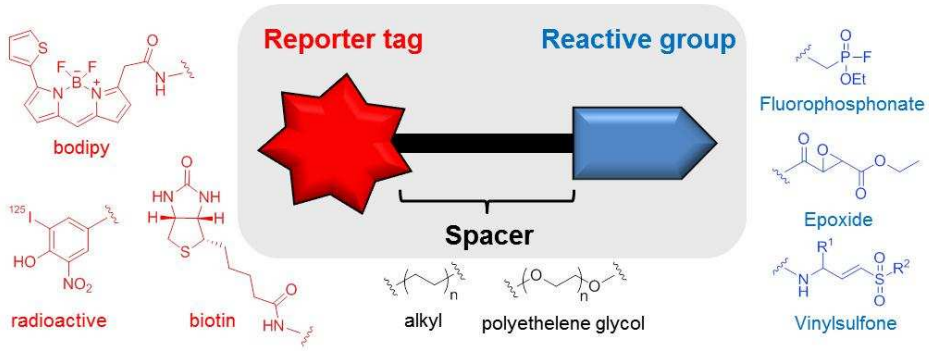

Figure 6: Schematic structure of an activity based probe which contains a reactive group (*blue*), a spacer region (*black*) and a reporter tag (*red*), surrounded by examples of chemical structures for each structural element.

First, a reactive group - often deduced from known irreversible enzyme inhibitors. Hydrolytic enzymes are particular suited for the development of ABPs as these enzymes are catalyzing this reaction often via a covalent intermediate. To this end, the catalytically active amino acid residue is attacking an electrophilic entity on the ABP resulting in a covalent modification of the active-sites. The target specificity of individual probes is thereby based on mechanistic differences of the various classes of enzymes. For example, threonine, serine and cysteine proteases are using different catalytically active amino acids and thus display a specific reactivity towards different reactive groups.

The second component is the spacer or linker region which has the role to provide sufficient space between the reporter and the reactive group to prevent undesirable steric hindrances. In addition, variation of the chemical composition of the spacer has influence on the solubility and membrane permeability of the probes. The spacer region often consists of alkane chains or polyethylene glycol units. It also allows the incorporation of 'specifity elements' to more selectively target a distinct enzyme or family of enzymes, e.g. proteases.[49; 50]

Third, a reporter tag for detection and/or isolation of probe-labeled enzymes from proteomes. Examples of reporter tags involve fluorophores, such as rhodamine or bodipy, biotin or radioactive labels for the detection of covalently modified target-enzymes. Fluorescent and the much less used radioactive tags can be detected easily (in contrast to a biotin-tag, where western-blot approaches are necessary) by direct scanning of the resolved SDS-gels with a fluorescence or radioactivity scanner. Despite these advantages, biotin is still

often used because this tag allows to both perform gel-based ABPP and gel-free ABPP applications via affinity purifications of labeled enzymes using (strept)avidin-beads (c.f. *Chapter 2.4.5*).[49]

2.4.3 Classes of ABPs

2.4.3.1 Directed probes

ABPs can be classified as either mechanism-based or affinity-based depending on the mode by which the covalent linkage with the enzyme is established. Mechanism-based ABPs (also known as directed ABPs) are mainly based on irreversible enzyme inhibitors (or suicide inhibitors) and use electrophilic warheads that specifically react with catalytic residues in the enzyme's active site.[51] A beneficial feature of direct ABPs is that they ideally possess excellent target selectivities within a family of enzymes sharing cognate mechanism and function and minimal interfamily cross-reactivity. Several directed probes for various enzyme classes are known so far, including ABPs for serine-hydrolases[52], several protease families[53; 54], phosphatases[55], glycosidases[56], etc.. Many of them have also been used in plant research (*Fig. 7*).

Serine hydrolases can be addressed with fluorophosphonates (*Fig. 7*) that react with the catalytic serine residue in this class of enzymes. Due to their high reactivity, fluorophosphonate-probes have emerged as powerful tools to study serine hydrolase activities in plants.[57]

The epoxide probe DCG-04 (*Fig. 7*), originally derived from the natural product E-64, selectively targets papain-like cysteine proteases in plants.[58]

The acyloxymethyl ketone electrophile (*Fig. 7*) is known to target cysteine proteases.[59] This type of electrophile is equipped with low reactivity towards weak nucleophiles and thus is efficiently addressed by catalytically active thiol residues located in the active site of cysteine proteases. The direct AOMK probe depicted in Figure 7 has for example been used to profile the cysteine protease AvrPphB, an effector of the plant pathogen *Pseudomonas syringae,* which is injected into the host plant cell to cleave specific kinases for disrupting immune signaling.[60] Of note, a number of other AOMK probes containing either a single

amino acid or an extended peptide sequence have been shown to target other cysteine proteases like caspases, legumains, gingipains and cathepsins in human cells.[59]

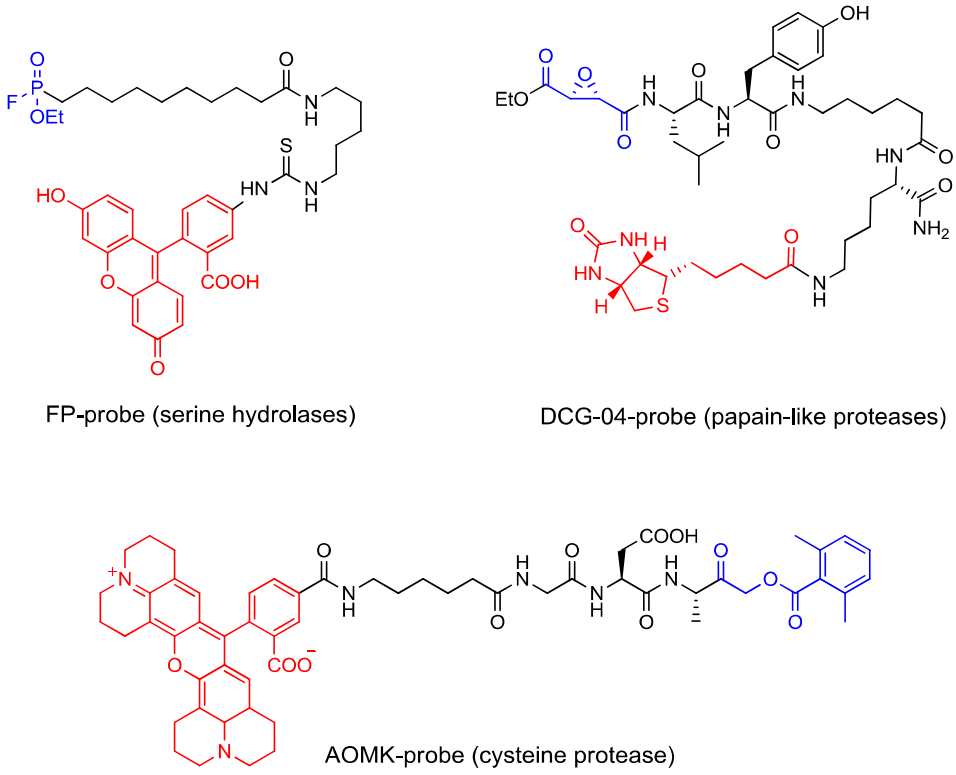

Figure 7: Examples of established directed probes that have been used in plant research. Reactive groups are colored in blue, reporter tags are highlighted in red and spacers and selectivity-providing groups are colored in black.

2.4.3.2 Non-directed probes

Another possibility to develop new reactive groups for ABPP is the non-direct approach, in which combinatorial chemistry libraries of molecules equipped with general electrophilic entities are screened towards a certain target enzyme. These reactive groups often possess new and unpredictable chemical features and sometimes contribute to the discovery of new ABPs for new enzyme targets. By following this concept, multiple non-directed probe libraries for several mechanistically distinct enzyme classes were developed. This approach has significantly expanded the scope of ABPP for those enzyme classes that lack obvious susceptible catalytic residues and was recently also used in in plant research.[53]

Such non-directed *β*-lactone probes were for example generated for monitoring protease activities in plant extracts (*Fig. 8*). Unexpectedly, this probe resulted in labeling of the *N*-terminus of PsbP, a non-proteolytic protein of photosystem II. Inhibitor studies and reverse genetics led to the discovery that this unusual modification was mediated by a single plant-specific, papain-like cysteine protease called RD21. In cellular extracts, RD21 accepted both *β*-lactone probes and peptides as donor molecules and ligates them, probably through a thioester intermediate, to unmodified *N*-termini of acceptor proteins.[61]

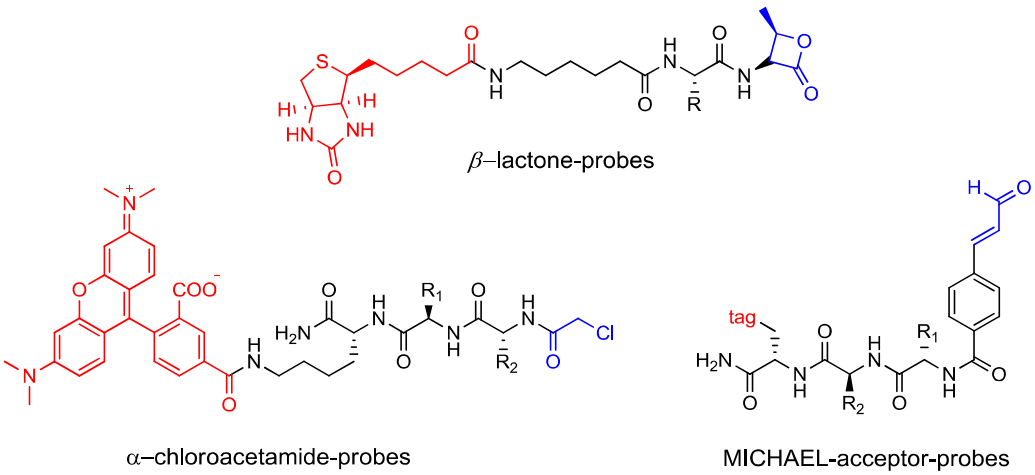

Figure 8: Examples of established non-directed probes for ABPP. Reactive groups are colored in blue, reporter tags are highlighted in red and spacers are colored in black.

The *α*-chloroacetamide group also has features that are beneficial for undirected ABPP (*Fig. 8*). Its small size does not bias binding elements towards a specific class of enzyme, and it possesses reactivity towards a broad variety of nucleophilic amino acid residues. Upon screening of an *α*-chloroacetamide-based library in a mouse model system many enzymes previously unadressed by directed ABPP probes were uncovered.[62]

Of all the non-directed ABPP reactive groups, the MICHAEL acceptor system is probably the most frequently used (*Fig. 8*). This chemical entity is found in many natural products, often displaying mechanism-based activity via the 1,4-addition of cysteine residues, the preferred reacting partner of MICHAEL-acceptors in the proteome. Pitscheider and Sieber synthesized an undirected ABPP library based on cinnamic aldehydes as the reactive group (*Fig. 8*). Using this probe library, a virulence-associated secretory antigen from MRSA strains was identified.[63]

As noted, ABPP with electrophilic ABPs is only applicable to protein targets that possess nucleophilic active site residues (mainly Ser, Cys or Lys) susceptible to covalent

labeling. For enzymes with different enzymatic mechanisms, strategies have been developed in which photoreactive ABPs are used. These probes contain for example an additional photo-reactive crosslinker (*Fig. 9*), which is conjugated to a probe that tightly binds to an active site of the protein target.[64] Upon UV irradiation, these chemical groups are able to form highly reactive intermediates. Subsequently, these reactive species form covalent bonds with all types of protein residues that are in close spatial proximity.

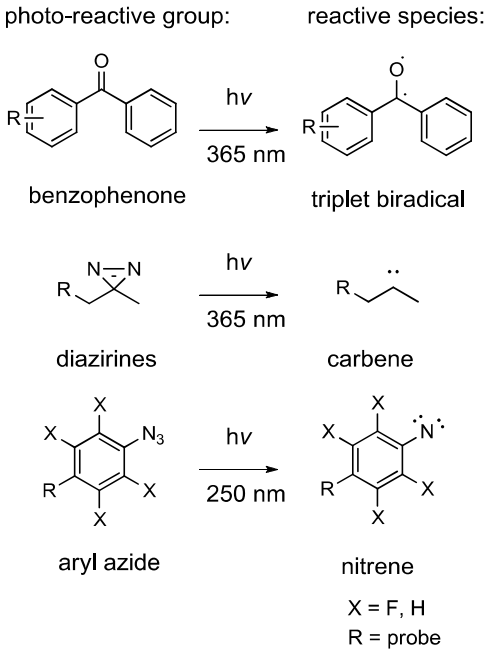

Figure 9: Examples of photo-reactive groups that can be incorporated into activity-based probes.

In a typical photo-reactive probe, the warhead is substituted by the incorporation of such a photo-crosslinker, in addition to a selectivity generating motif that is required to avoid random labeling. The integration of photo-reactive crosslinkers into natural products that lack electrophilic entities is also often used to elucidate the direct target of these compounds.[65] Finally, photo-reactive groups can also be used in a non-directed approach that has been termed as screening with "fully functionalized" small molecules.[66]

2.4.4 Two-step ABPP

A common limitation of in vivo applications of ABPP stem from the relative bulky nature of the reporter tags (e.g. biotin or rhodamine). The enlargement of the probes through these reporter tags often restricts the cell permeability and/or the distribution of the probes within the cells. The introduction of a two-step ABPP labeling strategy has allowed overcoming these difficulties. To this end, the reporter group is substituted with a small bioorthogonal chemical entity (mostly either alkyne or azide) which does not disturb membrane permeability.[26; 67]

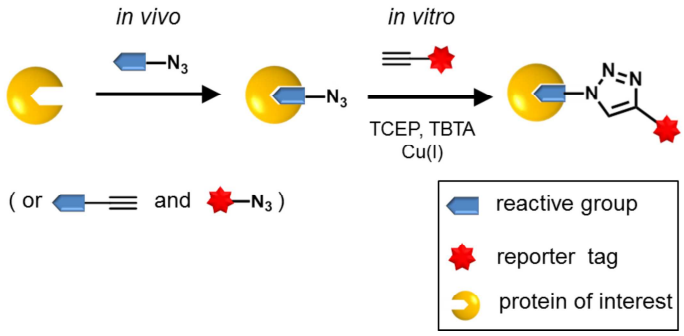

Figure 10: Principle of two-step ABPP. In contrast to standard ABPP, two-step ABPP enables the profiling of living cells and organism by treating them with "tag-free" azide- or alkyne-modified probes, which are subsequently conjugated in vitro forming a stable triazole product to visualize probe-labeled proteins.

Consequently, a reporter tag equipped with orthogonal functionalization (either alkyne or azide) is then attached to the probe after the labeling-experiment using for example the Cu-(I)-catalyzed version of HUISGEN's [2,3] cyclcoaddition to form a stable triazole product (*Fig. 10*).[68] This reaction is conducted using the whole, unpurified and probe-labeled proteome by applying TCEP as reducing agent, TBTA as stabilizing ligand and Cu-(I) as a catalyst. This approach has been widely used, for example to determine distinct activities of serine-hydrolases overexpressed in human cancer cell lines, which refused detection under in vitro conditions.[47]

2.4.5 Analytical platforms for ABPP

2.4.5.1 Gel-based approaches

Traditional ABPP approaches are gel-based methods because electrophoresis is the simplest method to resolve complex protein mixtures. Accordingly, all components of an ABP have to be stable at the conditions used for gel-electrophoresis. In gel-based ABPP approaches, the complex proteome is incubated with an ABP, resulting in covalent labeling of enzymes that are accessible for the probe. This complex mixture is then resolved by gel-electrophoresis and directly visualized using in-gel-fluorescent-scanning (fluorescent probes) or avidin-blotting (biotinylated probes). Two step ABPP approaches often apply both modes of detection, first using the attachment of fluorescent tags for rapid gel-based screening of proteomes and then linking biotinylated tags to allow avidin affinity chromatography, trypsin digest and mass spectrometry analysis for the identification of probe-labeled enzymes. In gel-based approaches, labelling patterns can be compared between samples but the elucidation of protein identies requires isolation of individual protein spots, their digestion and finally analysis of their mass, for example by MALDI or ESI mass spectrometry. The measured peptide masses are then compared against predicted mass values from a theoretical digestion of proteins, using a sequence database, resulting in the identification of a protein by a statistically significant number of matches.

2.4.5.2 Gel-free approaches

A gel-free approach is the Multidimensional Protein Identification Technology (MudPIT) that eliminates gel separations.[69] To this end, biotinylated probes are used and the labeled proteome is affinity-purified using avidin beads (*Fig. 11*). The affinity-purified fractions containing many proteins are then directly digested and the enormous number of generated peptides are separated by 2-dimensional liquid chromatography before entering the MS.[70] The procedure employs tandem mass spectrometry, i.e. after the mass of a peptide is measured, the peptide is fragmented using a collision-induced dissociation cell and the masses of the fragmentation products are also determined.[71] Extensive computational efforts then allow transforming this data into an amino acid sequence. Consequently, one identified peptide is

often sufficient to elucidate a target protein. This connotes a sensitivity advantage that allows identification of minor proteins in a biological fraction that conceivably cannot be detected by gel-based ABPP approaches. ABPP-MudPIT approaches were applied for example to profile enzyme activities in primary human breast tumors, resulting in the identification of more than 50 probe-labeled enzymes in a single experiment.[72] MudPIT approaches do however not enable a straightforward identification of the probe-labeled peptides. Consequently, a second concept known as the ASPP strategy was furthermore developed.[73] In this approach, the probe-labeled proteome is trypsin-digested before affinity-purification with beaded avidin. Therefore, only the probe-labeled peptides are subjected to the LC-MS/MS analysis and a direct determination of the binding site and thus of the catalytic amino acid can be ensured.

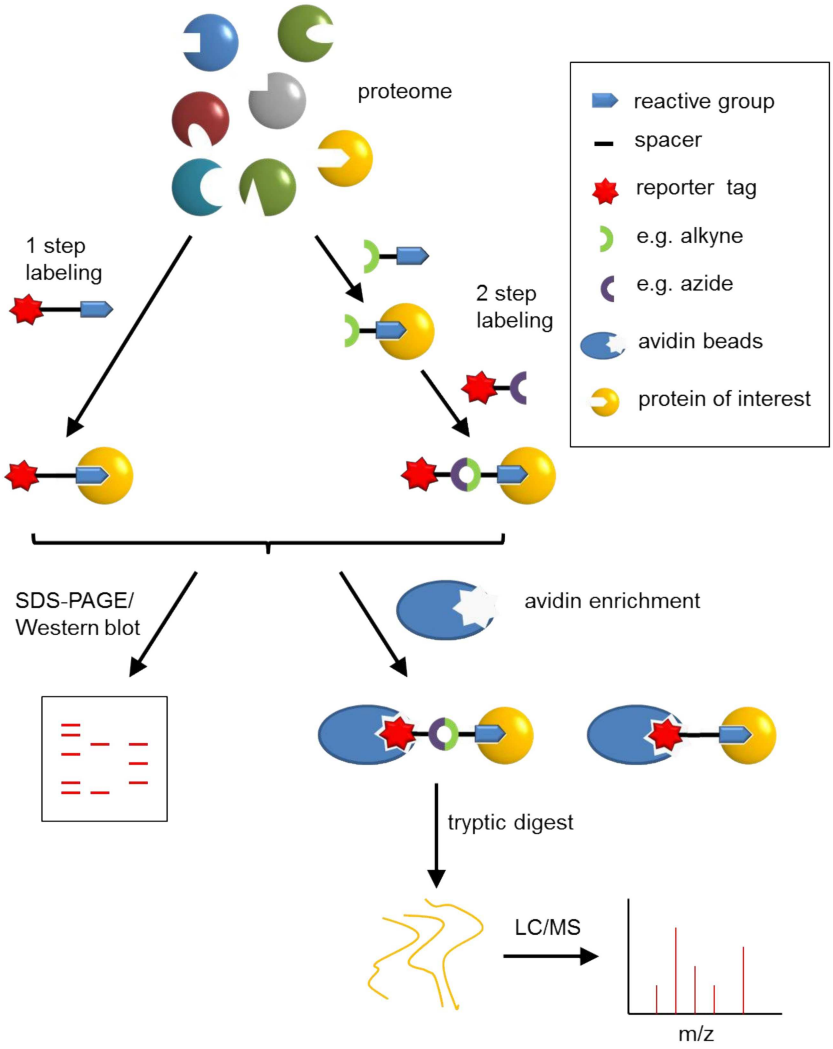

Figure 11: General procedure for gel-based and gel-free (MudPIT) ABPP experiments. (Adapted and modified from Overkleeft *et al.* [74])

In order to quantify the mass spectrometrical analysis of ABPP experiments, novel approaches (that originally stem from quantitative mass spectrometry approaches) have also been introduced in ABPP. To this end, stable isotope labels are incorporated into proteins. Stable isotopes preserve the physico-chemical characteristics of proteins and thus do not bias the activity. However, they differ in mass which enables their simultaneous detection and relative quantification. Mann and coworkers established a quantitative proteomic approach, the so called **s**table **i**sotope **l**abeling by **a**mino acids in **c**ell culture (SILAC).[75; 76] SILAC makes use of the requisition of mammalian cells for essential amino acids. Hence, cells are cultured either under normal conditions (natural abundant amino acids) or supplemented with isotope labeled essential amino acids (e.g. ^{13}C labeled L-arginine and ^{13}C, ^{15}N labeled L-lysine), which are fully integrated into cellular proteome. Different lysates are used for the pulldown with the active ("heavy" isotope labeled lysate) and with the inactive control probe ("light" lysate). The eluted proteins from both experiments are combined, processed and analyzed by MS. The use of isotopically labeled amino acids leads to a similar retention time for each peptide but to a difference in the molecular mass detected by MS. Therefore, a relative quantity of the "heavy" to the "light" peptide can be deduced from the ratio of the ion intensities. SILAC was for example used in the identification of tubulin and CSE1L as targets of tubulexins.[77] Morever, MT-ND1 and epoxide hydrolase 1 (EPHX1) were identified as primary targets of an antiproliferative 5-benzoylindole derivative in cancer cells by using the SILAC approach.[66; 78]

Another approach for quantitative proteomics is the use of **i**sotope-**c**oded **a**ffinity **t**ags (ICAT).[79] The ICAT probe contains an affinity tag (e.g. biotin), an isotopically labeled linker and a reactive group (warhead). The principle of ICAT comprises again two separate experiments (with two lysates treated independently with one of "heavy" and "light" probe) with subsequent pooling of the two different treated proteomes followed by digestion, affinity purification and relative quantification via MS. The ICAT approach was used for example to identify cytosolic MDHs as potential protein targets of the E7070 class of anticancer agents.[80]

2.4.6 Comparative ABPP

In a comparative ABPP approach, samples of proteomes obtained under different conditions are directly compared. For example, proteomes of healthy organisms can be compared with proteomes from diseased organisms via ABPP, resulting in different signal patterns.

Nowadays, many examples of this ABPP technology can be found in literature. As a prominent example, comparative ABPP has been used to identify some serine hydrolases that are dysregulated in aggressive cancer cells.[81]

2.4.7 Competitive ABPP

This versatile ABPP approach has also been developed to screen for enzyme inhibitors. To this end, a competitive ABPP experiment is performed which relies on determining enzyme activity states after pre-incubation with prospective enzyme inhibitors. A competitive ABPP approach offers several advantages towards the conventional screening of inhibitors. For example, targeted enzymes are tested in their native environment which ensures that potential post-translational modifications required for enzyme-activity are also considered. Moreover, this approach renders the recombinant expression and purification of proteins unneccessary due to use of whole native proteomes. Furthermore, there is the possibility to characterize simultaneously reversible[82] as well as irreversible inhibitors[83] against various enzymes. This approach is also suitable for those enzymes with unknown substrates as long as the enzyme is accessible to probe-labeling. Reversible inhibitors must be screened under kinetically controlled conditions, whereas the analysis of irreversible inhibitors is more straightforward and can even be performed in living organisms.[84]

2.4.8 ABPP with natural product-derived probes

Furthermore, the design of reactive groups may also makes use of protein-reactive natural products as starting point for novel selective probes.[85] Natural-products (NPs) are often very specific towards a particular enzyme and are therefore well suited for the design of probes, for which no mechanism-based inhibitor is available. For performing ABPP approaches with NPs, the target identification is undoubtedly the key step. To this end, the natural products need to be modified with an appropriate reporter-tag for transforming them into prospective probes. The corresponding reporter-tags can be incorporated into NPs either by total synthesis or via a regioselective modification (e.g. by alkylation, acylation etc.) of the NP. Such reporter-tagged NPs (tagged for example with biotin and/or alkyne/azide) can then be

incubated with proteomes. The corresponding target proteins are labeled by the NP-probes and enriched using for example immobilized (strept)avidin. Such affinity-purified proteins are then passed to either gel-based or gel-free identification techniques, mass spectrometry analysis and database searches for identifying labeled proteins (c.f. *Fig. 11*). For NPs that lack obvious electrophilic moieties for form covalent bonds, photo-reactive groups are often also attached (c.f. *Fig. 9*).

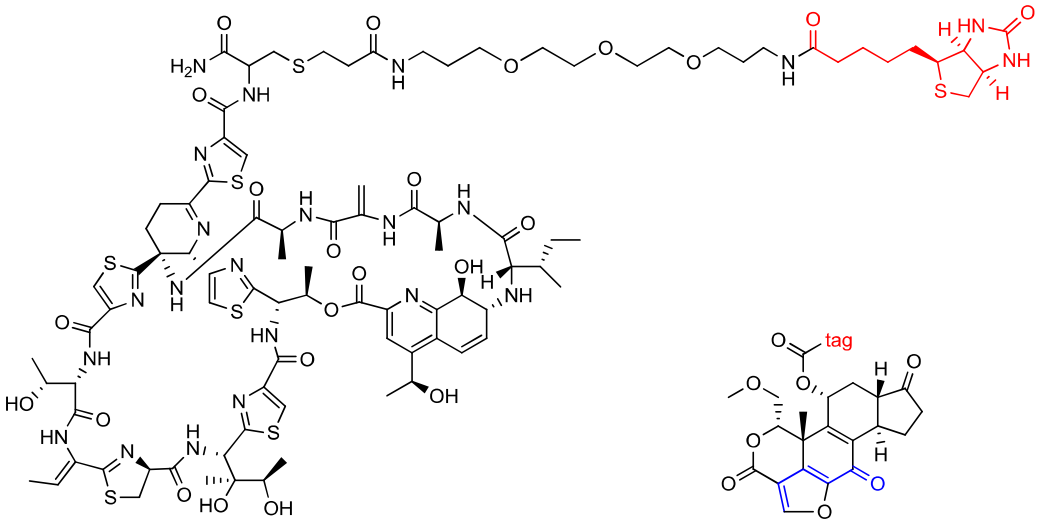

Figure 12: Examples of reporter-tagged natural products. Reactive groups are colored in blue, reporter tags are highlighted in red. The respective major protein targets are depicted in brackets.

To illustrate this NP-based approach, some examples will subsequently be given: Thiostrepton is a natural product isolated from various *Streptomyces* strains and has caused a great deal of scientific attention due to its potent antibiotic but also antiproliferative activity in human cancer cells. For pull-down experiments, the natural product thiostrepton was modified via 1,4 MICHAEL-type addition of a thiol-linked biotin tag to form a bioactive

probe (*Fig. 12*). In subsequent ABPP pull-down experiments, the transcription factor FOXM1 was found to be a direct target of thiostrepton in MCF-7 breast cancer cells.[86]

Wortmannin is a natural product that belongs structurally to the furanosteroids and is produced by the fungus *Penicillium wortmannii*. The capability of Wortmannin as a bioactive lead structure has inspired the development of Wortmannin-derived probes (*Fig. 12*). Attachment of fluorescent labels (bodipy and rhodamine) to the Wortmannin scaffold through esterification of a deacetylated alcohol side chain has enabled the identification of the binding partners of Wortmannin. Such an approach has allowed Yee and coworkers to confirm the reactivity of Wortmannin against phosphatidyl-inositol 3-kinase and related enzymes.[87]

HUN-7293 is a fungal cyclodepsipeptide that inhibits the expression of vascular cell adhesion molecule (VCAM). HUN-7293 associates irreversible to its protein targets and thus does not become covalently bond, which hampers target identification. Therefore, MacKinnon and coworkers generated a photoaffinity probe by incorporation of a photoleucine instead of leucine residue during chemical synthesis of HUN-7293 (*Fig. 12*). This probe was then able to covalently bind to HUN-7293 binding partners through photoactivation of the photoreactive diazirine group of photoleucine after UV irradiation. Additionally, an alkyne group was also introduced in HUM-7293, thereby enabling visualization of the target protein after a click reaction with rhodamine azide after UV irradiation of the probe-labeled proteome. This protocol enabled the identification of Sec61α as the direct target protein of HUN-7293. Sec61α participates in the forming of translocation channels at the beginning of the secretion pathway for all proteins in the endoplasmic reticulum. Hence, the molecular target of HUN-7293 could be directly detected by using ABPP.[65]

The marine natural product symplostatin 4 has been attracting many scientists due to its potent antimalarial properties. By adding a propargyl moiety to its *N*-terminus, this natural product was transferred into a natural product-derived probe (*Fig. 12*). Subsequent ABPP experiments revealed that plasmodial falcipains were the direct targets of symplostatin 4.[88]

2.5 Solid phase supported synthesis

Solid phase peptide synthesis (SPPS) has reached a major place in polypeptide synthesis since its invention by Merrifield in the early sixties of the 20th century and was awarded with the Nobel Prize in 1984.[89] Today, solid phase peptide synthesis has become an integral part for

the structure elucidation and total synthesis of natural products having a peptidic structure such as hormones, antibiotics, or plenty of other bioactive peptides. The definition of a peptide is not strict; most often, the benchmark for a peptide is a maximum of 50 amino acids and larger polypeptides are correspondingly then called proteins. Nowadays, synthetic peptides synthesized via solid supported methods have found widespread application in all areas of biomedical research.[90]

2.5.1 Peptide bond formation

Peptide synthesis relies on the controlled formation of a peptide (amide) bond between two amino acids with concurrent release of one water molecule, thus turning polypeptide synthesis into a repetitive condensation reaction. The condensation reaction however cannot proceed spontaneously but requires a pre-activation of the carboxyl component (**A**) of one amino acid, which holds additionally a selectively blocked *N*-terminus (*Fig. 13*). The *N*-terminal primary amine of the second amino acid (**B**), which possesses *vice versa* a selectively blocked carboxyl function, attacks the activated carboxyl component via a nucleophilic attack to give the dipeptide **A-B**. After selective deblocking of either the *N*-terminal or *C*-terminal protection group, the dipeptide **A-B** can enter again into the cyclic reaction flow.

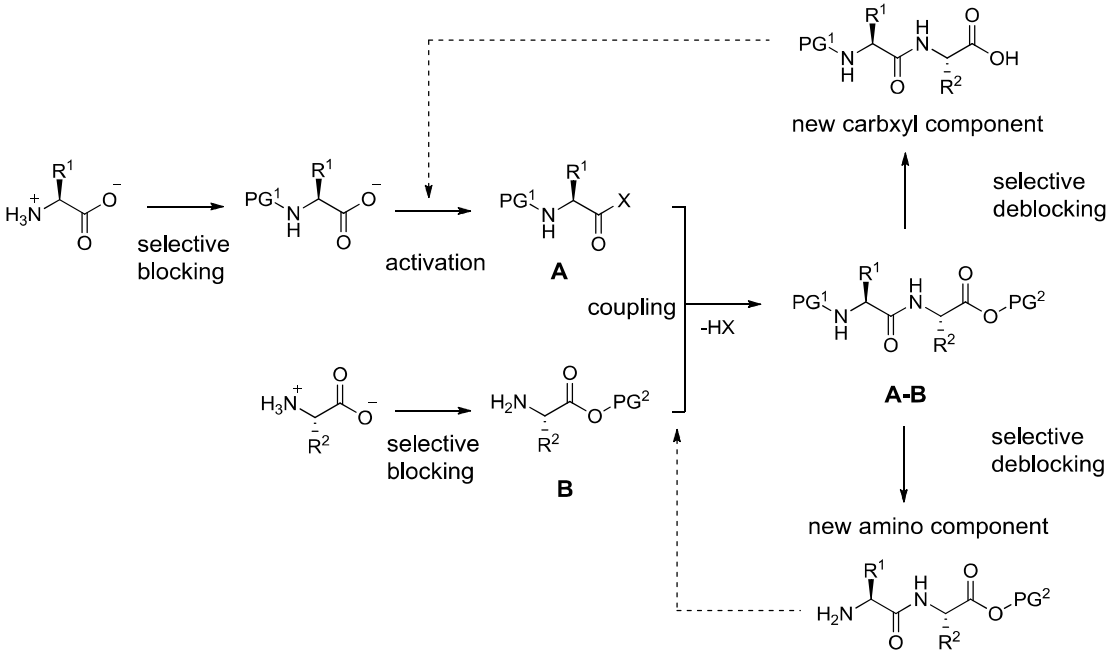

Figure 13: The multi-step process of peptide synthesis (adapted and modified from Ref. [91]).

To overcome unintentional side reactions during peptide synthesis, all additional reactive functional groups have to be blocked by protection groups. Hence, peptide bond formation can be regarded as a three-step procedure:

1. The preparation of a selectively and partially protected amino acid which results in a non-zwitter ionic amino acid derivative.
2. The formation of the peptide bond. To this end, the carboxyl function of the *N*-protected amino acid has to be transformed into an activated intermediate capable of reacting with the nucleophilic amine of the second amino acid.
3. The chemoselective cleavage of the protecting groups. To this end, two different deprotection approaches are differentiated. At the end of the synthesis, a complete deprotection of all protection groups of the peptide has to be performed. In contrast, during iterative assembly of the different amino acid building blocks, a selective cleavage of the N-terminal or C-terminal amino acid protection is required (*Fig 13*).

For activating the carboxylic acid of the carboxyl component (**A**), a broad spectrum of methods is nowadays available and often used in practical synthetic applications.[92] For example, acyl azides[93], mixed anhydrides[94], carbodiimides[95] and active esters[96] of HOBt or HOAt which are often indirectly derived from phosphonium or guanidinium/uronium type coupling reagents are often used.

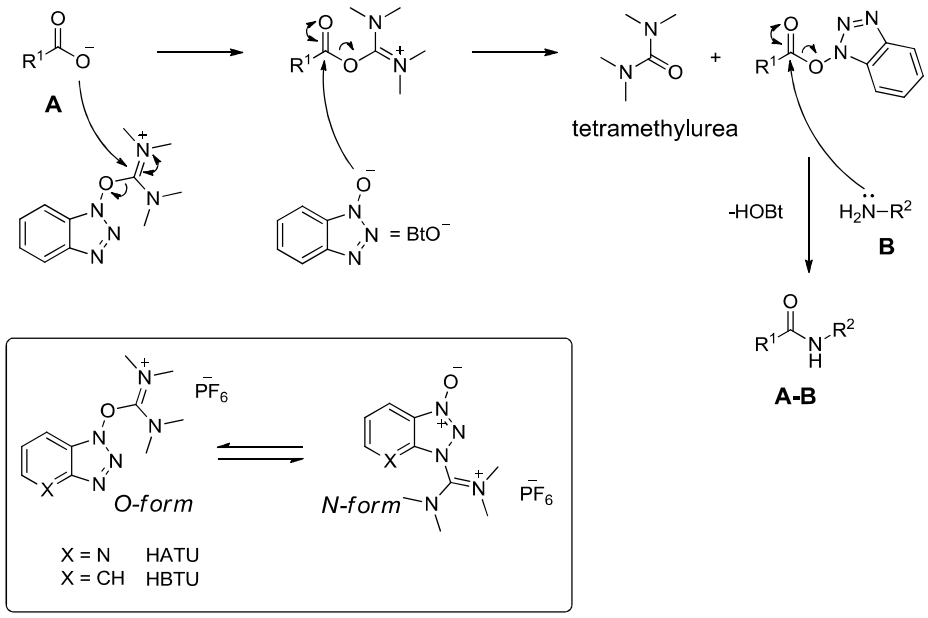

Figure 14: Mechanism of peptide bond formation via activation of guanidinium/uranium salts of hydroxybenzotriazole derivatives.

These HOBt and HOAt-based coupling reagents predominantly exist in the guanidinium or *N-form*, which is less reactive than the uronium *O-form*.[97] However, mechanistically the guanidinium reagents like HBTU are nucleophilically attacked by the carboxylate of the *N*-protected amino acid which results in an *O*-acylisouronium salt intermediate (*Fig. 14*). This highly reactive intermediate is then attacked by hydroxybenzotriazole to yield the corresponding active ester. This intermediate is then susceptible for the nucleophillic attack by the amine of the second amino acid (**B**) thereby finally leading to the peptide bond (**A-B**).

2.5.2 Protecting group strategies

The entire process of peptide synthesis is however complicated by the presence of additional functional groups in the side chain of half of all proteinogenic amino acids which makes a further selective protection indispensable (*Table 1*). Due to the different synthetic demands with respect to selectivity, a precise distinction must be made between the transient and semi-permanent (side chain-) protection groups. The transient protection groups are required for temporary protection of the amino function involved in subsequent bond formation. These transient protection groups must be cleaved selectively under conditions which do not impair the stability of the peptide backbone already present or the stability of the semi-permanent protection groups at the amino acid side chains. The semi-permanent protection groups are commonly cleaved after assembly of the desired peptide chain or, once in a while, also at an intermediate stage to perform e.g. regio-selective reactions with amino acid side chain. In these deprotection reactions, only those deblocking reagents can be used that do not harm the final product. The selection of protecting groups must also be carried out in accordance with the envisaged synthesis strategy. Normally, orthogonal protecting group strategies are used in peptide synthesis. Orthogonal protecting groups can be cleaved selectively while all other protecting groups stay intact. To this end, the chemical cleavage mechanisms of the different protecting groups should be chemically different to achieve an optimum degree of orthogonality. For instance, the application of Boc as the transient protection group excludes the use of semi-permanent protection groups at amino acid side chains with comparable acid-lability. Hence, semi-permanent protection in Boc tactics must avail protection groups that remain intact during the recurring acidic Boc cleavages. In contrast, Fmoc as the transient protection group is cleaved after each coupling step by treatment with secondary amine bases. In this case, side chain protection may apply *tert*-butyl or Boc-like protection groups.

Consequently, this tactic is denoted in literatue as the Fmoc/tBu or Fmoc/Boc or as the SHEPPARD-strategy.[98] Special protection schemes may also be required, for instance if a certain peptide strand needs to be branched via side chain funtionalization or for subsequent cyclization reactions. In small scale applications such as laboratory peptide syntheses, the Fmoc/tBu strategy is nowadays mostly used since it is more applicable than the Boc-tactics due to the avoidance of irritant chemicals (e.g. HF) used in the synthesis. As the name denotes, Fmoc-chemistry uses the Fmoc group for *N*-amino protection, which is usually removed by piperidine or DBU in DMF. Fmoc-compatible side chain protecting groups are primarily ether, esters or urethane-type derivatives of *tert*-butanol (*Table 1*). In the course of a common Fmoc-based peptide synthesis, the side chain protecting groups are ideally removed at the same time as the corresponding cleavage from the resin, often by the use of TFA as the cleavage reagent.

Table 1: Selected protecting group schemes for the maximum protection approach using the Fmoc/*t*Bu protocol.

	Fmoc/*t*Bu protocol
Transient protection group	Fmoc
Semi-permanent protection groups	
Asp/Glu	O*t*Bu
Arg	Pbf
Lys	Boc
His	Trt
Cys	Trt
Ser	*t*Bu
Thr	*t*Bu
Tyr	*t*Bu
Trp	Boc
Asn/Gln	Trt

Examples of important amino-protecting groups used in SPPS are given in the subsequent paragraphs.

2.5.2.1 The *tert*-Butoxycarbonyl protecting group

The *tert*-Butoxycarbonyl group (Boc) is attuned with the majority of the most common coupling methods to accomplish peptide bond formations. It can be cleaved using mild acidic conditions and is robust towards many reaction conditions like catalytic hydrogenation,

alkaline hydrolysis and diverse reductive conditions. The frequently used deprotection procedure is the treatment with pure or diluted TFA which efficiently cleaves Boc groups giving the free amine together with simultaneous elimination of carbon dioxide and isobutene (*Fig. 15*).[99]

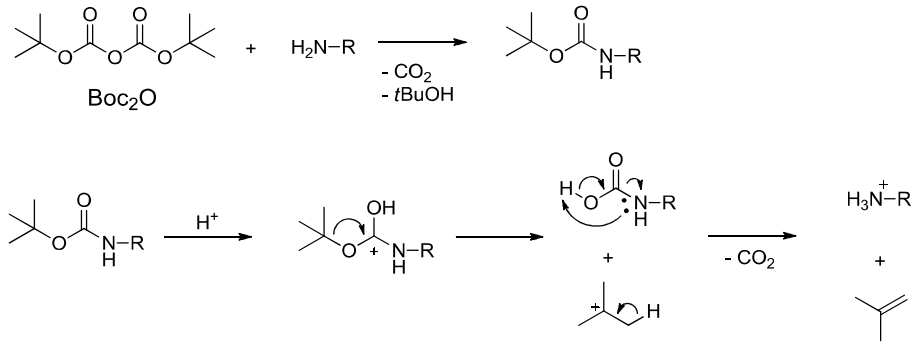

Figure 15: Mechanism of the introduction and of the acidolytic cleavage of the *tert*-butoxycarbonyl group.

The installation of the Boc-protection group on an amine is easily achieved by reaction with di-*tert*-butyldicarbonate (Boc_2O) (*Fig. 15*). To this end, amino acid salts are for example treated with Boc_2O in an aqueous sodium bicarbonate solution often containing solubilizing additives such as dioxane.

2.5.2.2 The 9-Fluorenylmethoxycarbonyl group

The 9-Fluorenylmethoxycarbonyl group (Fmoc) is the only amine urethane type protection group of practical significance that enables a cleavage under mildly basic conditions.[100] The practical benefit of the Fmoc-protection group is its particular sensitivity towards secondary amines, which allows deprotection of the amino group with dilute solutions of piperidine or diethylamine in DMF; for example, 20% piperidine in DMF is usually used in solid phase peptide synthesis. The deprotection reaction procceeds according to an E1cB mechanism, i.e. after an initial proton abstraction, the formed carbanion (a stabilized dibenzocyclopentadienyl anion), which is the conjugated base of the substrate eliminates in a second step from the substrate. The so formed dibenzofulvene subsequently reacts with piperidine to give a stable adduct as a by-product of the cleavage reaction (*Fig. 16*). This piperidine adduct has a unique UV absorption with a maximum at $\lambda = 301$ nm which allows to monitor the cleavage reaction by photometric measurements. The reagents Fmoc-Cl and Fmoc-OSu (9-Fluorenylmethyl-*N*-

succinimidyl carbonate) are mostly used for the installation of the Fmoc protecting group. The acid stability, combined with the mildly basic cleavage conditions, allows the application of acid-labile semi-permanent protecting groups (such as Boc) to mask side chain functionalities.

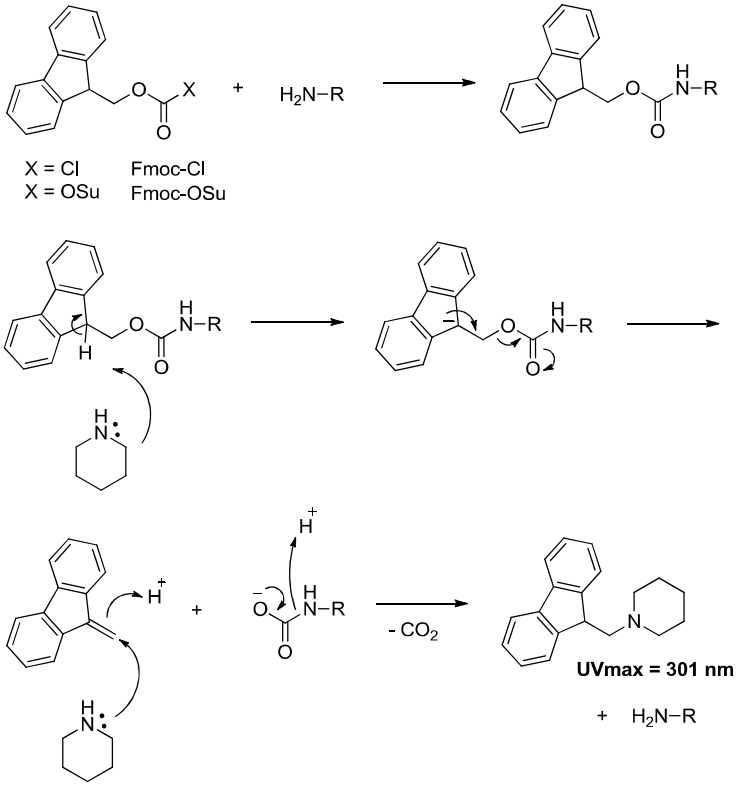

Figure 16: Mechanism of Fmoc introduction and base induced cleavage.

2.5.2.3 The *N*-Allyloxycarbonyl group

The *N*-Allyloxycarbonyl group (Alloc) is completely orthogonal to Boc and Fmoc and finds therefore application in syntheses in which a third orthogonality is needed, e.g. the syntheses of cyclic peptides or selective cross-links at side chain functionalities. The deprotection step involves palladium(0)-catalyzed allyl transfer to nucleophiles such as amines or organosilanes (*Fig. 17*).

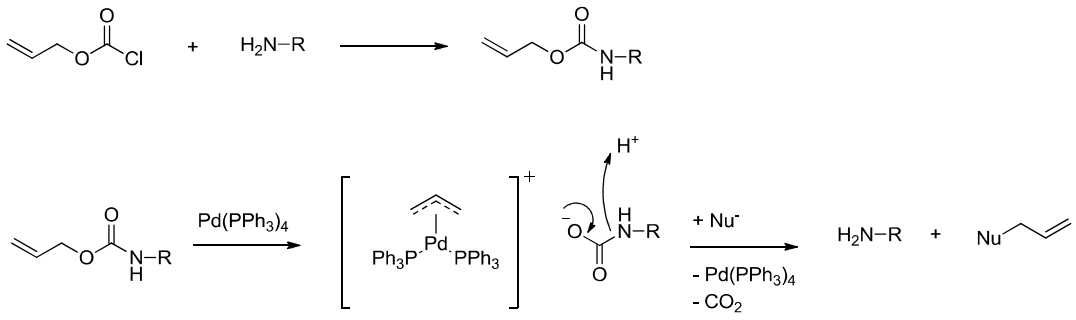

Figure 17: Mechanism of introduction and cleavage of Alloc-protecting groups.

The installation of the Alloc protecting group is quite similar to the introduction of the Fmoc protecting group. Thus, this protecting group is mostly introduced with a SCHOTTEN-BAUMANN-like reaction, i.e. an acylation of the primary amine by an acid chloride of a corresponding formic acid derivative.[101]

2.5.3 The principle of solid phase supported peptide synthesis (SPPS)

Despite some remarkable solution phase peptide synthesis of even whole proteins, solution phase peptide synthesis is generally highly elaborate and time-intensive due to the need to separate all interim peptide-intermediates from potential by-products as well as from coupling reagents. In addition, the solubility of the growing peptide chain is often an indispensable problem. Therefore, solid phase peptide synthesis has more and more become the standard method for the generation of all types of peptides. Solid phase peptide synthesis begins with the coupling of the first amino acid of the peptide via its carboxyl group to an insoluble polymer resin. The linkage to a solid matrix allows an easy separation of the resin-bound product from either reagents or dissolved product by simple filtration. To this end, an amino acid which is protected at its *N*-terminus is reacted with the functional group of the linker to form a covalent linkage (*Fig. 18*; Step 1). Subsequently, the *N*-terminal transient protection group is removed (*Fig. 18*; Step 2) and the next amino acid component is coupled (*Fig. 18*; Step 3). Steps 2 and 3 are then repeated until the required peptide sequence has been assembled. Finally, the covalent bond between the linker moiety and the peptide chain is cleaved. In many cases the permanent side chain protecting groups may be simultaneous

removed (*Fig. 18*; Step 4). The insoluble polymeric support is then separated from the cleaved product, for example by filtration (e.g. by suction through a frit).

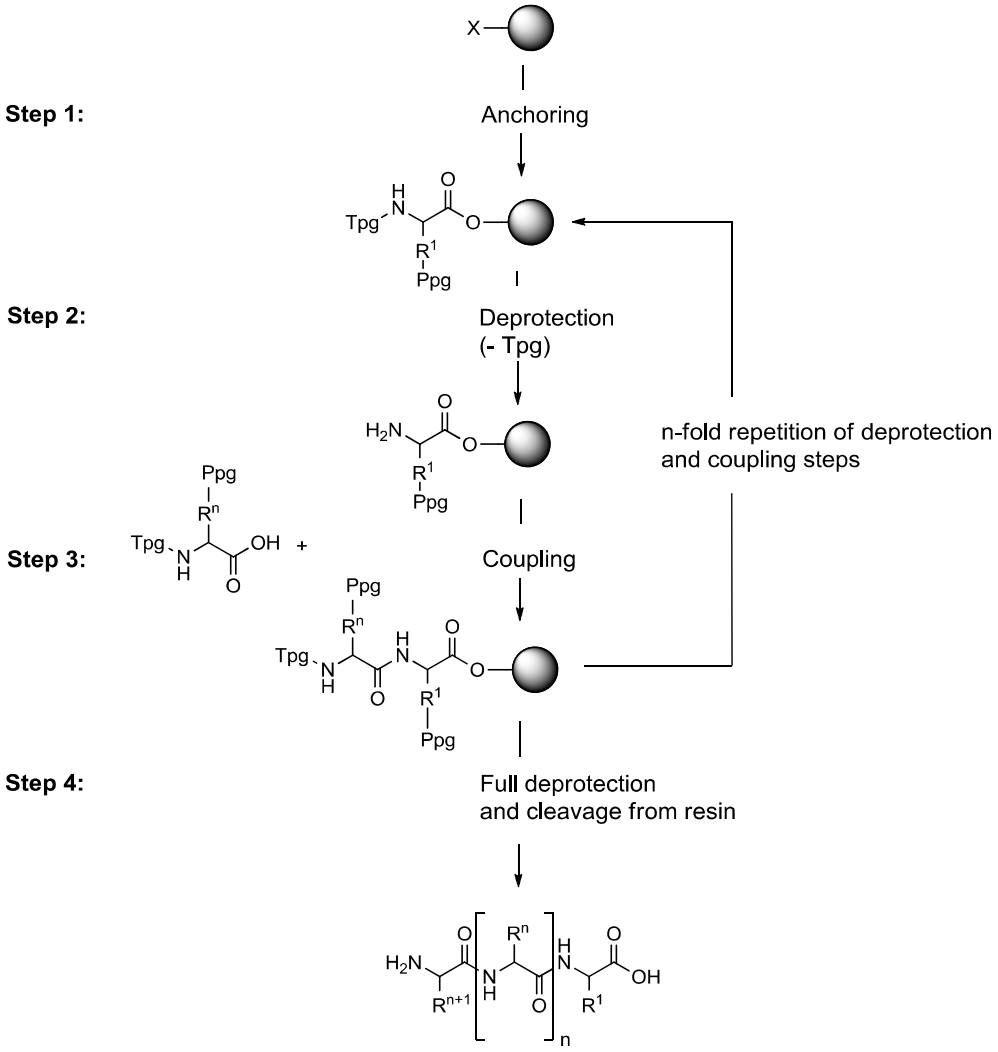

Figure 18: Process of solid phase peptide synthesis. Tpg = transient protecting group; Ppg = permanent protecting group; R = aa side chains; X = Cl

Thus, during the synthesis, the reaction products (i.e. intermediates or final product) remain covalently linked to the solid support during the whole synthesis, whereas by-products and the excess of coupling reagents are removed by filtration. This simple technical operation and the potential for automation of this "Merrifield synthesis" have revolutionized peptide chemistry.

The solid polymer support thereby plays a key role for a successful outcome of any SPPS. The polymeric support must fulfill several inevitable requirements. It has to be chemically inert, mechanically stable and completely insoluble in organic solvents, thereby allowing simple reagent separation by filtration. Moreover, it must comprise an appropriate

quantity of reactive sites to which the first C-terminal amino acid of the peptide is usually anchored. Finally, non-covalent interactions between the resin and the growing peptide chain should be as minimal as possible.

Similar to a carboxyl-protecting group, the resin linkage must be orthogonal to the transient protecting group utilized during synthesis and has to be stable under all employed chemical conditions throughout the whole synthetic process. Furthermore, cleavage under mild conditions without harming the fully assembled peptide backbone must also be possible. Commonly, a copolymer of polystyrene with 1% divinyl benzene as cross linker is used as a resin in SPPS. Therefore, the dry resin beads are normally 20-80 μm in diameter, and are capable to swell to its five- or six-fold volume in different organic solvents (e.g. DCM or DMF which are frequently used in SPPS). Thus, the polymeric resin after suspension in these solvents should not be considered as a static solid matrix but more as a well-solvated gel with mobile polymeric chains. This situation eases diffusional access of the reagents to all reaction sites. The heterogeneous reaction systems utilized in SPPS are typically two- or three-fold slower than comparable homogenous solution reactions.[91] The reaction sites are evenly distributed within the polymeric resin, and the reaction rates of the early coupling and deprotection steps are commonly similar to those at the end of a synthesis. The growing mass ratio of peptide/resin material does not regularly diminish the efficiency of further chain elongations, although the swelling performance in nonpolar solvents can be decreased.

The installation of anchoring groups on the polymeric resin is another pre-condition for their application in peptide synthesis. There are numerous different linker systems currently available for SPPS and solid-phase organic synthesis. As linkers must be considered as protecting groups for the *C*-terminal carboxyl group of the synthesized peptide, their design and implementation has to reflect these chemical properties. For example, different anchor groups are used if the *C*-terminus of the anticipated peptide should be obtained as a ’free’ carboxylate, a carboxamide or an alcohol. As for most peptide syntheses, a ‘free’ carboxylate C-terminus is required, the first amino acid is mostly connected to the resin via an ester bond.

3. AIMS OF THE PHD THESIS

The aim of this PhD thesis was the generation of small molecule modulators for functional chemical biology investigations in plants.

To this end, several approaches were followed. The main project of this thesis was focused on the chemical synthesis of bioactive plant growth-modulating natural products and their subsequent evaluation as potential chemical probes to decipher root growth biology. The acquisition of water and nutrients by plant roots is a fundamental aspect of agriculture and strongly depends on adequate root branching. The plant root system consists of a primary root originating from the plant embryo and of lateral roots, resulting in a branched root system to provide continuous access to new soil resources for nutrients and water. Within this thesis, new synthetic molecules that modulate the process of root development and that can be used as chemical probes should be discovered and characterized. To this end, a natural product approach was followed, i.e. derivatives of natural products with known plant growth modulatory properties were synthesized and derivatized for structure-activity relationship (SAR) -studies as a starting point for subsequent target identification studies.

Along these lines, a first total synthesis of Rotihibin A should be established. This lipopeptidic natural product features a vast array of non-proteinogenic amino acid (in fact, only one of the six amino acids is a regular proteinogenic amino acid) and this natural product was described in literature as a potent root-growth inhibitor in plants (*Fig 19*).[102] The synthesis should be conducted via solid phase supported synthesis after previous amino acid building block synthesis.

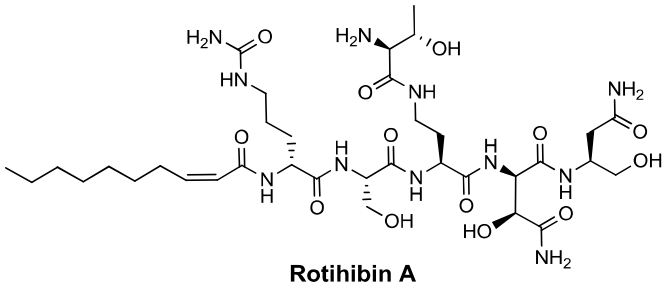

Figure 19: Chemical structure of the plant growth-modulating natural product Rotihibin A.

Subsequently, a whole series of derivatives should be synthesized to elucidate the underlying structure-activity relationships. To determine the bioactivity of these compounds, gene-reporter assays with transgenic plants should be carried out.

In a second project, related to the chemical synthesis of plant growth-modulating natural products, it was envisaged to synthesize a focused library of derivatives of the Brevicompanine natural product family (a class of reverse prenylated hexahydropyrrolo [2,3-*b*]indole alkaloids); these natural products were also reported as plant growth regulators. To this end, a focused library of Brevicompanine derivatives should be synthesized and used to study the structure-activity relationships and to get initial insights into the mode-of-action of this compound class (*Fig. 20*).[103; 104]

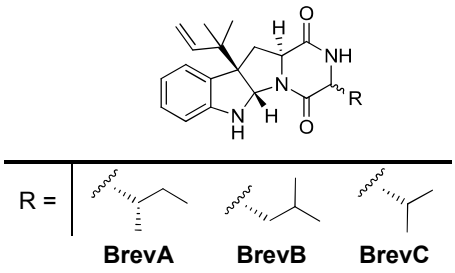

Figure 20: Chemical structures of Brevicompanine A, B and C.

In a third, slightly different project, novel activity-based probes should be synthesized to expand the scope of ABPP approaches in plants. To date, only a limited number of probes for this purpose are available and this subproject aims to expand the chemical toolbox into this direction. Therefore, in the first part of the thesis the outreach of acyl-phosphate probes, for profiling protein kinases and other ATP binding proteins in plants, should be expanded by directed synthesis of functional derivatives of a recently published biotinylated adenosine acyl phosphate probe.[105]

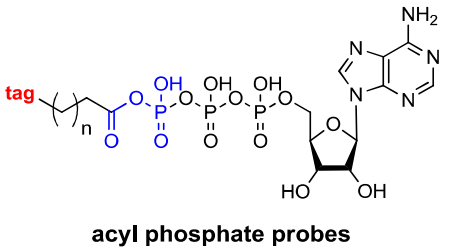

Figure 21: General structure of envisaged acyl phosphate probes. Probes are built up from ATP, an acyl phosphate warhead (blue), an alkyl linker and a reporter tag (red).

These probes represent an ATP-derivative which is modified with a reactive acyl phosphate group at the γ-phosphate followed by an appropiate reporter-tag (*Fig. 21*). This type of probes was previously shown to act by binding to the P-loop (phosphate binding domain) of ATP-binding proteins. At this binding site, it is cleaved by a conserved lysine residue, thereby inducing irreversible ATPase inhibition and transfer of a reporter group to the protein. The synthesized acyl phosphate probes should be utilized to launch a new approach to explore the ATP-binding proteome of the model plant *Arabidopsis thaliana*.

4. RESULTS AND DISCUSSION

4.1 Studies on Rotihibin A, a plant growth regulator from *Streptomyces graminofaciens*

In a screening campaign for plant growth regulators from bacterial origin, the group of Suzuki and coworkers found that a culture filtrate of *Streptomyces graminofaciens* (strain 3C02) inhibited the growth of lettuce seedlings. The strain 3C02 was isolated from a soil sample collected in Bunkyoku, Tokyo, Japan. Based on analytical data, the active substances were identified as lipo-peptidal compounds (*Fig. 22A*), named Rotihibin A (**1**) and B.[102; 106] Rotihibin A (**1**) is thereby by far the major bioactive secondary metabolite, while Rothibin B was isolated in only low amounts.

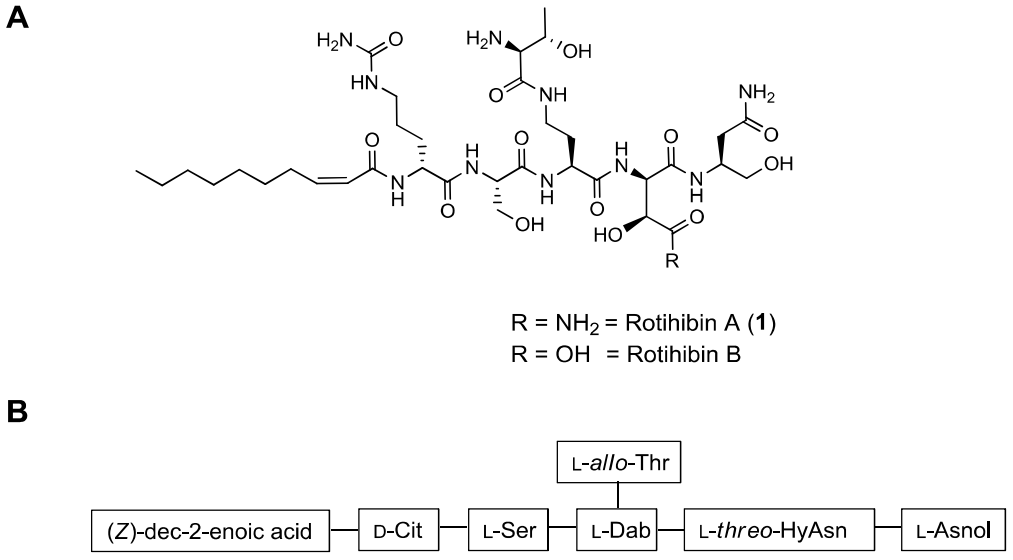

Figure 22: (A) Chemical structures of Rotihibin A (**1**) and Rotihibin B. (B) Schematic depiction of chemical components of Rotihibin A (**1**).

Lipopeptides (LPs) are characterized by a lipid tail linked to a short linear or cyclic oligopeptide. LPs represent a structurally diverse group of metabolites produced by various bacterial and fungal genera including for example *Aspergillus*, *Streptomyces* and

Pseudomonas.[107] LPs have received considerable attention for their antimicrobial, cytotoxic, antitumour, immunosuppressant and surfactant properties.

Intensive analytical studies including various NMR experiments and MS/MS analyses revealed that **1** is mainly build up from non-proteogenic, highly modified amino acids and amino alcohols including D-citrulline, L-diaminobutyric acid, L-*allo*-threonine, L-*threo*-*β*-hydroxyasparagine and L-amino-hydroxybutanamide (L-asparaginol) in addition to a lipophilic chain (*Z*)-dec-2-enoic acid and L-serine as the only common proteinogenic amino acid (*Fig. 22A, B*).[106] The high ratio of non-proteinogenic amino acids within Rotihibins suggests that the biosynthesis of these compounds could be non-ribosomal as it is already known for several other lipopeptides like surfactin[108] or fengycin[109]. In fact, most LPs are biosynthesized by large nonribosomal peptide synthetases (NRPSs) via a thiotemplate process.[110]

Interestingly and in contrast to other LPs, Rotihibin A (**1**) displayed no relevant antimicrobial activity against several bacterial and fungal strains.[106] Although many LPs from microbial origin furthermore show antitumor activities, Rotihibin A (**1**) also did not demonstrate any effect on mammalian cells. In contrast, **1** was reported to display a strong bioactivity on plants. In particular, Rotihibin A (**1**) inhibited the root growth of lettuce seedlings at a dose of 1-2 ppm (1-2 µg/ml), while Rotihibin B was significantly less active. Rotihibin A (**1**) application was however not lethal up to a concentration of 150 ppm (150 µg/ml). Moreover, Rotihibin A-treated plants were reported to recover to their normal growth after they were transferred into fresh media lacking **1**.[106]

Since Rotihibin A (**1**) was found to be the major and most active metabolite, the focus of the following synthetic work and biological assessment was therefore put on Rotihibin A (**1**). To the best of our knowledge, no synthesis of Rotihibin A (**1**) has been reported so far.

4.1.1 Synthetic considerations towards Rotihibin A

In contrast to a laborious solution synthesis, a more straightforward solid-phase strategy that also enables easy derivatization of Rotihibin A (**1**) was envisioned. For the synthesis of Rotihibin A (**1**), a solid phase Fmoc-based strategy was envisaged. To this end, an orthogonal protection group strategy was designed involving various protection groups that enabled the usage of three different complementary deprotection procedures.

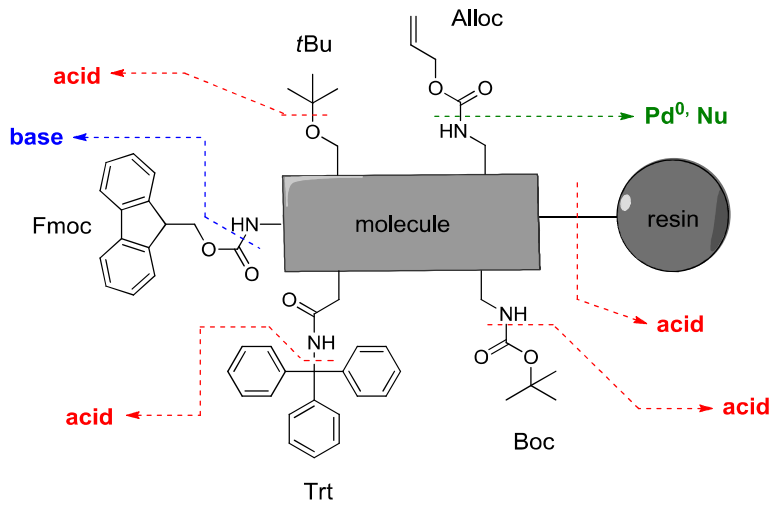

Figure 23: Schematic representation of the employed protection group strategy for SPPS of Rotihibin A (**1**). Red arrows: acid labile protecting groups (*t*Bu = *tert*-butyl; Trt = triphenyl methyl; Boc = *tert*-butoxycarbonyl; resin = 2-chlorotrityl chloride resin), blue arrow: base labile protecting group (Fmoc = 9-Fluorenylmethyl-oxycarbonyl), green arrow: Pd^0 mediated cleavage (Alloc = Allyloxycarbonyl).

As the transient protecting group for the primary α-amine of the *N*-terminus of each amino acid building block, the base-labile Fmoc (9-fluorenylmethyloxycarbonyl)-protecting group was chosen (*Fig 23*). The Fmoc method allows for a mild deprotection procedure, which uses basic conditions, usually 20% piperidine in DMF for removal the Fmoc group.[100] In contrast to acid labile protecting group such as Boc, the basic cleavage of Fmoc leads to neutral amine residues and no additional neutralization of the peptide-resin is necessary. The Fmoc group is stable towards acidic conditions and is removed via base-induced β-elimination. The removal of the transient α-amine protecting group (Fmoc) under mild basic conditions therefore enabled the simultaneous use of acid-labile protecting groups, such as *t*Bu, Boc and trityl (permanent protection groups) as protecting groups for side-chain protection of functional groups. Consequently, the permanent protection groups guarding side chain functionalities were orthogonal towards the stability of the transient α-amine protection group. This orthogonal protecting group strategy is common in organic synthesis.

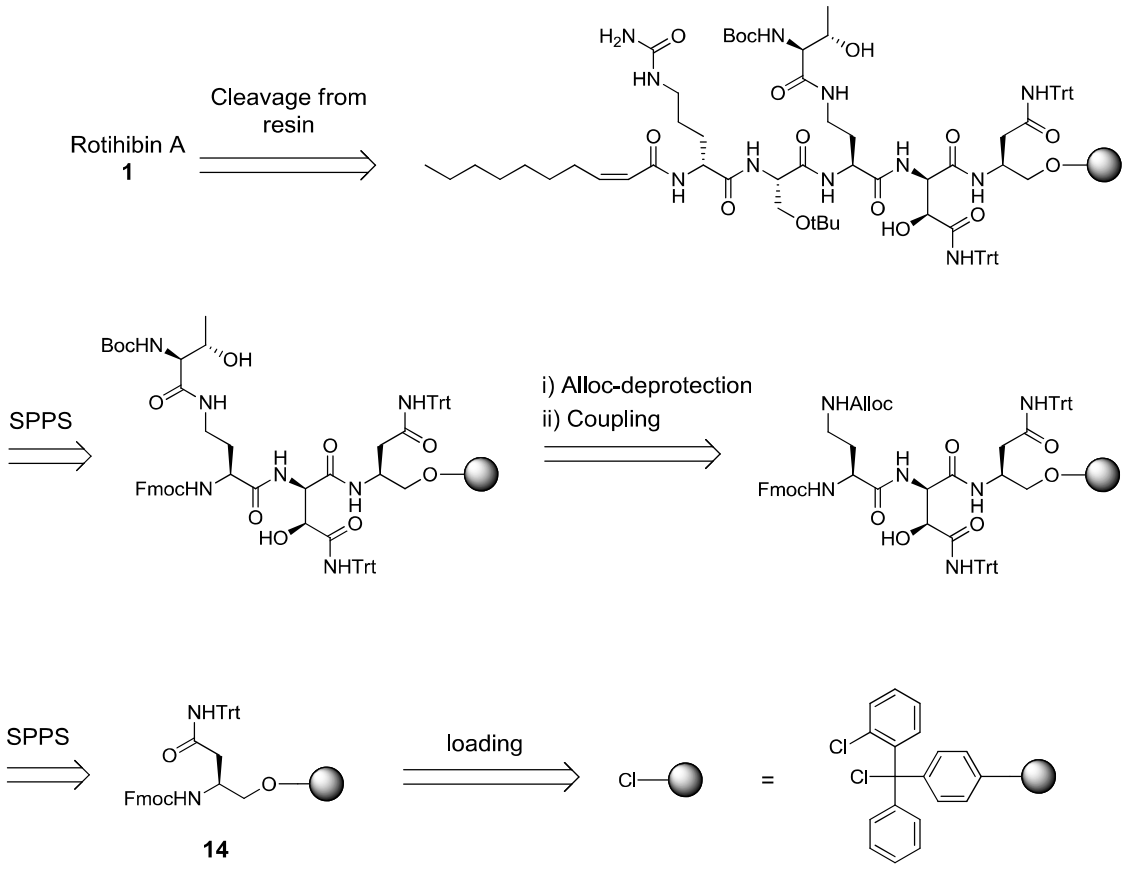

Figure 24: Projected synthetic route towards Rotihibin A (**1**).

The installation of Boc-L-*allo*-threonine on the *γ*-amine of the diaminobutyric acid side chain required a third orthogonal protection group, which needed to be stable towards acidic and basic conditions (*Fig. 23*). For that reason, the Alloc protecting group was chosen. This protecting group is removed by a palladium-mediated (usually $Pd(PPh_3)_4$) transfer of the allyl unit to nucleophiles such as morpholine and is therefore mechanistically different (and orthogonal) to basic and acidic deprotection conditions.

As the natural product Rotihibin A (**1**) features an amino alcohol on its C-terminus, a direct anchoring of such an alcohol represents the most convenient method for immobilizing of the peptide to the solid support. To allow this, the resin needed to have a suitable functionality that allows the attachment of a primary alcohol as well as feature acid lability to enable deprotection of the permanent protecting groups and cleavage from the resin in one single step. Thus, a 2-chlorotrityl chloride resin was selected, which is known to enable on the one hand the anchoring of primary alcohols and on the other the cleavage under acidic conditions.

Before starting with the final total solid phase synthesis (*Fig. 24*) of Rotihibin A (**1**), the amino acid building blocks equipped with suitable protecting groups first have to be available. The corresponding amino acid derivatives are shown in Figure 25.

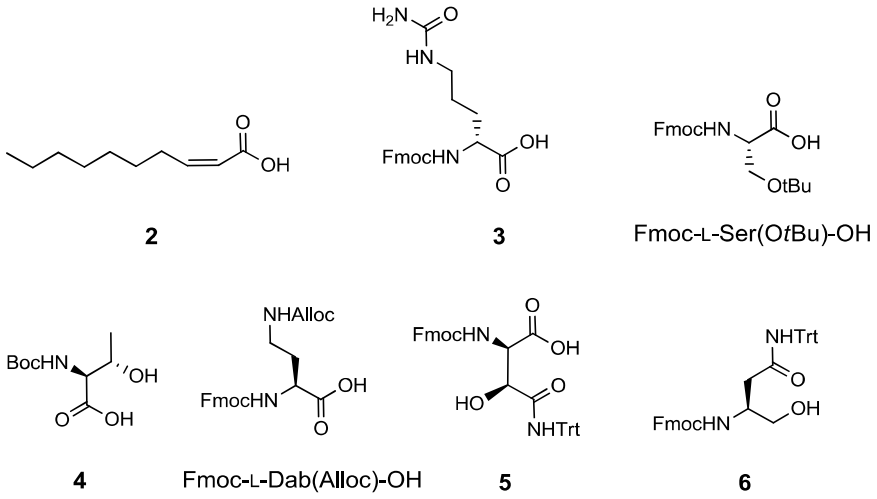

Figure 25: Chemical structures of the required building blocks for the solid-phase synthesis of Rotihibin A (**1**) via Fmoc-based strategy.

From these different amino acid derivatives, only Fmoc-L-Ser(OtBu)-OH and Fmoc-L-Dab(Alloc)-OH were commercially available. The remaining building blocks were chemically synthesized as descripted in the following paragraph.

4.1.2 Synthesis of required building blocks

- **Synthesis of (*Z*)-dec-2-enoic acid (2):**

The lipophilic tail in Rotihibin A (**1**) features a *Z*-configured *α,β*-unsaturated carboxylic acid entity. For the preparation of this building block **2**, classical carbonyl olefination reactions were considered and the HORNER-WADSWORTH-EMMONS (HWE) variation of the WITTIG olefination that is a commonly used reaction for the preparation of *α,β*-unsaturated esters was chosen.[111] To this end, phosphonates such as methyl phosphonoacetates are deprotonated with strong bases. The resulting phosphonate anions are strongly nucleophilic and react readily with carbonyl compounds under mild conditions. Nevertheless, this reaction preferentially gives more stable *E*-olefins.[112] Still and Gennari have however developed a modification of

this olefination reaction that provides access to *Z*-alkenes with excellent stereoselectivity.[113] To this end, phosphonates with electron-withdrawing groups such as trifluoroethyl residues and strongly dissociated base systems like NaH or KHMDS are used which enables the preparation of nearly exclusive *Z*-alkenes. The *Z*-alkene is preferably formed because the reaction proceeds through a sterically less hampered and thus thermodynamically more stable (*erythro*) transition state.

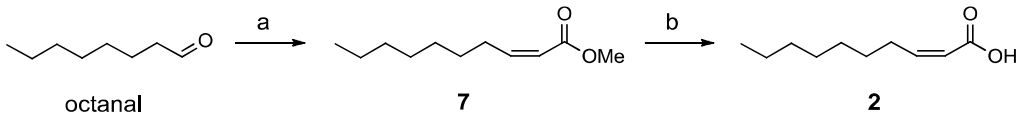

Scheme 1: Preparation of (*Z*)-dec-2-enoic acid (**2**). (a) Methyl-*P,P*-bis(2,2,2-trifluoroethyl)phosphonoacetate, NaH, THF, -78°C, 1 h, 90%. (b) LiOH, H_2O, THF, MeOH, 0°C→50°C, 5 h, 98%.

The synthesis of **2** therefore started with commercially available octanal which was converted through methyl-*P,P*-bis-(2,2,2-trifluoroethyl)-phosphonoacetate into the *α,β*-unsaturated methyl ester **7** with the desired (*Z*)-configuration (*Scheme 1*). The formation of the (*Z*)-configuration was confirmed by an examination of the corresponding coupling constants in the ^{1}H-NMR spectrum. Finally, the methyl ester **7** was hydrolyzed with aqueous lithium hydroxide, thereby yielding the desired building block (*Z*)-dec-2-enoic acid (**2**).

- **Synthesis of Fmoc-D -Cit-OH (3) and Boc-L-*allo*-Thr-OH (4)**

The preparation of Fmoc-D-Cit-OH (**3**) and Boc-L-*allo*-Thr-OH (**4**) was easily accomplished by protecting the corresponding free amino acids with Fmoc-OSu and Boc_2O, respectively (*Scheme 2*).[114] Synthesis of both building blocks (**3**, **4**) occurred smoothly without any special incidents and they were subsequently used for the solid phase synthesis of Rotihibin A (**1**).

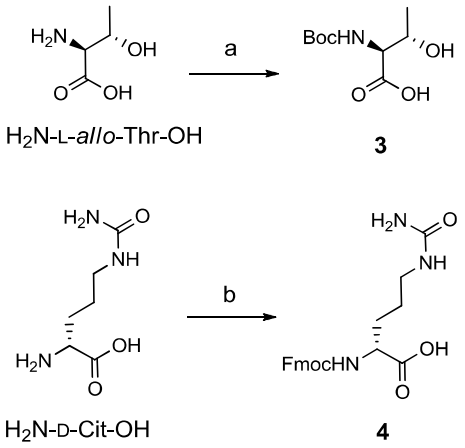

Scheme 2: Synthesis of building blocks **3** and **4** (a) Boc_2O, $NaHCO_3$, H_2O/dioxane, 0°C→rt, 16 h, 93%. (b) Fmoc-OSu, $NaHCO_3$, H_2O/dioxane, 0°C→rt, 16 h, 85%.

- **Synthesis of orthoganally protected L-*threo*-*β*-hydroxyasparagine (5)**

The preparation of the non-proteogenic L-*threo*-*β*-hydroxyasparagine derivative (**5**) that was fully compatible with Fmoc-solid phase synthesis was a key step in the synthesis of Rotihibin A (**1**). A few methods for the preparation of L-*threo*-*β*-hydroxyasparagine have been described in the literature.[115; 116; 117; 118] We first compared three of these strategies to gain on overview which one would be best suited. As the required building block was needed in rather large quantity, we particularly considered the overall yield and the temporal effort for its synthesis. A short overview of the selected literature reports is given below.

A synthesis of othoganally protected L-*threo*-*β*-hydroxyasparagine was reported from Cardillo and Guzmán-Martinez.[115; 118] It is based on the regioselective deprotonation of *N*-benzoyl dimethylaspartate at the *β*-position, followed by a diastereoselective iodocyclization for generation of a *trans*-oxazoline. Acidolytic hydrolysis of this *trans*-oxazoline in 6 N HCl under reflux then yields the L-*threo*-hydoxyaspartate **8**. The published synthetic protocol also included the attachment of the protecting groups, i.e. the transformation of **8** to the desired building block **5**, which was achieved in 8 steps and an overall yield of 22% (*Fig. 26*).[118] .

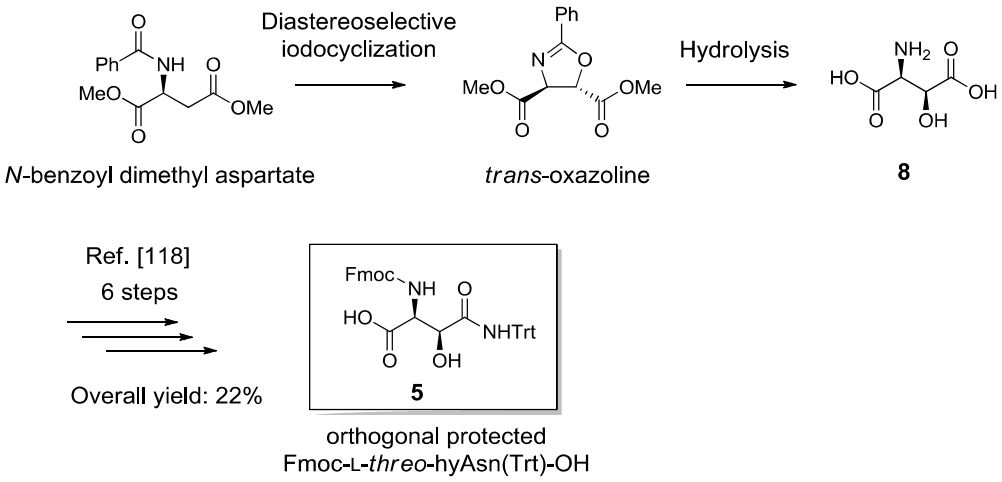

Figure 26: Synthesis of orthogonally protected L-*threo*-hyAsn as developed by Cardillo and Guzmán-Martinez.[115; 118]

An alternative synthesis was developed by Boger and coworkers.[116] In their approach, the proper stereochemistry was introduced through a SHARPLESS asymmetric aminohydroxylation (AA) of a 4-methoxycinnamate methyl ester (*Fig. 27*).[119]

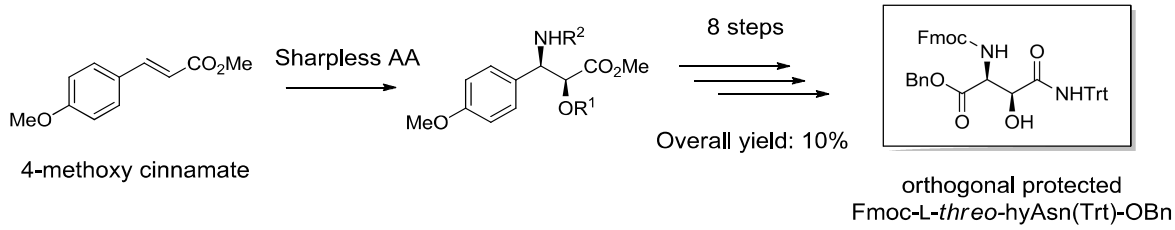

Figure 27: Synthesis of orthogonally protected L-*threo*-hyAsn as developed by Boger *et al.*[116]

The synthesis by Boger and coworkers comprises as a key step a SHARPLESS AA followed by various protection groups exchanges, amidation of the γ-carboxylate residue and oxidation of the aromatic system to a *C*-terminal carboxylic acid using ruthenium tetraoxide. In total, this synthesis consists of nine synthetic steps with an overall yield of 10%.

A third synthetic route was developed by Bionda and coworkers.[117] This approach includes an enantioresolution of commercial available racemic D,L-*threo*-hydroxyaspartate to yield enantiomerically pure L-*threo*-hydroxyaspartate. The subsequently required decoration of **8** with appropriate protecting groups can be achieved by adapting the synthetic route of Guzmán-Martinez (*Fig. 28*).[118]

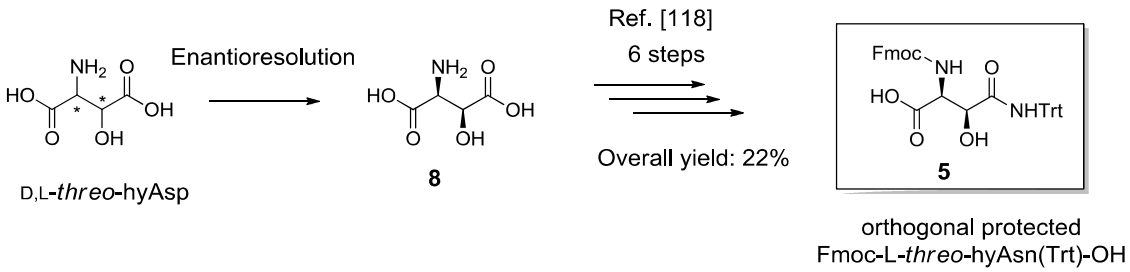

Figure 28: Synthesis of orthogonally protected L-*threo*-hyAsn as developed by Bionda and Guzmán-Martinez.[117; 118]

A comparison of these different routes (*Table 2*) reveals that the combined synthesis from Bionda and Guzmán-Martinez should be the most efficient one, featuring seven synthetic steps in total and a calculated overall yield of 22%.

Table 2: Comparison of three published syntheses towards **5**.

Reference	Total steps	Overall yield
[115] + [118]	8	22%
[116]	9	10%
[117] + [116]	7	22%

Therefore, the synthetic route was put into practice as illustrated in Scheme 3. First, an enantioresolution of commercially obtained D,L-*threo*-hydroxyaspartate by co-crystallization with an equimolar amount of salt-free L-lysine was performed and resulted in a precipitation of enantiomerically pure L-*threo*-hyAsp*L-Lys salt from a solvent mixture of water and methanol, whereas D-*threo*-hyAsp*L-Lys remained in the mother liquor. The precipitated crystals were isolated by filtration and L-lysine was subsequently removed by ion exchange chromatography yielding pure L-*threo*-hyAsp (**8**).

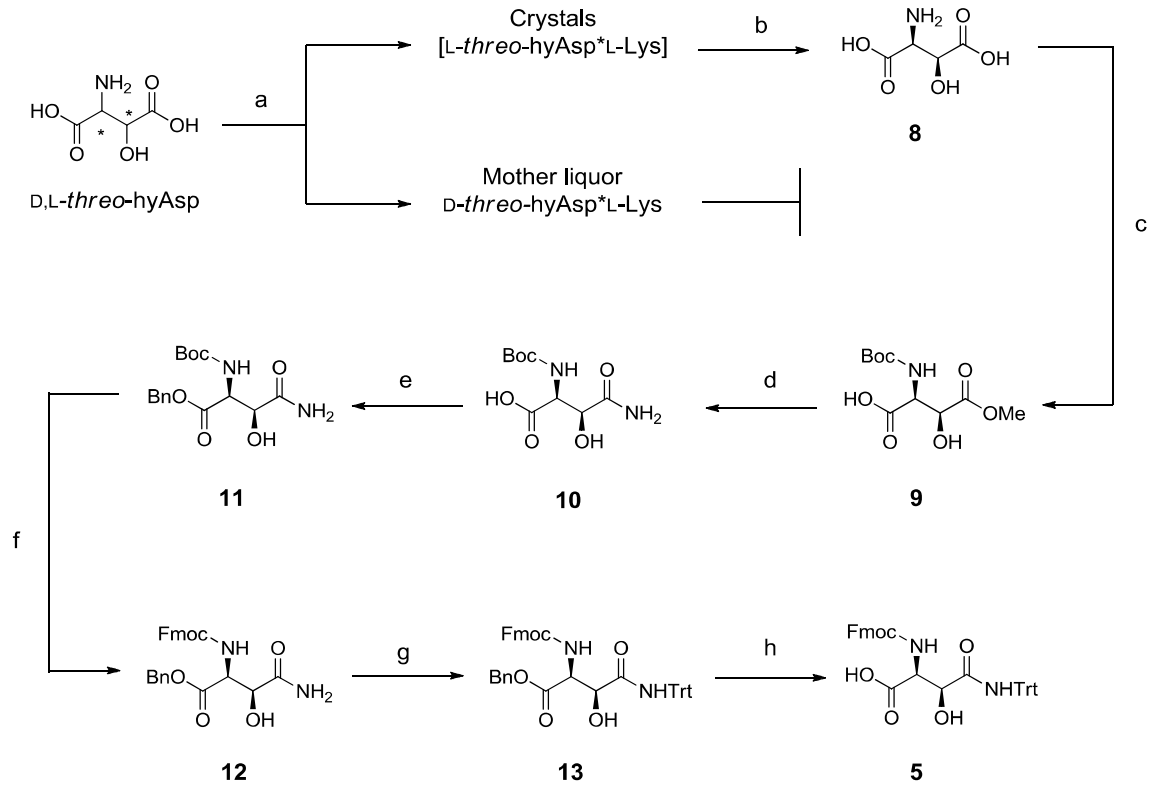

Scheme 3: Synthetic route towards orthogonally protected L-*threo*-*β*-hydroxyasparagine **5**. (a) L-lysine, H_2O, MeOH, 40°C→4°C, o.n. (b) ion exchange chromatography using DOWEX 1x4-50, eluent: 2 M AcOH, 63% (over 2 steps). (c) i) HCl, MeOH, reflux, 3 h, ii) Boc_2O, 10% Na_2CO_3, dioxane, 0°→rt, o.n., 98%. (d) 7 N NH_3 in MeOH, rt, 4 d, 98%. (e) BnBr, $NaHCO_3$, DMF, 0°C→rt, 24 h, 66%. (f) i) 4 N HCl in dioxane, rt, 2 h, ii) Fmoc-OSu, $NaHCO_3$, dioxane, H_2O, 0°C→rt, o.n., 98%. (g) Trt-OH, H_2SO_4 (cat.), Ac_2O, AcOH, 50°C, 2.5 h, 74%. (h) 1 atm. H_2, Pd/C, EtOH, rt, 1 h, 76%.

In the following two-step sequence, L-*threo*-*β*-hydroxyaspartatic acid (**8**) was first treated with methanolic hydrogen chloride to give the side chain mono-methylester followed by a treatment with di-*tert*-butyl dicarbonate to protect the *N*-terminus, thereby yielding the Boc-protected mono-methylester **9**. Subsequent aminolysis of **9** using 7 N ammonia in methanol provided the carboxamide **10**. The carboxyl group at the *C*-terminus of **10** was transferred into the corresponding benzyl ester **11** using benzyl bromide and standard alkylation conditions. At this point, the required protection group exchange of the *N*-terminal protection group was performed. Hence, compound **11** was deprotected with 4 N hydrogen chloride in dioxane and reprotection of the free amine group was achieved using Fmoc-OSu and aqueous sodium bicarbonate in dioxane yielding the Fmoc-protected benzyl ester **12**. As unprotected carboxamide groups of asparagine residues are susceptible to side reactions during peptide couplings (e.g. deamidation, L-succinimidyl formation etc.),[120] the carboxamide was

subsequently protected with a trityl protecting group. To this end, **12** was treated with triphenylmethanol and catalytic amounts of sulfuric acid in a mixture of acetic anhydride and acetic acid, thus providing compound **13**. Finally, hydrogenolysis of benzyl ester **13** was performed. Therefore, **13** was hyrdogenated with a palladium/coal catalyst under an hydrogen atmosphere which led to the desired target compound L-*threo*-Fmoc-*β*-hyAsn(Trt)-OH (**5**) in an overall yield of 22%.

- **Synthesis of Fmoc-Asnol(Trt) (6)**

The preparation of the 1,2-amino alcohol **6** was easily conducted in one step via reduction, using as a start material commercially available Fmoc- and trityl-protected asparagine (*Scheme 4*).

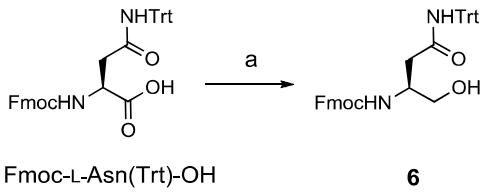

Scheme 4: Synthesis of building block **6**. (a) IBCF, NMM, THF, H_2O $NaBH_4$, -10°C, 0.5 h, 94%.

Reduction of a carboxyl group of *N*-protected amino acids to an alcohol function is known to be possible by sodium borohydride reduction of a mixed anhydride intermediate in THF. Therefore, the *N*-protected amino acid was first reacted with *iso*butyl chloroformate to form the mixed anhydride; next, sodium borohydride was added, thereby reducing the latter to the corresponding primary alcohol **6** which was used as a building block in the solid phase synthesis of Rotihibin A (**1**).

4.1.3 Total synthesis of Rotihibin A

With all building blocks in hands, the first total solid phase synthesis of Rotihibin A (**1**) was then established and conducted according to Scheme 5. To this end, commercially available chloro-2-chlorotrityl resin with an initial loading of 0.3 mmol/g was manually loaded with the amino alcohol **6**. Since primary alcohols are more difficult to deprotonate than carboxylic acids (which are more often loaded on such resins), a suitable base was required for the loading reaction. Conseqently, the loading was conducted using an excess of amino alcohol **6** and pyridine as a base resulting in an attachment of the amino alcohol to the solid phase via an ether bond. The loading reaction was terminated after 16 h by adding methanol to remove any remaining reactive chlorine-functionalities. An Fmoc-loading assay subsequently revealed that this procedure resulted in a loading of 0.3 mmol/g (loading yield of 25%) which is well within the range of comparable amino alcohol loadings.[121]

The loaded resin **14** was then used for the stepwise manual assembly of the natural sequence of Rotihibin A (**1**). Correspondingly, the transient *N*-terminal Fmoc-protection group was cleaved via base induced *β*-elimination using the standard procedure. The amide couplings of the following two building blocks were then performed using standard coupling reagents (HBTU, HOBt, DIPEA) with a Fmoc-cleavage in between. For the installation of Boc-L-*allo*-threonine (**3**) onto the Dab side chain, the Alloc-side chain protecting group had to be removed first. This was achieved by $Pd(PPh_3)_4$ as a catalyst and morpholine as a scavenging nucleophile; the reaction was furthermore performed in degassed dichloromethane under an inert atmosphere. In order to remove the catalyst after the reaction, a more stringent washing procedure was required after Alloc-cleavage. The following iterative assembly of the next four building blocks was once more performed via standard coupling conditions (and in between Fmoc-cleavage) and yielded the fully assembled resin-bound peptide. Treatment of the resin-bound peptide with TFA (95%) then cleaved all permanent side chain protecting groups as well as the relase from the resin. Such strong acidic conditions for final cleavage were necessary since the ether bond is more acid-resistant than the more often used ester bond linkage which can already be cleaved by acetic acid. The mixture was filtrated, diethyl ether was added to precipitate the crude lipo-peptide and the residue isolated and purified by preparative RP-HPLC purification.

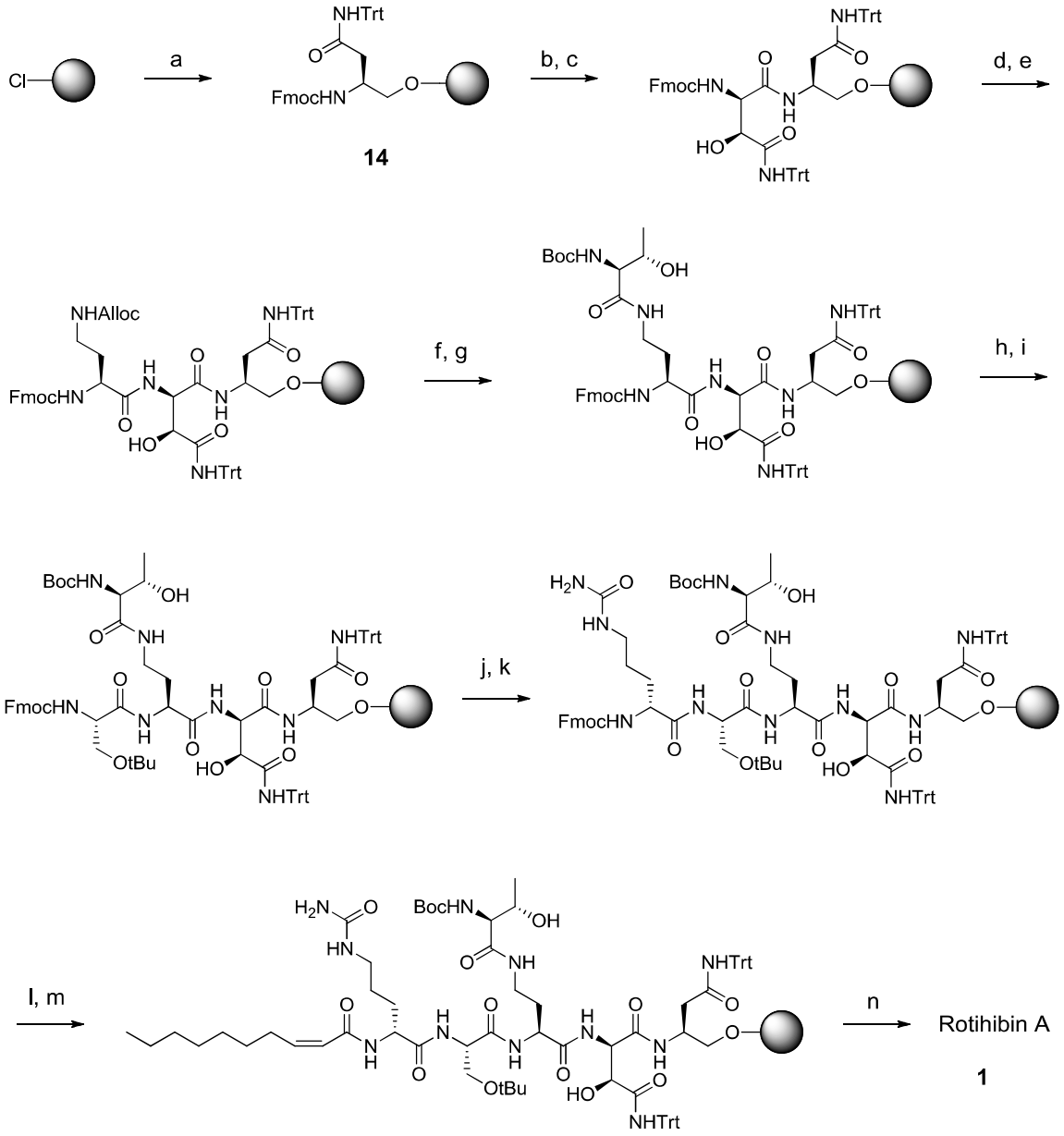

Scheme 5: Total solid phase supported synthesis of Rotihibin A (**1**). (a) i) **6**, pyridine, DCM, rt, 16 h, 25%. ii) MeOH, rt, 30 min. (b) 20% piperdine in DMF, rt, 2 x 15 min., (c) **5**, HBTU, HOBt, DIPEA, DMF, rt, 2 h. (d) 20% piperdine in DMF, rt, 2 x 15 min., (e) Fmoc-Dab(Alloc)-OH, HBTU, HOBt, DIPEA, DMF, rt, 2 h. (f) $Pd(PPh_3)_4$, morpholine, DCM, rt, 1.5 h. (g) **4**, HBTU, HOBt, DIPEA, DMF, rt, 2 h. (h) 20% piperdine in DMF, rt, 2 x 15 min., (i) Fmoc-Ser(O*t*Bu)-OH, HBTU, HOBt, DIPEA, DMF, rt, 2 h. (j) 20% piperdine in DMF, rt, 2 x 15 min., (k) **3**, HBTU, HOBt, DIPEA, DMF, rt, 2 h. (l) 20% piperdine in DMF, rt, 2 x 15 min., (m) **2**, HBTU, HOBt, DIPEA, DMF, rt, 2 h. (n) TFA, TIS, H_2O, rt, 2 h, 31% overall yield.

All recorded analytical data matched to those of isolated Rotihibin A (**1**), thus proving that the total synthesis of this natural product was successfully established in eight total steps. After purification, a single product was obtained with an overall yield of 31%, (based on the initial loading of 0.3 mmol/g) and the identity of this compound was established by mass

spectrometry and NMR experiments (*Fig. 29*). All recorded analytical data matched to those of isolated Rotihibin A (**1**), thus proving that the total synthesis of this natural product was successfully established in eight total steps.

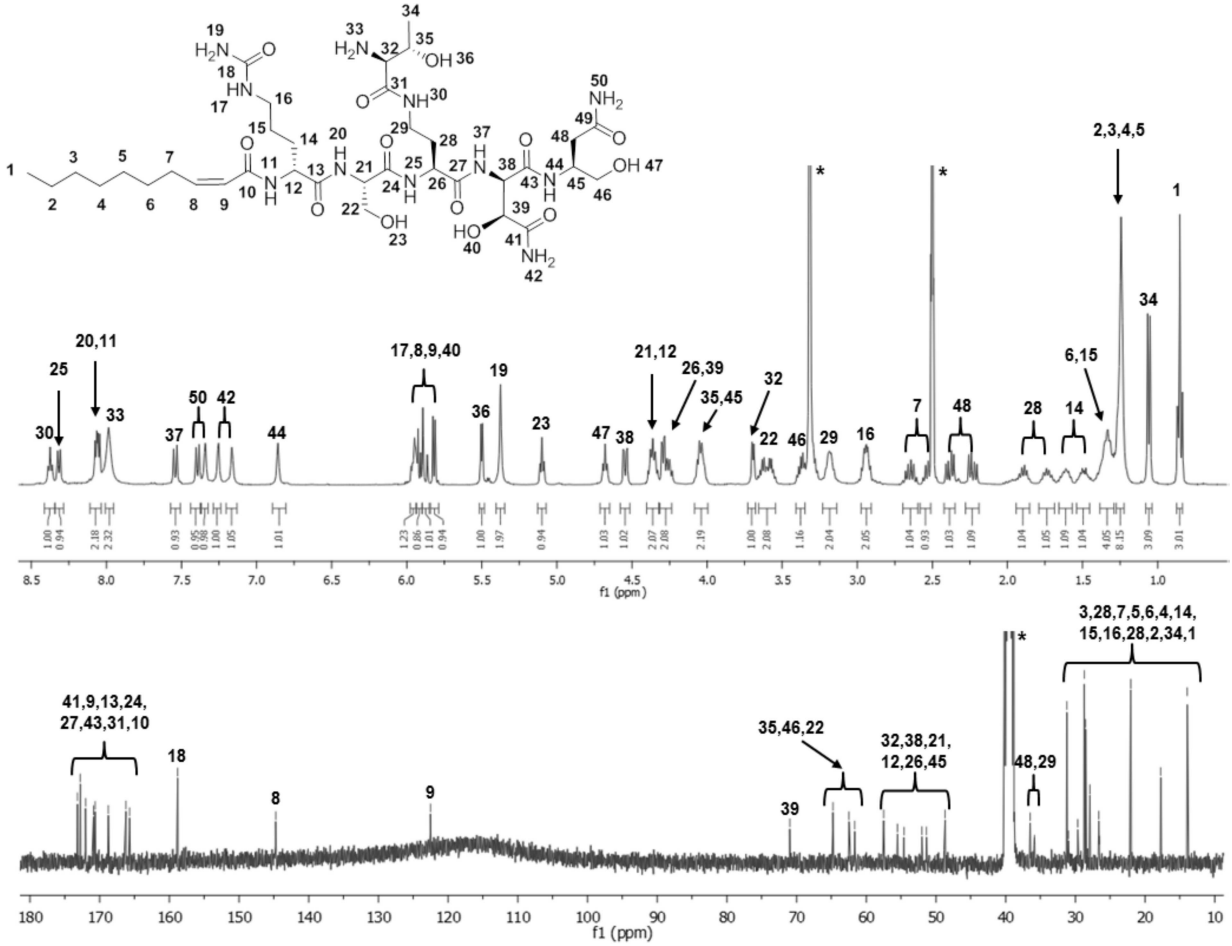

Figure 29: ^{1}H- and ^{13}C-NMR spectra of Rotihibin A (**1**) and assignment of the signals in accordance with Suzuki and coworkers.[106] (Astericks indicate solvent residual peaks of DMSO and H_2O)

4.1.4 Synthesis of Rotihibin A derivatives for SAR studies

By application of the antecedent synthesis route, a straightforward access to Rotihibin A analogues was also possible via simple exchange of building blocks (Scheme 6).

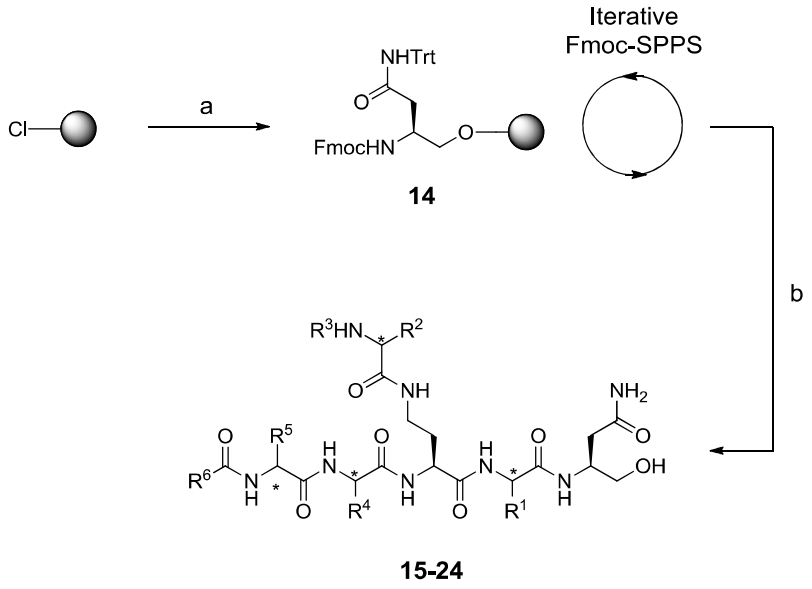

Scheme 6: Synthesis of Rotihibin A derivatives using the previously established synthetic conditions (cf. *Scheme 5*). (a) i) **6**, pyridine, DCM, rt, 16 h, 25%. ii) MeOH, rt, 30 min. (b) TFA, TIS, H_2O, rt, 2 h. R^1-R^6 = cf. *Table 3*.

Different derivatives were generated to investigate which residues (R^1-R^6) were essential for the observed biological activity and thus to gain insight into the underlying structure-activity-relationships (SAR). As a side effect, these studies also allowed to elucidate which positions of Rotihibin A are amenable for modification, thereby offering suggestions for the design of a Rotihibin A-derived activity-based probe for identification of its cellular targets.

One exciting modification was the replacement of the *α,β*-unsaturated fatty acid tail by a saturated lipophilic tail (**15**). *α,β*-Unsaturated carboxamides are principally susceptible to 1,4-MICHAEL-type additions by nucleophiles such as for example active site cysteine residues, thus potentially leading to a covalent reaction product; this substitution was therefore performed to test if Rotihibin A potentially acts via an irreversible, covalent mechanism.

The modification of compound **16** was the inversion of the stereogenic center at the *α-C* position of the citrulline residue to explore whether the stereochemistry at this position is required for the biological activity (*Table 3*).

Table 3: Chemical structures of synthesized derivatives **15-24**. Structural modifications to the natural product Rotihibin A are highlighted in red (in **17**, **22** and, **24**, one amino acid has been left out).

Chemical structures of derivatives 15-24	
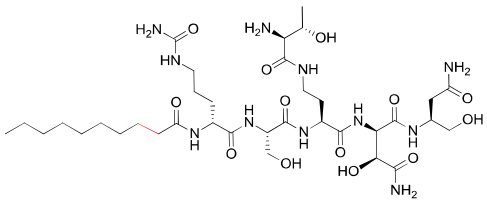 **15**	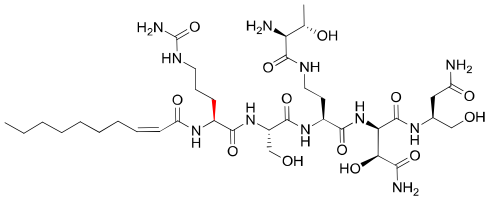 **16**
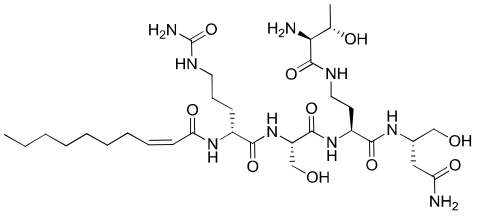 **17**	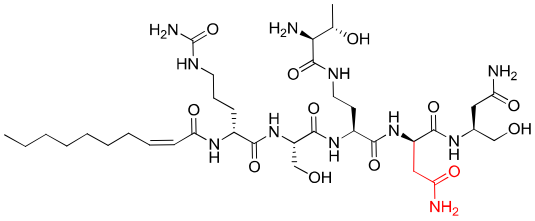 **18**
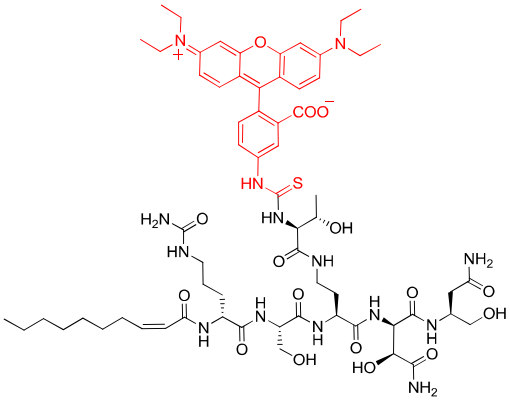 **19**	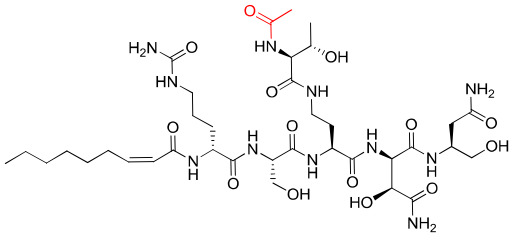 **20**
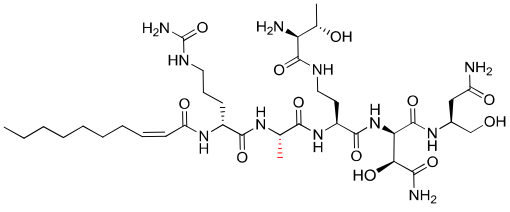 **21**	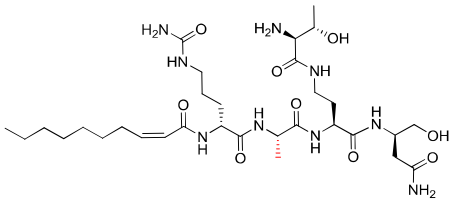 **22**
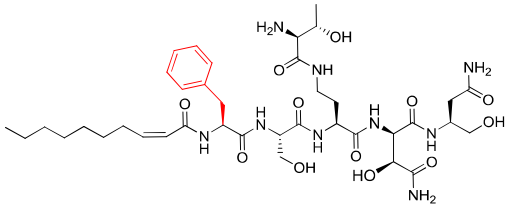 **23**	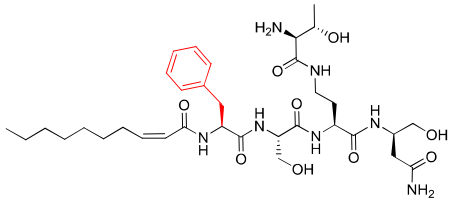 **24**

The derivatives **17** and **18** were synthesized to examine the impact of the unusual *β*-hydroxyasparagine residue for biological activity. Consequently, in compound **17** the *β*-hydroxyasparagine was not incorporated into the final sequence. In compound **18**, the *β*-hydroxyasparagine residue was substituted by the standard proteogenic L-asparagine residue and thus was bearing no *β*-hydroxy group on this position. It is known, that additional hydroxyl groups at the *β*- or *γ*-position of amino acids could mimic the tetrahedral transition state during the hydrolysis of peptide bonds.[122] Therefore, it is of great interest to examine the biological task of this particular structural element.

The derivatives **19** and **20** were generated by modifying the primary amine of the L-*allo*-threonine residue from Rotihibin A (**1**). Since the free *N*-terminus of the L-*allo*-threonine is the only primary amine residue in Rotihibin A (**1**), this particular reactivity could be easily exploited to react selectively with either acetic anhydride (thus yielding the acetyl derivative **20**) or rhodamine-isothiocyanate (to obtain the fluorophore tagged derivative **19**). These modifications allowed to explore the relevance of the primary amine for bioactivity. Furthermore, the rhodamine-tagged derivative **19** could be used for imaging studies if it retained its bioactivity.

Compounds **21** and **22** were generated to probe the function of the L-serine residue in Rotihibin A (**1**). These compounds featured a standard L-alanine residue instead. As serine is an amino acid known to be often post-translational modified, e.g. by phosphorylation, it was interesting to study its significance for bioactivity. In derivative **22**, this substitution was furthermore accompanied by a deletion of the *β*-hydroxyasparagine residue.

Finally, the biological significance of the amino acid D-citrulline was investigated. Thus compound **23** was synthesized in which D-citruline was substituted by the bulky aromatic amino acid L-phenylalanine. In compound **24**, this substitution was furthermore complemented by a deletion of L-*threo*-*β*-hydroxyasparagine.

4.1.5 Biological evaluation of Rotihibin A and derivatives thereof

4.1.5.1 Growth inhibitions studies with *Arabidopsis* seedlings

The biological evaluation was conducted in close collaboration with the Kombrink group (MPI for Plant Breeding Reseach in Cologne). First, biological experiments were performed

to confirm that synthetic Rotihibin A (**1**) displayed the reported bioactivities. As *Arabidopsis thaliana* is the best-established model organism in plant science and due to the fact that there are many mutants of this organism available, this plant system was chosen for the biological evaluation.[123]

The general phenotype of Rotihibin A (**1**) treated *Arabidopsis* seedlings were manifested in a universal retarded plant growth (*Fig. 30*). This was particularly noticeably in a delayed growth behavior of the cotyledons as well as in a hampered growth of the primary root. Besides this, a reduced number of lateral roots were also observed. Therefore, the observed phenotype matched with the reported root growth impairment.

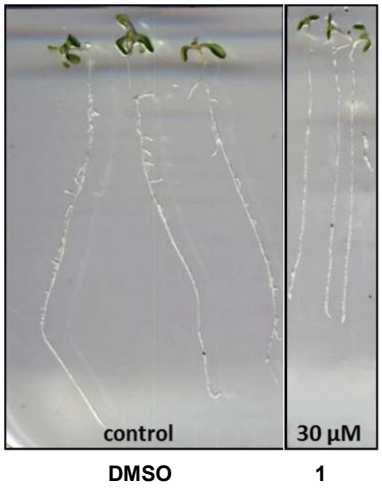

Figure 30: Phenotypic response of *Arabidopsis* seedlings ecotype Col-0 WT towards 30 µM of Rotihibin A (**1**).

Consequently, the corresponding plant growth phenotypes were also determined for all other derivatives **15-24**. To this end, *Arabidopsis* seedlings were grown in well plates containing media with various concentrations of derivatives **15-24**. Ten days after germination (DAG), the size of the cotyledons, the primary root length (PRL) and the lateral root density (LRD) were microscopically assigned. The size of the cotyledons of *Arabidopsis* seedlings in response to different concentrations of all derivatives **15-24** is depicted in Figure 31. The cotyledon size of the seedlings treated with Rotihibin A (**1**) is decreasing when probe concentrations are increased. At 100 µM of **1**, the average size was reduced to approximately 20% of the size of untreated seedlings. For compound **15** together with **16**, **17**, **18**, **19, 20, 22** and **24**, a weaker effect was observed. Although also these compounds show a decreased cotyledon size at higher concentrations, the absolute size shrinkage was much less. In contrast, a substantial decline of the cotyledon size was also observed for compound **21**. Already at a concentration of 10 µM of **21**, the cotyledon size was shrinking to 30% in

comparison to the control (DMSO). **21** showed an even stronger effect than the actual natural product Rotihibin A (**1**). Compound **23** also displayed the expected dose-activity relationship and at a concentration of 100 µM, the cotyledon size was reduced around 80% compared to the size of the control experiment. In contrast, the closely related compound **24** showed no significant effect.

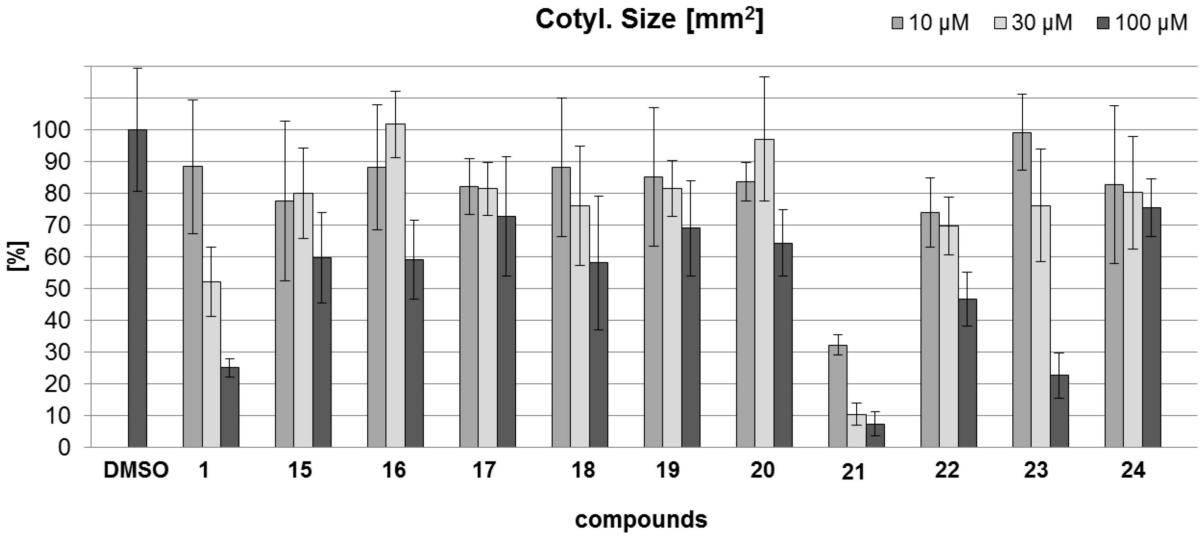

Figure 31: Cotyledon size of *Arabidopsis* seedlings ecotype Col-0 WT [DAG10] in the presence of various concentration of Rotihibin A (**1**) and **15-24** (100% ≡ 20.88 mm^2). Error bars indicate the standard deviation of at least three independent experiments.

Next, the length of the primary roots of the *Arabidopsis* seedlings after treatment with compounds **15-24** was determined (*Fig. 32*). Also in this assay, Rotihibin A (**1**) induced a growth inhibiting effect. At 100 µM, the root length was 70% less than non-treated roots. A similar outcome was observed with **15** which displayed a similar inhibitory potency as Rotihibin A (**1**). This finding is somehow surprising as **15** did not induce a comparable effect on the cotyledon size. In contrast, compounds **16**, **17**, **18**, **19, 20, 22** and **24** showed only a negligible inhibitory potency on root growth inhibition. Of note, compound **21** displayed the strongest inhibitory effect, at 100 µM, the root length was decreased by 98%. Nevertheless, none of the compounds was generally toxic as the seedlings showed no signs of lethality after compound treatments up to a concentration of 100 µM. A particular case was compound **23** which showed an inhibitory effect only at a concentration of 100 µM where a root length reduction of 80% was observed.

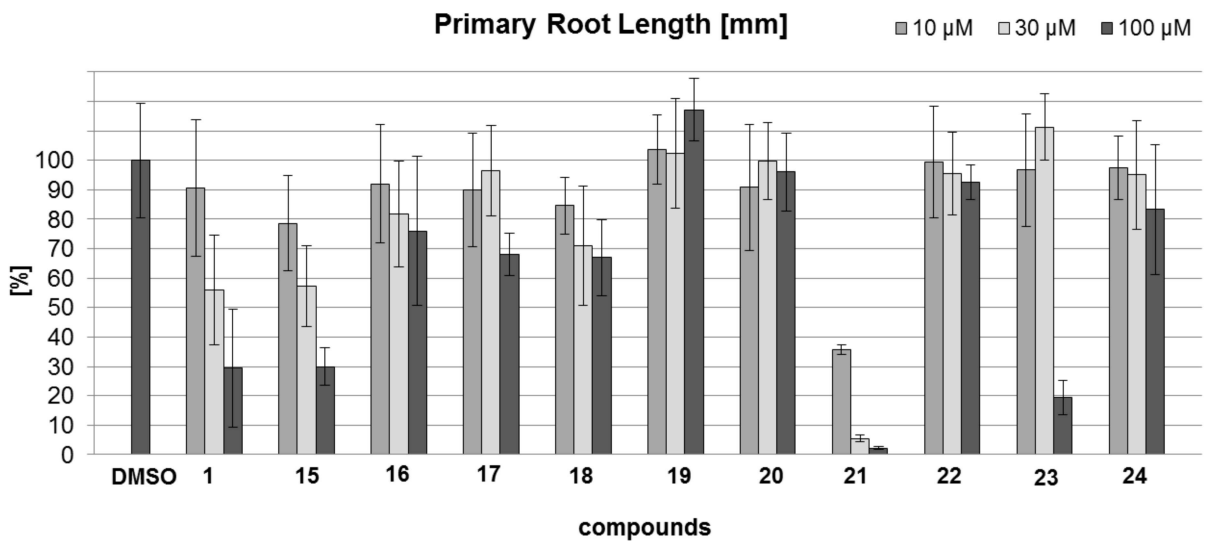

Figure 32: Primary root lengths of *Arabidopsis* seedlings ecotype Col-0 WT [DAG10] after treatment with varying concentrations of Rotihibin A (**1**) and derivatives **15-24** (100% ≡ 26.44 mm). Error bars indicate the standard deviation of at least three independent experiments.

By using the same root growth assay, the lateral root density was next determined by relating the absolute number of lateral roots with the length of the primary root (*Fig. 33*). A strong effect on the lateral root density was observed after treatment with Rotihibin A (**1**). At 100 µM, the lateral root density of the treated seedlings was reduced to 3% if compared to the control. Compound **15** showed a quite similar inhibitory effect at 100 µM, displaying a lateral root density reduction of 90%. As expected from the root length and cotyledon size measurements, compounds **16**, **17**, **18**, **19**, **20**, **22** and **24** showed also only a minor inhibitory effect on the lateral root density. Compound **21** however showed once again the strongest effect. Already at 30 µM, lateral root formation was completely inhibited. Finally, compound **23** revealed a relevant inhibitory effect on lateral root density only at a concentration of 100 µM.

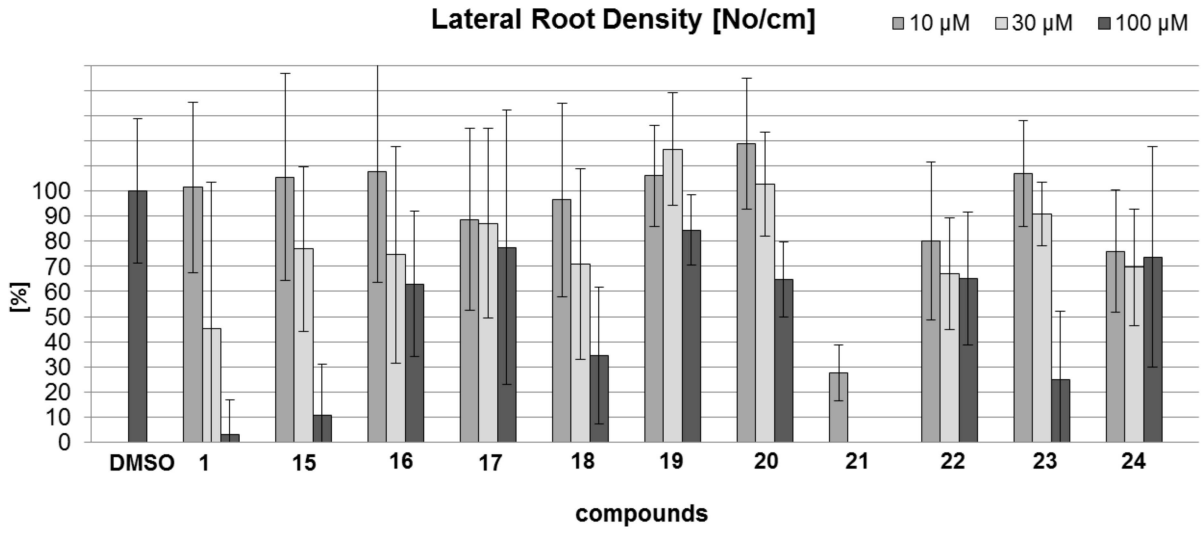

Figure 33: Lateral root density of *Arabidopsis* seedlings ecotype Col-0 WT [DAG10] after treatment with varying concentrations of Rotihibin A (**1**) and the derivatives **15**-**24** (100% ≡ 3.42 No/cm). Error bars indicate the standard deviation from at least three independent experiments.

Taken together, these experiments indicate that the hydroxyasparagine residue seems to play a crucial role for bioactivity. Compounds such as **17**, **22** or **24** which lack this moiety were completely inactive in the performed assays. The reduced bioactivity of compound **18** in which the hydroxyasparagine residue is replaced by an asparagine moiety, resulting in a derivative in which only the OH-group of this residue has been removed further supports this hypothesis. Surprisingly, the *α,β*-unsaturated amide system (i.e. a Michael system) of the lipophilic tail does not seem to be particulary important for bioactivity because compound **15** which lacks the corresponding double bond showed almost the same inhibitory effect than Rotihibin A (**1**). In contrast, the unusual D-stereochemistry of the citrulline residue appears to be essential for the growth inhibitory effect. The derivative with the reverse stereochemistry at this position, i.e. compound **16**, produced a far less distinctive growth inhibited phenotype. Moreover, a modification at the primary amine of the L-*allo*-threonine residue also does not seem to be tolerated as indicated by the observed phenotype after treatment with compounds **19** and **20**. The substitution of the L-serine residue with an L-alanine moiety as featured in compound **21** produced a remarkable inhibitory effect. Already at a concentration of 10 µM the cotyledon size, the primary root length and the lateral root density was decreased by more than 50%. Nevertheless, also in this case, the plant showed no lethal phenotype. Compound **23** in which the D-citrulline residue was replaced by an L-phenylalanine moiety, showed only an inhibitory effect at 100 µM; although this was not further investigated, a closer inspection

of the compound treated seedlings suggests that that this unusual effect might be caused by an undesirable toxic effect that is however rather weak as it was only observed at high concentrations.

4.1.5.2 Cell proliferation studies with *Arabidopsis* cell cultures

Whole plant growth inhibition studies are relatively easy in handling and generate a facile readout. Nevertheless, an accurate quantification of growth inhibition is hampered by a large variation as plant growth depends on many factors. In addition, two more-or-less independent processes contribute to the overall plant growth, i.e. cell division and cell elongation.[124] To better characterize the observed growth effects, additional proliferation experiments with *Arabidopsis* cell cultures were therefore next performed. One of the major advantages of such a cell culture-based growth inhibition assay is the unmatched consistency and reproducibility of experimental results. Moreover, plant cell cultures can be synchronized by means of blocking the cell cycle at one particular phase. Conditions constrictive for cell proliferation at one stage lead to accumation of cells at that phase. Once the restrictive stimulus is removed, all cells resume cell division in a synchronous way.[125]

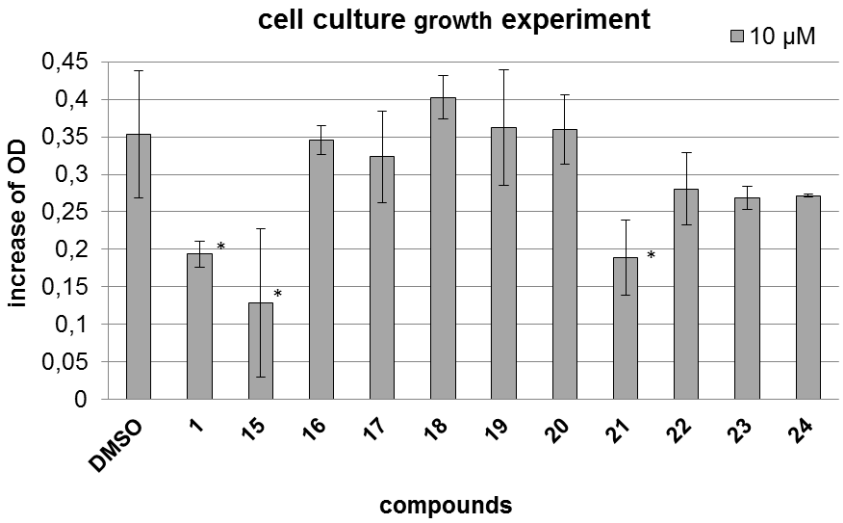

Figure 34: Measurement of cell proliferation in presence of Rotihibin A (**1**) and its derivatives. *Arabidopsis* cell cultures (Col-0) were incubated with 10 µM of **1** and **15**-**24** for 72 h and the increase in OD was determined by measuring the ratio between the OD after 72 hours and at the time point 0. Asterisks indicate the active derivatives with an OD increase of less than 0.2. Error bars indicate the standard deviation of at least three independent experiments.

The effect on proliferation can thereby easily be determined by measuring the optical density (OD) of the cultures. The outcome of the treatment of cell cultures of *Arabidopsis* cells with 10 µM of every derivative (**1** and **15**-**24**) is displayed in Figure 34. The results obtained by this assay corresponded very well to the results from the growth inhibition experiments with whole *Arabidopsis* seedlings. As before, compounds **1**, **15** and **21** showed the strongest effects. To confirm these findings, these three compounds were then tested at varying concentrations (*Fig. 35*). These results indicate that the compounds have a similar dose dependent effect on proliferation in cell culture as previously shown in the whole plant growth inhibition studies. Of note, the compounds displayed a higher activity in cell culture probably due to the lack of typical plant cell walls which act normally as an additional physical diffusion barrier. Correspondingly, a significant growth retarding effect was already observed at a concentration of 3 µM for compound **1**, **15** and **21**.

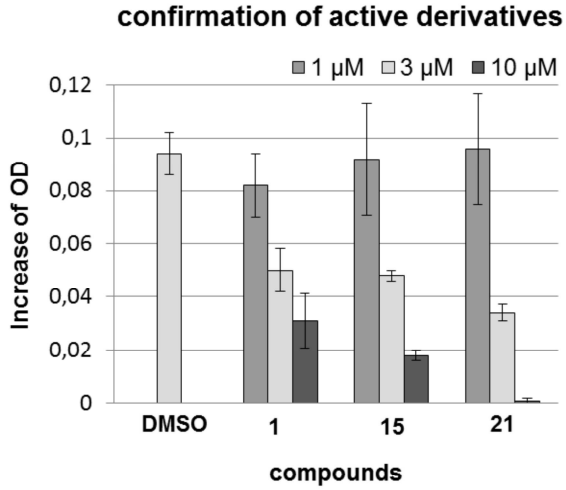

Figure 35: Measurement of cell proliferation in presence of compound **1**, **15** and **21**. Arabidopsis cell culture (Col-0) were incubated with various concentrations of **1**, **15** and **21** for 72 h and the increase in OD was determined by measuring the ratio between the OD after 72 hours and at the time point 0. Error bars indicate the standard deviation of at least three independent experiments.

4.1.5.3 Evaluation of Rotihibin A and derivatives in a cyclin B-reporter plant assays

A chemical genetic screen based on the *β*-glucuronidase (GUS) reporter gene system was subsequently performed to identify transcriptional events that were affected by Rotihibin A (**1**) treatment.[126] To this end, transgenic plant lines for measuring the 'promoter activity' via the insertion of a DNA construct consisting of the DNA sequence of the GUS

enzyme fused behind the promoter sequence of different genes were used. Such plants therefore allow determining the promoter activity state via GUS staining in living plants. The expressed enzyme GUS produces an insoluble, blue dye after addition of an artificial colorless substrate X-Gal (*Fig. 36*).

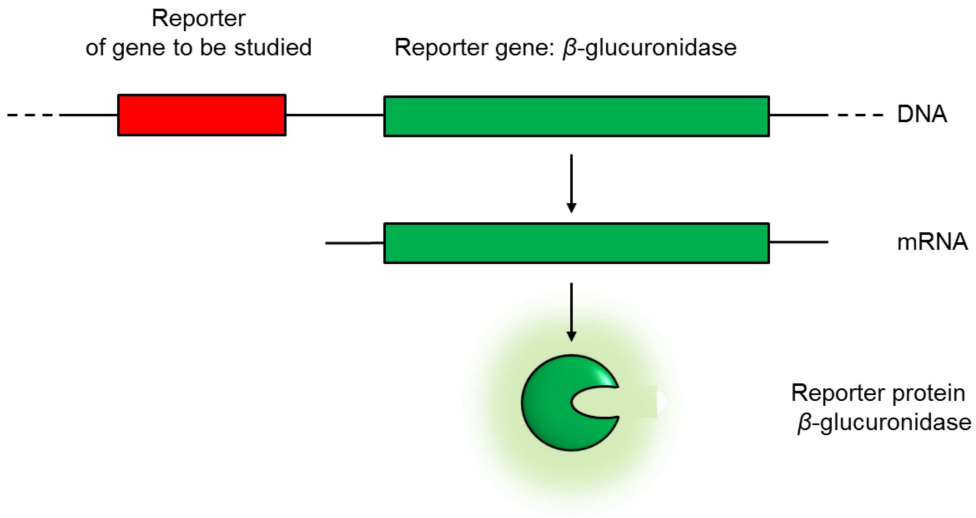

Figure 36: Schematic representation of the GUS reporter gene system.

Along these lines, the reporter activities of genes that are known to play roles in plant pathogen defense were analyzed as Rotihibin A (**1**) is biosynthesized by a bacterial species. Furthermore, genes involved in plant hormone responses were investigated. As plant hormones are critical key players in plant growth and development and as Rotihibin A (**1**) was found to affect plant growth, it was reasonable to assume that Rotihibin A (**1**) may modulate plant hormone function. In addition, the reporter activity of cyclin B as a general mitotic marker was investigated. This screen revealed that Rotihibin A (**1**) was affecting the mitotic cycle of the plants (*Table 4*).

Table 4: Gene constructs used to characterize Rotihibin A (**1**)'s mode of action. Rotihibin A (**1**, 30 µM) was added to the corresponding transgenic ROI::GUS *Arabidopsis* seedlings followed by GUS staining (ROI: Gene reporter of interest, X = no change of reporter activity upon treatment with **1** (30 µM). ✓ = reduction of reporter activity upon treatment with **1** (30 µM).

Impact of Rotihibin A on diverse gene reporter		
ROI::GUS	**role**	**1** (30 µM)
WRKY29::GUS	→immune response	X
VSP1::GUS	→plant defense	X
DR5::GUS	auxin depended promoter	X
DC3::GUS	ABA and mannitol depended promoter	X
Cyclin B::GUS	mitotic protein	✓

The acquisition of water and nutrients by plant roots is strongly dependent on root branching. In fact, the proper development of lateral roots plays a central role for the plants to guarantee steady acesss to new soil resources. Lateral roots originate from a subset of xylem pole pericycle cells that undergo asymmetric cell division. These are formed nearby, nevertheless distantly from the primary root tip and starts from a small number of pericycle founder cells (meristemic cells) that undergo cell-divisions, giving rise to a single layered primordium.[127] Subsequent cell-divisions yield a lateral primoradium which then grows through the outer cell layers and finally emerges from the primary root to form a lateral root.

Generally, tissues within a plant that are able to promote growth by mitosis are called meristems. Plants are equipped with meristematic tissue in several locations. For example, roots and shoots have meristematic tissue at their tips called apical meristems that are in charge of the elongation of both organs. Meristematic cells are entirely developed and completely functional at maturity, but unlike other cells in the plant, they stay totipotent. Thus, meristematic cells can be induced to develop into any plant tissue at any developmental stage of the plant.[128] Therefore, meristematic plant cells can be considered as analogues of mammalian totipotent stem cells from early embryonic stages. Plants grow larger either by cell division or by cell elongation. Primary plant growth is triggered by meristematic tissue because it is the primary site of cell proliferation, namely mitosis, in the plant. Meristematic tissue is however not autarkic and its fate is regulated by several plant hormones. For instance, giberellins provoke cell division in the shoot meristem, thus stimulating plant growth.[129] Cytokinins and auxins are also essential growth regulators.[28] Auxin promotes

growth by provoking cell elongation, while cytokinins are thought to induce both cell division and elongation.[130]

As all new cells of a plant are formed in the meristem, this tissue plays an important role in general plant growth. It was therefore not surprising that the reporter activity of cyclin B could only be observed in the meristematic areas, since this is the only place in the plant where mitosis takes place (*Fig. 37*).Consequently, DMSO treatment of the cycB::GUS reporter plant line resulted in a blue stain in the area where the meristemic cells are located, namely the root meristem, the shoot meristem and in the lateral primordia which represents the usual reporter activity of cyclin B in mitotic plant cells. In presence of 30 µM Rotihibin A (**1**), this signal was strongly reduced (*Fig. 37*). This pinpoints that cyclin B levels are also strongly reduced in these living plants which are usually required to complete the mitotic cycle. Consequently, the meristemic cells were not able to fulfill cell division anymore which would explain the observed dwarfed phenotype after incubation with Rotihibin A (**1**).

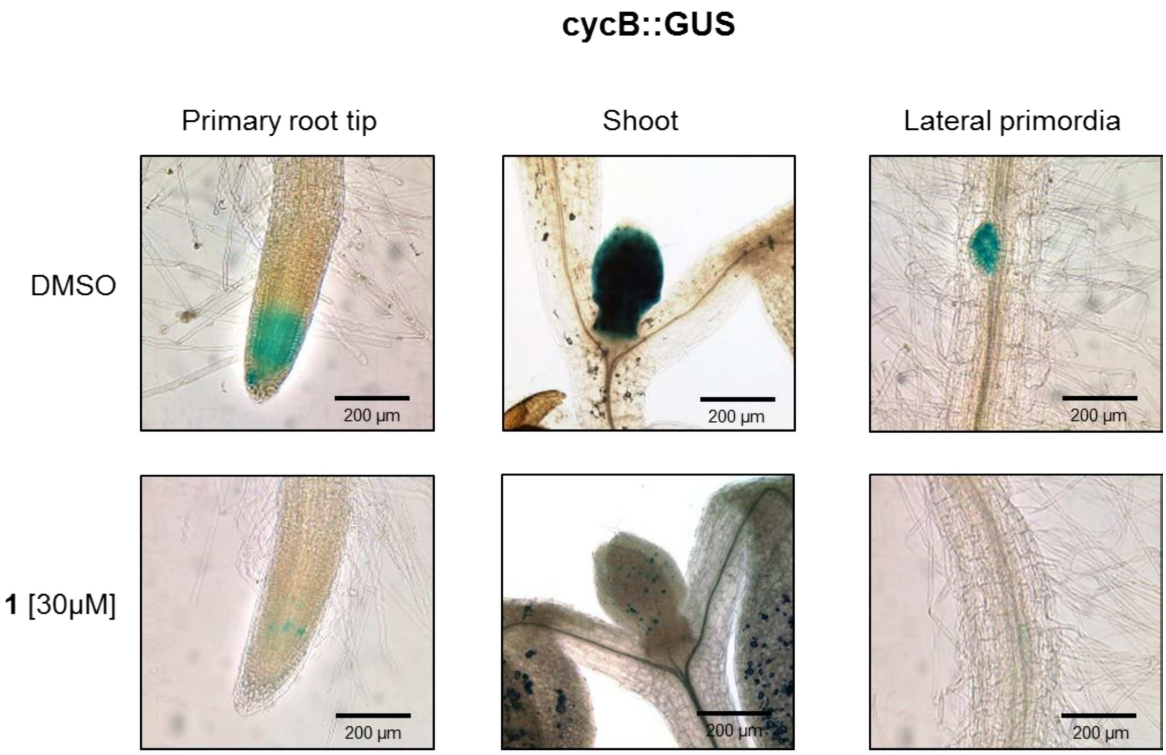

Figure 37: Histochemical GUS staining of 10 days old cycB::GUS *Arabidopsis* seedlings after 24 h treatment with or without **1**. Blue staining reflects reporter activity of cyclin B and thus also the approximate expression level. The images show representative distribution patterns of GUS staining in the primary root tip, the shoot and in the lateral primordia. Scale bar: 200 µm.

These findings lead to the conclusion that primary plant growth which is caused by mitotic cell proliferation in the meristemic tissue of the *Arabidopsis* seedlings is inhibited by Rotihibin A (**1**). Subsequently, the same set of experiments was also performed with the Rotihibin derivatives and a strong correlation between a dwarfed phenotype and the cyclin B reporter activity was observed. Along these lines, derivatives that showed no effect on plant growth also did not show any reduction in cyclin B reporter activity, while active compounds displayed this phenotype.

As a control to prove that the transgenic cycB::GUS plants still respond with the same phenotypic effect towards Rotihibin A (**1**) as wild-type plants (cf. *Fig. 31-33*), the transgenic plants were likewise treated with various concentrations of **1** (*Fig. 38*)**.**

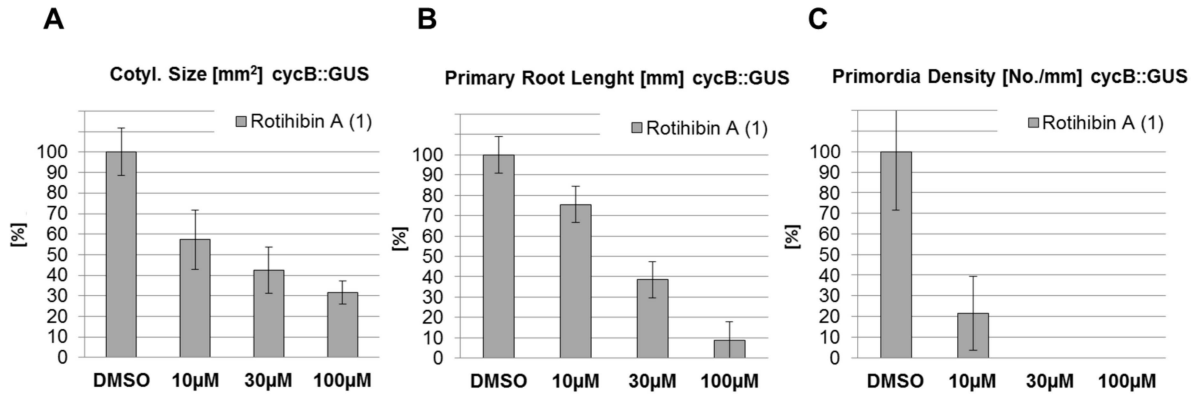

Figure 38: (**A**): Cotyledon size of transgenic *Arabidopsis* seedlings [10 DAG] in presence of **1** (100% ≡ 6.88 mm^2). (**B**): Primary root length of transgenic *Arabidopsis* seedlings in presence of **1** (100% ≡ 22.30 mm). (**C**) Lateral primordia density of transgenic *Arabidopsis* seedlings in presence of **1** (100%≡ 0.28 No./cm). Error bars indicate the standard deviation of at least three independent experiments.

As depicted in Figure 38, Rotihibin A (**1**) had a comparable impact on the cotyledon size, the primary root length and the lateral primordia density in transgenic cycB::GUS plants like in the wild-type plants (cf. *Fig. 31-33*).

The total synthesis and derivatization of Rotihibin A (**1**) together with the subsequent biological evaluation revealed structural entities within the natural compound that strongly contribute to bioactivity and allowed therefore a first glance at structure-activity relationships (SAR). The upcoming challenge will now be to design, according to these SAR-insights, a functional and bioactive natural product derived probe. To this end, all necessary groups, which account for a probe (c.f. *Chapter 2.4.2*), have to be integrated into the chemical structure of Rothibin A (**1**) without compromising the bioactivity. The present study gave the

first hints at which positions an incorporation of, for example, photo-reactive groups might be possible and at which positions chemical modifications are not tolerated regarding bioactivity. Finally, a bioactive Rotihibin A-derived probe, together with the synthesized Rothibin A (**1**) would be a meaningful tool to further study the mode-of-action of Rothibin A (**1**) and to promote the understanding of the well-orchestrated physiology underlying plant growth by the chance of revealing unknown networking cellular proteins.

4.2 Studies towards plant growth regulators Brevicompanine A, B & C

During a screening campaign to discover novel plant growth regulators from fungal sources, Kimura and Kusano isolated three diketopiperazines Brevicompanine A (**25**), B (**26**) and C (**27**) from a culture filtrate of *Penicillium brevicompactum* and found that they feature plant growth-regulating properties. [103,104] Compounds **25** and **26** were thereby elucidated to display inhibitory activities upon the hypocotyl elongation of lettuce seedlings at a concentration of 100 mg/L. In contrast, **25**, **26** and **27** accelerated the root growth of lettuce seedlings in proportion to its concentration from 10 $mg \cdot l^{-1}$ to 300 $mg \cdot l^{-1}$ (**26**) and from 1 $mg \cdot l^{-1}$ to 100 $mg \cdot l^{-1}$ (**25**, **27**). Interestingly, it was also reported that compounds **25** and **26** showed no inhibitory effects on the root and stem elongation of rice seedlings up to 300 mg l^{-1}.

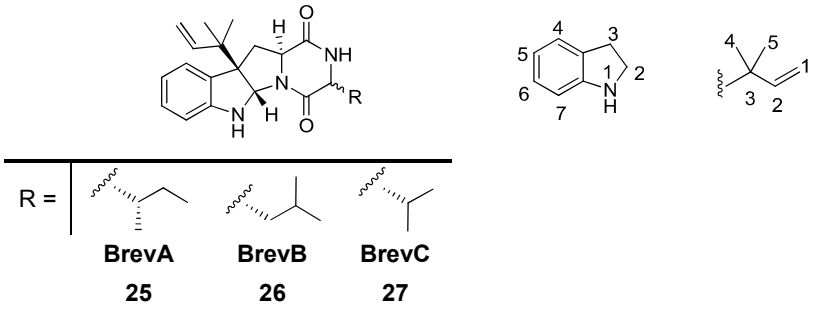

Figure 39: **(A)** Structures of Brevicompanine A (**25**), B (**26**) & C (**27**); **(B)** Atomic numbering of prenyl and indoline moieties.

Brevicompanine A (**25**), B (**26**) and C (**27**) can be regarded as a diketopiperazine product of a **h**exahydro**p**yrrolo[2,3-*b*]**i**ndole (HPI) moiety derived from L-tryptophan with either a D-leucine, a D-*allo*-isoleucine or a D-valine residue (*Fig. 39*). L-Tryptophan from primary

metabolism thereby serves as the biogenetic precursor for generation of the HPI-skeleton.[131] In Brevicompanines, this HPI moiety is substituted with an inverted prenyl (*α,α*-dimethylallyl) group at the C3 position which is a common structural element in various natural compounds like Amauromine[132], Fructigenines[133] and Flustramines[134]. Besides L-tryptophan, most of these substances contain a second amino acid and form cyclic dipeptides with a diketopiperazine structure or a derivative thereof, like it is the case for brevicompanines. Prenylated indole alkaloids are widely distributed in terrestrial and marine organisms.[131] Most of these alkaloids feature a wide range of biological and pharmacological activities.

The synthesis of Brevicompanine A (**25**) and B (**26**) and its *allo*-derivatives (these are derivatives that feature a L-amino acid configuration instead of the natural D configuration) has already been published.[135] A total synthesis of Brevicompanine C (**27**) however has so far not been reported. More importantly, the biological activity of brevicompanines is still insufficiently evaluated; in particular, no direct target proteins of these compounds have yet been elucidated. The establishment of a total synthesis route to Brevicompanines could thereby open the possibility to generate in a second step also analogues that might allow to deduce structure-activity relationships (SAR) and might represent starting points for subsequent target identification.

Consequently, a total chemical synthesis of Brevicompanine A (**25**), B (**26**) and C (**27**) and its *allo*-derivatives was performed, following essentially the route of Kitahara and coworkers.[135] This allowed gaining access to sufficient quantities for further studying in vitro and in vivo activities of these compounds.

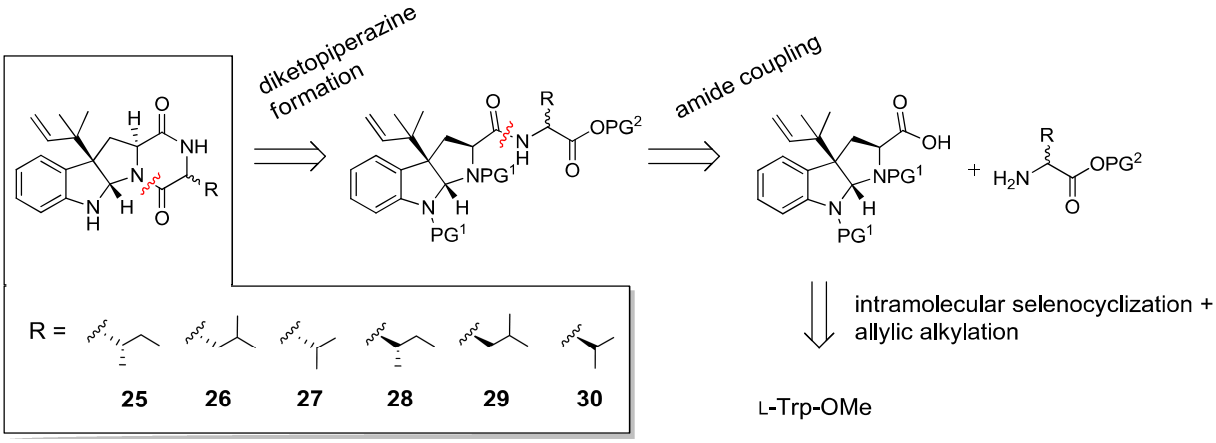

Figure 40: Retrosynthesis for generation of Brevicompanines and derivatives thereof. PG = protection group.

The retrosynthesis of Brevicompanines started with the disconnection of the two amide bonds of the diketopiperazine entity which leads to the reverse prenylated hexahydropyrrolo[2,3-*b*]indole (HPI)-skeleton together with the corresponding amino acid (*Fig. 40*). The HPI-moiety was generated starting from L-tryptophan methyl ester via heteroatom-mediated intramolecular selenocyclization, followed by selenoxide elimination and alkylation of a reverse prenyl nucleophile as discussed in the subsequent paragraphs.

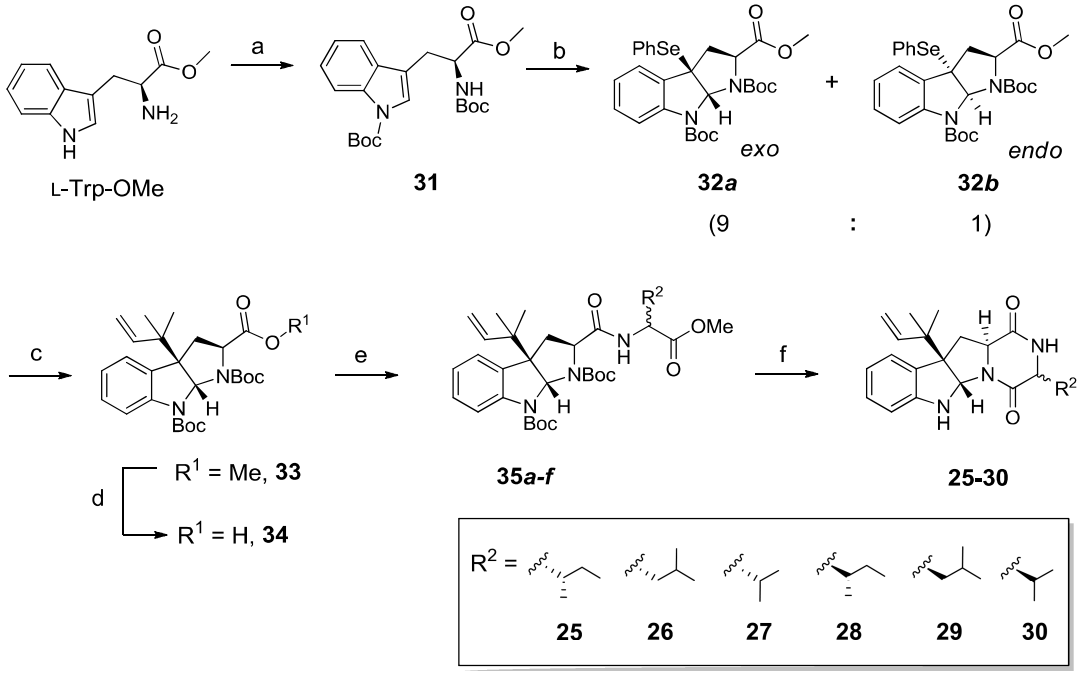

Scheme 7: a) Boc_2O, NaOH, NBu_4HSO_4, DCM, 0°C → rt, 16 h., 83%. b) *N*-(phenylseleno)phtalimide, p-TSA, Na_2SO_4 DCM, rt, 8 h, 47% (ratio of diastereomers). c) MeOTf, prenyl tributylstannane, 2,6-di-*tert*-butylpyridine, ACN, -78°C → reflux, 20 h, 96% (ratio of diastereomers). d) NaOH, THF, MeOH, reflux, 16 h, 97%. e) EDC*HCl, HOBt, DIPEA, *aa* methyl ester, DCM, rt, 12 h, 35- 93%. f) i: TMSI, ACN, 0°C → rt, 4 h; ii: NH_4OH, MeOH, rt, 2 h, 10-38%.

The synthesis started with L-tryptophan methyl ester, which was converted to the corresponding bis-(Boc) derivative **31** using Boc anhydride under phase transfer conditions (*Scheme 7*). The reaction occurred smoothly and with excellent yields. The tricyclic architecture of the HPI moiety was subsequently build up by a two-step procedure developed by Danishefsky and coworkers using *N*-(phenylseleno)-phtalimide and *p*-TSA to give the 3-seleno-modified pyrroloindoles **32a** and **32b**.[136] Sodium sulfate was used in this selenocyclization to remove the crystal water from the usage of the hydrated form of *p*-TSA. The cyclization occurred under gentle conditions yielding **32a** and **32b** as a 9:1 ratio of inseparable diastereomers. The relative high degree of stereoselection in this intramolecular

selenocyclization might thereby be explained by the thermodynamic stability of the pre-*exo* and pre-*endo* intermediates (*Fig. 41*). In this model, the cyclization of the pre-*endo* intermediate might be hampered by steric effects of the PG^2 at the carboxyl group with the indole moiety; the ratio of **32a** and **32b** might therefore be a consequence of the different thermodynamic stabilities of the *exo* and *endo* products as well as the reversibility of the cyclization of the pre-*exo* and pre-*endo* intermediates.

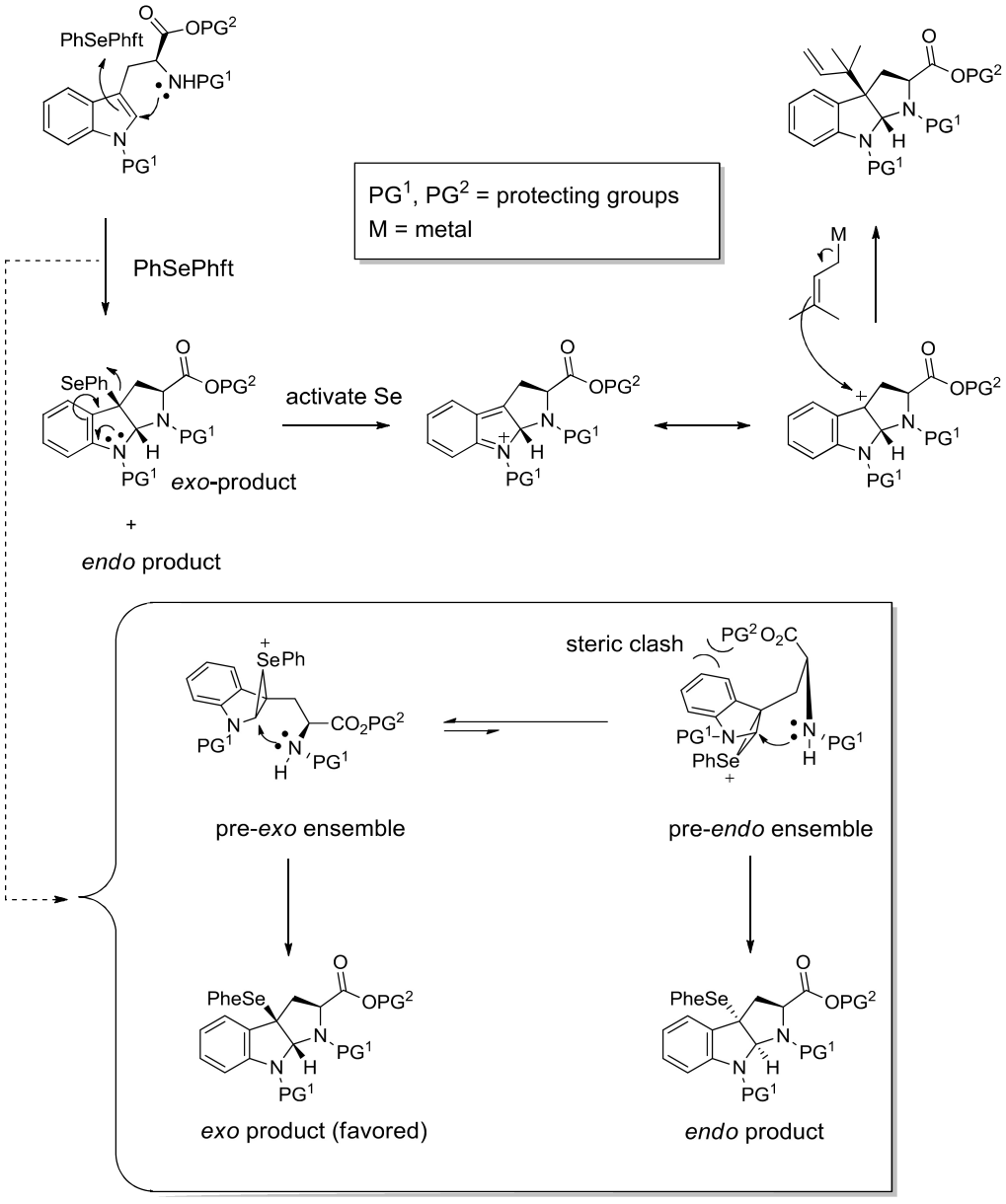

Figure 41: Mechanism of intramolecular selenocyclisation and the formulation of a hypothesis for explaining the favored formation of the exo-product. (Adapted and modified from Depew *et al.*[137])

The next step in the synthesis was the selenoxide elimination using MeOTf for oxidizing the selenium species **32a,b** and eliminating the phenyl selenide resulting in the formation of a

cationic species. This can be alkylated via allylic transposition with prenyl tributylstannane, yielding compound **33** (still as a mixture of diastereomers) in excellent yields (*Scheme 7*). Next, the hydrolysis of methyl ester **33** to the free carboxylic acid **34** was accomplished under basic conditions. This step then also enabled a separation of the diastereomeric mixture by repeated flash chromatography. Subsequent coupling of the corresponding amino acid methyl ester using standard solution coupling reagents yielded the fully protected linear precursor **35**. The cleavage of the two Boc protecting groups of compounds **35** with TMSI in anhydrous acetonitrile at 0 °C generated the diamine which was directly subjected to a reaction with methanolic ammonia. This resulted in hydrolysis of the methyl ester and a spontaneous formation of the diketopiperazines **25-30**. Following this route, Brevicompanine A (**25**), B (**26**) and C (**27**) as well as the isomeric compounds *allo*-Brevicompanine A (**28**), B (**29**) and C (**30**) were synthesized. All analytical data of synthetic Brevicompanines thereby agreed with those published for the natural compounds.[103; 104] For Brevicompanine C and its *allo*-derivative (**27** & **30**), this was the first total synthesis reported so far.

For identifying the cellular target of these compounds, a probe was designed for performing pull-down experiments. The probe should host several important functionalities for such an approach. First, it should present a recognition site consisting of the natural product core-structure (i.e. the HPI-diketopiperazine residue), responsible for binding to potent target proteins. Second, the probe should contain a moiety for reporter attachment. This is essential to visualize target proteins and to go on with affinity-purification. To this end, an alkyne-moiety to attach a suitable reporter via bioorthogonal Click-chemistry was chosen. Therefore, two different probes have been developed: In the first one (**37**), only an alkyne residue was introduced into the final product via diketopiperazine ring formation with a propargyl glycine residue (*Scheme 8*).

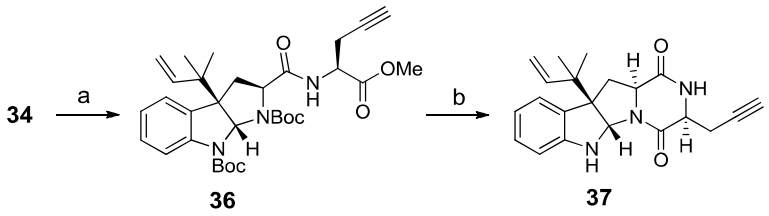

Scheme 8: Synthesis of compound **37**. a) EDC*HCl, HOBt, DIPEA, L-propargyl glycine methylester, DCM, rt, 12 h, 41%. b) i: TMSI, ACN, 0°C→rt, 4 h; ii: NH_4OH, MeOH, rt, 2 h, 15%.

The probe **37** was successfully synthesized according to Scheme 8. As Brevicompanines however feature no 'obvious' electrophilic functionalities which might react in a covalent

manner with nucleophilic groups on target proteins, a second probe was designed that also featured a benzophenone residue for photo-cross-linking. The benzophenone residue photolyzes upon exposure to UV-light to give highly reactive triplet-state ketone intermediates (*Fig. 9*). The energized electron of an activated benzophenone can then insert into a hydrogen-carbon bonds and other reactive functionalities to give covalent linkages with target proteins. As a covalent linkage is much more applicable for pull-down experiments, a photo-reactive group was installed as depicted in Scheme 9.

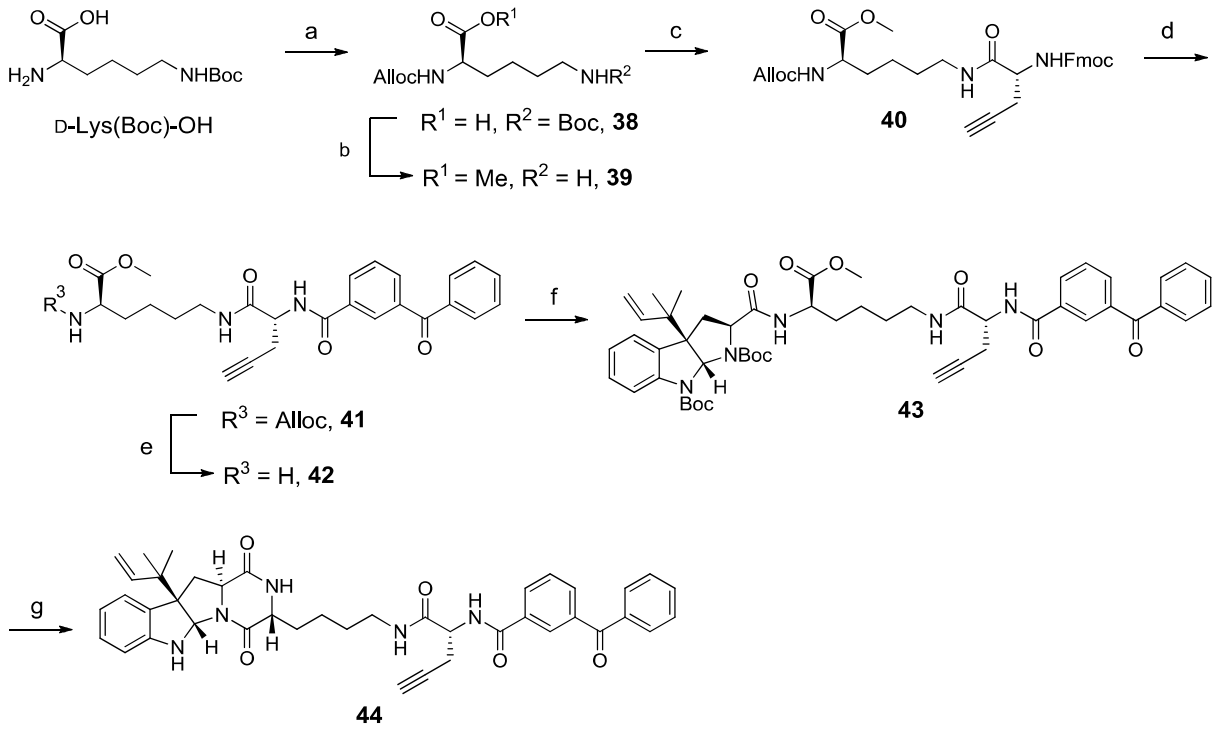

Scheme 9: Synthesis of photoreactive probe **44**. a) Alloc-Cl, $NaHCO_3$, H_2O/dioxane, 0°C→rt, 16 h, 99%. b) $SOCl_2$, MeOH, 0°C→reflux, 5 h, 95%. c) **39a**, EDC*HCl, HOBt, DIPEA, DCM, rt, 16 h, 72% d) i) DEA, CAN, rt, 2 h. ii) 3-benzoylbenzoic acid, EDC*HCl, HOBt, DIPEA, DCM, rt, 4 h, 65%. e) $Pd(PPh_3)_4$, dimedone, THF, rt, 1.5 h, 44%. f) **34**, PyBOP, HOBt, DIPEA, DCM, rt, 1.5 h, 26% g) i) TMSOTf, DCM, 0°C, 1.5 h. ii) LiOH, MeOH, THF, H_2O, rt, 3 h.. iii) PyBOP, HOBt, DIPEA, DCM, rt, 16 h, 20%.

The synthesis of the photoreactive probe **44** started with D-Lys(Boc)-OH for maintaining the stereochemistry found in the natural products which all have D-amino acids within the diketopiperazine heterocycle (*Fig. 38*). Starting from commercially available D-Lys(Boc)-OH, the free amino group was first protected with Alloc (**38**). The *C*-terminus was subsequently protected as a methyl ester using thionyl chloride in methanol which directly also cleaved the Boc protecting group, resulting in amine **39** in 95% yield over both steps. Next, the free amine **39** was coupled to Fmoc-protected L-propargyl glycine using standard coupling reagents to

introduce the alkyne moiety for reporter attachment. This gave the desired dipeptide **40** in 72% yield. The Fmoc-group was cleaved and coupling of 3-benzoylbenzoic acid was conducted to insert the photo-reactive group into the molecule resulting in compound **41** in 65% yield. Palladium(0)-mediated deprotection of the Alloc-group (**42**) and coupling to carboxylic acid **34** provided **43**. **43** was then treated with TMSOTf to cleave the Boc-protecting groups and to give the corresponding free diamine. Subsequently, the methyl ester was hydrolyzed using lithium hydroxide followed by diketopiperazine formation performed with standard coupling conditions to yield 20% (over 3 steps) of the photoreactive probe **44**.

4.2.1 Biological evaluation of Brevicompanines and derivatives thereof

The biological activities of compounds **25-30**, as well as of **37** and **44** were examined in collaboration with the Kombrink group (MPI Cologne) using a bioassay with *Arabidopsis* seedlings. As a readout, the effect of the Brevicompanines on root length and lateral root density was examined as Brevicompanines were reported to act as plant growth regulators. Surprisingly, no enhancement of root growth in *Arabidopsis* could be observed as published for lettuce seedlings. Instead, each of the compounds showed inhibitory effects on the primary root growth of *Arabidopsis* seedlings in response to increasing concentrations (*Fig. 42*). Interestingly, the natural products **25**, **26** and **27** showed a stronger effect than their *allo*-isomers **28-30**. This may indicate a stereospecific structure-activity-relationship (SAR) and suggests that the D-amino acids within the diketopiperazine moiety are favorable for this biological activity. The best inhibitory activity was observed for Brevicompanine B (**26**). Brevicompanine A (**25**) showed only slightly weaker bioactivities. Of note, both compounds possess a D-conformation within the diketopiperazine residue and both compounds feature the most hydrophobic amino acid side-chain in the diketopiperazine heterocycle. Subsequently, the inhibitory activities of the synthesized probes **37** and **44** were determined. The inhibition of the root growth by **37** and **44** was not as good as the inhibition triggered by **25-30**. Although the photoreactive probe **44** had the required D-stereochemistry within its diketopiperazine moiety, it showed almost no activity. The reduced inhibition of root growth might result from the bulky residues (benzophenone etc.) that might impart steric hindrance on the corresponding binding event(s). Probe **37** with its L-stereochemistry within the diketopiperazine possessed a less hydrophobic side chain (L-propargyl glycine) residue than for example *allo*-Brevicompanine B (**29**) which might also be required to retain activity.

Nevertheless both probes, **37** and **44**, displayed inhibitory activity towards the lateral root density at 100 µM (*Fig. 43*). However, both probes also indicated an inhibition of the primary root growth at a concentration of 300 µM (data not shown).

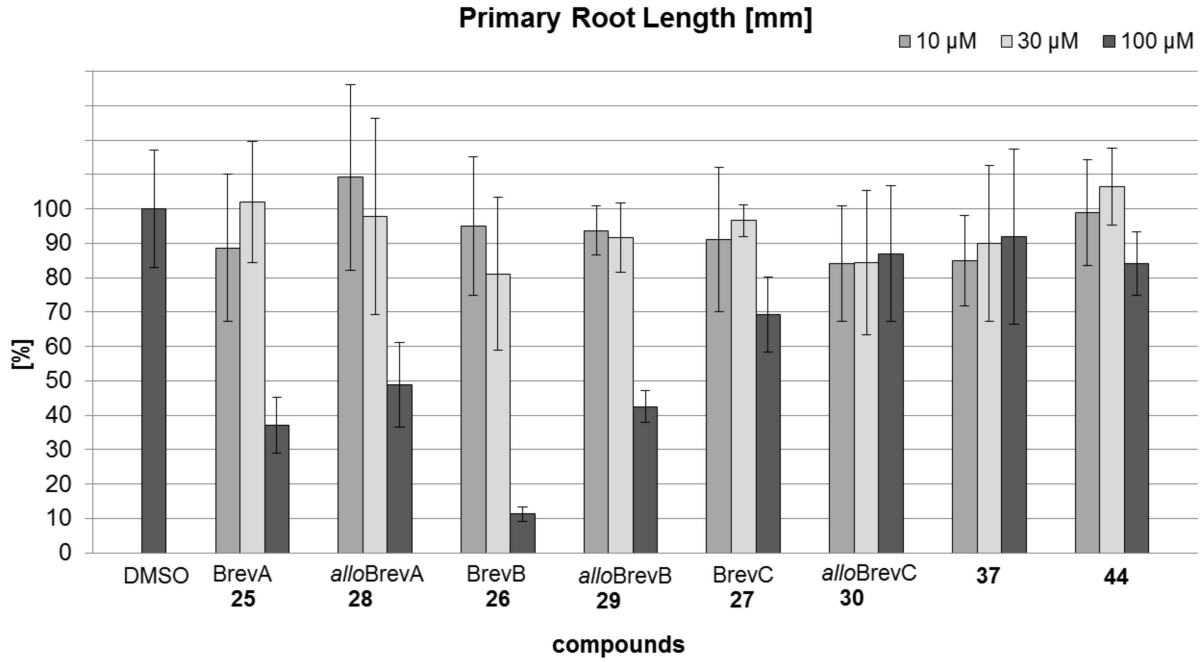

Figure 42: Primary Root Length of *Arabidopsis* (Col-0) seedlings [DAG10] in the presence of varying concentrations of **25-30**, **37** and **44** (100% ≡ 23.8 mm). Error bars indicate the standard deviation of at least three independent experiments.

In addition, the lateral root density (LRD) of *Arabidopsis* seedlings was examined. The LRD also decreased upon increasing concentrations of compounds **25-30** (*Fig. 43*). However, a correlation between stereochemistry of the diketopiperazine moiety and alteration of LRD could not be deduced.

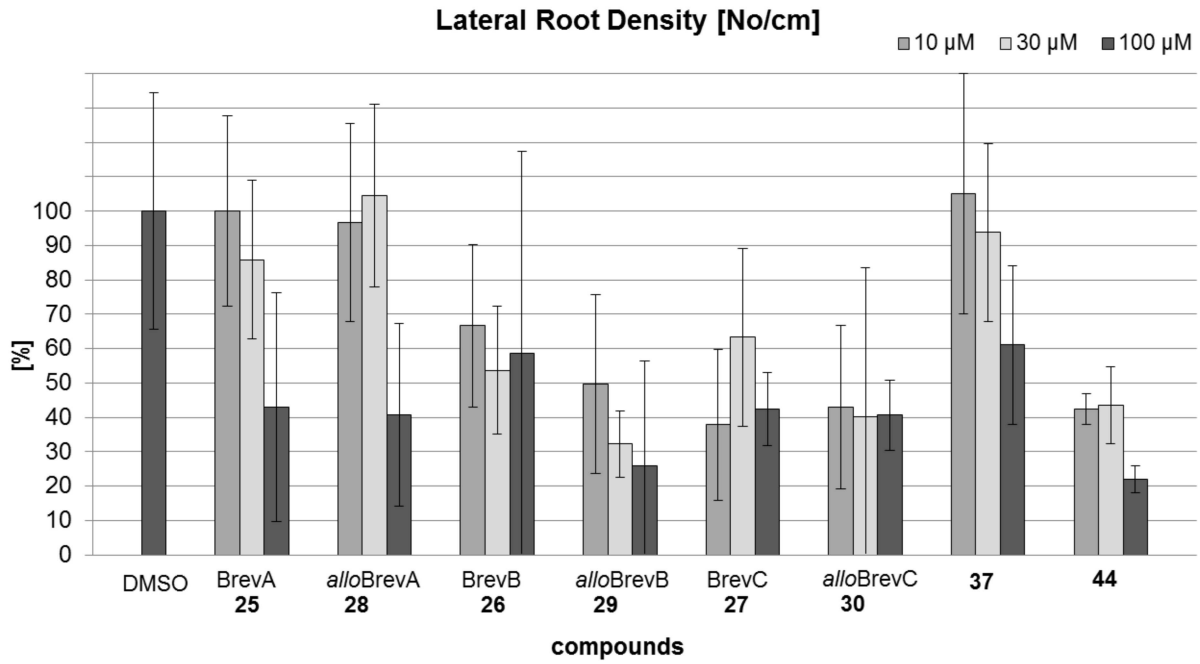

Figure 43: Lateral root density of *Arabidopsis* (Col-0) seedlings [DAG10] in the presence of varying concentrations of **25**-**30**, **37** and **44** (100% ≡ 1.77 No/cm). Error bars indicate the standard deviation of at least three independent experiments.

Altogether, these growth inhibition studies with the synthesized Brevicompanines and derivatives thereof (**25-30**) revealed inhibitory effects on the primary root growth of *Arabidopsis* seedlings and a correlation between the stereochemistry of the diketopiperazine moiety and inhibition efficiency. A growth enhancing effect as described for lettuce seedlings could not be observed. These findings may conclude that the target protein(s) of **25**, **26** and **27** on lettuce seedlings should be different from *Arabidopsis* seedlings.

However, since the acquisition of water and nutrients by plant roots strongly depended on root branching, the inhibition of the latter might be of further interest to elucidate the several processes of root expansion and to reveal more networking cellular proteins respectively. Therefore, the two natural product-based probes **37** and **44** were designed for identifying the corresponding target protein(s).

4.2.2 ABPP experiments for cellular target elucidation

For target elucidation of Brevicompanines, *Arabidopsis* leaf extracts were incubated with probe **37** and **44**, respectively. In a first experiment, an *Arabidopsis* lysate was preincubated with various concentrations of probe **37** and then with the corresponding "click-reagents" to attach a fluorescent reporter tag (Rhodamine) after labelling. Subsequent SDS gel analysis of such treated proteome should then reveal potential targets. Figure 44A depicts that no covalent labeling was observed using probe **37**. This issue might indicate that Brevicompanines – as expected from their molecular structure- bind to their targets in a non-covalent fashion.

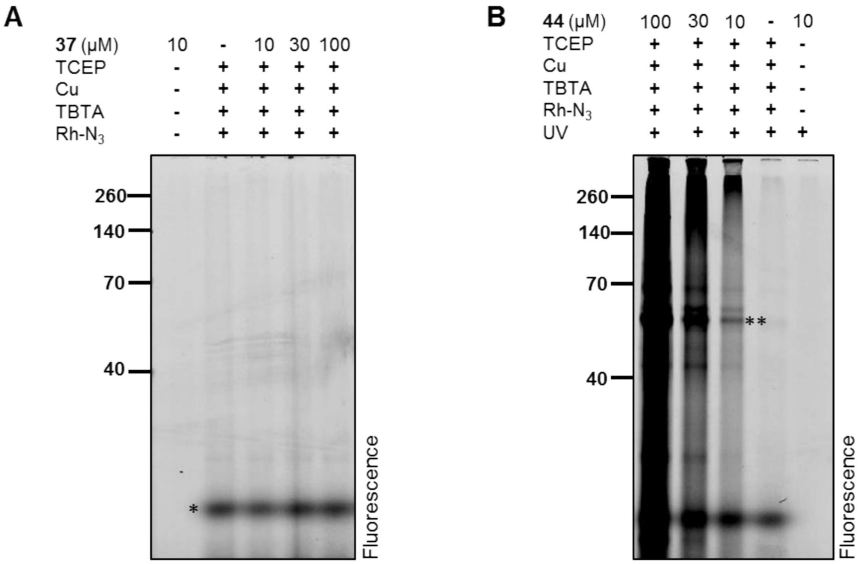

Figure 44: **(A)** Labeling of *Arabidopsis* leaf extracts with probe **37**. **(B)** Labeling of Arabidopsis leaf extracts with probe **44**. (* = signal of free rhodamine-azide; ** = this labeled band is most likely to be the abundant protein RuBisCo)

In a second experiment, *Arabidopsis* leaf extracts were incubated with varying concentrations of probe **44**, and then irradiated with UV-light (360 nm) to initiate photo-crosslinking with target proteins. Afterwards the samples were treated with "click reagents" to attach again the fluorescent reporter tag. The outcome of this treatment is depicted in Figure 30B. A distinct band (**, *Fig. 44B*) was labeled by probe **44** at a concentration of 10 µM. The size of the labeled protein is about 50 kDa which however most probably is labeling of the abundant protein RuBisCo and thus a non-specific cross-link.[138] Remarkably, increasing concentrations of **44** led to rather unspecific photo-crosslinking within the *Arabidopsis* leaf proteome (*Fig. 44B*). At a concentration of 100 µM the signal was unquestionably oversaturated.

Altogether, the current target identification studies are inconclusive. It is not clear if no target could be found due to technical or due to inherent problems with the probes. Further investigations that may help to shed light on this could be competition experiments with the natural products and **44** to confirm whether the labeled protein at 50 kDa is as expected non-specific or represents specific labeling. Additional pull-down experiments using biotinylated reporter tags and streptavidin enrichment could also be helpful for paving the path to the cellular targets of Brevicompanines. Finally, also alternative photo-affinity probes that display a stronger bioactivity might be required for target identification.

However, due to the overall rather weak bioactivities of Brevicompanines and the time limitations from the PhD, such experiments were not performed within the frame of this thesis.

4.3 Synthesis of acyl-ATP probes for profiling of ATP binding proteins in *A. thaliana*

Adenosine triphosphate (ATP) is the biochemical fuel of all living organisms. The phosphor-anhydride linkages in an ATP molecule are responsible for the high energy content of this molecule. Hydrolysis of these bonds releases this chemical energy that can then be used to drive metabolic reactions. In all living organisms, numerous proteins that are able to bind and hydrolyse ATP are found. An important and very large class of ATP-binding proteins are protein kinases which transfer the γ-phosphate from ATP to substrates. Nearly all signalling pathways rely on protein kinase cascades which precisely regulate cellular processes as for example cell division and differentiation. In the genome of the model plant *Arabidopsis thaliana*, over 1000 protein kinases and hundreds of other ATP binding proteins are encoded.[5] Due to their diverse and important roles, kinases have been intensively studied in plant science.[139; 140]

The study of the ATP-binding proteome is an elaborate task considering the remaining hundreds of uncharacterized kinases in plants. Therefore, new chemical biological approaches are necessary to study kinases and other ATP binding proteins in plants. For visualizing ATP-dependent enzymes, a directed activity-based probe named BHAcATP (**5**) has recently been introduced (c.f. *Table 5*).[105] This probe represents an ATP-derivative which is modified with a reactive acyl phosphate group at the γ-phosphate followed by a reporter-tag. The acyl

phosphate probes target ATP binding sites and covalently label conserved lysine residues located in the ATP binding pocket. Such conserved lysine residues have been found for a huge number of kinases in their ATP binding site (*Fig. 45B*) and during ATP binding, these lysine residues are in very close proximity to the γ-phosphate (*Fig. 45C*).[141] The acyl phosphate might therefore serve as an electrophilic warhead because a mixed carboxylic phosphoric anhydride residue is chemically rather reactive. Consequently, the electrophilic acyl phosphate within the probes can be attacked by the ε-amino group of a lysine, resulting in an irreversible acylation of the lysine with the reporter-tag accompanied by a release of ATP (*Fig. 45A*).

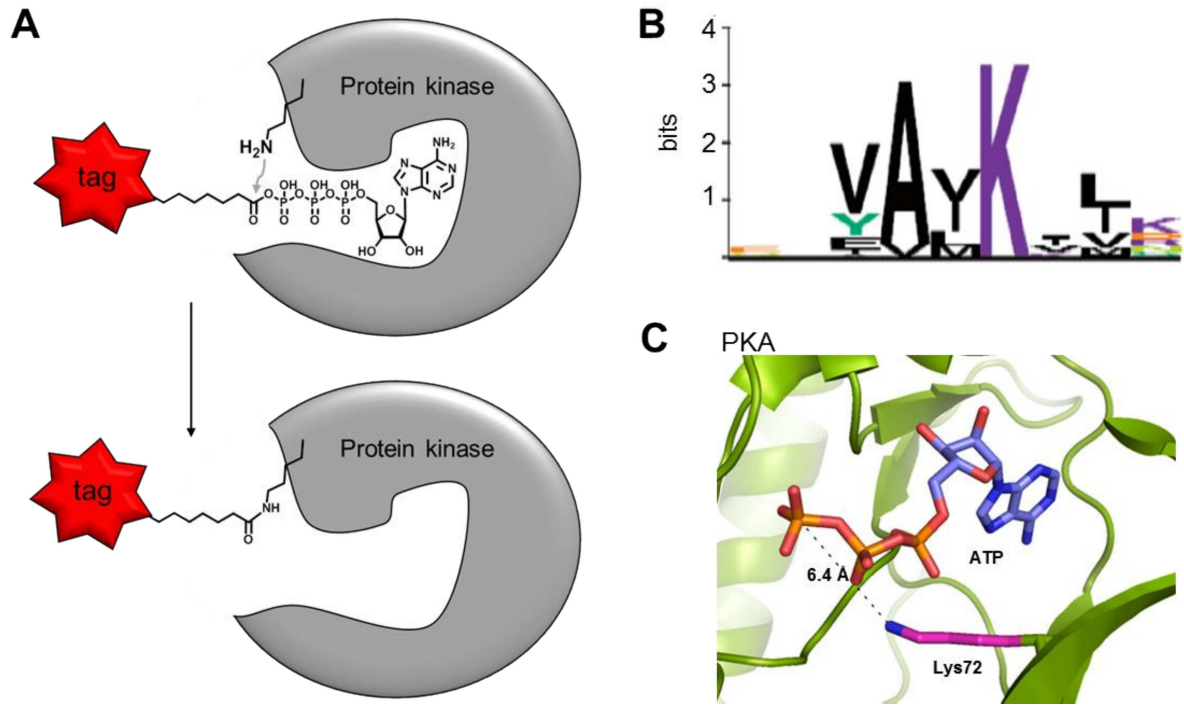

Figure 45: **A)** Mechanism of labeling with acyl phosphate probes. Probes consist of ATP that is modified into an acyl phosphate warhead, an alkyl linker and a reporter tag. The ATP entity is binding to the ATP-binding pocket of a protein, the nucleophilic ε-NH_2 from nearby lysine is attacking the acyl phosphate resulting in a covalent binding of the tag to the protein. **B)** Sequence logo representation (the size of each letter at a given position corresponds to the proportion of sequences, expressed in bits, containing this residue). Diagram shows the region of nine residues around the conserved lysine in the ATP binding loop based on an alignment of all protein kinases. **C)** Crystal structure of Protein Kinase A (PKA) in complex with ATP. Catalytic lysine (Lys72) is shown in magenta. The ε-NH_2 is about 6.4 Å away from the γ-phosphate of ATP. (This figure was made using Protein Data Bank coordinates for Protein Kinase A (4DH1).[142])

For a global analysis of ATP-dependent enzymes within the *Arabidopsis* proteome, a set of acyl phosphate probes on the basis of ATP were therefore synthesized (Table 5).[105]

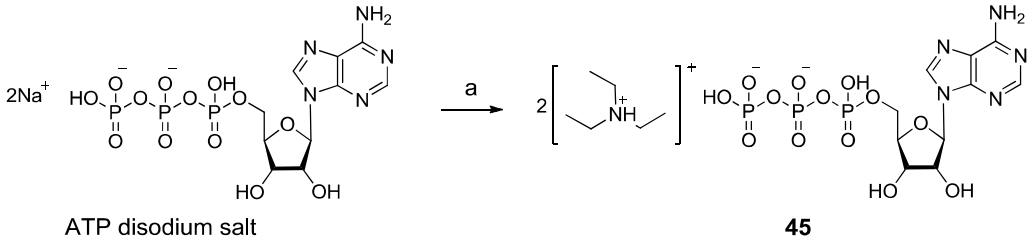

Scheme 10: Cation exchange of disodium ATP. a) DEAE Sephadex A-25, $NHEt_3CO_3$

To this end, the protocol of Patricelli and coworkers was essentially followed.[105] The synthesis of the corresponding probes starts with a cation exchange of disodium ATP to enhance the ATP solubility in organic solvents. To this end, the commercially available disodium salt of ATP was converted to the triethyl ammonium salt **45** by passing it through an ion-exchange column packed with DEAE-Sephadex A-25. The ATP disodium salt was applied to this column and eluted with 0.5 M $NH(Et)_3CO_3$. The fractions containing ATP-$NH(Et)_3^+$ were pooled and lyophilized to form a white solid (*Scheme 10*).

As a first ATP probe derivative, a biotin-tagged derivative was synthesized. To this end, a linker was attached to biotin, resulting in **48** after coupling and methyl ester hydrolysis (*Scheme 11*). To minimize the steric influence of biotin as a reporter tag, 6-aminohexanoic acid was introduced as an additional spacer.

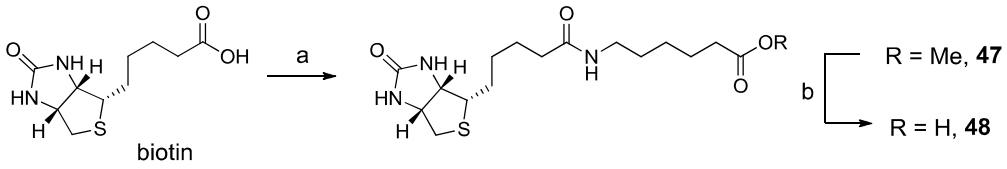

Scheme 11: Synthesis of biotinyl-linker **48**. a) **46**, HBTU, HOBt, TEA, DMF, rt, 0.5 h, 85%. b) LiOH, H_2O, MeOH, 0°C→rt, 1 h, 99%.

48 was then coupled with previously prepared ATP compound **45**, thereby yielding compound **49** (*Scheme 12*).

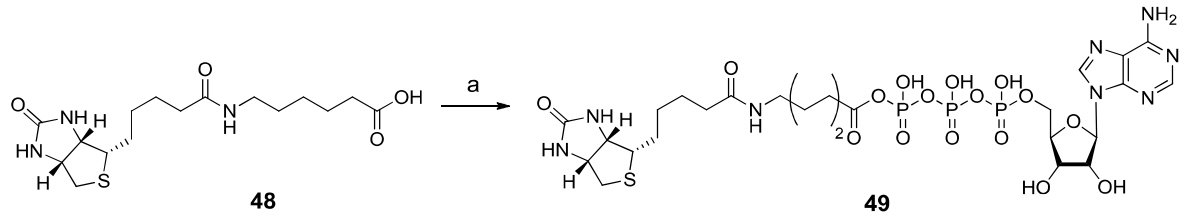

Scheme 12: Synthesis of BHAcATP (**49**). a) TEA, IBCF, **45**, dioxane/DMF/DMSO, 0°C→rt, 20 h, 6%.

The crude acyl phosphate **49** was then purified manualy by RP-C_{18} silica gel using water as eluent. The manual purification became necessary as HPLC purification of **49** led to decomposition of the desired product.

By a simple exchange of the last acylation step (*Scheme 12*), four additional acyl phosphate probes (**49**-**52**) were successfully synthesized. Altogether, three different types of reporter tags were introduced into the ATP probes: a biotin-tagged derivative (**49**), two fluorophore-tagged derivatives (**51**, **52**) and an alkyne tagged version (**50**) have been developed successfully by adapting the synthetic route of Patricelli (*Table 5*).[105]

Table 5: Chemical structures of synthesized acyl phosphate probes.

Chemical structure	Cpd (type of tag)
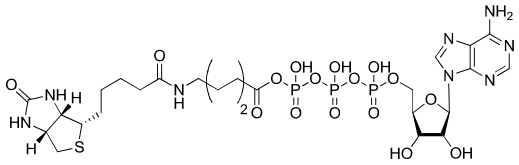	**49** *(biotin-tag)*
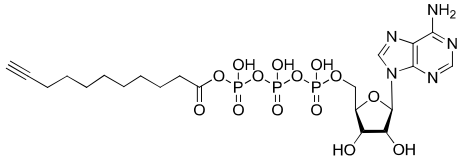	**50** *(click-tag)*
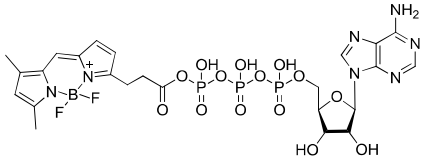	**51** *(fluorescence-tag)*
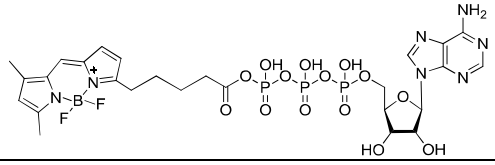	**52** *(fluorescence-tag)*

With the bodipy-tagged probes **51** & **52**, a direct visualization after labeling is possible whereas the biotin-tagged version **49** needs to be blotted and the alkyne-tagged probe **50** is only effective when a two-step ABPP experiment is executed. In a very first experiment, the

reactivity of the acyl phosphate towards the ε-amine of lysine was evaluated. Therefore, a 0.2 mM solution of probe **49** was incubated with salt-free lysine (1 mM) in water. After one hour, samples were taken and subjected to the LC-MS. MS and MS/MS spectra of the precursor ion were recorded (*Fig. 46*). This revealed that after one hour (which represents approximately the incubation time used in biological experiments) most of the probe **49** was converted to the lysine acylation product. This proves the general reactivity of acyl phosphates towards lysine side chain residues. It however also raises the question if not any lysine residue located at the surface of proteins might be reactive enough to react with acyl phosphate probes.

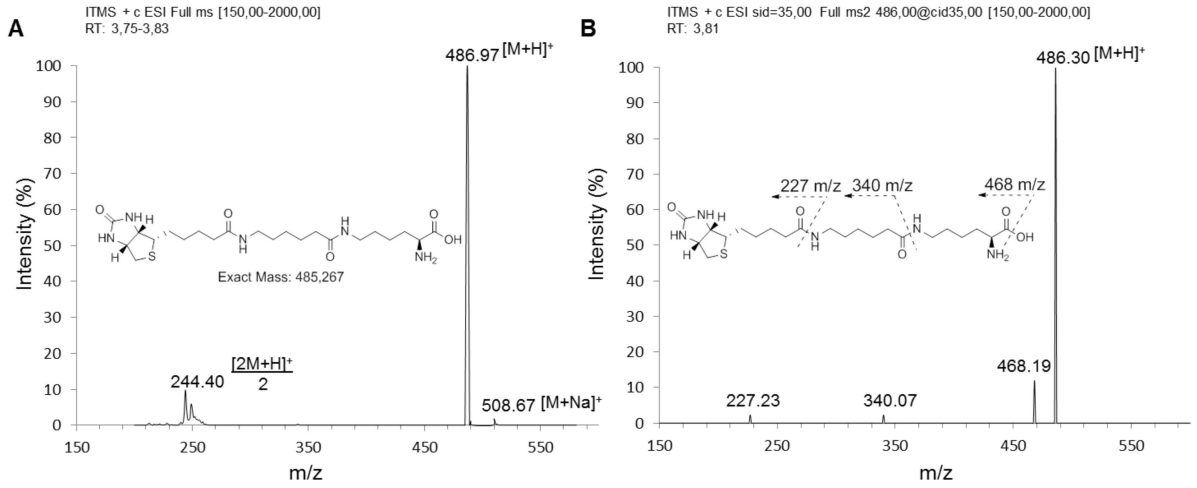

Figure 46: Analysis of acylation of L-lysine with **49**. (**A**) Positive ESI-MS spectrum of the acylation product after LC. (**B**) MS/MS spectrum of the precursor ion (486 m/z) resulted in three different fragmentations.

In collaboration with the van der Hoorn group (MPI Cologne), the labeling pattern of each probe was therefore evaluated in biological ABPP experiments. In Figure 47 is shown the typical labeling profiles of the acyl phosphate probes **49-52**. Coomasie brilliant blue (CBB) staining indicates the equal loading. In each experiment, *Arabidopsis* leaf extracts were labeled with probes **49-52**, respectively. In case of probe **49**, the biotinylated proteins were detected on protein blots using streptavidin HRP. For probe **50**, a two-step ABPP experiment was performed and the probe-labeled proteome was incubated in a second step with the "click-reagents" (Cu(I), TBTA, TCEP) and a trifunctional reporter tag (Tri-N_3) including a biotin and an additional rhodamine as reporter tags (which makes a bifunctional detection possible - either Strep-HRP blot or direct in-gel fluoresecence scanning, *Fig 47B,C*). The labeling profile of the bodipy-tagged probes **51** and **52** could be easily detected by direct in-gel fluorescence scanning.

Figure 47A shows a characteristic labeling profile of **49** in *Arabidopsis* leaf extracts. It can be seen that a wide range of proteins are adressed by the biotinyl-tagged acyl phosphate probe **49**, as expected from the fact that the ATP-binding cleft within ATP-binding proteins is highly conserved. Figure 47B shows the labeling profile of the alkyne-tagged probe **50** detected by Western-blot and Figure 47C shows the same labeling profile detected by in-gel fluorescence scanning. Again, a widespread labeling was observed, although not as strong as for the biotinyl-tagged probe **49**. A comparison of these labeling patterns with those of the two bodipy-tagged probes which only differed in the length of their linker region, showed interesting results (*Fig. 47C, D*): Only the probe with the shorter alkyl-chain **51** produced a comparable labeling pattern with the probe **49** (biotin) and **50** (alkyne). In contrast, probe **52** did not display labeling which cannot be explained easily and would require further investigations.

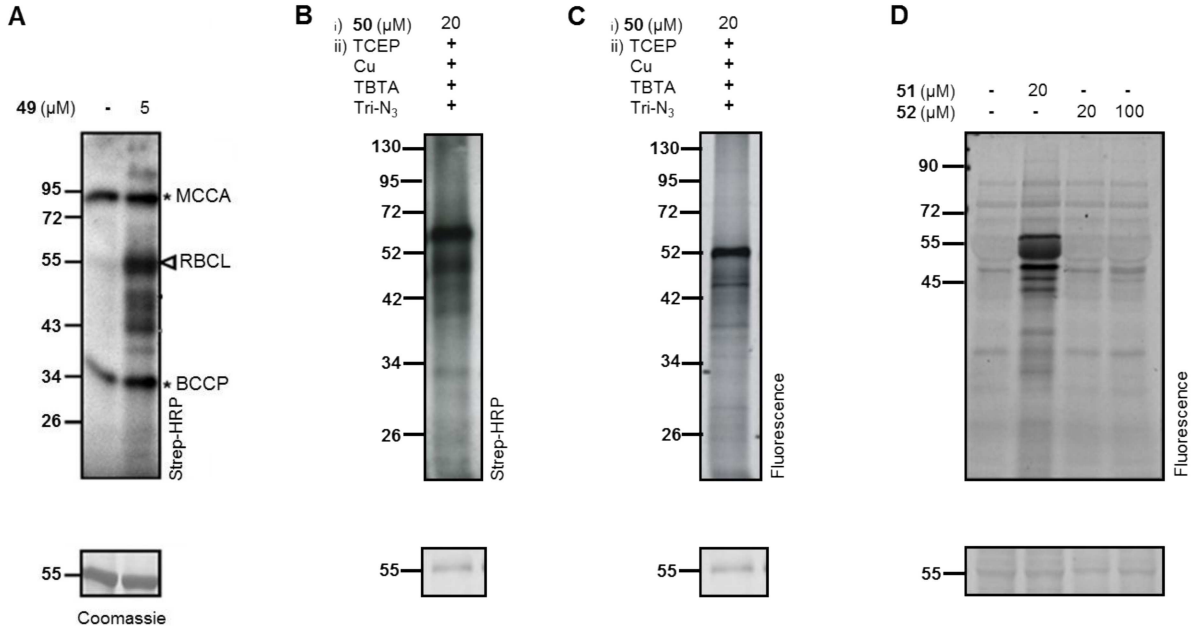

Figure 47: Labeling patterns produced from acyl phosphate probes **49**, **50**, **51** and **52** on *Arabidopsis* leaf extracts. (**A)** Labeling profile of **49** (MCCA = 3-methylcrotonyl-CoA carboxylase, RBCL = ribulose-1,5-bisphophate carboxylase oxygenase, BCCP = biotin carboxyl carrier protein) **(B)** Labeling profile of probe **50** after "click-reaction" using Strep-HRP blot for detection. **(C)** Labeling profile of probe **50** after "click-reaction" using in-gel fluorescence scanning for detection. **(D)** Labeling profile of probe **51** and **52** using in-gel fluorescence scanning for detection. (Labeling experiments performed by Joji Villamor, MPI Cologne)

Next, different labeling conditions were tested with probe **49** (*Fig. 48*). The labeling pattern of **49** towards an increasing concentration demonstrated that probe labeling is optimal using

probe concentrations below 60 µM. Higher probe concentrations instead led to massive labeling that hampers any assignment of signals (*Fig. 48A*).

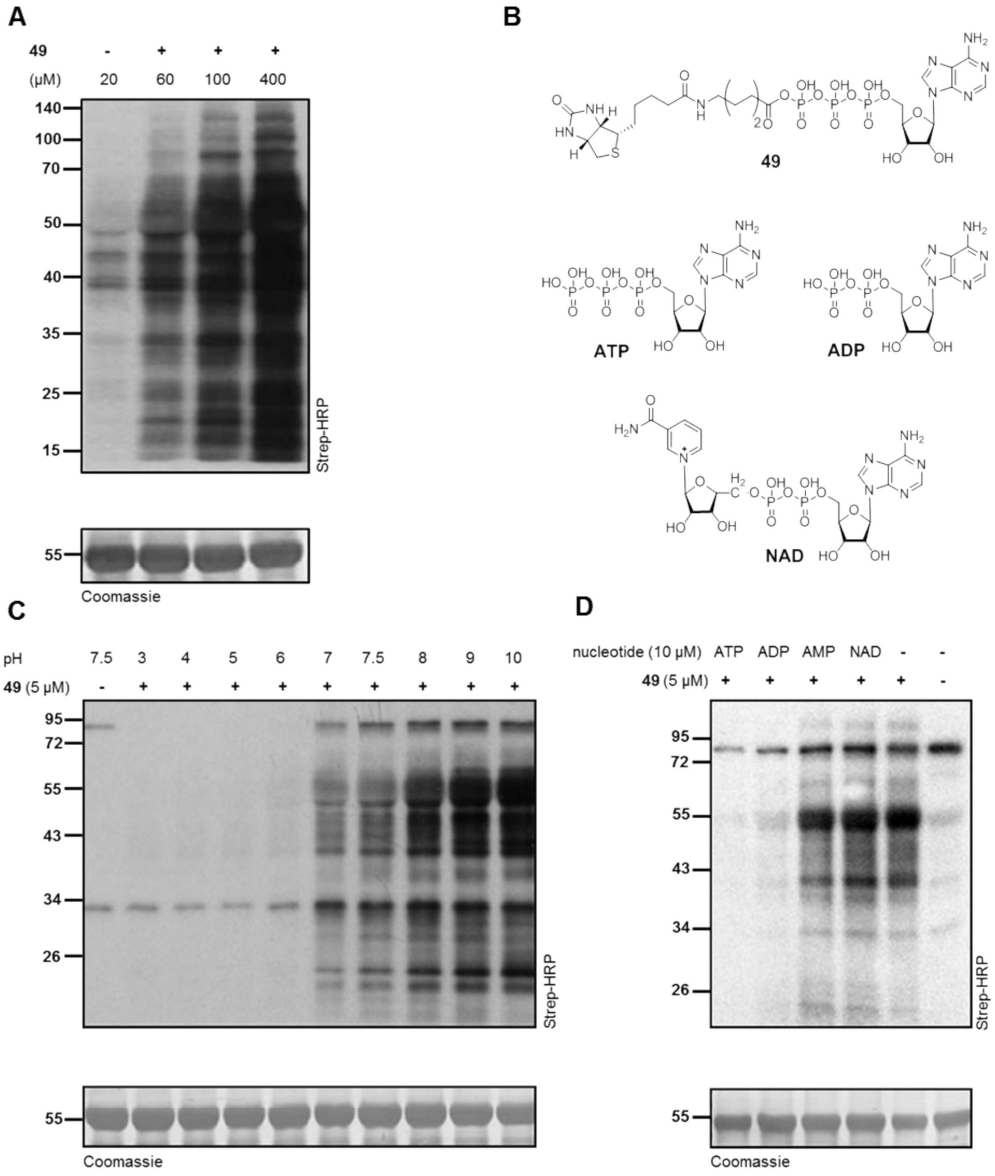

Figure 48: Labeling pattern of probe **49** depends on conditions. **(A)** Labeling patterns of probe **49** in relation to probe concentration. **(B)** Chemical structures of probe **49**, ATP (Adenosine-5'-triphosphate), ADP (Adenosine-5'-diphosphate), AMP (Adenosine-5'-monophosphate) and NAD^+ (Nicotinamide adenine dinucleotide). **(C)** pH-dependency of labeling with probe **49**. **(D)** Probe (**49**)-labeling was competed with ATP and ADP, but not with AMP and NAD. (Adapted and modified from Villamor *et al.*[143])

In subsequent experiments, a probe concentration of 5 µM was used. First, the pH-dependency regarding probe-labeling was investigated. To this end, the *Arabidopsis* leaf extracts were labeled with **49** at various pH levels (*Fig. 48C*). This revealed that labeling with

49 is strongly pH dependent. At acidic pH, only weak or even no labeling was observed, while intense labeling occurs at neutral to basic pH (*Fig. 48C*).

In a second competitive ABPP experiment, a suppression of labeling with probe **49** by various nucleotides was investigated (*Fig. 48B, D*). This experiment series disclosed that a pre-incubation of ATP suppressed labeling of **49** very efficiently. Interestingly, also ADP could outcompete probe-labeling, whereas AMP and NAD^+ could not. This evidenced that ATP-binding proteins were susceptible for labeling with probe **49** and that the ATP-binding pocket has most likely been addressed. This demonstrated that the labeling event was selective.

Finally, probe **49** was used in pull-down experiments in *Arabidopsis* leaf extracts using streptavidin beads to enrich probe-labeled proteins followed by gel-electrophoresis, trypsin digest and LCMS/MS analysis to identify the probe-labeled proteins. From this procedure, in total 112 proteins could be identified from *Arabidopsis* leaf extracts incubated with probe **49**. 13 of these proteins were also detectable in the no-probe-control as background signals. Some of them were endogenously biotinylated proteins such as MCCA (3-methylcrotonyl-CoA carboxylase) at 80 kDa or BCCP (biotin carboxyl carrier protein) at 34 kDa (*Fig. 47A*). All 112 detectable proteins were selected by spectral counts which revealed that the significant signal in the region of 55 kDa is attributed to the labeling of a subunit of the chloroplastic ATPase (ATPB) and the large subunit of ribulose-1,5-bisphophate carboxylase oxygenase (RBCL) (*Fig. 47A*). The majority of all detectable proteins were ATP-binding proteins like RBCL. It emerged that only 21 of the total 112 labeled proteins could be assigned to protein kinases, including receptor-like kinases (RLKs), MAP kinases (MPKs) and calcium dependent kinases (CPKs). Since there are more than 1000 protein kinases encoded by the *Arabidopsis* genome, this represents a rather tiny section that was labeled by probe **49**.[5] This may be caused by several reasons. One reason could be that not all protein kinases were expressed in the analyzed tissue (here: leaf). However, the analysis of labeling sites using protein databases showed that the biotinylated probe **49** targets predominantly but not exclusively the ATP binding pockets of a broad range of protein kinases and other unrelated ATP binding proteins.

Overall, these results demonstrate that the probes **49-52** generally compile a powerful toolbox to study and identify ATP binding activities in native plant proteomes, which has not been done before. Future studies could involve, for example the identification of selective inhibitors of *Arabidospis* kinases or to study the activation of kinases upon external stimuli by using the probes **49-52**.

5. SUMMARY AND OUTLOOK

During this PhD project, syntheses of small molecule modulators for functional chemical biological investigations in plants were accomplished. Two different approaches were thereby followed:

In the first approach and main project of this thesis, chemical syntheses of bioactive plant growth-modulating natural products and their subsequent evaluation as potential chemical probes to decipher root growth biology were successfully performed.

In this context, the first total synthesis of the natural product Rotihibin A (**1**) was successfully achieved (c.f. *Chapter 4.1*). This lipopeptidic natural product features a vast array of non-proteinogenic amino acids and the natural product **1** was described in literature as a potent root-growth inhibitor. The developed first total synthesis of Rotihibin A (**1**) was based on a solid phase synthesis after previous amino acid building block generation and allowed to confirm the previous structural assignment. After confirmation of the reported bioactivity via bioassays using living plants, a whole set of Rotihibin A derivatives (**15**-**24**) for structure-activity relationship studies was synthesized by the developed synthetic route. In these studies, several structural features with a critical role for bioactivity could be revealed. Moreover, assays with different *Arabidopsis* reporter lines and cell-based assays demonstrated that Rotihibin A (**1**) impairs root growth via inhibiton of cell mitosis. These studies therefore open the possibility to generate chemical probes for protein target identification in the future.

In a second project, a focused library of derivatives of the Brevicompanine natural product family was successfully generated (compounds **25**-**30**). The Brevicompanines belong to a natural product class that are characterized by a **h**exahydro**p**yrrolo**i**ndole (HPI) moiety, derived from L-tryptophan, which undergoes a diketopiperazine formation with a second amino acid residue.

The chemical synthesis of these compounds was succeffully achieved via a heteroatom-mediated intramolecular selenocyclization followed by an allylic transposition and finally the formation of the diketopiperazine (c.f. *Chapter 4.2*). The biological evaluation of this compound series was executed in cooperation with the Kombrink group (MPI Cologne). In these studies, the synthesized compounds showed root growth inhibition properties reminiscent of cytokines. The best inhibitory activity showed compound **26**. The corresponding structure-activity-relationship studies furthermore revealed that growth

inhibition required a D-configured amino acid within the diketopiperazine heterocycle. The determined structure-activity relationships then allowed the generation of a series of first photoaffinity- and alkyne-tagged Brevicompanine derivatives **37** and **44** usable for target identification studies. Although the subsequent target identification studies did not yet result in the elucidation of a target, they nevertheless demonstrated the general feasibility of such an approach. In future studies, an optimization of pull-down procedures as well as the generation of structurally alternative natural product-based probes can be envisioned to finally elucidate the cellular target.

In the second approach, activity-based probes were synthesized to expand the scope of ABPP approaches in plants (c.f. *Chapter 4.3*). To this end, diverse acyl-phosphate probes **49-52** with different reporter groups for profiling protein kinases and other ATP binding proteins in plants were successfully synthesized. These probes entail an ATP-derivative which is modified with a reactive acyl phosphate group at the γ-phosphate followed by a reporter-tag. This type of probes was shown to act by binding to the P-loop of ATP-binding proteins. At this binding site, the acyl-phosphate probes are nucleophilically attacked by a conserved lysine residue, resulting in a transfer of the reporter group onto the lysine residue and thus irreversible ATPase inhibition and covalent labeling of the enzyme. The synthesized acyl phosphate probes were utilized to launch a new approach to explore the ATP-binding proteome of the model plant *Arabidopsis thaliana*. The biological evaluation of all probes were performed in cooperation with the van der Hoorn group (MPI Cologne). However, the labeling pattern of all acyl phosphate probes showed a comparable broad-range labeling, since all ATP-binding proteins should be susceptible to these probes. By using the biotinylated acyl phosphate probe **49** in ABPP and pull-down approaches, the first in-depth analysis of targets in a plant proteome was possible. The labeled proteins include a few well-characterized ATP-binding proteins, and many ATP-binding proteins that have not been studied so far. A total of 112 proteins, of which 21 were protein kinases, were identified in the labeling experiments while only 13 of these proteins were also identified in the no-probe-control. The analysis of labeling sites using the protein database showed that the biotinylated probe **49** targets predominantly but not exclusively the ATP binding pockets of a broad range of protein kinases and other unrelated ATP binding proteins. These studies therefore demonstrated that the acyl-phosphate probes **49-52** generally compile a powerful toolbox to study and identify ATP binding activities in native plant proteomes. .

6. ZUSAMMENFASSUNG UND AUSBLICK

Im Rahmen dieser Dissertation wurden chemische Synthesen von niedermolekularen Modulatoren zur Durchführung von chemisch-biologischen Ansätzen in Pflanzen entwickelt. Dazu wurden zwei verschiedene Strategien verfolgt.

Bei dem ersten Ansatz und Hauptprojekt dieser Dissertation wurden chemische Synthesen von bioaktiven Pflanzenwachstums-modulierenden Naturstoffen und deren nachfolgende biologische und biochemische Evaluierung erfolgreich durchgeführt.

In diesem Zusammenhang wurde eine erste erfolgreiche Totalsynthese des Naturstoffes Rotihibin A (**1**) realisiert (vgl. *Kapitel 4.1*). Dieser lipopeptidische Naturstoff besteht aus einer Vielzahl von nicht-proteinogenen Aminosäuren und wurde in der Literatur als potenter Hemmstoff für das Wurzelwachstum bei Pflanzen beschrieben. Die Totalsynthese wurde nach vorangegangener Bausteinsynthesen an der festen Phase mittels Fmoc-Strategie erfolgreich abgeschlossen. Dabei wurde auch gleichzeitig die vorher nur mittels Spektroskopie bestimmte Struktur und Stereochemie des isolierten Naturstoffes bestätigt. Nachdem die beschriebene Bioaktivität in Bioassays reproduziert werden konnte, wurde eine kleine Substanzbibliothek von Rotihibin A-Derivaten (**15**-**24**) für Struktur-Wirkungsuntersuchungen unter Verwendung der vorher etablierten Synthese generiert. In diesen Untersuchungen konnten mehrere strukturelle Eigenschaften des Naturstoffes identifiziert werden, die essentiell für den Erhalt der Bioaktivität sind. Des Weiteren konnte unter Heranziehung verschiedener transgener *Arabidopsis* Reporter-Linien und zellbasierter Assays gezeigt werden, dass Rotihibin A (**1**) die Hemmung des Wurzelwachstums über eine Inhibition des mitotischen Zellzyklus erreicht. Zukünftige Arbeiten können nun die aus diesen Studien gewonnenen Struktur-Wirkungsbeziehungen ausnutzen, um entsprechende bioaktive Naturstoff-basierte Sonden zur Aufklärung der molekularen Zielproteine von Rotihibin A (**1**) zu generieren.

Ergänzend hierzu wurde des Weiteren eine Synthese einer fokussierten Bibliothek von Derivaten (**25**-**30**) der Brevicompanin-Naturstoffklasse (vgl. *Kapitel 4.2*) durchgeführt. Diese Naturstoffklasse zeichnet sich strukturell durch ein an der C3-Position revers-prenyliertes **H**exahydro**p**yrrolo[2,3-*b*]**i**ndol (HPI)- Grundgerüst aus, welches aus einem L-Tryptophan abgeleitet werden kann. Die HPI-Aminosäure bildet dann mit einer weiteren Aminosäure ein Diketopiperazinderivat. Die erfolgreiche chemische Synthese dieser Verbindungen gelang mittels einer Heteroatom-vermittelten, intramolekularen Selenocyclisierung, gefolgt von einer

reversen Prenylierung und schließlich der Bildung des gemischten Diketopiperazins. Die biologische Evaluierung dieser so erstellten Verbindungsbibliothek (**25**-**30**) wurde in Kooperation mit der Arbeitsgruppe von Erich Kombrink (MPI Köln) realisiert. Dabei zeigten diese Verbindungen Wurzelwachstums-hemmende Eigenschaften, wobei Verbindung **26** die stärkste inhibitorische Aktivität zeigte. In diesen Studien konnte des Weiteren gezeigt werden, dass eine Aminosäure mit D-Konfiguration innerhalb des Diketopiperazin-Heterozyklus sich günstig auf die biologische Aktivität auswirkte. Die so gewonnen Struktur-Wirkungsbeziehungen konnten direkt in der Generierung von Photoaffinitäts- und Alkin modifizierten Brevicompanin-Derivaten (**37**, **44**) für die Zielproteinidentifizierung umgesetzt werden. Leider gelang bisher jedoch noch keine Aufklärung des molekularen Targets. Zukünftige Arbeiten müssten diesbezüglich eine Optimierung der Pull-down Strategien anstreben oder die Synthese von Brevicompanin-Sonden mit besseren Bioaktivtäten beinhalten, um abschließend die zellulären Zielproteine der Brevicompanin-Naturstoffklasse aufzuklären.

In einem zweiten aktivitäts-basierten Ansatz wurden neuartige molekulare Sonden für die aktivitäts-basierte Proteinprofilierung in Pflanzen synthetisiert (vgl. *Kapitel 4.3*). Dazu wurden verschiedene Acyl-Phosphat-Sonden (**49**-**52**) generiert, um Kinasen und andere ATP-bindene Proteine in *Arabidopsis thaliana* zu studieren. Diese Sonden basierten auf ATP, welches am γ-Phosphat mit einem reaktiven Acyl-Phosphatrest und mit verschiedenen Reportereinheiten versehen wurden. Für diese Art von Sonden wurde bereits gezeigt, dass sie an die P-Schleife (die Phosphat-bindene Schleife) von ATP-bindenen Proteinen binden. An dieser Phosphat-bindenen Kavität befindet sich in vielen ATP-bindenen Proteinen ein konserviertes Lysin. Dieses Lysin greift nukleophil das Acyl-Phosphat der Sonden an, wodurch die Reportereinheit kovalent auf den Lysinrest übertragen wird. Dadurch werden diese Enzyme kovalent markiert und die ATPase-Aktivität der jeweiligen Enzyme gleichzeitig inhibiert. Diese neu synthetisierten Acyl-Phosphat-Sonden wurden dann dazu benutzt, einen neuen chemisch-biologischen Ansatz zu entwickeln, um das ATP-bindene Proteom der Modellpflanze *Arabidopsis thaliana* zu untersuchen. Die biologische Evaluierung dieser Sonden wurde von der Arbeitsgruppe um R. van der Hoorn (MPI Köln) durchgeführt. Die Markierungsmuster aller synthetisierten Sonden (**49**-**52**) zeigten, dass eine Vielzahl von Enzymen für Sonden dieser Art zugänglich war. Diese Tatsache entsprach den Erwartungen, dass prinzipiell alle ATP-bindenen Proteine durch diese Art von Sonden adressierbar sind. Durch die Verwendung der biotinylierten Acyl-Phosphatsonde **49** in ABPP und pull-down Experimenten konnte eine erste eingehende Analyse der für die Sonde

zugänglichen ATP-bindenen Proteine in Pflanzenproteomen berichtet werden. Die markierten Proteine beinhalteten einige gut charakterisierte ATP-bindene Proteine und viele weitere ATP-bindende Proteine, die bis jetzt noch für keine Studien zugänglich waren. Insgesamt wurden in diesem chemisch-biologischen Ansatz 112 Proteine, davon 21 Proteinkinasen, als Zielproteine der Acyl-Phosphatsonde **49** in Pflanzen identifiziert. Die Analyse der genauen Bindungsstelle der Sonde **49** ergab, dass hauptsächlich die ATP-Bindungstaschen (P-Schleife) modifiziert wurden. In diesen Studien stellten sich solche Acyl-Phosphat-Sonden daher als besonders hilfsreiches chemisches Werkzeug für das Studium des ATP-bindenen Proteoms in Pflanzen dar.

7. EXPERIMENTAL PART

7.1 General methods and instruments

Chemicals

All chemicals were purchased from Alfa Aesar, Acros, ABCR, Senn Chemicals, Bachem, Carl Roth, Fluka, TCI chemicals, Merck, Novabiochem, Riedel de Haen, Iris, Roth, Invitrogen, or Sigma-Aldrich and were used without any further purification. Anhydrous solvents in the highest available quality were purchased from the same suppliers.

Thin layer chromatography (TLC)

TLC was performed on Merck aluminum pre-coated silica gel plates (20 × 20 cm, $60F_{254}$). Spots were detected using UV irradiation at 254 nm or by soaking the TLC plates with developing solution A or B. Subsequently, the TLC plates were heated to visualize the respective spots. Eluents and R_f values are given in the particular experimental description. Reversed-phase TLC was carried out on Merck aluminum pre-coated silica gel plates (60 RP-18 F_{254S}) utilizing UV irradiation at 254 nm or the following developing reagents to visualize the spots.

Developing solution A: 20 g of phosphomolybdic acid hydrate in 80 mL ethanol

Developing solution B: 1.5 g $KMnO_4$, 10 g K_2CO_3 and 1.25 mL of 10% aq. NaOH in 200 mL water

Silica gel flash liquid chromatography

Column chromatography purifications were performed with silica gel from Acros (particle size 35-70 µm). Reversed-phase chromatography was performed with LiChroprep RP-18 (40-63 µm) from Merck.

Reactions under inert atmosphere using balloon technique

In order to run air or moisture sensitive reactions, all glassware was thoroughly dried in an oven at 100 °C for 12 h. Next, the flasks were evacuated from air in the vacuum and flushed by argon gas. This was carried out using a two-way vacuum line or by an argon-filled balloon. An argon filled balloon that was connected to the flask via a septum was also used to provide the necessary pressure compensation for reactions under inert atmosphere.

Reversed-phase liquid chromatography - electrospray ionization mass spectrometry (LC-MS)

LC-MS analyses were performed on a LC-MS system from Thermo Scientific with an Eclipse XDB-C18 (5 µm) column from Agilent (peak detection at 210 nm) and a Thermo Scientific LCQ Fleet^{TM} ESI-Spectrometer. For positive mode measurements, a linear gradient of solvent B (0.1% formic acid in acetonitrile) in solvent A (0.1% formic acid in water) was used at 1 mL/min flow rate. For negative mode measurements, a linear gradient of solvent C (5 mM NH_4OAc in acetonitrile) in solvent D (5 mM NH_4OAc in H_2O) at 1 mL/min flow rate was employed.

Gradient for positive mode: 0 min / 10% B → 1 min / 10% B → 10 min / 100% B → 12 min / 100% B → 15 min / 10% B
Gradient for negative mode: 0 min / 10% C → 1 min / 10% C → 10 min / 100% C → 12 min / 100% C → 15 min / 10% C

Preparative reversed-phase high performance liquid chromatography (prep HPLC)

Purification of the compounds was carried out on a Shimadzu HPLC system (Prominence UFLC) with a RP-C_{18}-column from Phenomenex (Phenomenex Luna® 5 µm C18(2), 100 x 21.20 mm)) and peak detection at 210 and 254 nm. Linear gradients of solvent B (0.1% TFA in acetonitrile) in solvent A (0.1% TFA in water) were applied at a 25 mL/min flow rate.

Freeze drying

Freeze-drying or lyophilisation was conducted with a Freeze Dryer ALPHA 2-4 LD plus (CHRIST). To this end, an aqueous solution of the substance was frozen separately in round-bottom flasks using liquid nitrogen. As the time required for the drying process is affected by the thickness of the ice layer, the samples were frozen under rotation which leads to the formation of a thin uniform ice layer inside the glass vessel. Thus frozen samples were submitted to the freeze dryer. The samples were usually completely lyophilized after 24 h.

Nuclear magnetic resonance spectroscopy (NMR)

Nuclear magnetic resonance (NMR) spectra were recorded on a Bruker Avance II 400 system (400 MHz for ^{1}H- and 100 MHz for ^{13}C-NMR) or a Bruker Avance II 700 MHz system (700 MHz for ^{1}H and 176 MHz for ^{13}C-NMR). ^{1}H NMR spectra are reported in the following manner: chemical shifts (δ) in ppm calculated with reference to the residual signals of undeuterated solvent, multiplicity (s, singlet; d, doublet; t, triplet; dd, doublet of doublet; dt, doublet of triplet; m, multiplet; b, broad signal), coupling constants (J) in Hertz (Hz), and number of protons (H).

Optical rotation

Optical rotations were measured with a Polartronic universal polarimeter from Schmidt + Haensch. The concentrations (given in g/100 ml) and the solvent used are given with the respective experimental data. The wavelength of the light is 589 nm (the sodium D line).

$$[\alpha]_{\lambda}^{T} = \frac{\alpha}{l\,x\,c} \qquad [1]$$

l = length of the cuvette in decimeter

$_C$ = concentration (g/100 ml)

λ = wavelength (typically: 589 nm)

T = temperature (typically: 20 °C)

7.2 Synthesis of Rotihibin A and derivatives

7.2.1 Syntheses of building blocks

(*Z*)-methyl dec-2-enoate (7):

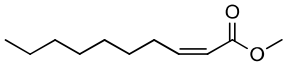

7

To a solution of methyl *P*,*P*-bis(2,2,2-trifluoroethyl)phosphonoacetate (1.272 g, 4 mmol) in anhydrous THF (16 ml) was added cautiously a solution of NaH (60% dispersion in mineral oil, 224 mg, 5.6 mmol) in dry THF (4 ml) at -78 °C under argon atmosphere. This mixture was stirred for 15 min. at -78 °C, then octanal (512 mg, 4 mmol) dissolved in anhydrous THF (4 ml) was added. This mixture was stirred for 1 h at -78 °C. After TLC indicated completion of the reaction, saturated aqueous NH_4Cl solution (20 ml) was added and the quenched reaction mixture was warmed to rt. The product was twice extracted into diethyl ether. The organic layers were combined, dried over Na_2SO_4, filtered and evaporated. The resulting residue was purified by flash chromatography (SiO_2, CH/DEE 50:1).

Yield: 611 mg (3.6 mmol, 90%) as colorless oil, *ee* % E/Z 1:9 (by TLC)
TLC (CH/DEE = 20:1): $R_f = 0.43$
^{1}H NMR (400 MHz, $CDCl_3$): δ = 6.23 (dt, J = 11.5, 7.5 Hz, 1H), 5.76 (dt, J = 11.5, 1.7 Hz, 1H), 3.71 (s, 3H), 2.64 (qd, J = 7.5, 1.7 Hz, 2H), 1.30 (dd, J = 12.1, 6.8 Hz, 10H), 0.91 – 0.87 (m, 3H)
^{13}C NMR (101 MHz, $CDCl_3$): δ = 167.06, 151.19, 119.28, 51.10, 31.93, 29.41, 29.24, 29.18, 22.77, 14.22

(*Z*)-dec-2-enoic acid (2):

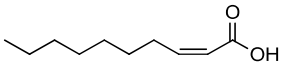

2

To a solution of **7** (132 mg, 0.72 mmol) in THF/MeOH (3:1, 8 ml) was added 1 M LiOH (2 ml, 2 mmol) at 0 °C. After this, the solution was allowed to warm to rt and was then heated up to 50 °C and stirred at this temperature for 5 h. The reaction was monitored by TLC (DEE/CH 1:20). The reaction mixture was diluted with 1 M HCl (10 ml) and extracted three times with DCM. The combined organic layers were dried (Na_2SO_4), filtered and concentrated under reduced pressure giving the title compound which was used in following steps without further purification.

Yield: 120 mg (0.71 mmol, 98%) as a colorless oil

^{1}H NMR (400 MHz, $CDCl_3$): δ = 6.35 (dt, *J* = 11.5, 7.6 Hz, 1H), 5.83 – 5.75 (m, 1H), 2.66 (qd, *J* = 7.5, 1.7 Hz, 2H), 1.39 – 1.18 (m, 10H), 0.88 (t, *J* = 6.9 Hz, 3H)

^{13}C NMR (101 MHz, $CDCl_3$): δ = 171.34, 153.73, 118.95, 31.91, 29.37, 29.22, 29.10, 27.08, 22.78, 14.22

LC-MS (ESI): t_R = 9.28 min, calcd. for $C_{10}H_{17}O_2^-$ $[M-H]^-$: 169.12, found 169.54

Fmoc-D-Cit-OH (3):

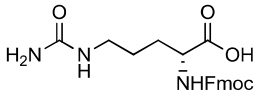

3

H-D-Cit-OH (500 mg, 2.85 mmol) was dissolved in water (10 ml) and $NaHCO_3$ (479 mg, 5.7 mmol) was added under stirring. The resulting solution was cooled to 0 °C and Fmoc-OSu (1.44 g, 4.28 mmol) was slowly added as a solution in dioxane (10 ml). The resulting solution was stirred at 0 °C for 1 h and allowed to warm to rt while stirring overnight. Subsequently, water (10 ml) was added and the aqueous layer was extracted twice with EtOAc. The organic layer was re-extracted twice with sat. $NaHCO_3$. The combined aqueous layers were acidified to a pH of 1 by addition of 1 N HCl and then extracted three times with EtOAc. The combined organic layers were dried (Na_2SO_4) and concentrated. The obtained residue was purified by flash chromatography (SiO_2, DCM/MeOH 9:1) which led to the desired product.

Yield: 0.953 g (2.4 mmol, 85%) as a colorless solid

TLC (DCM/MeOH = 9:1): $R_f = 0.2$

^{1}H NMR (400 MHz, $CDCl_3$): δ = 7.72 (d, J = 7.5 Hz, 2H), 7.61 – 7.51 (m, 2H), 7.35 (t, J = 7.4 Hz, 2H), 7.26 (td, J = 7.5, 1.1 Hz, 2H), 4.41 – 4.28 (m, 2H), 4.19 (dt, J = 13.8, 6.0 Hz, 2H), 3.09 (t, J = 6.7 Hz, 2H), 1.84 (td, J = 13.4, 7.9 Hz, 1H), 1.75 – 1.59 (m, 1H), 1.60 – 1.44 (m, 2H)

^{13}C NMR (101 MHz, $CDCl_3$): δ = 174.31, 160.31, 156.67, 143.78, 143.63, 141.19, 127.62, 126.98, 124.95, 119.83, 66.85, 57.55, 53.49, 47.03, 39.34, 29.29, 25.84

LC-MS (ESI): t_R = 7.70 min, calcd. for $C_{21}H_{24}N_3O_5^+$ $[M+H]^+$: 398.17, found 398.00

Boc-L-*allo*-Thr-OH (4):

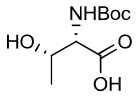

4

L-*allo*-Thr-OH (1 g, 8.38 mmol) was dissolved in 10% aqueous Na_2CO_3 (20 ml) and cooled to 0 °C in an ice-bath. A solution of Boc_2O in dioxane (20 ml) was added dropwise. The reaction mixture was allowed to warm to rt and stirred 16 h at ambient temperature. After that, all volatiles were removed using reduced pressure and the residue was taken up in EtOAc/1 N HCl (1:1, 50 ml). The organic layer was separated, dried over Na_2SO_4, filtered and concentrated.

Yield: 1.7 g (7.8 mmol, 93%) as a colorless glasslike solid

^{1}H NMR (400 MHz, $CDCl_3$): δ = 5.70 (s, 1H), 4.27 (d, *J* = 47.8 Hz, 1H), 4.16 (s, 1H), 1.43 (s, 9H), 1.32 – 1.22 (m, 3H)

^{13}C NMR (101 MHz, $CDCl_3$): δ = 174.00, 156.62, 85.35, 80.89, 69.33, 28.40, 27.54, 18.96

LC-MS (ESI): t_R = 2.76 min, calcd. for $C_9H_{16}NO_5^-$ $[M-H]^-$: 218.10, found 218.48

L-*threo*-β-hydroxyaspartic acid (8):

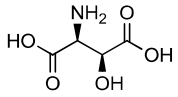

8

Enantioresolution of D,L-*threo*-β-*hydroxyaspartic acid*: Enantioresolution of D,L-*t*HyAsp was performed following the described method of Bionda and coworkers.[117] A racemic mixture of D,L-*t*HyAsp (purchased from TCI Deutschland GmbH) (2 g, 13.68 mmol) was dissolved in water (16 ml) by smooth heating (~40 °C). L-lysine in a salt-free form (1.96 g, 13.68 mmol) was subsequently added to this solution. After dissolution of all compounds, MeOH (13 ml) was added in small portions. The resulting mixture was slowly cooled to rt and then cooled to 4°C and kept overnight to crystallize. Precipitated crystals were filtered off, washed with a small amount of cold MeOH and recrystallized from water (10.6 ml) by addition of MeOH (8.6 ml). Crystals consisting of [L-Lys*L-*t*HyAsp] were collected by filtration and dried under reduced pressure. Subsequently, the ion-exchanger resin DOWEX 1x4-50 was loaded into a column and converted to the OH^--form by washing with 5 to 10 volumes of 1 M NaOH. The resin was thereby washed slowly to ensure that the whole washing procedure last at least 1 h. Next, the resin was washed with $H_2O_{(dest.)}$ until the pH of the eluent was neutral. Then, the resin was flushed with 1 N AcOH which converted the resin to its acetate form. The excess of acetic acid was rinsed off by applying $H_2O_{(dest.)}$ again until the pH was neutral. The previously obtained crystals were dissolved in water (2 ml) and applied on the ion-exchanger. Once L-Lys was eluted from the column by using 0.5 M AcOH as the eluent, the eluent was changed to 2 M AcOH to elute enantiomerically pure L-*t*HyAsp. Fractions containing L-*t*HyAsp were combined and evaporated yielding the title compound, which was used in the next steps without any further purification.

Yield: 0.64 g (4.3 mmol, 63 %) as a colorless solid

^{1}H NMR (400 MHz, DMSO): δ = 4.08 (d, J = 8 Hz, 1H), 3.82 (d, J = 8 Hz, 1H)

^{13}C NMR (101 MHz, DMSO): δ = 172.74, 168.57, 66.74, 54.02

Boc-L-*threo*-β-HyAsp(OMe)-OH (9):

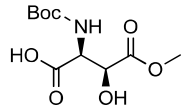

9

8 (135 mg, 0.73 mmol) was dissolved in a solution of concentrated HCl (120 µl) in MeOH (3 ml) at 0 °C. The reaction mixture was refluxed for 3 h, allowed to cool to rt and concentrated using reduced pressure. The crude product was dried under high vacuum and used without further purification in the following reaction. The free amine was dissolved in an aqueous solution of 10% Na_2CO_3 (3 ml) at 0 °C. Next, a solution of Boc_2O (0.488 g, 2.19 mmol) in dioxane (3 ml) was added dropwise and the resulting mixture was stirred at rt overnight. After removing all volatiles using a rotary evaporator, the residue was dissolved in EtOAc and washed with 1 N HCl. The organic layer was separated, dried (Na_2SO_4) and concentrated to dryness. The crude product was purified using flash chromatography (SiO_2, DCM/MeOH: 5:1) thereby yielding the title compound.

Yield: 194 mg (0.72 mmol, 98%) as colorless oil

TLC (DCM/MeOH = 5:1): R_f = 0.33 (smeary)

$[\alpha]^{22}_D$: +18 (*c* 1.00, MeOH)

^{1}H NMR (400 MHz, MeOD): δ = 4.73 (d, *J* = 1.9 Hz, 1H), 4.56 (d, *J* = 22.0 Hz, 1H), 3.75 (d, *J* = 11.5 Hz, 3H), 1.43 (s, 9H)

^{13}C NMR (101 MHz, MeOD): δ = 173.85, 157.58, 80.82, 72.51, 58.30, 52.88, 28.59

LC-MS (ESI): t_R = 5.16 min, calcd. for $C_{10}H_{17}NNaO_7^+$ $[M+Na]^+$: 286.09, found 286.63

Boc-L-*threo*-β-HyAsn-OH (10):

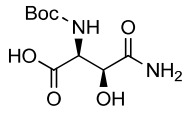

10

9 (250 mg, 0.95 mmol) was transferred to a 50 ml round bottom flask and dissolved in 7 M NH_3 in MeOH (20 ml). The flask was sealed properly using a septum and the solution was stirred for 4 days at rt until reaction was completed according to LC/MS analysis. The

reaction mixture was concentrated to dryness and used in the following steps without further purification.

Yield: 230 mg (0.93 mmol, 98%) as colorless oil
TLC (DCM/MeOH = 5:1): R_f = 0.3 (smeary)
[α]$^{22}_{D}$: -9 (*c* 1.00, MeOH)
^{1}H NMR (400 MHz, MeOD): δ = 4.67 (s, 1H), 4.52 (s, 1H), 1.43 (s, 9H)
^{13}C NMR (101 MHz, MeOD): δ = 178.06, 157.84, 80.71, 73.47, 66.82, 28.81
LC-MS (ESI): t_R = 3.92 min, calcd. for $C_9H_{16}N_2NaO_6^+$ $[M+Na]^+$: 271.09, found 271.90

Boc-L-*threo*-β-HyAsn-OBn (11):

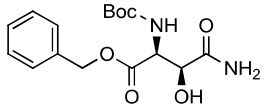

11

A solution of **10** (468 mg, 1.89 mmol) in DMF (10 ml) was cooled to 0 °C. Subsequently, the solution was treated with $NaHCO_3$ (317 mg, 3.77 mmol) and benzyl bromide (894 µl, 5.22 mmol). The resulting reaction mixture was stirred for 2 h at 0 °C and then for 24 h at rt. H_2O (50 ml) was added to quench the reaction. The obtained aqueous mixture was extracted three times with EtOAc. The organic layers were separated, combined and washed three times with H_2O. The organic layer was dried (Na_2SO_4), filtered and concentrated. Finally, the crude product was purified using flash chromatography (SiO_2, DCM/MeOH: 30:1) yielding the title compound.

Yield: 418 mg (1.24 mmol, 66%) as a colorless solid
TLC (DCM/MeOH = 9:1): R_f = 0.5
[α]$^{22}_{D}$: -18 (*c* 1.00, MeOH)
^{1}H NMR (400 MHz, MeOD): δ = 7.45 – 7.27 (m, 5H), 5.21 (s, 2H), 4.71 (d, *J* = 1.9 Hz, 1H), 4.57 (t, *J* = 10.1 Hz, 1H), 1.38 (s, 9H)
^{13}C NMR (101 MHz, MeOD): δ = 176.53, 172.03, 158.10, 137.12, 129.54, 129.26, 129.11, 80.93, 72.76, 68.25, 58.16, 28.62
LC-MS (ESI): t_R = 6.70 min, calcd. for $C_{16}H_{22}N_2NaO_6^+$ $[M+Na]^+$: 361.14, found 361.85

Fmoc-L-*threo*-β-HyAsn-OBn (12):

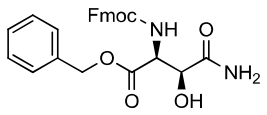

12

11 (400 mg, 1.18 mmol) was dissolved in 4 N HCl in dioxane (10 ml) and stirred for 2 h at rt. Next, all volatiles were removed using rotary evaporation. The obtained residue was dried under high vacuum for at least 2 h. The resulting solid was dissolved in H_2O (9 ml), $NaHCO_3$ (200 mg, 2.38 mmol) was added and the solution was cooled to 0 °C. To this solution was added Fmoc-OSu (616 mg, 1.82 mmol) as a solution in ice-cold dioxane (9 ml). The reaction mixture was stirred overnight at rt. Afterwards, the solution was diluted by addition of EtOAc (70 ml) and saturated aqueous $NaHCO_3$ (50 ml). The aqueous layer was separated and extracted three times with EtOAc. The organic layers were combined, dried (Na_2SO_4), filtered and concentrated. The resulting residue was dissolved in a minimum of 20% MeOH in $CHCl_3$ and the title compound precipitated by addition of cyclohexane.

Yield: 544 mg (1.18 mmol, >98%) as a white solid

TLC (DCM/MeOH = 19:1): $R_f = 0.3$

$[\alpha]^{22}_D$: -16 (*c* 0.80, $CHCl_3$)

^{1}H NMR (400 MHz, MeOD): δ = δ 7.80 (d, *J* = 7.7 Hz, 2H), 7.65 (d, *J* = 7.5 Hz, 2H), 7.40 – 7.26 (m, 9H), 5.26 – 5.17 (m, 2H), 4.66 – 4.62 (m, 1H), 4.36 (dd, *J* = 10.0, 6.7 Hz, 1H), 4.22 (m, 2H)

^{13}C NMR (101 MHz, MeOD): δ = 176.46, 171.75, 158.82, 145.27, 142.52, 137.10, 129.55, 129.26, 129.09, 128.78, 128.21, 126.36, 126.28, 120.89, 72.81, 68.33, 58.62

LC-MS (ESI): t_R = 8.33 min, calcd. for $C_{26}H_{25}N_2O_6^+$ $[M+H]^+$: 461.17, found 461.53

Fmoc-L-*threo*-β-HyAsn(Trt)-OBn (13):

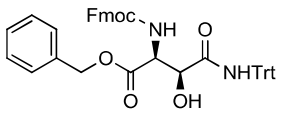

13

12 (544 mg, 1.18 mmol) and triphenylmethanol (3.07 g, 11.8 mmol) were suspended in acetic acid (10 ml) and heated to 50 °C. To this mixture, a catalytic amount of conc. H_2SO_4 (41 µl, 0.706 mmol) was added. The resulting muddy mixture was stirred at 50 °C for 2.5 h. After cooling to rt, the reaction mixture was diluted by addition of EtOAc (70 ml) and washed with a saturated, aqueous $NaHCO_3$ solution (100 ml). The organic layer was separated and the aqueous layer was extracted once more with EtOAc. The organic layers were combined, dried (Na_2SO_4), filtered and concentrated using rotary evaporation. The crude product was purified by flash chromatography (SiO_2, CH/EA: 5:1) yielding the desired product.

Yield: 608 mg (0.87 mmol, 74%) as a white solid

TLC (CH/EA = 2:1): $R_f = 0.3$

$[\alpha]^{22}_D$: -12 (*c* 0.93, $CHCl_3$)

^{1}H NMR (400 MHz, MeOD): δ = 7.82 – 7.72 (m, 2H), 7.75 – 7.58 (m, 2H), 7.41 – 7.13 (m, 24H), 5.21 (s, 2H), 4.82 (d, *J* = 2.1 Hz, 1H), 4.68 – 4.62 (m, 1H), 4.52 (dd, *J* = 13.2, 9.7 Hz, 1H), 4.17 (m, 2H)

^{13}C NMR (101 MHz, MeOD): δ = 172.19, 171.77, 158.93, 145.75, 145.32, 145.04, 142.56, 142.47, 137.09, 129.87, 129.54, 129.29, 129.23, 129.01, 128.91, 128.80, 128.74, 128.24, 128.12, 126.53, 126.22, 120.89, 73.42, 71.53, 68.59, 68.32, 58.63, 48.25

LC-MS (ESI): t_R = 11.28 min, calcd. for $C_{45}H_{38}N_2NaO_6^+$ $[M+Na]^+$: 725.26, found 726.26

Fmoc-L-*threo*-β-HyAsn-OH (5):

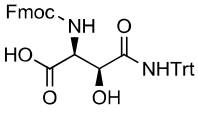

5

13 (608 mg, 0.87 mmol) was dissolved in ethanol (10 ml). 10 wt. % Pd/C (60.8 mg, 0.57 mmol) was carefully added to the solution. The atmosphere within the flask was exchanged to 1 atm H_2 and stirred for 1 h. The catalyst was removed by filtration through a

pad of Celite and the filter cake was rinsed with ethanol. The filtrate was evaporated to dryness under reduced pressure and the residue was purified by flash chromatography (SiO_2, $CHCl_3$→$CHCl_3$/MeOH 1:1) which delivered the desired product.

Yield: 401 mg (0.66 mmol, 76%) as a colorless glasslike solid
TLC (DCM/MeOH = 1:1): R_f = 0.3 (smeary)
[α]$^{22}_D$: -16 (*c* 1.00, $CHCl_3$/MeOH 1:1)
^{1}H NMR (400 MHz, DMSO): δ = 8.40 (s, 1H), 7.89 (dd, J = 7.5, 2.7 Hz, 2H), 7.81 (d, J = 7.5 Hz, 1H), 7.77 (d, J = 7.5 Hz, 1H), 7.40 (dd, J = 7.4, 3.5 Hz, 2H), 7.25 – 7.13 (m, 18H), 4.47 (d, J = 2.1 Hz, 1H), 4.44 – 4.29 (m, 2H), 4.19 (t, J = 6.6 Hz, 2H)
^{13}C NMR (101 MHz, DMSO): δ = 173.83, 170.19, 156.29, 144.59, 143.75, 140.66, 128.40, 127.58, 127.06, 126.61, 125.56, 125.43, 120.03, 72.25, 69.16, 66.01, 57.19, 46.62
LC-MS (ESI): t_R = 10.19 min, calcd. for $C_{38}H_{32}N_2NaO_6^+$ $[M+H]^+$: 635.22, found 635.59

Fmoc-L-Asn(Trt)-ol (6):

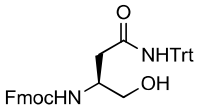

6

Fmoc-L-Asn(Trt)-OH (2.98 g, 5 mmol) was dissolved in THF (5 ml) and cooled to -10 °C. To this solution were added successively *N*-methyl morpholine (0.604 ml, 5.5 mmol) and *iso*butyl chloroformate (0.72 ml, 5.5 mmol). After 5 min., a solution of $NaBH_4$ (0.24 g, 6.3 mmol) in H_2O (6.3 ml) was added at once (strong gas evolution was observed). The mixture was stirred for 0.5 h and then quenched by addition of a saturated aqueous $NaHCO_3$ solution (20 ml). The product was extracted twice with EtOAc (2x 40 ml). The organic layers were combined and washed extensively with 1 M $KHSO_4$ and brine, dried over Na_2SO_4, filtered and concentrated under reduced pressure which delivered the title compound.

Yield: 2.75 g (4.73 mmol, 94%) as a white solid
[α]$^{22}_D$: +17 (*c* 1.00, DCM)
^{1}H NMR (400 MHz, MeOD): δ = 7.77 (d, J = 7.5 Hz, 2H), 7.61 (t, J = 6.9 Hz, 2H), 7.36 (t, J = 7.4 Hz, 2H), 7.23 (d, J = 17.9 Hz, 17H), 4.48 – 4.24 (m, 2H), 4.15 (dd, J = 13.1, 6.8 Hz, 1H), 3.96 (d, J = 5.7 Hz, 1H), 3.46 (tt, J = 34.9, 17.4 Hz, 2H), 2.59 – 2.40 (m, 2H)
^{13}C NMR (101 MHz, MeOD): δ = 170.84, 156.57, 144.28, 143.93, 141.43, 128.72, 128.16,

127.86, 127.34, 127.23, 125.20, 120.12, 71.01, 67.02, 64.31, 50.12, 47.29, 39.45

LC-MS (ESI): t_R = 10.26 min, calcd. for $C_{38}H_{34}N_2NaO_4^+$ $[M+Na]^+$: 605.24, found 605.71

General methods for solid phase peptide synthesis (SPPS) using the Fmoc-strategy

Method A: *Fmoc-determination:*

Loadings of Fmoc-protected peptide resins were quantitatively determined using a UV/Vis spectrophotometer. For Fmoc-determinations, a small sample of ~5 mg of dried resin was added to a 25 ml conical flask and the portion was weighted exactly. A freshly prepared 20% piperidine in DMF solution (5 ml) was added (in total 10 ml of the 20% piperidine/DMF was prepared, either for serial dilution of the sample and as a reference). The resulting suspension was shaken at rt on an orbital shaker for 20 min. The resin within the flask was allowed to settle down and the UV absorption of 1 ml (or a dilution thereof) of the cleavage solution was measured at λ = 301 nm. The measured value which was adjusted by dilution of the sample was always between 0.1 and 1 to ensure accurate results. The measurements were repeated at least three times. The loading of the resin was calculated using the following equation and used in subsequent steps to calculate resin amount and/or reagent equivalents.

$$c = \frac{A_{301} \cdot V \cdot F}{\varepsilon_{301} \cdot d \cdot m} \qquad [2]$$

c = resin load (mmol/g)

A_{301} = absorption value, λ = 301 nm

V = Volume of cleavage solution

F = dilution factor (e.g. 3, 5…)

ε_{301} = extinction coefficient (7800 $M^{-1}cm^{-1}$)

d = thickness of cuvette

m = weighed mass of the resin

Method B: *Amino acid coupling condition*

All subsequent amino acid couplings were performed in a syringe reactor using the corresponding Fmoc-amino acids (4 eq.) and HOBt (4 eq.), HBTU (4 eq.) and DIPEA (4 eq.) (always 4 eq. if not specified in the experimental description). To this end, the respective Fmoc-N_{α}-amino acid, HOBT, HBTU and DIEA were dissolved in an adequate amount of DMF (~5 ml) and stirred for a few minutes in a separate flask to preactivate the amino acid. This solution was then added to a syringe reactor containing the resin and the suspension was shaken for 2 h at rt. Finally, the reaction solution was discarded and the resin was washed sequentially with 3 x DMF, 3 x DCM, 3 x MeOH, 3 x DCM and 3 x DMF.

Method C: *Kaiser test*

Amino acid coupling reactions were monitored by the Kaiser test to evaluate the efficiency of amide bond formation as the Kaiser test allows to determine the presence of primary amines on solid support. For the Kaiser test, the following solutions were used:

Solution I: 5% Ninhidrin in ethanol
Solution II: 20% phenol in ethanol
Solution III: 0.4 ml of 0.001 M $KCN_{(aq)}$ in pyridine (20 ml)

A few resin beads were transferred into a small glass tube. 3 drops of solution I, 2 drops of solution II and 3 drops of solution III were sequentially added and the resulting suspension was mixed well and placed for 5 min in a pre-heated oven (100 °C). The formation of a blue solution indicated the presence of primary amines. To reduce the occurrence of false negative results, a positive control was always performed in parallel.

Method D: *Base induced cleavage of Fmoc protection group*

A solution of 20% piperidine in DMF was added to the resin and this suspension was agitated for 15 min. The cleavage solution was discarded. This procedure was repeated once more. Afterwards the resin was extensively washed by an alternation of 3 x DMF, 3 x DCM, 3 x MeOH, 3 x DCM and 3x DMF.

Method E: *Pd catalyzed cleavage of the Alloc protecting group*

The resin was washed extensively with DCM and subsequently dried overnight under high vacuum. The dried resin was transferred to a flame dried conical 25 ml flask under argon atmosphere. Anhydrous and degassed DCM (3 ml) was added to the resin and to this suspension degassed morpholine (24 eq.) was added dropwise followed by a degassed solution of $Pd(PPh_3)_4$ (0.25 eq.) in anhydrous DCM (2 ml). The resulting reaction suspension was shaken under an argon atmosphere and light exclusion on an orbital shaker for 90 min at rt. The reaction suspension was transferred into a syringe reactor and washed 3 x with DCM, 3 x DMF, 3 x with a 0.02 M solution of Et_2NCS_2Na in NMP and 5 x with DMF.

Method F: *Microcleavage for LC/MS analysis*

After a critical synthetic step or if the Kaiser test (*method C*) showed incomplete couplings, a microcleavage was implemented to analyze a small amount of the intermediate product by LC/MS analysis. To this end, 1-2 mg of resin beads was transferred to a separate, small syringe reactor (2 ml). The cleavage cocktail (95% TFA, 2.5% TIS, 2.5% H_2O, 500 µl) was added and the resulting suspension was shaken for 1 h at rt. The solution was transferred to a small 5 ml flask and all volatiles were removed under reduced pressure. The crude residue was dissolved in H_2O/ACN (1:1, 500 µl), filtered, transferred to a LC/MS vial and injected in a LC-MS apparatus.

Method G: *Final cleavage of side-chain protecting groups and cleavage of peptidyl alcohols from 2-chlorotrityl resin*

The cleavage cocktail (95% TFA, 2.5% TIS, 2.5% H_2O, 5 ml) was added to the peptide-loaded resin. The resulting suspension was agitated for 2 h at rt, then filtered and transferred to a 50 ml falcon tube. This falcon tube was replenished with ice-cold diethyl ether to precipitate the crude peptidyl alcohols. The suspension was put into the freezer for 15 min, then the precipitate was isolated by centrifugation (2200 g, 15 min, 4°C), decanted and the obtained pellet washed with ice-cold diethyl ether (40 ml) and centrifuged once more. Finally, the crude pellet was dried under a continuous stream of N_2-gas.

Method H: *Preparative HPLC purification of peptidyl alcohols*

A maximal amount of 50 mg crude product was dissolved in ACN/H_2O + 0.1% TFA (1:4, 5 ml). Linear gradients of solvent B (0.1% TFA in acetonitrile) in solvent A (0.1% TFA in water) were applied at a 25 ml/min flow rate and a peak detection at 210 nm. The binary gradient was adjusted according to the polarity of the product (elution time ~ 30-40 min). Fractions (each 18 ml) were collected corresponding to product peak. ACN was removed by rotary evaporation at reduced pressure. The aqueous solution was finally lyophilized.

7.2.2 Solid phase synthesis of Rotihibin A

Coupling of 6 to 2-Chlorotrityl chloride resin (14):

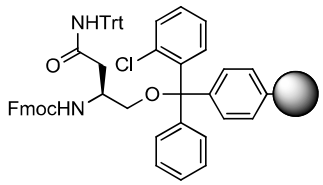

14

2-Chlorotrityl resin (250 mg, *c* = 1.22 mmol/g) was transferred into a flame dried Rosenbaum-reactor under an argon atmosphere. Separately, **6** (532.5 mg, 0.915 mmol) was dissolved in anhydrous DCM (8 ml) and pyridine (147 µl, 1.83 mmol) was added. This solution was transferred to the Rosenbaum-reactor and the suspension was shaken on an orbital shaker for 16 h under an argon atmosphere. Methanol (4 ml) was added and the mixture was shaken for further 30 min to terminate the reaction and to quench the resin. The loaded resin was washed alternately with DCM (3x), DMF (3x) and again with DCM (3x) and then dried under high vacuum. The loading of the resin was quantified using *method A*.

Loading: 0.3 mmol/g (25%)

Solid phase synthesis of Rotihibin A (1):

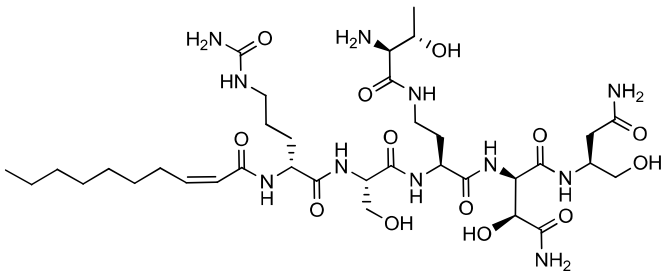

1

General procedure I: **Solid phase synthesis using Fmoc-strategy**

The resin **14** (250 mg, 0.075 mmol) was placed in a syringe reactor and the Fmoc-protecting group was removed using *method D*. The coupling of **5** was performed according to *method B*. To this end, 2 eq. of **5** were used. The quantities of the reagents were as follows:

5:	92 mg, 0.15 mmol
HBTU:	56.8 mg, 0.15 mmol
HOBT:	20 mg, 0.15 mmol
DIPEA:	25 µl, 0.15 mmol
DMF:	5 ml

After this step, a microcleavage, performed according to *method F,* showed a complete turnover.

Deprotection of the Fmoc-protecting group was performed using *method D*. The coupling of Fmoc-Dab(Alloc)-OH was performed according to *method B*. The quantities of the reagents were as follows:

Fmoc-L-Dab(Alloc)-OH:	127.3 mg, 0.3 mmol
HBTU:	113.7 mg, 0.3 mmol
HOBT:	40 mg, 0.3 mmol
DIPEA:	50 µl, 0.3 mmol
DMF:	5 ml

Cleavage of the Alloc-protecting group of CTC-asparaginol(Trt)-hyAsn(Trt)-Dab(Alloc)-Fmoc was carried out using *method E*. A Kaiser test, performed according to *method C,* showed the presence of primary amines which ensured full Alloc-cleavage.

The subsequent coupling of **4** was performed according to *method B*. The quantities of the reagents were as follows:

4:	60.3 mg, 0.3 mmol
HBTU:	113.7 mg, 0.3 mmol
HOBT:	40 mg, 0.3 mmol
DIPEA:	50 µl, 0.3 mmol
DMF:	5 ml

Cleavage of the Fmoc-protection group of CTC-asparaginol(Trt)-hyAsn(Trt)-Dab(Boc-*allo*-Thr)-Fmoc was carried out using *method D*.

The coupling of Fmoc-L-Ser(O*t*Bu)-OH was performed corresponding to *method B*. The quantities of the reagents were as follows:

Fmoc-L-Ser(O*t*Bu)-OH:	115 mg, 0.3 mmol
HBTU:	113.7 mg, 0.3 mmol
HOBT:	40 mg, 0.3 mmol
DIPEA:	50 µl, 0.3 mmol
DMF:	5 ml

Cleavage of the Fmoc-protection group of CTC-asparaginol(Trt)-hyAsn(Trt)-Dab(Boc-*allo*-Thr)-Ser(O*t*Bu)-Fmoc was carried out using *method D*.

The subsequent coupling of **3** was performed corresponding to *method B*. The quantities of the reagents were as follows:

3:	120 mg, 0.3 mmol
HBTU:	113.7 mg, 0.3 mmol
HOBT:	40 mg, 0.3 mmol
DIPEA:	50 µl, 0.3 mmol
DMF:	5 ml

Cleavage of the Fmoc-protection group of CTC-asparaginol(Trt)-hyAsn(Trt)-Dab(Boc-*allo*-Thr)-Ser(O*t*Bu)-Cit-Fmoc was carried out using *method D*.

The coupling of **2** was performed corresponding to *method B*. The quantities of the reagents were as follows:

2:	51.6 mg, 0.3 mmol
HBTU:	113.7 mg, 0.3 mmol
HOBT:	40 mg, 0.3 mmol
DIPEA:	50 µl, 0.3 mmol
DMF:	5 ml

The final cleavage of side-chain protecting groups and the cleavage from 2-chlorotrityl resin were carried out in one step according *method G*. The preparative purification was conducted via RP-HPLC corresponding to *method H,* which yielded the desired product.

Yield: 19.8 mg (0.0234 mmol, 31% overall yield) as a white solid

$[\alpha]^{23}_{D}$: +8 (*c* 0.50, DMSO)

^{1}H NMR (400 MHz, DMSO): δ = 8.37 (t, J = 5.4 Hz, 1H), 8.32 (d, J = 7.1 Hz, 1H), 8.07 (d, J = 7.2 Hz, 1H) 8.05 (d, J = 7.6 Hz, 1H), 7.99 (s br., 2H), 7.53 (d, J = 8.8 Hz, 1H), 7.39 (d, J = 8.3 Hz, 1H), 7.34 (s, 1H), 7.25 (d, J = 2 Hz, 1H), 7.17 (d, J = 2 Hz, 1H), 6.83 (s, 1H), 5.96 (m, 1H), 5.92 (m, 1H), 5.88 (d, J = 11.6 Hz, 1H), 5.82 (d, J = 5.9 Hz, 1H), 5.50 (d, J = 4.2 Hz, 1H), 5.38 (s, 2H), 5.10 (t, J = 5.2 Hz, 1H), 4.67 (t, 5.6 Hz, 1H), 4.54 (dd, J = 2.4, 8.8 Hz, 1H), 4.36 (m, 2H), 4.29 (dd, J = 2.4, 6 Hz, 1H), 4.26 (dd, J = 7.2, 14 Hz, 1H), 4.05 (m, 2H), 3.69 (d, J = 4.6 Hz, 1H), 3.60 (m, 2H), 3.38 (m, 2H), 3.16 (m, 2H), 2.94 (m, 2H), 2.65 (m, 1H), 2.54 (m, 1H), 2.38 (dd, J = 6.4, 14.8 Hz, 1H), 2.23 (dd, J = 6.8, 14.8 Hz, 1H), 1.89 (m, 1H), 1.73 (m, 1H), 1.61 (m, 1H), 1.49 (m, 1H), 1.35 (m, 4H), 1.24 (m, 8H), 1.06 (d, J = 6.5 Hz, 3H), 0.85 (t, J = 6.9 Hz, 3H)

^{13}C NMR (101 MHz, DMSO): δ = 173.18, 172.76, 172.03, 170.87, 170.64, 168.75, 166.22, 165.70, 158.80, 144.74, 122.52, 70.97, 64.78, 62.47, 61.65, 57.49, 55.50, 54.59, 52.00, 51.35, 48.67, 36.47, 35.86, 31.20, 30.98, 29.65, 28.72, 28.51, 27.91, 26.62, 26.57, 22.04, 17.72, 13.93

LC-MS (ESI): t_R = 4.89 min, calcd. for $C_{35}H_{64}N_{11}O_{13}^{+}$ $[M+H]^{+}$: 846.47, found 846.52

HR-MS (ESI): calcd. for $C_{35}H_{64}N_{11}O_{13}^{+}$ $[M+H]^{+}$: 846.468, found 846.469

7.2.3 Solid phase synthesis of Rotihibin A-derivatives

Solid phase synthesis of RotA-DB (15):

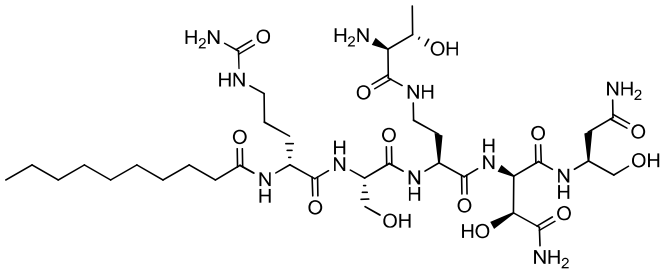

15

The synthesis was carried out following the *general procedure I* by the use of the corresponding building blocks. All subsequent deprotection- and coupling-steps were accomplished using *method D*, *B* and *E*. The analysis of intermediate products was performed in compliance with *method C* and *F*. The final cleavage from 2-chlorotrityl resin and the preparative purification were conducted according to *method G* and *method H* which yielded the title compound.

Yield: 16.2 mg (0.019 mmol, 26% overall yield) as a white solid

^{1}H NMR (400 MHz, DMSO-d_6): δ = 8.37 (t, J = 5.4 Hz, 1H), 8.28 (d, J = 7.2 Hz, 1H), 8.04 (d, J = 7.6 Hz, 1H), 7.98 (m, 3H), 7.52 (d, J = 8.7 Hz, 1H), 7.37 (d, J = 8 Hz, 1H), 7.34 (s, 1H) 7.25 (d, J = 2 Hz, 1H), 7.18 (d, J = 2 Hz, 1H), 6.86 (s, 1H), 5.92 (t, J = 5.9 Hz, 1H), 5.80 (d, J = 5.9 Hz, 1H), 5.49 (d, J = 4.2 Hz, 1H), 5.37 (s, 2H), 5.07 (t, J = 5.3 Hz, 1H), 4.67 (t, J = 5.4 Hz, 1H), 4.53 (dd, J = 8.8, 2.3 Hz, 1H), 4.34 (m, 1H), 4.27 (m, 3H), 4.05 (m, 2H), 3.69 (s, 1H), 3.60 (m, 2H), 3.37 (m, 2H), 3.19 (m, 2H), 2.94 (m, 2H), 2.36 (dd, J = 6.4, 14.8 Hz, 1H), 2.23 (dd, J = 6.4, 14.8 Hz, 1H), 2.11 (m, 2H), 1.89 (m, 1H), 1.74 (m, 1H), 1.58 (m, 1H), 1.45 (m, 3H), 1.26 (m, 12H), 1.06 (d, J = 6.5 Hz, 3H), 0.86 (t, J = 6.8 Hz, 3H)

LC-MS (ESI): t_R = 5.02 min, calcd. for $C_{35}H_{66}N_{11}O_{13}^+$ $[M+H]^+$: 848.48, found 849.09

Solid phase synthesis of RotA-L-Cit (16):

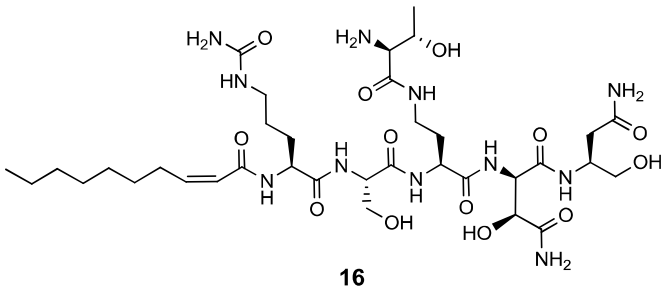

16

The synthesis was carried out following the *general procedure I* and by the use of the corresponding building blocks. All subsequent deprotection- and coupling-steps were accomplished using *method D*, *B* and *E*. The analysis of intermediate products was performed in compliance with *method C* and *F*. The final cleavage from 2-chlorotrityl resin and the preparative purification were conducted according to *method G* and *method H*, which yielded the title compound.

Yield: 21.0 mg (0.025 mmol, 33% overall yield) as a white solid

^{1}H NMR (400 MHz, DMSO): δ = 8.35 (t, J = 5.4 Hz, 1H), 8.18 (d, J = 7.2 Hz, 1H), 8.04 (d, J = 7.6 Hz, 1H) 8.03 (d, J = 7.6 Hz, 1H), 7.99 (s br., 2H), 7.61 (d, J = 9.2 Hz, 1H), 7.45 (d, J = 8.4 Hz, 1H), 7.34 (s, 1H), 7.25 (d, J = 2 Hz, 1H), 7.17 (d, J = 2 Hz, 1H), 6.87 (s, 1H), 5.94 (m, 2H), 5.89 (m, 1H), 5.84 (m, 1H), 5.50 (d, J = 4.0 Hz, 1H), 5.39 (s, 2H), 5.04 (t, J = 5.2 Hz, 1H), 4.68 (t, 5.6 Hz, 1H), 4.56 (dd, J = 2.4, 8.8 Hz, 1H), 4.35 (m, 2H), 4.29 (m, 2H), 4.05 (m, 2H), 3.69 (m, 2H), 3.62 (m, 2H), 3.37 (m, 2H), 3.18 (m, 2H), 2.94 (m, 2H), 2.59 (m, 2H), 2.38 (dd, J = 6.4, 14.8 Hz, 1H), 2.23 (dd, J = 6.8, 14.8 Hz, 1H), 1.89 (m, 1H), 1.73 (m, 1H), 1.64 (m, 1H), 1.49 (m, 1H), 1.35 (m, 4H), 1.24 (m, 8H), 1.06 (d, J = 6.5 Hz, 3H), 0.85 (t, J = 6.9 Hz, 3H)

LC-MS (ESI): t_R = 5.04 min, calcd. for $C_{35}H_{64}N_{11}O_{13}^+$ $[M+H]^+$: 846.47, found 846.75

HR-MS (ESI): calcd. for $C_{35}H_{64}N_{11}O_{13}^+$ $[M+H]^+$: 846.468, found 846.468

Solid phase synthesis of RotA-hyAsn (17):

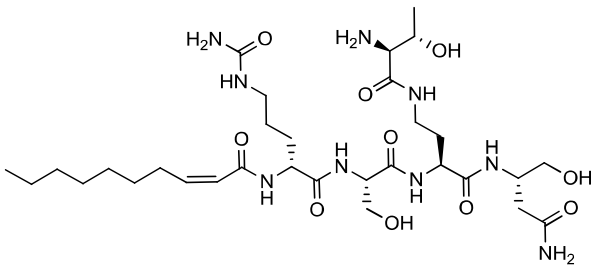

17

The synthesis was carried out following the *general procedure I* by the use of the corresponding building blocks. All subsequent deprotection- and coupling-steps were accomplished using *method D*, *B* and *E*. The analysis of intermediate products was performed in compliance with *method C* and *F*. The final cleavage from 2-chlorotrityl resin and the preparative purification were conducted according to *method G* and *method H*, which yielded the title compound.

Yield: 24.6 mg (0.034 mmol, 45% overall yield) as a white solid

^{1}H NMR (400 MHz, DMSO): δ = 8.35 (t, J = 5.2 Hz, 1H), 8.17 (d, J = 7.4 Hz, 1H), 8.11 (d, J = 7.6 Hz, 1H), 8.08 (d, J = 7.6 Hz, 1H), 7.99 (s br., 2H), 7.45 (d, J = 8.2 Hz, 1H), 7.19 (s, 1H), 6.79 (s, 1H), 5.96 (m, 1H), 5.92 (m, 1H), 5.87 (d, J = 11.6 Hz, 1H), 5.49 (d, J = 4.2 Hz, 1H), 5.37 (s, 2H), 5.11 (t, J = 5.2, 1H), 4.66 (s, 1H), 4.32 (m, 2H), 4.20 (m, 1H), 4.02 (m, 2H), 3.66 (m, 2H), 3.57 (m, 1H), 3.21 (m, 1H), 3.10 (m, 1H), 2.95 (m, 2H), 2.65 (m, 1H), 2.54 (m, 1H), 2.32 (dd, J = 6.4, 14.8 Hz, 1H), 2.14 (dd, , J = 6.4, 14.8 Hz, 1H), 1.94 (m, 1H), 1.72 (m, 1H), 1.61 (m, 1H), 1.50 (m, 1H), 1.36 (m, 4H), 1.24 (m, 8H), 1.06 (d, J = 6.5 Hz, 3H), 0.85 (t, J = 6.4 Hz, 3H)

LC-MS (ESI): t_R = 4.94 min, calcd. for $C_{31}H_{58}N_9O_{10}^+$ $[M+H]^+$: 716.43, found 716.73

HR-MS (ESI): calcd. for $C_{31}H_{58}N_9O_{10}^+$ $[M+H]^+$: 716.430, found 716.431

Solid phase synthesis of RotA-L-Asn (18):

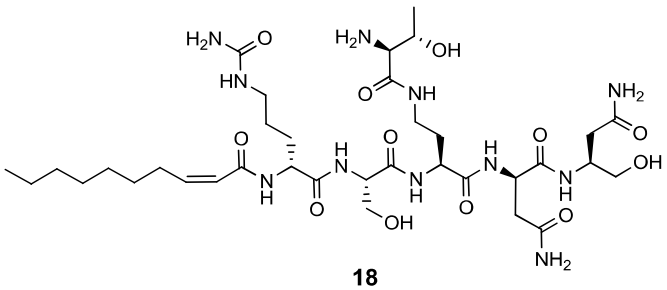

18

The synthesis was carried out following the *general procedure I* by the use of the corresponding building blocks. All subsequent deprotection- and coupling-steps were accomplished using *method D*, *B* and *E*. The analysis of intermediate products was performed in compliance with *method C* and *F*. The final cleavage from 2-chlorotrityl resin and the preparative purification were conducted according to *method G* and *method H*, which yielded the title compound.

Yield: 3.64 mg (0.0043 mmol, 6% overall yield) as a white solid

^{1}H NMR (400 MHz, DMSO): δ = 8.37 (t, J = 5.4 Hz, 1H), 8.22 (d, J = 5.6 Hz, 1H), 8.1 (m, 2H), 7.98 (s br., 2H), 7.61 (m, 1H), 7.55 (m, 1H), 7.31 (s, 1H), 7.26 (s, 1H), 6.91 (s, 1H), 6.81 (s, 1H), 5.96 (m, 2H), 5.89 (m, 1H), 5.49 (d, J = 3.2 Hz, 1H), 5.37 (s, 2H), 5.12 (t, J = 4.0 Hz, 1H), 4.64 (t, 4.4 Hz, 1H), 4.45 (m, 1H), 4.33 (m, 2H), 4.22 (m, 1H), 4.02 (m, 2H), 3.69 (d, J = 2.8 Hz, 1H), 3.62 (m, 2H), 3.20 (m, 2H), 2.94 (m, 2H), 2.67 (m, 1H), 2.54 (m, 1H), 2.35 (m, 1H), 2.19 (dd, J = 65.6, 12.0 Hz, 1H), 1.89 (m, 1H), 1.73 (m, 1H), 1.61 (m, 1H), 1.49 (m, 1H), 1.42 (m, 4H), 1.24 (m, 8H), 1.06 (d, J = 5.2 Hz, 3H), 0.85 (t, J = 5.2 Hz, 3H)

LC-MS (ESI): t_R = 6.00 min, calcd. for $C_{35}H_{64}N_{11}O_{12}^+$ $[M+H]^+$: 830.47, found 830.40

Solid phase synthesis of RotA-Rh (19):

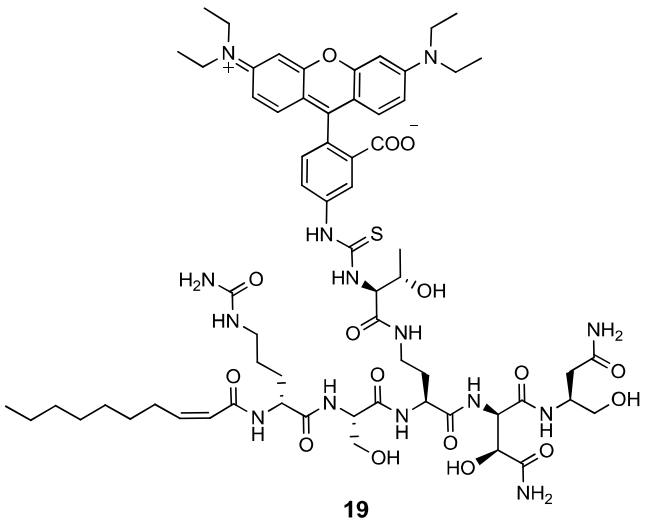

19

1 (1.5 mg, 1.7 µmol) was dissolved in DMF (0.5 ml). To this solution, Rhodamine B isothiocyanate (5 mg, 9.3 µmol) and DIPEA (5 µl, 29 µmol) were added. The reaction mixture was stirred in the dark at ambient temperature for 4 h. All volatiles were removed under reduced pressure and the residue was purified via HPLC according to *method H*.

Yield: 1.2 mg (0.9 µmol, 53%) as a purple solid

LC-MS (ESI): t_R = 6.18 min, calcd. for $C_{64}H_{93}N_{14}O_{16}S^+$ $[M+H]^+$: 1345.66, found 1345.77

Solid phase synthesis of RotA-Ac (20):

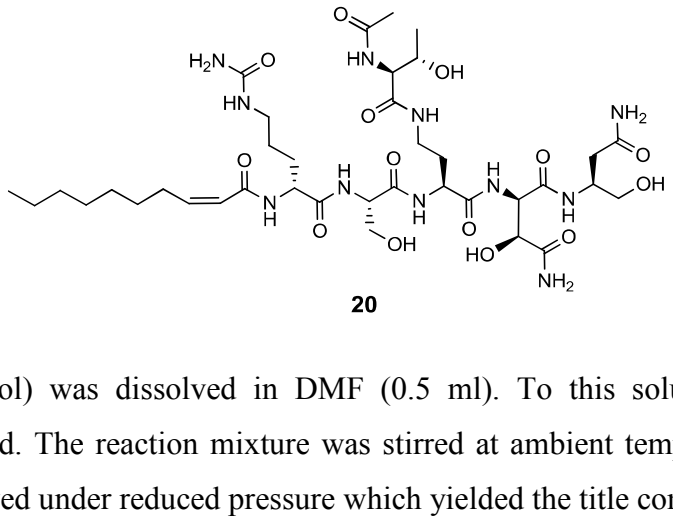

20

1 (1.5 mg, 1.7 µmol) was dissolved in DMF (0.5 ml). To this solution, Ac_2O (20 µl, 0.2 mmol) was added. The reaction mixture was stirred at ambient temperature for 2 h. All volatiles were removed under reduced pressure which yielded the title compound.

Yield: 1.5 mg (1.7 µmol, quant.) as a white solid

LC-MS (ESI): t_R = 5.39 min, calcd. for $C_{37}H_{66}N_{11}O_{14}^+$ $[M+H]^+$: 888.48, found 888.56

Solid phase synthesis of RotA-Ala (21):

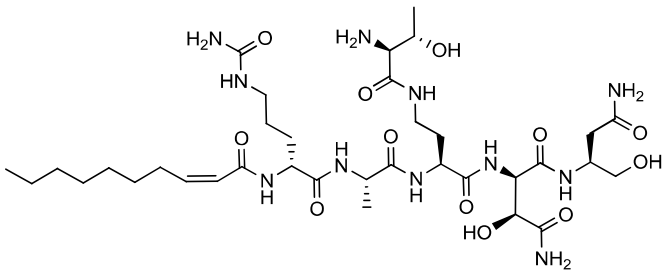

21

The synthesis was carried out following the *general procedure I* by the use of the corresponding building blocks. All subsequent deprotection- and coupling-steps were accomplished using *method D*, *B* and *E*. The analysis of intermediate products was performed in compliance with *method C* and *F*. The final cleavage from 2-chlorotrityl resin and the preparative purification were conducted according to *method G* and *method H*, which yielded the title compound.

Yield: 7.1 mg (8.5 µmol, 11% overall yield) as a white solid

^{1}H NMR (400 MHz, DMSO): δ = 8.36 (t, J = 5.6 Hz, 1H), 8.20 (d, J = 7.2 Hz, 1H), 8.16 (d, J = 7.2 Hz, 1H), 7.99 (m, 3H), 7.47 (d, J = 8.4 Hz, 1H), 7.43 (d, J = 8.8 Hz, 1H), 7.33 (s, 1H), 7.27 (d, J = 1.6 Hz, 1H), 7.13 (d, J = 1.6 Hz, 1H), 6.85 (s, 1H), 5.94 (m, 2H), 5.89 (m, 2H), 5.50 (d, J = 2.0 Hz, 1H), 5.38 (s, 2H), 4.66 (s, 1H), 4.53 (dd, J = 2.4, 8.8 Hz, 1H), 4.31 (m, 2H), 4.28 (m, 2H), 4.05 (m, 2H), 3.69 (t, J = 4.4 Hz, 1H), 3.31 (m, 2H), 3.18 (m, 2H), 2.94 (m, 2H), 2.63 (m, 1H), 2.53 (m, 1H), 2.36 (dd, J = 6.4, 14.8 Hz, 1H), 2.23 (dd, J = 6.8, 14.8 Hz, 1H), 1.89 (m, 1H), 1.72 (m, 1H), 1.59 (m, 1H), 1.49 (m, 1H), 1.33 (m, 4H), 1.25 (m, 8H), 1.23 (s, 3H), 1.06 (d, J = 6.4 Hz, 3H), 0.85 (t, J = 7.2 Hz, 3H)

LC-MS (ESI): t_R = 4.92 min, calcd. for $C_{35}H_{64}N_{11}O_{12}^+$ $[M+H]^+$: 830.47, found 830.56

Solid phase synthesis of RotA-Ala-hyAsn (22):

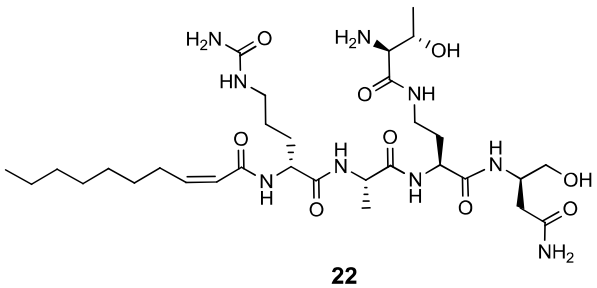

22

The synthesis was carried out following the *general procedure I* by the use of the corresponding building blocks. All subsequent deprotection- and coupling-steps were accomplished using *method D*, *B* and *E*. The analysis of intermediate products was performed in compliance with *method C* and *F*. The final cleavage from 2-chlorotrityl resin and the preparative purification were conducted according to *method G* and *method H*, which yielded the title compound.

Yield: 4.1 mg (5.8 μmol, 7.8% overall yield) as a white solid

^{1}H NMR (400 MHz, DMSO): δ = 8.33 (t, J = 5.2 Hz, 1H), 8.26 (d, J = 7.2 Hz, 1H), 8.07 (d, J = 7.2 Hz, 1H), 8.02 (d, J = 8.0 Hz, 1H), 7.99 (s br., 2H), 7.46 (d, J = 8.0 Hz, 1H), 7.23 (s, 1H), 6.81 (s, 1H), 5.93 (m, 3H), 5.49 (s, 1H), 5.37 (s, 2H), 4.25 (m, 3H), 4.01 (m, 2H), 3.69 (t, J = 3.6 Hz, 1H), 3.60 (m, 2H), 3.31 (m, 2H), 3.14 (m, 2H), 2.94 (m, 2H), 2.63 (m, 1H), 2.54 (m, 1H), 2.29 (dd, J = 6.4, 14.8 Hz, 1H), 2.18 (dd, J = 6.8, 14.8 Hz, 1H), 1.87 (m, 1H), 1.72 (m, 1H), 1.59 (m, 1H), 1.49 (m, 1H), 1.33 (m, 4H), 1.25 (m, 8H), 1.23 (s, 3H), 1.05 (d, J = 6.4 Hz, 3H), 0.85 (t, J = 6.8 Hz)

LC-MS (ESI): t_R = 4.98 min, calcd. for $C_{31}H_{58}N_9O_9^+$ $[M+H]^+$: 700.44, found 700.64

Solid phase synthesis of RotA-Phe (23):

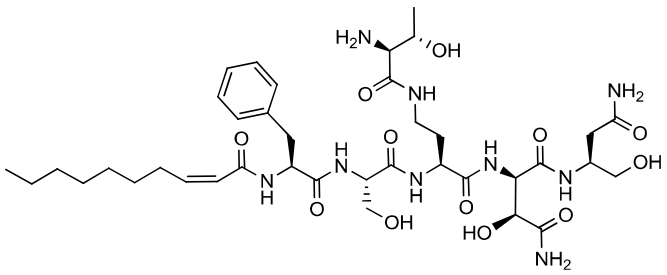

23

The synthesis was carried out following the *general procedure I* by the use of the corresponding building blocks. All subsequent deprotection- and coupling-steps were accomplished using *method D*, *B* and *E*. The analysis of the intermediate products was performed in compliance with *method C* and *F*. The final cleavage from 2-chlorotrityl resin and the preparative purification were conducted according to *method G* and *method H*, which yielded the title compound.

Yield: 4.0 mg (4.8 µmol, 6.5% overall yield) as a white solid

^{1}H NMR (400 MHz, DMSO): δ = 8.35 (t, J = 5.6 Hz, 1H), 8.23 (d, J = 7.2 Hz, 1H), 8.17 (d, J = 7.6 Hz, 1H) 8.06 (d, J = 8.4 Hz, 1H), 7.93 (s br., 2H), 7.62 (d, J = 8.8 Hz, 1H), 7.45 (d, J = 8.4 Hz, 1H), 7.35 (s, 1H), 7.25 (m, 5H), 7.16 (m, 2H), 6.87 (s, 1H), 5.84 (m, 3H), 5.49 (d, J = 4.4 Hz, 1H), 5.09 (t, J = 5.2 Hz, 1H), 4.67 (t, 5.6 Hz, 1H), 4.62 (m, 1H), 4.56 (dd, J = 2.4, 8.8 Hz, 1H), 4.36 (dd, J = 5.6, 13.2 Hz, 1H), 4.30 (dd, J = 2.4, 6 Hz, 1H), 4.03 (m, 2H), 3.69 (m, 2H), 3.62 (m, 1H), 3.37 (m, 1H), 3.28 (m, 1H), 3.20 (m, 2H), 3.07 (m, 1H), 2.74 (m, 1H), 2.40 (m, 2H), 2.23 (dd, J = 6.8, 14.8 Hz, 1H), 1.89 (m, 1H), 1.73 (m, 1H), 1.23 (m, 10H), 1.05 (d, J = 6.4 Hz, 3H), 0.85 (t, J = 7.2 Hz, 3H)

LC-MS (ESI): t_R = 5.78 min, calcd. for $C_{38}H_{62}N_9O_{12}^+$ $[M+H]^+$: 836.45, found 836.58

Solid phase synthesis of RotA-Phe-hyAsn (24):

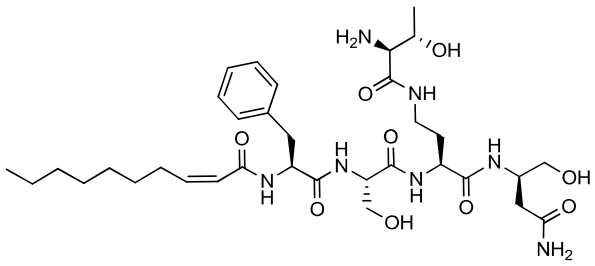

24

The synthesis was carried out following the *general procedure I* by the use of the corresponding building blocks. All subsequent deprotection- and coupling steps were accomplished using *method D*, *B* and *E*. The analysis of intermediate products was performed in compliance with *method C* and *F*. The final cleavage from 2-chlorotrityl resin and the preparative purification were conducted according to *method G* and *method H* which yielded the title compound.

Yield: 5.0 mg (7.1 μmol, 9.5% overall yield) as a white solid

^{1}H NMR (400 MHz, DMSO): δ = 8.32 (t, J = 6.0 Hz, 1H), 8.13 (d, J = 7.6 Hz, 1H), 8.08 (d, J = 7.6 Hz, 1H) 8.07 (d, J = 8.4 Hz, 1H), 7.93 (s br., 2H), 7.66 (d, J = 8.4 Hz, 1H), 7.25 (m, 5H), 7.17 (m, 1H), 6.81 (s, 1H), 5.88 (m, 1H), 5.77 (m, 1H), 5.47 (d, J = 4.4 Hz, 1H), 5.11 (t, J = 5.2 Hz, 1H), 4.71 (t, 5.6 Hz, 1H), 4.62 (m, 1H), 4.33 (dd, 6.2, 13.2 Hz, 1H), 4.25 (dd, J = 8, 14.0 Hz, 1H), 4.03 (m, 2H), 3.66 (m, 2H), 3.58 (m, 1H), 3.34 (m, 1H), 3.28 (m, 1H), 3.14 (m, 3H), 2.75 (m, 1H), 2.40 (m, 2H), 2.17 (dd, J = 6.8, 14.8 Hz, 1H), 1.89 (m, 1H), 1.70 (m, 1H), 1.23 (m, 10H), 1.05 (d, J = 6.4 Hz, 3H), 0.85 (t, J = 7.2 Hz, 3H)

LC-MS (ESI): t_R = 5.92 min, calcd. for $C_{34}H_{56}N_7O_9^+$ $[M+H]^+$: 706.41, found 706.64

7.3 Synthesis of Brevicompanines

Boc-Trp(Boc)-OMe (31):

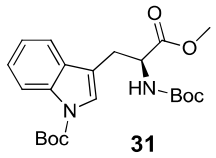

31

Freshly grounded NaOH (4 g, 100 mmol) was added to a solution of L-tryptophan methyl ester hydrochloride (5 g, 19.63 mmol) and tetrabutylammonium hydrogen sulfate (666 mg, 1.963 mmol) in DCM (200 ml). This mixture was stirred for 2 h at rt. Di-*tert*-butyl dicarbonate (13.52 ml, 58.90 mmol) was added and the mixture was stirred o.n. at rt. This mixture was filtered through a pad of celite and evaporated in vacuo. The residue was purified by flash chromatography (30% EA inCH) to afford the title compound.

Yield: 6.82 g (16.3 mmol, 83%) as colorless oil

TLC (EA/CH = 1:2): $R_f = 0.6$

^{1}H NMR (400 MHz, $CDCl_3$): δ = 8.11 (d, *J* = 7.2 Hz, 1H), 7.49 (d, *J* = 7.7 Hz, 1H), 7.39 (s, 1H), 7.34 – 7.27 (m, 1H), 7.22 (t, *J* = 7.4 Hz, 1H), 5.12 (d, *J* = 7.6 Hz, 1H), 4.65 (dd, *J* = 12.8, 5.5 Hz, 1H), 3.69 (s, 3H), 3.22 (ddd, *J* = 34.8, 14.7, 5.4 Hz, 2H), 1.66 (s, 9H), 1.44 (s, 9H)

^{13}C NMR (101 MHz, $CDCl_3$): δ = 172.38, 155.15, 149.64, 146.83, 135.44, 130.64, 124.57, 124.15, 122.61, 118.95, 115.32, 115.15, 85.21, 83.70, 79.98, 53.77, 52.38, 28.38, 28.27, 27.48.

LC-MS (ESI): t_R = 10.85 min, calcd. for $C_{22}H_{30}N_2NaO_6^+$ $[M+Na]^+$, 441.20, found 440.92

(2*S*,3a*R*,8a*R*)-1,8-di-*tert*-butyl-2-methyl-3a-(phenylselanyl)-3,3a-dihydropyrrolo[2,3-b]indole-1,2,8(2H,8aH)-tricarboxylate (32*a/b*):

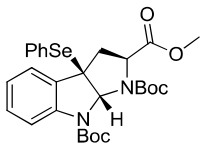

32*a/b*

To a suspension of **31** (923 mg, 2.2 mmol), *N*-phenylselenophthalimide (1 g, 3.3 mmol) and powdered Na_2SO_4 (3.13 g, 22 mmol) in DCM (5 ml) was added *p*-toluenesulfonic acid (41.8 mg, 0.22 mmol). The resulting mixture was stirred for 8 h, filtered through a pad of Celite, and the filtered solids rinsed with DCM. The filtrate was washed with 1 N NaOH (3 times), and the combined aqueous layers re-extracted with DCM. The combined organic layers were dried over Na_2SO_4, filtered, concentrated and purified by gel chromatography (silica gel, EA/CH 1:9) to yield the title compound as a 9:1 ratio of diastereomers.

Yield: 587 mg (1.02 mmol, 47%) as an off-white solid

TLC (EA/CH = 1:2): $R_f = 0.64$

^{1}H NMR (400 MHz, $CDCl_3$): δ = 7.32 (m, 4H), 7.23 – 7.14 (m, 4H), 7.02 (dd, *J* = 14.1, 6.6 Hz, 1H), 6.27 (s, 1H), 3.90 (dd, *J* = 9.7, 6.6 Hz, 1H), 3.65 (s, 3H), 2.90 (dd, *J* = 12.7, 6.6 Hz, 1H), 2.38 (dd, *J* = 12.7, 9.8 Hz, 1), 1.55 (d, *J* = 4.4 Hz, 18H).

^{13}C NMR (101 MHz, $CHCl_3$): δ = 171.24, 152.22, 142.07, 137.62, 132.8, 129.3, 129.2, 128.9, 124.1, 123.9, 123.5, 123.4, 123.0, 117.7, 117.6, 83.0, 82.7, 81.6, 80.9, 59.1, 52.1, 38.5, 28.3, 28.2

LC-MS (ESI): t_R = 13.3 min, calcd. for $C_{28}H_{34}N_2NaO_6Se^+$ $[M+Na]^+$, 597.15, found 597.00

(2*S*,3a*R*,8a*R*)-1,8-di-*tert*-butyl 2-methyl 3a-(2-methylbut-3-en-2-yl)-3,3a-dihydropyrrolo [2,3-b]indole-1,2,8(2H,8aH)-tricarboxylate (33):

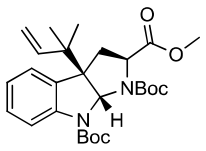

33

A solution of **32*a/b*** (588 mg, 1.02 mmol) and 2,6-di-*tert*-butylpyridine (1.03 ml, 4.59 mmol) in DCM (10 ml) was cooled under an argon atmosphere to -78 °C. Methyl trifuoromethanesulfonate (520 µl, 4.59 mmol) was added, followed by prenyl tributylstannane (1.5 ml, 3 mmol). The solution was allowed to warm to rt over 6 hours, and was then refluxed for 14 hours. The mixture was cooled to rt, quenched by addition of an equal volume of sat. $NaHCO_3$ solution and the organic layer was separated. The aqueous layer was extracted with DCM (2 times). The combined organic layers were washed with brine, dried over Na_2SO_4, filtered, concentrated and purified by gel chromatography (silicagel, EA/CH 1:5) to give the title compound as a 9:1 mixture of diastereomers.

Yield: 480 mg (0.98 mmol, 96%) as a white foam

TLC (EA/CH = 1:5): $R_f = 0.53$

^{1}H NMR (400 MHz, $CDCl_3$): δ = 7.23 (d,J =8.0 Hz, 1H), 7.18 – 7.15 (m, 1H), 7.14 (d, J = 0.7 Hz, 1H), 7.04 (t, J= 7.5 Hz, 1H), 6.14 (s, 1H), 5.86 (m, 1H), 5.07 (d, J = 10.8 Hz, 1H), 5.00 (d, J=17.4 Hz, 1H), 3.80 (dd, J = 10.2, 6.6 Hz, 1H), 3.70 (s, 3H), 2.37 (dd, J = 12.4, 6.6 Hz, 1H), 2.27 (dd, J = 12.4, 10.1 Hz, 1H), 1.52 (s, 9H), 1.43 (s, 9H), 0.97 (m, 6H)

^{13}C NMR (101 MHz, DMSO): δ = 172.81, 152.55, 143.33, 143.10, 133.91, 128.63, 125.11, 124.91, 123.52, 117.30, 114.38, 81.2, 81.0, 78.6, 61.3, 58.98, 51.95, 40.27, 34.89, 27.87, 27.70, 22.36, 21.97

LC-MS (ESI): t_R = 9.09 min, calcd. for $C_{27}H_{38}N_2NaO_6^+$ $[M+Na]^+$: 509.26, found 509.07

(2*S*,3a*R*,8a*R*)-1,8-bis(*tert*-butoxycarbonyl)-3a-(2-methylbut-3-en-2-yl)-1,2,3,3a,8,8a-hexahydropyrrolo[2,3-b]indole-2-carboxylic acid (34):

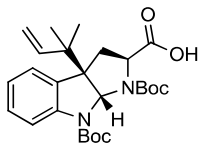

34

33 (146 mg, 0.30 mmol) was refluxed o.n. in a mixture of THF (2.5 ml), methanol (2.5 ml), 1 N NaOH (1.5 ml) and water (1 ml). The mixture was allowed to cool to rt and was carefully acidified to pH 4 by addition of 5% citric acid solution. The resulting solution was extracted with ethyl acetate (4x10 ml), the combined organic layers were dried over Na_2SO_4, filtered, concentrated and purified by gel chromatography (silica gel, 35:60:5 EA:CH:AcOH) two times to separate the mixture of diastereomers.

Yield: 138 mg (0.29 mmol, 97%) as a white solid

TLC (EA/CH/AcOH = 35:60:5): $R_f = 0.45$

^{1}H NMR (400 MHz, $CDCl_3$): δ = 7.35 (m, 1H), 7.23 (d, *J* = 7.8 Hz, 1H), 7.17 (d, *J* = 7.0 Hz, 1H), 7.05 (t, *J* = 7.6, 1H), 6.15 (s, 1H), 5.91 – 5.80 (m, 1H), 5.13 – 4.96 (m, 2H), 3.81 (dd, *J* = 10.2, 6.6 Hz, 1H), 2.43 (dd, *J* = 12.4, 6.6 Hz, 1H), 2.34 (dd, *J* = 12.4, 10.2 Hz, 1H), 1.68 – 1.60 (m, 2H), 1.54 (s, 9H), 1.25 (s, 9H), 0.92 (m, 6H).

^{13}C NMR (101 MHz, $CDCl_3$): δ = 171.38, 152.38, 143.28, 128.73, 126.41, 124.86, 123.44, 118.02, 114.57, 114.22, 100.14, 97.20, 81.64, 78.79, 60.57, 59.41, 40.50, 29.84, 28.52, 27.99, 26.98, 23.15, 22.29

LC-MS (ESI): t_R = 8.38 min, calcd. for $C_{26}H_{36}N_2NaO_6^+$ $[M+Na]^+$: 495.25, found 495.13

(2*S*,3a*R*,8a*R*)-di-*tert*-butyl 2-(((R)-1-methoxy-4-methyl-1-oxopentan-2-yl)carbamoyl)-3a-(2-methylbut-3-en-2-yl)-3,3a-dihydropyrrolo[2,3-b]indole-1,8(2H,8aH)-dicarboxylate (35*a*):

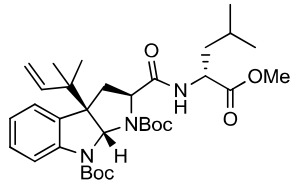

35*a*

To a solution of **34** (170 mg, 0.36 mmol) in DCM (10 mL) was added DCC (67 mg, 0.33 mmol), HOBt (40.5 mg, 0.3 mmol), and D-leucine methylester (90.8 mg, 0.5 mmol). The resulting mixture was stirred at room temperature for 12 h, followed by dilution with ether (20 ml). The side product DCU was removed by filtration and the organic layer washed with 1 N HCl, saturated aq. $NaHCO_3$ solution, and brine. The organic layer was dried over Na_2SO_4, filtered, and concentrated under reduced pressure to yield a light yellow foam. Flash chromatography with acetone/CH (1:9) as the eluent then yielded the title compound.

Yield: 139 mg (0.23 mmol, 93%) as a white foam

TLC (acetone/CH = 1:9): $R_f = 0.22$

^{1}H NMR (400 MHz, DMSO): δ = 7.36 (s, 1H), 7.32 (d, *J* = 7.4 Hz, 1H), 7.27 (t, *J* = 7.3 Hz, 1H), 7.10 (t, *J* = 7.6 Hz, 1H), 5.98 (s, 1H), 5.83 (dd, *J* = 16.9, 10.7 Hz, 1H), 5.03 (d, *J* = 10.8 Hz, 1H), 4.95 (d, *J* = 17.2 Hz, 1H), 4.33 (s, 1H), 3.61 (s, 1H), 3.59 (s, 3H), 2.41 (dd, *J* = 12.5, 6.9 Hz, 1H), 2.16 – 2.04 (m, 1H), 1.85-1.6 (m, 3H), 1.57 – 1.27 (m, 18H), 0.95 – 0.81 (m, 12H)

^{13}C NMR (101 MHz, DMSO): δ = 172.63, 167.11, 158.58, 147.37, 147.23, 146.45, 146.26, 143.43, 128.38, 127.35, 125.23, 113.84, 94.13, 79.48, 52.21, 51.66, 51.45, 43.38, 27.92, 26.32, 24.09, 22.78, 22.03, 21.81

LC-MS (ESI): t_R = 12.73 min, calcd. for $C_{33}H_{49}N_3NaO_7^+$ $[M+Na]^+$: 622.35, found 622.27

Brevicompanine B (26):

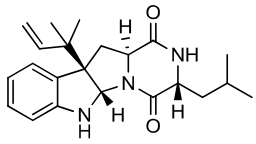

26

To a stirred solution of **35*a*** (50 mg, 0.083 mmol) in ACN (1 ml) at 0 °C was added TMSI (100 mg, 0.498 mmol). After 30 min of stirring, the reaction was allowed to warm to rt and stirred for further 3 h. The reaction was quenched by addition of saturated aq. $NaHCO_3$ solution (1 ml) and then extracted twice with DCM. The combined organic layers were dried over Na_2SO_4 and concentrated to dryness. The residue was dissolved in methanol (1 ml) and ammonium hydroxide (0.1 ml) was added. The resulting mixture was stirred for 2 h at room temperature and concentrated to dryness under reduced pressure. The residue was taken up in ACN/H_2O (1:1, 3 ml), filtered and purified directly via preparative RP-HPLC to yield the title compound.

Yield: 3.5 mg (9.53 µmol, 12%) as a white solid

^{1}H NMR (400 MHz, DMSO): δ = 8.37 (d, *J* = 3.8 Hz, 1H), 7.16 (d, *J* = 7.4 Hz, 1H), 6.99 (t, *J* = 7.5 Hz, 1H), 6.62 (t, *J* = 7.4 Hz, 1H), 6.53 (d, *J* = 7.8 Hz, 1H), 6.49 (s, 1H), 6.00 (dd, *J* = 17.3, 10.8 Hz, 1H), 5.76 (s, 1H), 5.45 (s, 1H), 5.07 (dd, *J* = 17.2, 14.2 Hz, 2H), 3.79 (dd, *J* = 11.1, 6.2 Hz, 1H), 3.64 (dt, *J* = 14.2, 8.1 Hz, 1H), 2.36 (dt, *J* = 12.8, 6.4 Hz, 1H), 2.23 – 2.14 (m, 1H), 1.79-1.40 (m, 3H), 1.38 – 1.18 (m, 3H), 1.02 (s, 3H), 0.87 (m, 9H).

^{13}C NMR (101 MHz, DMSO): δ = 168.00, 165.72, 151.01, 144.07, 128.82, 128.42, 124.69, 117.23, 114.03, 108.42, 76.41, 60.28, 57.15, 42.92, 40.71, 37.13, 23.59, 22.89, 22.61, 22.22, 21.56

LC-MS (ESI): t_R = 8.29 min, calcd. for $C_{22}H_{30}N_3O_2^+$ $[M+H]^+$: 368.23, found 368.10

(2*S*,3a*R*,8a*R*)-di-*tert*-butyl 2-(((*S*)-1-methoxy-4-methyl-1-oxopentan-2-yl)carbamoyl)-3a-(2-methylbut-3-en-2-yl)-3,3a-dihydropyrrolo[2,3-b]indole-1,8(2H,8aH)-dicarboxylate (35*b*):

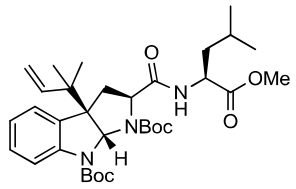

35*b*

To a solution of **34** (30 mg, 0.064 mmol) in DCM (2.5 mL) was added DCC (16.8 mg, 0.057 mmol), HOBt (10.1 mg, 0.053 mmol), and L-leucine methylester (22.7 mg, 0.088 mmol). The resulting mixture was stirred at room temperature for 12 h and diluted with ether (10 mL). The side product DCU was removed by filtration and the organic layer washed with 1 N HCl, saturated aq. $NaHCO_3$ solution, and brine. The organic layer was dried over Na_2SO_4, filtered, and concentrated under reduced pressure to yield the crude product. Flash chromatography with acetone/CH (1:9) as eluent yielded the title compound.

Yield: 16 mg (0,027 mmol, 62%) as a white foam

TLC (acetone/CH = 1:9): $R_f = 0.22$

^{1}H NMR (400 MHz, $CDCl_3$): δ = 7.39 (m, 1H), 7.22 (t, *J* = 7.7 Hz, 1H), 7.16 (d, *J* = 7.5 Hz, 1H), 7.05 (td, *J* = 7.5, 1.0 Hz, 1H), 6.14 (s, 1H), 5.87 (dd, *J* = 17.4, 10.8 Hz, 1H), 5.03 (dd, *J* = 24.9, 14.1 Hz, 1H), 4.64 (td, *J* = 8.6, 5.4 Hz, 1H), 3.70 (m, 3H), 3.68 – 3.61 (m, 1H), 2.42 – 2.34 (m, 2H), 2.04 (s, 1H), 1.79 – 1.59 (m, 3H), 1.53 (s, 9H), 1.42 (s, 9H), 1.03 (s, 3H), 0.93 (m, 9H).

^{13}C NMR (101 MHz, $CDCl_3$): δ = 169.10, 157.46, 152.51, 143.48, 142.95, 129.73, 128.61, 126.76, 125.02, 123.52, 118.80, 114.51, 81.65, 61.52, 60.54, 52.33, 50.63, 42.19, 40.48, 28.58, 28.37, 24.69, 23.14, 23.01, 22.04.

LC-MS (ESI): t_R = 12.74 min, calcd. for $C_{33}H_{49}N_3NaO_7^+$ $[M+Na]^+$: 622.35, found 622.37

***allo*-Brevicompanine B (29):**

29

To a stirred solution of **35*b*** (12 mg, 0.02 mmol) in ACN (0.3 ml) at 0 °C was added TMSI (19 µl, 0.12 mmol). After 30 min stirring, the reaction was allowed warm to room temperature and stirred for further 3 h. The reaction was stopped by addition of saturated aq. $NaHCO_3$ solution (0.3 ml) and then extracted twice with DCM. The combined organic layers were dried over Na_2SO_4 and concentrated to dryness. The residue was dissolved in methanol (1 ml) and then ammonium hydroxide (0.1 ml) was added. The resulting mixture was stirred for 2 h at room temperature and concentrated to dryness under reduced pressure. The residue was taken up in ACN/H_2O (1:1, 3 ml), filtered and purified directly via RP-HPLC to afford the title compound.

Yield: 2.1 mg (5.7 µmol, 30%) as a white solid

^{1}H NMR (400 MHz, DMSO): δ = 7.98 (s, 1H), 7.17 (d, *J* = 7.4 Hz, 1H), 7.04 – 6.96 (m, 1H), 6.62 (td, *J* = 7.4, 1.0 Hz, 1H), 6.53 (d, *J* = 7.8 Hz, 1H), 6.44 (s, 1H), 5.99 (dd, *J* = 17.3, 10.8 Hz, 1H), 5.39 (s, 1H), 5.11 – 5.00 (m, 2H), 4.00 (t, *J* = 5.2 Hz, 1H), 3.86 (dd, *J* = 10.8, 6.4 Hz, 1H), 2.39 – 2.31 (m, 1H), 2.27 – 2.17 (m, 1H), 1.92 – 1.66 (m, 2H), 1.48 – 1.36 (m, 1H), 1.04 (s, 3H), 0.91 – 0.80 (m, 9H)

^{13}C NMR (101 MHz, DMSO) δ 168.01, 165.73, 151.00, 144.08, 128.82, 128.43, 124.70, 117.23, 114.04, 108.42, 76.42, 60.28, 57.14, 54.86, 42.91, 40.72, 37.14, 23.60, 22.88, 22.63, 22.23, 21.56

LC-MS (ESI): t_R = 8.62 min, calcd. for $C_{22}H_{30}N_3O_2^+$ $[M+H]^+$: 368.23, found 368.07

(2*S*,3a*R*,8a*R*)-di-*tert*-butyl2-(((2*R*,3*S*)-1-methoxy-3-methyl-1-oxopentanyl)carbamoyl)-3a-(2-methyl-but-3-en-2-yl)-3,3a-dihydropyrrolo[2,3-b]indole-1,8(2H,8aH)-dicarboxylate (35*c*):

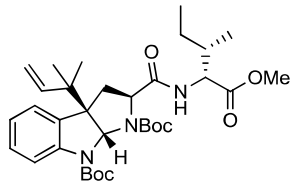

35*c*

To a solution of **34** (57 mg, 0.12mmol) in DMF (5 mL) was added PyBOP (75 mg, 0.144 mmol), HOBt (19.4 mg, 0.144 mmol), D-*iso*leucine methylester (22 mg, 0.12 mmol) and DIPEA (61 µl, 0.36 mmol). The resulting mixture was stirred at room temperature for 15 h. All volatiles were removed by reduced pressure and the crude product was taken up in EtOAc (15 ml). The organic layer was washed with 1 N HCl, saturated aq. $NaHCO_3$ solution and brine. The organic layer was dried over Na_2SO_4, filtered, and concentrated under reduced pressure to yield a pale yellow oil. Flash chromatography with the eluent acetone/CH (1:9) yielded the title compound.

Yield: 25 mg (0.042 mmol, 35%) as colorless oil

TLC (acetone/CH = 1:9): $R_f = 0.23$

^{1}H NMR (400 MHz, $CDCl_3$): δ = 7.37 (m, 1H), 7.22 (dt, J = 14.3, 3.6 Hz, 1H), 7.17 (t, J = 6.3 Hz, 1H), 7.11 – 7.02 (m, 1H), 6.31 – 6.08 (m, 2H), 5.86 (ddd, J = 17.5, 10.8, 6.7 Hz, 1H), 5.11 – 4.97 (m, 2H), 4.67 (dd, J = 9.1, 3.9 Hz, 1H), 3.72 (s, 3H), 3.72 – 3.69 (m, 1H), 2.50 – 2.45 (m, 1H), 2.33 (dd, J = 12.7, 10.5 Hz, 1H), 1.99 – 1.86 (m, 1H), 1.62 (s, 2H), 1.55 (s, 9H), 1.40 (s, 9H), 1.03 (d, J = 7.4 Hz, 3H), 0.97 (d, J = 7.8 Hz, 3H), 0.95 – 0.88 (m, 3H), 0.83 (d, J = 6.9 Hz, 3H)

^{13}C NMR (101 MHz, $CDCl_3$) δ 172.72, 152.64, 143.33, 142.83, 133.92, 128.66, 125.07, 123.58, 114.58, 81.78, 81.36, 79.53, 61.84, 55.09, 52.28, 40.48, 37.98, 28.59, 28.38, 27.06, 26.14, 23.08, 22.37, 14.73, 11.86

LC-MS (ESI): t_R = 11.65 min, calcd. for $C33H49N3NaO_7^+$ $[M+Na]^+$: 622.35, found 623.10

Brevicompanine A (25):

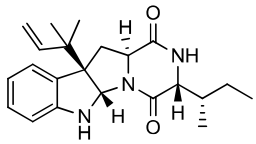

25

To a solution of **35*c*** (25 mg, 0.042 mmol) in dry DCM (4 ml) was added dropwise TMSOTf (76 µl, 0.42 mmol) under an argon atmosphere at 0 °C. This mixture was stirred for 1.5 h at 0 °C. The reaction mixture was diluted with saturated aq. $NaHCO_3$ solution and extracted three times with DCM. The combined organic layers were dried over Na_2SO_4, filtered and concentrated to dryness under reduced pressure. The resulting residue was dissolved in THF/MeOH (3:1, 4 ml) and cooled to 0 °C. To this solution, 0.5 N LiOH (252 µl, 0.126 mmol) was added and the resulting mixture was stirred for 16 h at rt. 1 N $KHSO_4$ (162 µl, 0.162 mmol) was added to the reaction mixture which was then diluted with saturated aq. $(NH_4)_2SO_4$ solution and extracted with DCM. The extract was dried over Na_2SO_4, filtered and concentrated to dryness. The resulting residue was dissolved in DCM (4 ml). To this solution was added PyBOP (26 mg, 0.050 mmol) and DIPEA (21 µl, 0.126 mmol) under an argon atmosphere. The resulting solution was stirred for 16 h at rt and then diluted by addition of saturated aq. $NaHCO_3$ solution. The resulting mixture was extracted with DCM, the organic layer was dried over Na_2SO_4, filtered and concentrated. The resulting crude product was purified by RP-HPLC to afford the title compound.

Yield: 1.7 mg (4.6 µmol, 11%) as colorless solid

^{1}H NMR (400 MHz, DMSO): δ = 7.15 (d, J = 6.9 Hz, 1H), 6.99 (t, J = 7.6 Hz, 1H), 6.61 (t, J = 6.9 Hz, 1H), 6.54 (d, J = 8.2 Hz, 1H), 6.00 (dd, J = 17.4, 10.8 Hz, 1H), 5.48 (s, 1H), 5.11 – 5.01 (m, 2H), 3.67 (d, J = 20.0 Hz, 2H), 2.41 (m, 1H), 2.03 – 1.96 (m, 1H), 1.41-1.23 (m, 2H), 1.04 (s, 3H), 0.88 (d, J = 10.7 Hz, 3H), 0.84 (q, J = 7.0 Hz, 3H), 0.67 (dt, J = 14.3, 6.9 Hz, 3H)

LC-MS (ESI): t_R = 8.20 min, calcd. for $C_{22}H_{30}N_3O_2^+$ $[M+H]^+$: 368.23, found 368.32

(2*S*,3a*R*,8a*R*)-di-*tert*-butyl 2-(((2*S*,3*S*)-1-methoxy-3-methyl-1-oxopentan-2-yl)carbamoyl)-3a-(2-methyl-but-3-en-2-yl)-3,3a-dihydropyrrolo[2,3-b]indole-1,8(2H,8aH)-dicarboxylate (35*d*):

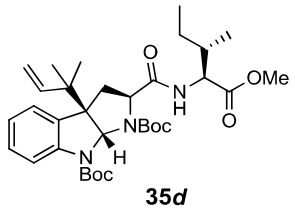

35*d*

To a solution of **34** (57 mg, 0.12mmol) in DMF (5 ml) was added PyBOP (75 mg, 0.144 mmol), HOBt (19.4 mg, 0.144 mmol), L-isoleucine methylester (22 mg, 0.12 mmol) and DIPEA (61 µl, 0.36 mmol). The resulting mixture was stirred at room temperature for 12 h. All volatiles were removed by reduced pressure and the crude product was taken up in EtOAc (15 ml). The organic layer was washed with 1 N HCl, saturated aq. $NaHCO_3$ solution, and brine. The organic layer was dried over Na_2SO_4, filtered, and concentrated under reduced pressure to yield a pale yellow oil. Flash chromatography with the eluents acetone/CH (1:9) then yielded the title compound.

Yield: 25 mg (0.042 mmol, 35%) as colorless oil

TLC (acetone/CH = 1:9): $R_f = 0.23$

^{1}H NMR (400 MHz, $CDCl_3$): δ = 7.45 – 7.29 (m, 1H), 7.22 (dd, J = 14.3, 6.2 Hz, 1H), 7.16 (t, J = 7.7 Hz, 1H), 7.05 (td, J = 7.5, 0.8 Hz, 1H), 6.23 (d, J = 8.7 Hz, 1H), 6.15 (s, 1H), 5.88 (dd, J = 17.4, 10.8 Hz, 1H), 5.10 – 4.97 (m, 2H), 4.57 (dd, J = 8.6, 5.1 Hz, 1H), 3.70 (s, 3H), 3.66 (dd, J = 15.7, 8.8 Hz, 1H), 2.49 – 2.25 (m, 2H), 1.93 – 1.80 (m, 1H), 1.63 (s, 2H), 1.56 – 1.52 (m, 9H), 1.40 (s, 9H), 1.03 (s, 3H), 0.94 – 0.87 (m, 9H)

^{13}C NMR (101 MHz, $CDCl_3$): δ = 172.39, 152.55, 143.49, 142.94, 128.62, 125.04, 123.47, 114.58, 81.67, 81.24, 79.20, 61.67, 56.28, 52.12, 40.50, 38.45, 28.59, 28.38, 27.06, 25.23, 23.15, 22.27, 15.48, 11.65

LC-MS (ESI): t_R = 11.56 min, calcd. for $C_{33}H_{49}N_3NaO_7^+$ $[M+Na]^+$: 622.35, found 623.14

***allo*-Brevicompanine A (28):**

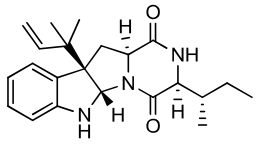

28

To a solution of **35*d*** (25 mg, 0.042 mmol) in dry DCM (4 ml) was added dropwise TMSOTf (76 µl, 0.42 mmol) under an argon atmosphere at 0 °C. The resulting mixture was stirred for 1.5 h at 0 °C. The reaction mixture was diluted by addition of saturated aq. $NaHCO_3$ solution and extracted three times with DCM. The combined organic layers were dried over Na_2SO_4, filtered and concentrated to dryness under reduced pressure. The resulting residue was dissolved in THF/MeOH (3:1, 4 ml) and cooled to 0 °C. To this solution, 0.5 N LiOH (252 µl, 0.126 mmol) was added and the mixture was stirred for 16 h at rt. 1 N $KHSO_4$ (162 µL, 0.162 mmol) was added to the reaction mixture, followed by dilution with saturated aq. $(NH_4)_2SO_4$ solution and the resulting mixture was extracted with DCM. The organic phase was dried over Na_2SO_4, filtered and concentrated to dryness. The resulting residue was dissolved in DCM (4 ml). To this solution was added PyBOP (26 mg, 0.050 mmol) and DIPEA (21 µL, 0.126 mmol) under an argon atmosphere. The resulting solution was stirred for 16 h at rt and then diluted with saturated aq. $NaHCO_3$ solution. Extraction with DCM, drying of the organic layer over Na_2SO_4, filtration and concentration to dryness then delivered the crude product which was purified by RP-HPLC to yield the title compound.

Yield: 1.5 mg (4.1 µmol, 10%) as colorless solid

^{1}H NMR (400 MHz, DMSO): δ = 7.16 (d, J = 7.1 Hz, 1H), 6.99 (t, J = 7.6 Hz, 1H), 6.62 (d, J = 6.7 Hz, 1H), 6.53 – 6.43 (m, 1H), 5.97 (dd, J = 17.4, 10.8 Hz, 1H), 5.45 (s, 1H), 5.06 (dd, J = 14.1, 8.6 Hz, 2H), 3.89 (m, 1H), 3.66 – 3.55 (m, 1H), 2.41 (dd, J 0 12 Hz, J = 11 Hz, 1H), 2.03 – 1.96 (m, 1H), 1.41-1.22 (m, 2H), 1.04 (s, 3H), 0.95 (d, J = 7.1 Hz, 3H), 0.84 (dd, J = 12.3, 4.8 Hz, 6H)

LC-MS (ESI): t_R = 8.54 min, calcd. for $C_{22}H_{30}N_3O_2^+$ $[M+H]^+$: 368.23, found 368.49

(2*S*,3a*R*,8a*R*)-di-*tert*-butyl 2-(((*R*)-1-methoxy-3-methyl-1-oxobutan-2-yl)carbamoyl)-3a-(2-methylbut-3-en-2-yl)-3,3a-dihydropyrrolo[2,3-b]indole-1,8(2H,8aH)-dicarboxylate (35*e*):

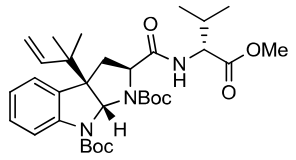

35e

To a solution of **34** (122.6 mg, 0.26mmol) in DCM (5 ml) was added PyBOP (162 mg, 0.31 mmol), HOBt (42 mg, 0.31 mmol), D-valine methylester (44 mg, 0.26 mmol) and DIPEA (222 µl, 1.3 mmol). The resulting mixture was stirred at room temperature for 12 h and diluted by addition with ether (10 ml). The organic layer was washed with 1 N HCl, saturated aq. $NaHCO_3$ solution and brine. The organic layer was dried over Na_2SO_4, filtered, and concentrated under reduced pressure to yield a light yellow foam. Flash chromatography, with the eluents DCM/MeOH (30:1) then yielded the title compound.

Yield: 52.7 mg (0.098 mmol, 38%) as a white foam

TLC (DCM/MeOH = 30:1): $R_f = 0.4$

^{1}H NMR (400 MHz, $CDCl_3$): δ = 7.36 (dd, *J* = 17.3, 9.9 Hz, 1H), 7.25 – 7.09 (m, 2H), 7.05 (td, *J* = 7.5, 1.0 Hz, 1H), 6.20 (d, *J* = 8.9 Hz, 1H), 6.16 (s, 1H), 5.86 (ddd, *J* = 17.2, 10.8, 6.4 Hz, 1H), 5.10 – 4.97 (m, 2H), 4.53 (dd, *J* = 8.9, 4.8 Hz, 1H), 3.72 (s, 3H), 3.71 (t, *J* = 1.8 Hz, 1H), 2.44 (dd, *J* = 12.8, 6.6 Hz, 1H), 2.31 (dd, *J* = 12.7, 10.5 Hz, 1H), 2.21 – 2.06 (m, 1H), 1.55 (d, *J* = 7.2 Hz, 9H), 1.41 (d, *J* = 6.7 Hz, 9H), 1.02 (d, *J* = 6.5 Hz, 3H), 0.96 – 0.86 (m, 9H)

^{13}C NMR (101 MHz, $CDCl_3$): δ = 172.35, 152.62, 143.31, 142.85, 133.88, 128.65, 125.05, 123.52, 118.37, 114.57, 81.75, 81.35, 79.48, 61.79, 56.78, 52.20, 40.47, 31.54, 28.57, 28.39, 23.08, 22.35, 18.99, 17.87

LC-MS (ESI): t_R = 11.29 min, calcd. for $C_{32}H_{47}N_3NaO_7^+$ $[M+Na]^+$: 608.33, found 608.23

Brevicompanine C (27):

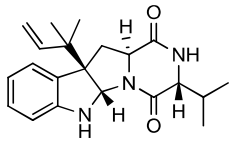

27

To a stirred solution of **35*e*** (40 mg, 0.068 mmol) in DCM (4 ml) at 0 °C was added TMSOTf (75 µl, 0.41 mmol). The resulting reaction mixture was stirred for 1.5 h at 0 °C. The reaction was quenched by addition of saturated aq. $NaHCO_3$ solution (1 ml) and then extracted twice with DCM. The combined organic layers were dried with Na_2SO_4 and concentrated to dryness. The residue was dissolved in methanol (1 ml) and ammonium hydroxide (0.1 ml) was added. The resulting mixture was stirred for 2 h at room temperature and concentrated to dryness under reduced pressure. The residue was taken up in ACN/H_2O (1:1, 3 ml), filtered and purified directly via RP-HPLC to yield the title compound.

Yield: 3.2 mg (9.07 µmol, 13%) as a white solid

^{1}H NMR (400 MHz, DMSO): δ = 7.15 (d, J = 7.3 Hz, 1H), 7.06 (t, J = 7.5 Hz, 1H), 6.99 (m, 2H), 6.61 (t, J = 7.0 Hz, 1H), 6.54 (s, 1H), 6.00 (dd, J = 17.4, 10.8 Hz, 1H), 5.47 (s, 1H), 5.07 (ddd, J = 18.7, 14.1, 1.4 Hz, 2H), 3.68 (dd, J = 11.3, 5.9 Hz, 1H), 3.53 (dd, J = 9.7, 5.6 Hz, 1H), 2.38 – 2.31 (m, 1H), 2.18 (t, J = 11.9 Hz, 1H), 1.04 (s, 3H), 0.86 (m, 9H)

^{13}C NMR (101 MHz, DMSO): δ = 167.81, 164.51, 162.29, 151.21, 144.09, 128.66, 128.44, 124.65, 117.23, 113.93, 108.24, 76.36, 61.57, 60.24, 57.43, 40.59, 38.23, 37.42, 35.76, 33.28, 30.76, 22.61, 22.26, 18.58, 17.19

LC-MS (ESI): t_R = 7.73 min, calcd. for $C_{21}H_{28}N_3O_2^+$ $[M+H]^+$: 354.22, found 354.12

(2*S*,3a*R*,8a*R*)-di-*tert*-butyl 2-(((*S*)-1-methoxy-3-methyl-1-oxobutan-2-yl)carbamoyl)-3a-(2-methylbut-3-en-2-yl)-3,3a-dihydropyrrolo[2,3-b]indole-1,8(2H,8aH)-dicarboxylate (35*f*):

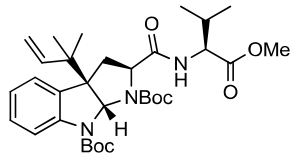

35*f*

To a solution of **34** (122.6 mg, 0.26 mmol) in DCM (5 ml) was added PyBOP (162 mg, 0.31 mmol), HOBt (42 mg, 0.31 mmol), L-valine methylester (44 mg, 0.26 mmol) and DIPEA (222 µl, 1.3 mmol). The mixture was stirred at room temperature for 12 h and diluted by the addition of ether (10 ml). The organic layer was washed with 1 N HCl, saturated aq. $NaHCO_3$ solution and brine. The organic layer was dried over Na_2SO_4, filtered, and concentrated under reduced pressure to yield a light yellow foam. Flash chromatography with the eluents DCM/MeOH (30:1) then yielded the title compound.

Yield: 60 mg (0.102 mmol, 40%) as a white foam

TLC (DCM/MeOH = 30:1): $R_f = 0.4$

^{1}H NMR (400 MHz, $CDCl_3$): δ = 7.40 (ddd, J = 21.0, 12.9, 4.7 Hz, 1H), 7.22 (dt, J = 7.4, 2.7 Hz, 1H), 7.18 – 7.14 (m, 1H), 7.05 (td, J = 7.5, 0.7 Hz, 1H), 6.23 – 6.18 (m, 1H), 6.15 (s, 1H), 5.88 (dd, J = 17.4, 10.8 Hz, 1H), 5.11 – 4.96 (m, 2H), 4.53 (dd, J = 8.7, 4.9 Hz, 1H), 3.70 (s, 3H), 3.70 – 3.62 (m, 1H), 2.51 – 2.29 (m, 2H), 2.12 (qt, J = 13.7, 6.9 Hz, 1H), 1.55 (d, J = 6.2 Hz, 9H), 1.41 (d, J = 6.2 Hz, 9H), 1.03 (s, 3H), 0.96 – 0.88 (m, 9H)

^{13}C NMR (101 MHz, $CDCl_3$): δ = 172.40, 152.54, 143.47, 142.94, 128.61, 125.05, 123.47, 114.59, 81.66, 81.23, 79.22, 61.71, 56.96, 52.16, 40.49, 31.91, 28.58, 28.47, 28.38, 23.14, 22.27, 21.18, 19.03, 17.84

LC-MS (ESI): t_R = 11.23 min, calcd. for $C_{32}H_{47}N_3NaO_7^+$ $[M+Na]^+$: 608.33, found 608.21

***allo*-Brevicompanine C (30):**

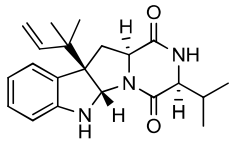

30

To a stirred solution of ***35f*** (40 mg, 0.068 mmol) in DCM (4 ml) at 0 °C was added TMSOTf (75 µl, 0.41 mmol). The resulting reaction mixture was stirred for 1.5 h at 0 °C. The reaction was quenched by addition of a saturated aq. $NaHCO_3$ solution (1 ml) and then extracted twice with DCM. The combined organic layers were dried over Na_2SO_4 and concentrated to dryness. The residue was dissolved in methanol (1 ml) and ammonium hydroxide (0.1 ml) was added. The resulting mixture was stirred for 2 h at room temperature and concentrated to dryness under reduced pressure. The residue was taken up in ACN/H_2O (1:1, 3 ml), filtered and purified directly via RP-HPLC to yield the title compound.

Yield: 3 mg (8.5 µmol, 12%) as a white solid

^{1}H NMR (400 MHz, DMSO): δ = 7.16 (d, J = 7.3 Hz, 1H), 6.99 (m, 2H), 6.62 (t, J = 7.4 Hz, 1H), 6.56 – 6.45 (m, 1H), 5.98 (dd, J = 17.3, 10.9 Hz, 1H), 5.46 (s, 1H), 5.13 – 4.98 (m, 2H), 3.90 (s, 1H), 3.78 (dd, J = 11.0, 5.6 Hz, 1H), 2.36 – 2.29 (m, 1H), 2.25 – 2.14 (m, 1H), 1.04 (s, 3H), 0.97 – 0.81 (m, 9H)

^{13}C NMR (101 MHz, DMSO): δ = 167.82, 164.61, 162.29, 151.21, 144.09, 128.66, 128.44, 124.65, 117.23, 113.93, 108.24, 76.36, 61.57, 60.24, 57.43, 40.59, 38.23, 37.42, 35.76, 33.28, 30.76, 22.61, 22.26, 18.58, 17.20

LC-MS (ESI): Rt = 8.03 min, calcd. for $C_{21}H_{28}N_3O_2^+$ $[M+H]^+$: 354.22, found 354.23

(2*S*,3a*R*,8a*R*)-di-tert-butyl 2-(((*S*)-1-methoxy-1-oxopent-4-yn-2-yl)carbamoyl)-3a-(2-methylbut-3-en-2-yl)-3,3a-dihydropyrrolo[2,3-b]indole-1,8(2H,8aH)-dicarboxylate (36):

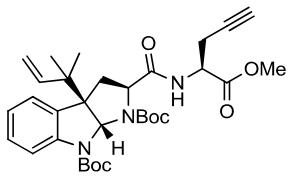

36

To a solution of **34** (190 mg, 0.4 mmol) in DCM (10 ml) was added EDC hydrochloride (99.32 mg, 0.52 mmol), HOBt (64.8 mg, 0.48 mmol) and L-propargylglycine methylester (130.4 mg, 0.8 mmol). The resulting mixture was stirred at room temperature for 12 h and diluted by addition of ether (10 ml). The organic layer was washed with 1 N HCl, saturated aq. $NaHCO_3$ solution and brine, dried over Na_2SO_4, filtered, and concentrated under reduced pressure to yield a light yellow foam. Flash chromatography with acetone/CH (1:9) as eluent then yielded the title compound.

Yield: 95 mg (0.17 mmol, 41%) as a white solid

TLC (acetone/CH = 1:9): $R_f = 0.32$

^{1}H NMR (400 MHz, $CDCl_3$): δ = 7.46 – 7.32 (m, 1H), 7.20 (dd, *J* = 19.6, 7.7 Hz, 2H), 7.05 (t, *J* = 7.8 Hz, 1H), 6.49 (d, *J* = 7.6 Hz, 1H), 6.16 (s, 1H), 5.86 (dd, *J* = 17.3, 10.8 Hz, 1H), 5.03 (dd, *J* = 22.4, 14.1 Hz, 2H), 4.77 – 4.70 (m, 1H), 3.78 (d, *J* = 6.7 Hz, 3H), 3.70 (dd, *J* = 10.4, 6.5 Hz, 1H), 2.76 (d, *J* = 2.3 Hz, 2H), 2.45 (dd, *J* = 12.6, 6.5 Hz, 1H), 2.32 (dd, *J* = 12.5, 10.6 Hz, 1H), 2.01 (t, *J* = 2.5 Hz, 1H), 1.56 (d, *J* = 6.6 Hz, 9H), 1.42 – 1.39 (m, 9H), 1.03 (s, 3H), 0.92 (s, 3H)

^{13}C NMR (101 MHz, $CDCl_3$): δ = 170.72, 152.54, 143.36, 142.98, 128.67, 125.03, 123.52, 114.55, 106.69, 100.14, 81.67, 78.66, 71.64, 61.64, 52.87, 50.53, 40.45, 28.57, 28.42, 27.06, 23.12, 22.54, 22.35

LC-MS (ESI): t_R = 11.83 min, calcd. for $C_{32}H_{44}N_3O_7^+$ $[M+H]^+$: 582.32, found 582.07

(3*R*,5a*S*,10b*R*,11a*S*)-10b-(2-methylbut-3-en-2-yl)-3-(prop-2-yn-1-yl)-2,3,5a,6,11,11a-hexahydro-1H-pyrazino[1',2':1,5]pyrrolo[2,3-b]indole-1,4(10bH)-dione (37):

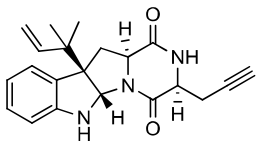

37

To a stirred solution of **36** (20 mg, 0.057 mmol) in ACN (0.5 ml) at 0 °C was added TMSI (54 µl, 0.342 mmol). After 30 min stirring, the reaction mixture was allowed to warm to room temperature and stirred for further 3 h. The reaction was quenched by addition of saturated aq. $NaHCO_3$ solution (0.5 ml) and then extracted twice with DCM. The combined organic layers were dried over Na_2SO_4 and concentrated to dryness. The residue was dissolved in methanol (1 ml) and then ammonium hydroxide (0.1 ml) was added. The resulting solution was stirred for 2 h at room temperature and concentrated to dryness under reduced pressure. The residue was taken up in ACN/H_2O (1:1, 3 ml), filtered and purified directly via RP-HPLC to afford the title compound.

Yield: 2.9 mg (8.3 µmol, 15%) as a white solid

^{1}H NMR (400 MHz, DMSO): δ = 8.12 (s, 1H), 7.16 (d, *J* = 6.8 Hz, 1H), 7.00 (td, *J* = 7.7, 1.1 Hz, 1H), 6.62 (td, *J* = 7.4, 1.0 Hz, 1H), 6.51 (d, *J* = 7.8 Hz, 1H), 5.97 (dd, *J* = 17.3, 10.8 Hz, 1H), 5.48 (s, 1H), 5.06 (ddd, *J* = 18.8, 14.1, 1.3 Hz, 2H), 4.17 (s, 1H), 3.81 (dd, *J* = 5.7, 4.2 Hz, 1H), 2.84 (t, *J* = 2.5 Hz, 1H), 2.79 – 2.64 (m, 1H), 2.56 – 2.52 (m, 1H), 2.34 (dd, *J* = 12.3, 5.9 Hz, 1H), 2.20 (t, *J* = 11.9 Hz, 1H), 1.03 (s, 3H), 0.94 – 0.84 (m, 3H)

^{13}C NMR (101 MHz, $CDCl_3$): δ = 167.63, 163.42, 151.19, 143.99, 137.64, 132.28, 128.85, 128.38, 124.75, 117.23, 113.89, 108.22, 80.10, 76.35, 73.28, 60.88, 57.98, 53.62, 40.73, 37.67, 22.69, 22.22, 21.64

LC-MS (ESI): t_R = 8.58 min, calcd. for $C_{21}H_{24}N_3O_2^+$ $[M+H]^+$: 350.19, found 350.00

Alloc-D-Lys(Boc)-OH (38):

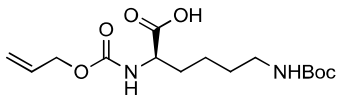

38

H-D-Lys(Boc)-OH (1 g, 4.06 mmol) was dissolved in water (10 ml) and $NaHCO_3$ (1.023 g, 12.18 mmol) was added under stirring. The resulting solution was cooled to 0 °C and allyl chloroformate (0.644 ml, 6.09 mmol) was slowly added as a solution in dioxane (10 ml). The resulting mixture was stirred for 1 h at 0 °C and allowed to warm to rt and stirred for further 16 h at rt. Water (10 mL) was added and the aqueous layer was extracted twice with EtOAc. The organic layer was re-extracted twice with a saturated aq. $NaHCO_3$ solution. The combined aqueous layers were acidified to pH of 1 with 10% HCl and extracted three times with EtOAc. The combined organic layers were dried over Na_2SO_4 and concentrated to dryness. The resulting residue was purified by flash chromatography (EtOAc/CH 1:1 + 0.1% AcOH) to yield the title compound.

Yield: 1.33 g (4.03 mmol, 99%) as a colorless solid

TLC (EA/CH = 1:1 + 0.1% AcOH): $R_f = 0.38$

^{1}H NMR (400 MHz, $CDCl_3$): δ = 5.88 (ddt, J = 16.1, 10.7, 5.6 Hz, 1H), 5.67 (d, J = 7.2 Hz, 1H), 5.23 (d, J = 17.2 Hz, 1H), 5.14 (dd, J = 10.4, 1.0 Hz, 1H), 4.55 (d, J = 5.3 Hz, 2H), 4.36 – 4.11 (m, 1H), 3.06 (d, J = 6.3 Hz, 2H), 1.77 (m, 2H), 1.46 (dd, J = 11.4, 5.2 Hz, 2H), 1.41 (s, 9H), 1.39 (m, 2H)

^{13}C NMR (101 MHz, $CDCl_3$): δ = 176.96, 176.58, 156.24, 132.69, 117.91, 65.99, 60.58, 53.72, 31.87, 29.41, 28.46, 22.33, 20.87

LC-MS (ESI): t_R = 5.41 min, calcd. for $C_{15}H_{25}N_2O_6^-$ $[M-H]^-$: 329.17, found 329.13

Alloc-D-Lys-OMe (39):

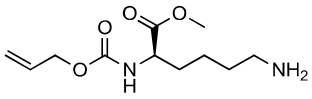

39

A solution of **38** (1.33 g, 4.03 mmol) in MeOH (10 ml) was cooled to 0 °C. To this solution was added dropwise $SOCl_2$ (1.37 ml, 18.9 mmol). The resulting mixture was allowed to warm to rt and then heated up to 50 °C for further 5 h. All volatiles were removed by reduced

pressure, affording the title compound which was used in the next steps without further purification.

Yield: 0.903 g (3.9 mmol, 95%) as a colorless solid

^{1}H NMR (400 MHz, $CDCl_3$): δ = 5.86 (s, 2H), 5.30 (d, J = 17.0 Hz, 1H), 5.20 (d, J = 10.0 Hz, 1H), 4.56 (s, 2H), 4.25 (d, J = 48.2 Hz, 1H), 3.74 (s, 3H), 3.22 – 2.93 (m, 2H), 1.83 (s, 4H), 1.50 (s, 2H)

^{13}C NMR (101 MHz, $CDCl_3$): δ = 173.15, 156.25, 132.82, 117.97, 66.03, 53.93, 52.76, 39.97, 31.73, 27.09, 22.53

LC-MS (ESI): t_R = 3.33 min, calcd. for $C_{11}H_{21}N_2O_4^+$ $[M+H]^+$: 245.15, found 244.89

Fmoc-L-propargyl glycine (39*a*):

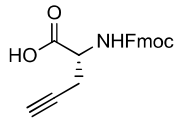

39*a*

To a solution of L-propargyl glycine (0.5 g, 4.42 mmol) in H_2O (10 ml) was added $NaHCO_3$ (0.744 g, 8.84 mmol). The resulting solution was cooled to 0 °C and Fmoc-Cl (1.71 g, 6.63 mmol) was slowly added as a solution in dioxane (10 ml). The resulting mixture was stirred at 0 °C for 1 h and then allowed to warm to rt overnight. Water (10 ml) was added and the aqueous layer was extracted two times with EtOAc. The organic layer was re-extracted twice with saturated aq. $NaHCO_3$ solution. The combined aqueous layers were acidified to pH 1 by addition of 1 N HCl and then extracted three times with EtOAc. The combined organic layers were dried over Na_2SO_4, filtered and concentrated in vacuo. The product was used without further purification.

Yield: 1.12 g (3.34 mmol, 76%) as a colorless solid

^{1}H NMR (400 MHz, $CDCl_3$): δ = 7.63 (d, J = 7.5 Hz, 2H), 7.49 (d, J = 7.4 Hz, 2H), 7.26 (t, J = 7.4 Hz, 2H), 7.18 (t, J = 7.4 Hz, 2H), 4.32 (dd, J = 10.3, 5.2 Hz, 1H), 4.25 (t, J = 6.6 Hz, 1H), 4.11 (t, J = 7.0 Hz, 1H), 2.64 (d, J = 13.6 Hz, 2H), 1.99 (s, 1H)

^{13}C NMR (101 MHz, $CDCl_3$): δ = 172.06, 156.11, 143.59, 141.15, 127.60, 126.96, 124.98, 119.82, 78.52, 71.31, 67.04, 52.20, 46.95, 22.24

LC-MS (ESI): t_R = 6.04 min, calcd. for $C_{40}H_{32}N_2NaO8^-$ $[2M-2H+Na]^-$: 691.21, found 692.01

(*R*)-Methyl 6-((*R*)-2-((((9H-fluoren-9-yl)methoxy)carbonyl)amino)pent-4-ynamido)-2-(((allyloxy) carbonyl)amino)hexanoate (40):

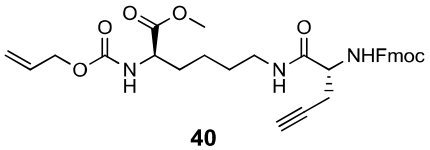

40

39 (200 mg, 0.82 mmol), EDC*HCl (314.4 mg, 1.64 mmol) and HOBt (121.78 mg, 0.902 mmol) were dissolved in DCM. To this solution, DIPEA (0.7 mL, 4.1 mmol) was added and the resulting mixture was stirred for 5 min at rt. In a separate flask, **23*a*** (274 mg, 0.82 mmol) was dissolved in DCM (3 mL) and added to the first reaction mixture. The resulting solution was stirred for 16 h at rt. All volatiles were removed by rotary evaporation. The resulting crude product was taken up in EtOAc (20 ml) and washed once with saturated aq. $NaHCO_3$ solution, once with 1 N HCl and once with brine. The organic layer was dried over Na_2SO_4, filtered and concentrated to dryness. The resulting crude product was purified by flash chromatography with DCM/MeOH (50:1) as eluent to yield the title compound.

Yield: 0.33 g (0.59 mmol, 72%) as a colorless solid

TLC (DCM/MeOH = 50:1): $R_f = 0.33$

^{1}H NMR (400 MHz, $CDCl_3$): δ = 7.77 (d, J = 7.5 Hz, 2H), 7.57 (t, J = 16.4 Hz, 2H), 7.41 (t, J = 7.5 Hz, 2H), 7.31 (dd, J = 17.1, 9.7 Hz, 2H), 5.90 (ddd, J = 22.8, 10.9, 5.7 Hz, 1H), 5.31 (m, 1H), 5.21 (dd, J = 10.4, 1.2 Hz, 1H), 4.56 (d, J = 5.3 Hz, 2H), 4.46 (m, 2H), 4.32 (m, 2H), 4.23 (t, J = 6.8 Hz, 1H), 3.75 (s, 3H), 3.28 (m, 2H), 2.87 – 2.52 (m, 2H), 2.15 – 2.10 (m, 1H), 1.87 – 1.78 (m, 2H), 1.55 (m, 2H), 1.41 (m, 2H)

^{13}C NMR (101 MHz, $CDCl_3$): δ = 173.00, 169.89, 156.09, 148.63, 143.83, 141.50, 132.70, 127.95, 127.25, 125.17, 120.21, 118.10, 72.08, 67.36, 66.06, 53.66, 52.60, 47.29, 39.30, 32.32, 28.87, 22.82, 22.38

LC-MS (ESI): t_R = 8.92 min, calcd. for $C_{31}H_{36}N_3O_7^+$ $[M+H]^+$: 562.25, found 563.04

(*R*)-Methyl 2-(((allyloxy)carbonyl)amino)-6-((*R*)-2-(3-benzoylbenzamido)pent-4-ynamido)hexanoate (41):

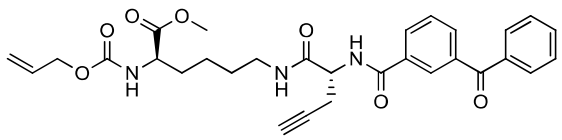

41

40 (330 mg, 0.92 mmol) was dissolved in ACN (9.2 ml). To this solution was added diethylamine (0.95 ml, 9.2 mmol) and the resulting mixture was stirred at rt for 2 h. The reaction mixture was concentrated to dryness and the resulting residue was dissolved in 90% aqueous ACN and washed three times with heptane. The heptane layer containing cleaved dibenzofulvene was discarded and the acetonitrile water phase was concentrated to dryness to yield the free amine (225 mg, 0.67 mmol) which was directly added to a solution of 3-benzoylbenzoic acid (180 mg, 0.8 mmol), HBTU (365 mg, 0.96 mmol), HOBt (122 mg, 0.9 mmol) and DIPEA (0.7 ml, 4.12 mmol) in DCM (8 ml). The resulting reaction mixture was stirred for 4 h at rt. The solvent was removed and the residue was taken up in EtOAc and washed sequentially with saturated aq. $NaHCO_3$ solution, 1 N HCl and brine. The organic layer was dried (Na_2SO_4), filtered and concentrated. The crude product was purified by gel chromatography (DCM/MeOH 50:1) to yield 326 mg (0.6 mmol, 67% over 2 steps) of the desired product.

Yield: 326 mg (0.6 mmol, 65%) as a colorless solid

TLC (DCM/MeOH = 50:1): $R_f = 0.14$

^{1}H NMR (400 MHz, $CDCl_3$): δ = 7.94 (d, J = 8.2 Hz, 2H), 7.85 (d, J = 8.4 Hz, 2H), 7.83 – 7.77 (m, 2H), 7.65 – 7.59 (m, 1H), 7.49 (dd, J = 10.6, 4.7 Hz, 2H), 7.34 (d, J = 7.0 Hz, 1H), 6.54 (s, 1H), 5.90 (ddd, J = 22.8, 10.8, 5.7 Hz, 1H), 5.41 (d, J = 8.1 Hz, 1H), 5.36 – 5.24 (m, 1H), 5.24 – 5.17 (m, 1H), 4.75 (dd, J = 12.9, 7.5 Hz, 1H), 4.57 (d, J = 5.6 Hz, 2H), 4.34 (m, 1H), 3.74 (s, 3H), 3.39 (m, 1H), 3.32 – 3.22 (m, 1H), 2.98 – 2.87 (m, 1H), 2.71 (ddd, J = 16.8, 7.8, 2.4 Hz, 1H), 2.17 (t, J = 2.5 Hz, 1H), 1.92 – 1.80 (m, 1H), 1.77 – 1.65 (m, 1H), 1.58 (m, 2H), 1.43 (m, 2H)

^{13}C NMR (101 MHz, $CDCl_3$): δ = 196.00, 174.85, 173.02, 169.96, 166.52, 156.10, 140.71, 137.12, 136.77, 133.08, 132.67, 130.30, 130.23, 128.62, 127.35, 118.13, 79.63, 72.19, 66.08, 60.55, 53.67, 52.61, 52.32, 39.43, 32.29, 28.80, 22.68, 22.41, 21.19, 20.62, 14.34

LC-MS (ESI): t_R = 8.01 min, calcd. for $C_{30}H_{34}N_3O_7^+$ $[M+H]^+$: 548.24, found 548.09

(*R*)-Methyl 2-amino-6-((*R*)-2-(3-benzoylbenzamido)pent-4-ynamido)hexanoate (42):

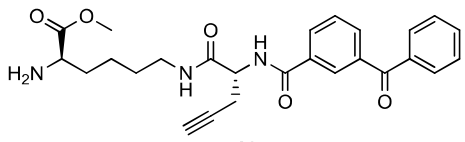

42

41 (326 mg, 0.6 mmol) was dissolved in dry THF (5 ml) under an argon atmosphere. Dimedone (589 mg, 4.2 mmol) followed by tetrakis(triphenylphosphine)palladium (70 mg, 0.06 mmol) were sequentially added as a solution in dry THF. The resulting reaction mixture was stirred until TLC indicated consumption of the whole starting material (≈ 1.5 h). The reaction mixture was concentrated to dryness and purified by flash chromatography (DCM/MeOH 19:1) to yield the title compound.

Yield: 120 mg (0.26 mmol, 44%) as a colorless solid
TLC (DCM/MeOH = 19:1): R_f = 0.22
LC-MS (ESI): t_R = 5.23 min, calcd. for $C_{26}H_{30}N_3O_5^+$ $[M+H]^+$: 464.21, found 464.30

(2*S*,3a*R*,8a*R*)-di-*tert*-butyl 2-(((*R*)-6-((*R*)-2-(3-benzoylbenzamido)pent-4-ynamido)-1-methoxy-1-oxo-hexan-2-yl)carbamoyl)-3a-(2-methylbut-3-en-2-yl)-3,3a-dihydropyrrolo [2,3-b]indole-1,8(2H,8aH)-di-carboxylate (43):

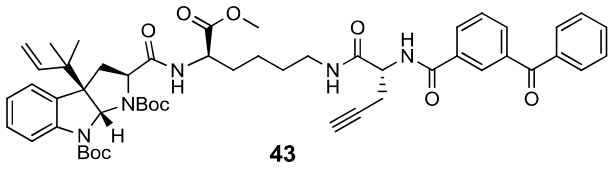

43

34 (61.3 mg, 0.13 mmol), PyBOP (81.12 mg, 0.156 mmol), HOBt (21.06 mg, 0.156 mmol) and DIPEA (111 µl, 0.65 mmol) were dissolved in DCM (4 ml). **42** (60 mg, 0.13 mmol) was dissolved separately in DCM (2 ml) and added to the reaction mixture. The resulting solution was stirred for 1.5 h at rt. The solvent was evaporated under reduced pressure and the resulting residue was taken up in EtOAc and washed sequentially with saturated aq. $NaHCO_3$ solution, 0.5 N HCl and brine. The organic layer was dried over Na_2SO_4, filtered and concentrated to dryness. The resulting crude product was purified by flash chromatography (silicagel, DCM/MeOH 30:1) to yield the desired product.

Yield: 30 mg (0.033 mmol, 26%) as a colorless solid

TLC (DCM/MeOH = 30:1): $R_f = 0.3$

^{1}H NMR (400 MHz, $CDCl_3$): δ = 7.94 (t, J = 6.9 Hz, 2H), 7.87 – 7.77 (m, 5H), 7.61 (dd, J = 16.1, 9.2 Hz, 2H), 7.49 (dd, J = 10.6, 4.4 Hz, 3H), 7.19 (dd, J = 14.2, 7.7 Hz, 1H), 7.11 – 7.01 (m, 1H), 6.72 (s, 1H), 6.47 (d, J = 11.7 Hz, 1H), 6.27 – 6.13 (m, 1H), 5.85 (ddd, J = 15.6, 10.7, 4.8 Hz, 1H), 5.14 – 4.94 (m, 2H), 4.73 (d, J = 6.7 Hz, 1H), 4.48 (d, J = 23.4 Hz, 1H), 3.72 (s, 3H), 3.41 (d, J = 2.9 Hz, 2H), 3.29 – 3.20 (m, 1H), 2.99 – 2.88 (m, 1H), 2.45 (dd, J = 12.5, 6.5 Hz, 1H), 2.32 (d, J = 12.4 Hz, 1H), 2.12 (dd, J = 20.5, 9.3 Hz, 2H), 1.95 (s, 2H), 1.89 – 1.63 (m, 2H), 1.55 (m, 9H), 1.34 (s, 9H), 1.06 – 0.93 (m, 6H), 0.89 (d, J = 10.3 Hz, 2H)

^{13}C NMR (101 MHz, $CDCl_3$): δ = 196.04, 172.65, 171.94, 170.25, 166.70, 152.65, 143.28, 140.52, 137.18, 133.03, 132.33, 130.23, 130.19, 128.75, 128.61, 128.59, 127.47, 127.34, 125.07, 114.61, 81.85, 77.37, 53.56, 52.50, 48.77, 40.48, 28.58, 28.53, 28.49, 28.47, 28.39, 28.09, 26.53, 26.44, 23.11, 22.34, 14.34

LC-MS (ESI): t_R = 5.23 min, calcd. for $C_{52}H_{62}N_5O_{10}^-$ $[M-H]^-$: 916.45, found 916.49

3-Benzoyl-*N*-((*R*)-1-((4-((3*R*,5a*S*,10b*R*,11a*S*)-10b-(2-methylbut-3-en-2-yl)-1,4-dioxo-2,3,4,5a,6,10b,11,11a-octahydro-1H-pyrazino[1',2':1,5]pyrrolo[2,3-b]indol-3-yl)butyl)amino)-1-oxopent-4-yn-2-yl) benzamide (44):

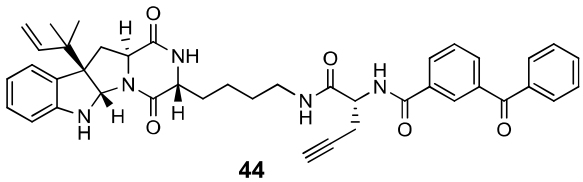

44

To a solution of **43** (25 mg, 0.027 mmol) in dry DCM (1.7 ml) was added dropwise TMSOTf (49 µl, 0.27 mmol) under an argon atmosphere at 0 °C. This mixture was stirred for 1.5 h at 0 °C. The reaction mixture was diluted by addition of saturated aq. $NaHCO_3$ solution and extracted three times with DCM. The combined organic layers were dried over Na_2SO_4, filtered and concentrated to dryness under reduced pressure. The resulting residue was dissolved in THF/MeOH (3:1, 2 ml) and cooled to 0 °C. To this solution, 0.5 N LiOH (162 µl, 0.081 mmol) was added and the mixture was stirred for 3 h at rt. 1 N $KHSO_4$ (162 µL, 0.162 mmol) was subsequently added to the reaction mixture which was then diluted by addition of saturated aq. $(NH_4)_2SO_4$ solution and extracted with DCM. The organic layer was dried over Na_2SO_4, filtered and concentrated to dryness. The resulting residue was dissolved

in DCM (3 ml). To this solution was added PyBOP (16.8 mg, 0.032 mmol) and DIPEA (9.5 µl, 0.054 mmol) under an argon atmosphere. The resulting solution was stirred for 16 h at rt and was then diluted by addition of saturated aq. $NaHCO_3$ solution and extracted with DCM. The organic layer was dried over $NaSO_4$, filtered and concentrated. The resulting crude product was purified by flash chromatography (DCM/MeOH 19:1) and afterwards by RP-HPLC to yield the desired product.

Yield: 3.7 mg (5.4 µmol, 20%) as a colorless solid

TLC (DCM/MeOH = 19:1): $R_f = 0.4$

^{1}H NMR (400 MHz, $CDCl_3$): δ = 8.18 (d, J = 7.9 Hz, 1H), 7.94 (d, J = 8.4 Hz, 1H), 7.90 – 7.84 (m, 2H), 7.82 – 7.78 (m, 2H), 7.66 – 7.59 (m, 1H), 7.50 (td, J = 7.7, 2.4 Hz, 2H), 7.31 (dd, J = 11.1, 6.8 Hz, 1H), 7.20 – 7.07 (m, 2H), 7.02 (dd, J = 10.5, 8.6 Hz, 1H), 5.99 – 5.87 (m, 1H), 5.67 (d, J = 3.8 Hz, 1H), 5.21 – 5.08 (m, 2H), 4.75 (dd, J = 13.6, 6.4 Hz, 1H), 3.95 (dt, J = 28.5, 14.4 Hz, 2H), 3.39 (dd, J = 13.2, 6.7 Hz, 1H), 3.31 – 3.17 (m, 1H), 2.98 – 2.84 (m, 1H), 2.75 (dd, J = 16.8, 7.7 Hz, 1H), 2.60 (dd, J = 12.7, 6.0 Hz, 1H), 2.54 – 2.28 (m, 2H), 2.20 – 2.11 (m, 1H), 1.96 – 1.72 (m, 2H), 1.57 (s, 2H), 1.46 – 1.38 (m, 2H), 1.26 (s, 1H), 1.20 – 1.07 (m, 3H), 1.03 (dd, J = 15.4, 8.6 Hz, 3H), 0.88 (dd, J = 7.5, 6.1 Hz, 2H)

LC-MS (ESI): t_R = 8.62 min, calcd. for $C_{41}H_{41}N_5O_5^+$ $[M+H]^+$: 686.33, found 686.26

7.4 Synthesis of acyl-ATP probes

Adenosine 5′-triphosphate triethyl-ammonium salt (45):

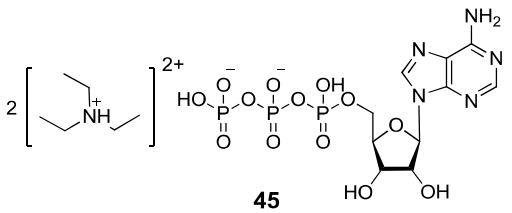

45

DEAE-Sephadex A-25 (purchased in the Cl^- form) was added to distilled water and the resulting suspension was kept at rt overnight. It was then washed by ten times decantation with 0.5 N NaOH and three times with water. The ion-exchanger was then suspended in 2 M aq. $NaHCO_3$ solution, packed into a column and washed extensively with 2 M $NaHCO_3$ solution. The resin material was then transferred to a large beaker and suspended in 0.04 M $NH(Et)_3HCO_3$ buffer (pH~7). The suspension was allowed to settle for 15 min and the

supernatant was decanted off. This was repeated two further times. Subsequently, DEAE-Sephadex A-25 was put into a glas-column and equilibrated additionally several times with 0.04 M aq. $NH(Et)_3HCO_3$ solution. Adenosine 5′-triphosphate disodium salt hydrate (1 g, 1.81 mmol) was dissolved in aq. 0.04 M $NH(Et)_3HCO_3$ solution (5 ml) and placed onto the column and allowed to seep into the column-material. The column-material was covered by a piece of cotton-wool to avoid flotation of the column material. The column was washed three times with a column volume of 0.04 M aq. $NH(Et)_3HCO_3$ solution. The product was eluated from column by applying 0.5 M aq. $NH(Et)_3HCO_3$ solution. Product containing fractions (UV-detection) were combined and lyophilized.

Preparation of 1 M $NH(Et)_3HCO_3$ -buffer, pH~7:

1 M aq. $NH(Et)_3HCO_3$ buffer was produced by adding gradually dry ice into a solution of H_2O (480 ml) and TEA (70 ml) under vigorous stirring until a pH of ~7 was reached.

6-Aminohexanoic acid methylester hydrochloride (46):

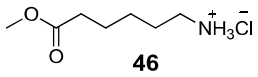

46

Methanol (20 ml) was cooled in a dry ice-acetone bath and thionyl chloride (0.31 ml, 4.191 mmol) was added dropwise over 30 min. At the same temperature, 6-aminohexanoic acid (500 mg, 3.81 mmol) was added portionwise and the dry-ice acetone bath was removed. The reaction mixture was allowed to warm to rt and then refluxed gently for 6 h. Removal of the volatiles under reduced pressure gave the title compound which was used in the next step without any further purification.

Yield: 889 mg (3.81 mmol, >99%) as a colorless crystalline solid

Methyl 6-(5-((3a*S*,4*S*,6a*R*)-2-oxohexahydro-1*H*-thieno[3,4-d]imidazol-4-yl)pentanamido) hexanoate (47):

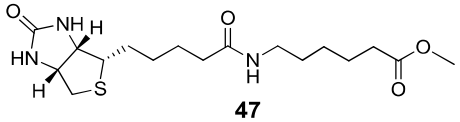

47

To a solution of **46** (284 mg, 1.56 mmol), biotin (366 mg, 1.56 mmol) and TEA (1.1 ml, 8 mmol) in DMF (4 ml) was added HBTU (591 mg, 1.56 mmol) and HOBt (210 mg, 1.56 mmol). After 0.5 h stirring at rt, water was added and the product was extracted with DCM. The organic phase was dried over Na_2SO_4, evaporated to dryness and the crude product was purified by silica gel chromatography (MeOH/DCM = 1:9) to obtain **47**.

Yield: 471 mg (1.27 mmol, 85%) as a colorless solid

TLC (MeOH/DCM = 1:9): Rf = 0.3

^{1}H NMR (400 MHz, $CDCl_3$): δ = 4.65 (s, 1H), 4.47 (s, 1H), 3.66 (s, 3H), 3.29 (s, 2H), 3.21 (s, 1H), 3.01 – 2.81 (m, 2H), 2.49 (s, 2H), 2.32 (t, *J* = 7.2 Hz, 2H), 1.84 – 1.53 (m, 8H), 1.48 (s, 2H), 1.37 (d, *J* = 6.9 Hz, 2H)

^{13}C NMR (CDCl3): δ = 174.4, 173.4, 164.2, 62.0, 60.4, 55.9, 51.8, 40.8, 39.4, 36.3, 34.1, 29.5, 28.4, 28.3, 26.6, 25.9, 24.7

LC-MS (ESI): t_R = 6.40 min, calcd. for $C_{17}H_{30}N_3O_4S$ $[M+H]^+$ 372.19, found 372.07

6-(5-((3a*S*,4*S*,6a*R*)-2-oxohexahydro-1*H*-thieno[3,4-d]imidazol-4-yl)pentanamido) hexanoic acid (48):

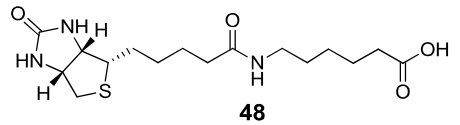

48

A solution of **47** (124 mg, 0.334 mmol) in H_2O/MeOH (1:1, 4 ml) was cooled to 0 °C. A 1 M solution of LiOH (24 mg, 1 mmol) in H_2O/MeOH (1:1, 1 ml) was added dropwise. The resulting solution was stirred for 1 h at rt until all starting material was used up (monitored by TLC; DCM/MeOH 9:1). MeOH was removed under reduced pressure and the aqueous layer was acidified by addition of 1 M HCl. The desired product **48** precipitated and was filtered off and dried in vacuo.

Yield: 119 mg (0.33 mmol, 99%) as a colorless solid

^{1}H NMR (DMSO-d^6) δ = 11.96 (s, 1H), 7.71 (s, 1H), 6.40 (s, 1H), 6.34 (s, 1H), 4.28 (m, 1H), 4.11 (m, 1H), 3.08 (m, 1H), 3.00 (dd, *J* = 12.6, 6.2 Hz, 2H), 2.82 (dd, *J* = 12.3, 4.9 Hz, 1H), 2.57 (d, *J* = 12.4 Hz, 1H), 2.18 (t, *J* = 7.4 Hz, 2H), 2.04 (t, *J* = 7.3 Hz, 2H), 1.68 – 1.42 (m, 6H), 1.32 (m, 6H)

^{13}C NMR (DMSO-d^6): δ = 174.4, 171.7, 162.7, 61.0, 59.2, 55.4, 38.2, 35.2, 33.6, 28.9, 28.2, 28.0, 26.0, 25.3, 24.2

LC-MS (ESI): t_R = 5.72 min, calcd. for $C_{16}H_{27}N_3O_4S$ $[M+H]^+$ 358.47, found 358.07

(+)-Biotin-Hex-acyl-ATP (BHAcATP) (49):

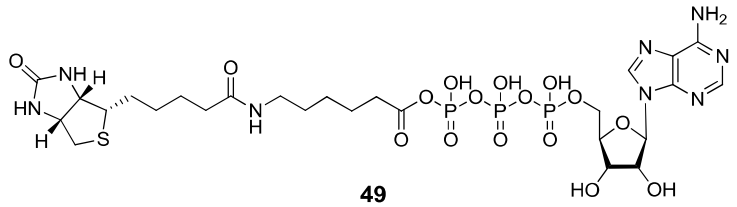

49

To a stirred suspension of **48** (30 mg, 0.085 mmol) in a dioxane/DMF/DMSO mixture (1:1:1, 3 ml) was added triethylamine (47 µl, 0.34 mmol) and *iso*butyl chloroformate (33 µl, 0.255 mmol) at 0 °C. The cloudy mixture was kept at this temperature for 20 min, allowed to warm to rt and then stirred for an additional 1.5 h. A solution of **45** (69 mg, 0.085 mmol) in anhydrous DMSO (1 ml) was added to the mixture. After 18 h, the reaction was quenched by addition of water (4 ml) and the solution was quickly extracted with ethyl acetate (3 x 4 ml). The aqueous layer was immediately frozen and lyophilized. The resulting solid was suspended in water (1 ml), transferred to a pre-equilibrated C18 column and eluted with water. Fractions containing product were immediately frozen and lyophilized.

Yield: 4.3 mg (5.1 µmol, 6%) as a colorless solid

LC-MS (ESI): t_R = 2.16 min, calcd. for $C_{26}H_{40}N_8O_{16}P_3S^-$ $[M-H]^-$ 845.15, found 845.13

Undec-10-ynoic-acyl-ATP (50):

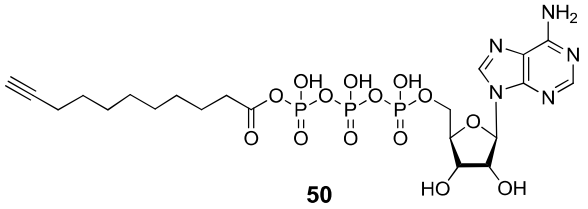

50

To a stirred suspension of undec-10-ynoic acid (15.5 mg, 0.085 mmol) in a dioxane/DMF/DMSO mixture (1:1:1, 3 ml) was added triethylamine (47 µl, 0.34 mmol) and *iso*butyl chloroformate (33 µl, 0.255 mmol) at 0 °C. The cloudy mixture was kept at this temperature for 20 min, allowed to warm to rt and then stirred for an additional 1.5 h. A solution of **45** (69 mg, 0.085 mmol) in anhydrous DMSO (1 ml) was added to the mixture. After 18 h, the reaction was quenched by addition of water (4 ml) and the solution was quickly extracted with ethyl acetate (3 x 4 ml). The aqueous layer was immediately frozen and lyophilized. The resulting solid was suspended in water (1 ml), transferred to a pre-equilibrated C18 column and eluted with water. Product containing fractions were immediately frozen and lyophilized.

Yield: 3.7 mg (5.5 µmol, 6.5%) as a colorless solid
LC-MS (ESI): t_R = 4.99 min, calcd. for $C_{21}H_{31}N_5O_{14}P_3^-$ $[M-H]^-$ 670.10, found 569.93

Bodipy(C3)-acyl-ATP (51):

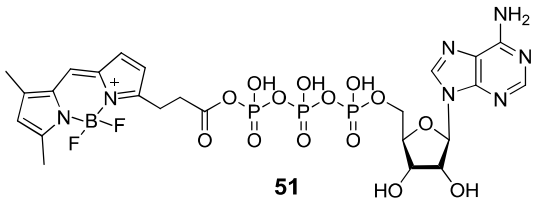

51

To a stirred suspension of BODIPY® FL propionic acid (5 mg, 17.1 µmol) in a dioxane/DMF/DMSO mixture (1:1:1, 1.5 ml) under light exclusion were added at 0 °C triethylamine (11 µl, 0.0684 mmol) and *iso*butyl chloroformate (7.1 µl, 0.00936 mmol). The resulting cloudy mixture was kept at this temperature for 20 min, allowed to warm to rt and then stirred for an additional 1.5 h. A solution of **45** (13.5 mg, 39.3 µmol) in anhydrous DMSO (0.5 ml) was added to the mixture. After 18 h, the reaction was quenched by addition of water (4 ml) and the solution was quickly extracted with ethyl acetate (3 x 4 ml). The

aqueous layer was immediately frozen and lyophilized. The resulting solid was suspended in water (1 ml), transferred to a pre-equilibrated C18 column and eluted with water. Fractions containing the product were combined, immediately frozen and lyophilized.

Yield: 1.8 mg (2.3 µmol, 14%) as a colorless solid
LC-MS (ESI): t_R = 4.83 min, calcd. for $C_{24}H_{27}BF_2N_7O_{14}P_3^-$ $[M-H]^-$ 780.09, found 779,87

Bodipy(C5)-Acyl-ATP (52):

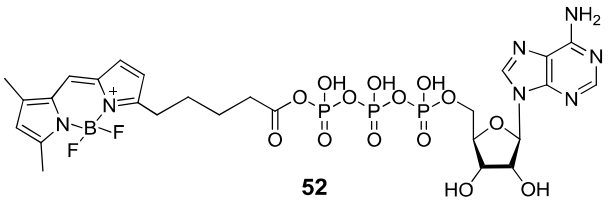

52

To a stirred suspension of BODIPY® FL pentanoic acid (1 mg, 3.12 µmol) in a dioxane/DMF/DMSO mixture (1:1:1, 1.5 ml) under light exclusion at 0 °C were added triethylamine (2 µl, 0.0125 mmol) and *iso*butyl chloroformate (1.3 µl, 0.00936 mmol). The resulting cloudy mixture was kept at this temperature for 20 min, allowed to warm to rt and then stirred for an additional 1.5 h. A solution of **45** (2.5 mg, 7.12 µmol) in anhydrous DMSO (0.5 ml) was added to the mixture. After 18 h, the reaction was quenched by addition of water (4 ml) and the solution was quickly extracted with ethyl acetate (3 x 4 ml). The aqueous layer was immediately frozen and lyophilized. The resulting solid was suspended in water (1 ml), transferred to a pre-equilibrated C18 column and eluted with water. Product containing fractions were immediately frozen and lyophilized.

Yield: 0.75 mg (0.89 µmol, 28%) as a colorless solid
LC-MS (ESI): t_R = 7.07 min, calcd. for $C_{26}H_{32}BClF_2N_7O_{14}P_3^-$ $[M-H]^-$ 843.09, found 843,44

7.5 Biological Procedures

List of buffers:

Phosphate buffered saline (10x PBS): 10.6 mM KH_2PO_4, 1552 mM NaCl, 30 mM Na_2HPO_4, pH 7.4.

SDS-PAGE gel-loading buffer (4x GLB): 280 mM SDS, 400 mM Tris, 40% glycerol, 1.4 M DTT, 0.6 mM Bromophenol Blue, pH 6.8.

MOPS (20x MOPS): 50 mM MOPS, 50 mM Tris Base, 0.1% SDS, 1 mM EDTA, pH 7.7.

Bis-Tris Buffer (1.25 M): 131 g Bis-Tris, 350 ml water, 40-50 ml HCl (25%), adjust to pH 6.6, adjust to 500 ml with water.

Coomassie-stain: 0.08% Coomassie Billiant blue G250, 1.6% ortho-phosphoric acid, 8% ammonium sulfate, 20% methanol.

Preparation of functional protein extracts from *Arabidopsis thaliana*

50-100 mg leaf material of two weeks old *Arabidospsis* seedlings (Col-0, WT) were transferred into a fresh Eppendorf tube and 400 µl 1x PBS buffer were poured into the same vessel. The leaf tissue was grinded up with an appropriate mortar to form a homogenous solution. The extract was cleared by centrifugation (13k g, 5 min, 4 °C) which resulted in a greenish pellet and a clear supernatant. The pellet was discarded and the clear supernatant, containing the water-soluble protein fraction of the *Arabidopsis* leaf proteome was transferred to a fresh Eppendorf tube. This protein extract was used subsequently or otherwise kept on ice.

Measuring protein concentration

The protein concentration was measured using a modified Bradford assay, called Roti-Nanoquant®. The assay was conducted according to the instruction given by the supplier. (http://www.carlroth.com/media/_nl-nl/usage/K880.pdf)

In vitro activity-based labeling of plant extracts

1 step ABPP:

The equivalent of 50 µg protein from the leaf extracts were transferred to a designated Eppendorf tube. The volume of this solution was adjusted to 49 µl with 1x PBS-buffer. 1 µl of the corresponding probe (fluorescent) was added and agitated properly (all chemicals were added as a solution in DMSO). The reaction mixture was incubated at rt in the dark for 1 h. The reaction was stopped by adding 16.5 µl of 4x GLB. The mixture was then incubated for 10 min at 70 °C and centrifuged briefly (10 s, 16k g) to spin down the water that condensed in the lid. The protein samples were resolved by gel-electrophoresis. Labeled proteins were detected by direct in-gel fluorescence scanning (532 nm) using a Typhoon® 9000 scanner (GE Healthcare). To ensure equal loading, a Coomassie stain was conducted. On that purpose the SDS-gel was stained o.n. in the Coomassie-stain and washed afterwards several times with pure water.

2 step ABPP:

The equivalent of 50 µg protein from the leaf extracts were transferred to a designated Eppendorf tube. The volume of this solution was adjusted to 45 µl with 1x PBS-buffer. Then 1 µl from an apropiate stock solution of the corresponding "click" probe was added and the mixture was agitated properly (all chemicals were added as a solution in DMSO). The reaction mixture was incubated at rt in the dark for 1 h. Subsequently, 1 µl rhodamine-azide (1 mM stock), 1 µl TBTA (5 mM stock), 1 µl TCEP (100 mM stock) and 1 µl $CuSO_4$ (50 mM stock) were added. The reaction mixtures were agitated and incubated subsequently at rt in the dark for 1 h. The reactions were stopped by adding 16.5 µl of 4x GLB to each reaction vessel. The mixture was then incubated for 10 min at 70 °C and centrifuged briefly (10 s, 16k g) to spin down the water that condensed in the lid. The protein samples were then resolved by gel-electrophoresis. Labeled proteins were detected by direct in-gel fluorescence scanning (532 nm) using a Typhoon® 9000 scanner (GE Healthcare). To ensure equal loading, a Coomassie stain was conducted. On that purpose the SDS-gel was stained o.n. in the Coomassie-stain and washed afterwards several times with pure water.

2 step photoaffinity ABPP:

The equivalent of 50 µg protein from the leaf extracts were transferred to a designated Eppendorf tube. The volume of this solution was adjusted to 45 µl with 1x PBS-buffer. 1 µl from an appropiate stock solution of the corresponding "photoaffinity" probe was added and the mixture was agitated properly (all chemicals were added as a solution in DMSO). The reaction mixture was incubated at rt and in the dark for 1 h. The samples were transferred into a shallow, translucent and uncovered 96-well plate. The plate was placed on ice subsequently and photoactivation was performed by placing a hand-held UV-lamp (λ = 360 nm) in a distance of 1 cm above the 96-well plate. A total UV irradiation time of 15 min was used. Subsequently, 1 µl rhodamine-azide (1 mM stock), 1 µl TBTA (5 mM stock), 1 µl TCEP (100 mM stock) and 1 µl $CuSO_4$ (50 mM stock) were added. The reaction mixtures were agitated and incubated subsequently at rt in the dark for 1 h. The reactions were stopped by adding 16.5 µl of 4x GLB to each reaction vessel. The mixture was incubated for 10 min at 70° C and centrifuged briefly (10 s, 16k g) to spin down the water condensed in the lid. The protein samples were resolved by gel-electrophoresis. Labeled proteins were detected by direct in-gel fluorescence scanning (532 nm) using a Typhoon® 9000 scanner (GE Healthcare). To ensure equal loading, a Coomassie stain was conducted. On that purpose the SDS-gel was stained o.n. in the Coomassie-stain and washed afterwards several times with pure water.

SDS-gelectrophoresis

Continuous SDS-Gels (11%: 30 ml 30% acrylamide/Bis-acrylamide, 22.8 ml Bis-Tris (1.25 M), 320 µl APS (10%), 64 µl TEMED, water 27.4 ml) were loaded in each pocket with 12 µl protein sample and transferred into designated devices (C.B.S Scientific). As running-buffer 1x MOPS buffer was used. The power-supply Consort EV261 was utilized attuned to 120 V, 75 mA and 30 W. A complete protein separation was achieved after 90 min.

8. REFERENCES

1. Somerville, C. & Koornneef, M. (2002). Timeline - A fortunate choice: the history of Arabidopsis as a model plant. *Nature Reviews Genetics* **3**, 883-889.

2. Haas, B. J., Jr, W., Ronning, C. M., Hannick, L. I*., et al.* (2005). Complete reannotation of the Arabidopsis genome: methods, tools, protocols and the final release. *BMC Biol.* 22, **3**.

3. Pang, P. P. & Meyerowitz, E. M. (1987). Arabidopsis Thaliana: a Model System for Plant Molecular-Biology. *Bio-Technol* **5**, 1177-1187.

4. Zupan, J. R. & Zambryski, P. (1995). Transfer of T-DNA from Agrobacterium to the Plant-Cell. *Plant Physiol.* **107**, 1041-1047.

5. Kaul, S., Koo, H. L., Jenkins, J., Rizzo, M*., et al.* (2000). Analysis of the genome sequence of the flowering plant Arabidopsis thaliana. *Nature* **408**, 796-815.

6. Wienkoop, S., Baginsky, S. & Weckwerth, W. (2010). Arabidopsis thaliana as a model organism for plant proteome research. *J. Proteomics* **73**, 2239-2248.

7. Mann, G. W., Joshi, H. J., Petzold, C. J. & Heazlewood, J. L. (2013). Proteome coverage of the model plant Arabidopsis thaliana: Implications for shotgun proteomic studies. *J. Proteomics* **79**, 195-199.

8. Drabovich, A. P., Berezovski, M. V., Musheev, M. U. & Krylov, S. N. (2009). Selection of smart small-molecule ligands: the proof of principle. *Anal. Chem.* **81**, 490-494.

9. Voet, D., Voet, G. V., Pratt, C. W., Ed. (2013). Principle of Biochemistry. 4th edit. Singapore: John Wiley & Sons, Inc.

10. Kendrew, J. C., Bodo, G., Dintzis, H. M., Parrish, R. G., Wyckoff, H. & Phillips, D. C. (1958). 3-Dimensional Model of the Myoglobin Molecule Obtained by X-Ray Analysis. *Nature* **181**, 662-666.

11. Geysen, H. M., Schoenen, F., Wagner, D. & Wagner, R. (2003). Combinatorial compound libraries for drug discovery: An ongoing challenge. *Nature Reviews Drug Discovery* **2**, 222-230.

12. Walsh, D. P. & Chang, Y. T. (2006). Chemical genetics. *Chem. Rev.* **106**, 2476-2530.

13. Newman, D. J. & Cragg, G. M. (2007). Natural products as sources of new drugs over the last 25 years. *J. Nat. Prod.* **70**, 461-477.

14. Hong, J. Y. (2011). Role of natural product diversity in chemical biology. *Curr. Opin. Chem. Biol.* **15**, 350-354.

15. Wetzel, S., Bon, R. S., Kumar, K. & Waldmann, H. (2011). Biology-Oriented Synthesis. *Angew Chem Int Edit* **50**, 10800-10826.

16. Kumar, K. & Waldmann, H. (2009). Synthesis of Natural Product Inspired Compound Collections. *Angew Chem Int Edit* **48**, 3224-3242.

17. Matcha, K., Madduri, A. V. R., Roy, S., Ziegler, S., Waldmann, H., Hirsch, A. K. H. & Minnaard, A. J. (2012). Total Synthesis of (-)-Doliculide, Structure-Activity Relationship Studies and Its Binding to F-Actin. *ChemBioChem* **13**, 2537-2548.

18. Chin, Y. W., Balunas, M. J., Chai, H. B. & Kinghorn, A. D. (2006). Drug discovery from natural sources. *Aaps J* **8**, 239-253.

19. Blackwell, H. E. & Zhao, Y. D. (2003). Chemical genetic approaches to plant biology. *Plant Physiol.* **133**, 448-455.

20. Zanders, E. D., Ed. (2005). Chemical Genomics. Vol. 310. Methods in Molecular Biology™: Humana Press.

21. Kidd, D., Liu, Y. S. & Cravatt, B. F. (2001). Profiling serine hydrolase activities in complex proteomes. *Biochemistry-Us* **40**, 4005-4015.

22. Taunton, J., Hassig, C. A. & Schreiber, S. L. (1996). A mammalian histone deacetylase related to the yeast transcriptional regulator Rpd3p. *Science* **272**, 408-411.

23. MacBeath, G. & Schreiber, S. L. (2000). Printing proteins as microarrays for high-throughput function determination. *Science* **289**, 1760-1763.

24. Lin, H. N. & Cornish, V. W. (2001). In vivo protein-protein interaction assays: Beyond proteins. *Angew Chem Int Edit* **40**, 871-875.

25. Sche, P. P., McKenzie, K. M., White, J. D. & Austin, D. J. (1999). Display cloning: functional identification of natural product receptors using cDNA-phage display. *Chem. Biol.* **6**, 707-716.

26. Speers, A. E. & Cravatt, B. F. (2004). Chemical strategies for activity-based proteomics. *ChemBioChem* **5**, 41-47.

27. Kawasumi, M. & Nghiem, P. (2007). Chemical genetics: Elucidating biological systems with small-molecule compounds. *J Invest Dermatol* **127**, 1577-1584.

28. Santner, A., Calderon-Villalobos, L. I. A. & Estelle, M. (2009). Plant hormones are versatile chemical regulators of plant growth. *Nat. Chem. Biol.* **5**, 301-307.

29. Davletova, S., Rizhsky, L., Liang, H. J., Zhong, S. Q., Oliver, D. J., Coutu, J., Shulaev, V., Schlauch, K. & Mittler, R. (2005). Cytosolic ascorbate peroxidase 1 is a central component of the reactive oxygen gene network of Arabidopsis. *Plant Cell* **17**, 268-281.

30. Park, S. Y., Fung, P., Nishimura, N., Jensen, D. R., *et al.* (2009). Abscisic acid inhibits type 2C protein phosphatases via the PYR/PYL family of START proteins. *Science* **324**, 1068-1071.

31. Kaschani, F. & van der Hoorn, R. (2007). Small molecule approaches in plants. *Curr. Opin. Chem. Biol.* **11**, 88-98.

32. Toth, R. & van der Hoorn, R. A. L. (2010). Emerging principles in plant chemical genetics. *Trends Plant Sci.* **15**, 81-88.

33. DeBolt, S., Gutierrez, R., Ehrhardt, D. W., Melo, C. V., Ross, L., Cutler, S. R., Somerville, C. & Bonetta, D. (2007). Morlin, an inhibitor of cortical microtubule dynamics and cellulose synthase movement. *Proc. Natl. Acad. Sci. USA* **104**, 5854-5859.

34. De Rybel, B., Audenaert, D., Vert, G., Rozhon, W., *et al.* (2009). Chemical Inhibition of a Subset of Arabidopsis thaliana GSK3-like Kinases Activates Brassinosteroid Signaling. *Chem. Biol.* **16**, 594-604.

35. Hayashi, K., Jones, A. M., Ogino, K., Yamazoe, A., Oono, Y., Inoguchi, M., Kondo, H. & Nozaki, H. (2003). Yokonolide B, a novel inhibitor of auxin action, blocks degradation of AUX/IAA factors. *The Journal of biological chemistry* **278**, 23797-23806.

36. Ballio, A. (1982). Interaction of Fusicoccin with Plant-Cell Plasma-Membranes. *Adv. Exp. Med. Biol.* **148**, 223-229.

37. Wurtele, M., Jelich-Ottmann, C., Wittinghofer, A. & Oecking, C. (2003). Structural view of a fungal toxin acting on a 14-3-3 regulatory complex. *Embo J* **22**, 987-994.

38. Groll, M., Schellenberg, B., Bachmann, A. S., Archer, C. R., Huber, R., Powell, T. K., Lindow, S., Kaiser, M. & Dudler, R. (2008). A plant pathogen virulence factor inhibits the eukaryotic proteasome by a novel mechanism. *Nature* **452**, 755-757.

39. Kolodziejek, I., Misas-Villamil, J. C., Kaschani, F., Clerc, J., *et al.* (2011). Proteasome Activity Imaging and Profiling Characterizes Bacterial Effector Syringolin A. *Plant Physiol.* **155**, 477-489.

40. Misas-Villamil, J. C., Kolodziejek, I., Crabill, E., Kaschani, F., Niessen, S., Shindo, T., Kaiser, M., Alfano, J. R. & van der Hoorn, R. A. L. (2013). Pseudomonas syringae pv. syringae Uses Proteasome Inhibitor Syringolin A to Colonize from Wound Infection Sites. *PLoS Pathog.* **9**.

41. Sheard, L. B., Tan, X., Mao, H. B., Withers, J., *et al.* (2010). Jasmonate perception by inositol-phosphate-potentiated COI1-JAZ co-receptor. *Nature* **468**, 400-405.

42. Katsir, L., Schilmiller, A. L., Staswick, P. E., He, S. Y. & Howe, G. A. (2008). COI1 is a critical component of a receptor for jasmonate and the bacterial virulence factor coronatine. *Proc. Natl. Acad. Sci. USA* **105**, 7100-7105.

43. Blackstock, W. P. & Weir, M. P. (1999). Proteomics: quantitative and physical mapping of cellular proteins. *Trends Biotechnol.* **17**, 121-127.

44. Anderson, N. L. & Anderson, N. G. (1998). Proteome and proteomics: New technologies, new concepts, and new words. *Electrophoresis* **19**, 1853-1861.

45. Wasinger, V. C., Zeng, M. & Yau, Y. (2013). Current status and advances in quantitative proteomic mass spectrometry. *Int. J. Proteomics* **2013**, 180605-180616.

46. Kidd, D., Liu, Y. & Cravatt, B. F. (2001). Profiling serine hydrolase activities in complex proteomes. *Biochemistry-Us* **40**, 4005-4015.

47. Speers, A. E. & Cravatt, B. F. (2004). Profiling enzyme activities in vivo using click chemistry methods. *Chem. Biol.* **11**, 535-546.

48. Ovaa, H. (2007). Active-site directed probes to report enzymatic action in the ubiquitin proteasome system. *Nature Reviews Cancer* **7**, 613-620.

49. Jeffery, D. A. & Bogyo, M. (2003). Chemical proteomics and its application to drug discovery. *Curr. Opin. Biotechnol.* **14**, 87-95.

50. Greenbaum, D. C., Arnold, W. D., Lu, F., Hayrapetian, L., *et al.* (2002). Small molecule affinity fingerprinting: a tool for enzyme family subclassification, target identification, and inhibitor design. *Chem. Biol.* **9**, 1085-1094.

51. Evans, M. J. & Cravatt, B. F. (2006). Mechanism-based profiling of enzyme families. *Chem. Rev.* **106**, 3279-3301.

52. Liu, Y. S., Patricelli, M. P. & Cravatt, B. F. (1999). Activity-based protein profiling: The serine hydrolases. *Proc. Natl. Acad. Sci. USA* **96**, 14694-14699.

53. van der Hoorn, R. A. L. & Kaiser, M. (2012). Probes for activity-based profiling of plant proteases. *Physiol. Plant.* **145**, 18-27.

54. Serim, S., Haedke, U. & Verhelst, S. H. L. (2012). Activity-Based Probes for the Study of Proteases: Recent Advances and Developments. *Chemmedchem* **7**, 1146-1159.

55. Zhu, Q., Huang, X., Chen, G. Y. J. & Yao, S. Q. (2003). Activity-based fluorescent probes that target phosphatases. *Tetrahedron Lett.* **44**, 2669-2672.

56. Williams, S. J., Hekmat, O. & Withers, S. G. (2006). Synthesis and testing of mechanism-based protein-profiling probes for retaining endo-glycosidases. *ChemBioChem* **7**, 116-124.

57. Kaschani, F., Nickel, S., Pandey, B., Cravatt, B. F., Kaiser, M. & van der Hoorn, R. A. L. (2012). Selective inhibition of plant serine hydrolases by agrochemicals revealed by competitive ABPP. *Bioorg. Med. Chem.* **20**, 597-600.

58. van der Hoorn, R. A. L., Leeuwenburgh, M. A., Bogyo, M., Joosten, M. H. A. J. & Peck, S. C. (2004). Activity profiling of papain-like cysteine proteases in plants. *Plant Physiol.* **135**, 1170-1178.

59. Kato, D., Boatright, K. M., Berger, A. B., Nazif, T., Blum, G., Ryan, C., Chehade, K. A. H., Salvesen, G. S. & Bogyo, M. (2005). Activity-based probes that target diverse cysteine protease families. *Nat. Chem. Biol.* **1**, 33-38.

60. Lu, H., Wang, Z., Shabab, M., Oeljeklaus, J., Verhelst, S. H., Kaschani, F., Kaiser, M., Bogyo, M. & van der Hoorn, R. A. (2013). A substrate-inspired probe monitors translocation, activation, and subcellular targeting of bacterial type III effector protease AvrPphB. *Chem. Biol.* **20**, 168-176.

61. Wang, Z., Gu, C., Colby, T., Shindo, T., Balamurugan, R., Waldmann, H., Kaiser, M. & van der Hoorn, R. A. L. (2008). beta-Lactone probes identify a papain-like peptide ligase in Arabidopsis thaliana. *Nat. Chem. Biol.* **4**, 557-563.

62. Barglow, K. T. & Cravatt, B. F. (2004). Discovering disease-associated enzymes by proteome reactivity profiling. *Chem. Biol.* **11**, 1523-1531.

63. Pitscheider, M. & Sieber, S. A. (2009). Cinnamic aldehyde derived probes for the active site labelling of pathogenesis associated enzymes. *Chem. Commun.*, 3741-3743.

64. Robinette, D., Neamati, N., Tomer, K. B. & Borchers, C. H. (2006). Photoaffinity labeling combined with mass spectrometric approaches as a tool for structural proteomics. *Expert Rev. Proteomics* **3**, 399-408.

65. MacKinnon, A. L., Garrison, J. L., Hegde, R. S. & Taunton, J. (2007). Photo-leucine incorporation reveals the target of a cyclodepsipeptide inhibitor of cotranslational translocation. *J. Am. Chem. Soc.* **129**, 14560-14561.

66. Cisar, J. S. & Cravatt, B. F. (2012). Fully Functionalized Small-Molecule Probes for Integrated Phenotypic Screening and Target Identification. *J. Am. Chem. Soc.* **134**, 10385-10388.

67. Speers, A. E., Adam, G. C. & Cravatt, B. F. (2003). Activity-based protein profiling in vivo using a copper(I)-catalyzed azide-alkyne [3+2] cycloaddition. *J. Am. Chem. Soc.* **125**, 4686-4687.

68. Kolb, H. C. & Sharpless, K. B. (2003). The growing impact of click chemistry on drug discovery. *Drug Discov. Today* **8**, 1128-1137.

69. Washburn, M. P., Wolters, D. & Yates, J. R. (2001). Large-scale analysis of the yeast proteome by multidimensional protein identification technology. *Nat. Biotechnol.* **19**, 242-247.

70. Speers, A. E. & Cravatt, B. F. (2009). Activity-Based Protein Profiling (ABPP) and Click Chemistry (CC)-ABPP by MudPIT Mass Spectrometry. *Curr. Protoc. Chem. Biol.* **1**, 29-41.

71. Wells, J. M. & McLuckey, S. A. (2005). Collision-induced dissociation (CID) of peptides and proteins. *Methods Enzymol.* **402**, 148-185.

72. Jessani, N., Niessen, S., Wei, B. Q., Nicolau, M.*, et al.* (2005). A streamlined platform for high-content functional proteomics of primary human specimens. *Nat. Methods* **2**, 691-697.

73. Adam, G. C., Burbaum, J., Kozarich, J. W., Patricelli, M. P. & Cravatt, B. F. (2004). Mapping enzyme active sites in complex proteomes. *J. Am. Chem. Soc.* **126**, 1363,1368.

74. Li, N., Overkleeft, H. S. & Florea, B. I. (2012). Activity-based protein profiling: an enabling technology in chemical biology research. *Curr. Opin. Chem. Biol.* **16**, 227-233.

75. Ong, S. E., Foster, L. J. & Mann, M. (2003). Mass spectrometric-based approaches in quantitative proteomics. *Methods* **29**, 124-130.

76. Blagoev, B., Kratchmarova, I., Ong, S. E., Nielsen, M., Foster, L. J. & Mann, M. (2003). A proteomics strategy to elucidate functional protein-protein interactions applied to EGF signaling. *Nat. Biotechnol.* **21**, 315-318.

77. Voigt, T., Gerding-Reimers, C., Ngoc Tran, T. T., Bergmann, S.*, et al.* (2013). A natural product inspired tetrahydropyran collection yields mitosis modulators that synergistically target CSE1L and tubulin. *Angew. Chem.* **52**, 410-414.

78. Oeljeklaus, J., Kaschani, F. & Kaiser, M. (2013). Streamlining chemical probe discovery: libraries of "fully functionalized" small molecules for phenotypic screening. *Angew. Chem.* **52**, 1368-1370.

79. Ranish, J. A., Yi, E. C., Leslie, D. M., Purvine, S. O., Goodlett, D. R., Eng, J. & Aebersold, R. (2003). The study of macromolecular complexes by quantitative proteomics. *Nat. Genet.* **33**, 349-355.

80. Oda, Y., Owa, T., Sato, T., Boucher, B.*, et al.* (2003). Quantitative chemical proteomics for identifying candidate drug targets. *Anal. Chem.* **75**, 2159-2165.

81. Jessani, N., Humphrey, M., McDonald, W. H., Niessen, S., Masuda, K., Gangadharan, B., Yates, J. R., Mueller, B. M. & Cravatt, B. F. (2004). Carcinoma and stromal enzyme activity profiles associated with breast tumor growth in vivo. *Proc. Natl. Acad. Sci. USA* **101**, 13756-13761.

82. Leung, D., Hardouin, C., Boger, D. L. & Cravatt, B. F. (2003). Discovering potent and selective reversible inhibitors of enzymes in complex proteomes. *Nat. Biotechnol.* **21**, 687-691.

83. Joyce, J. A., Baruch, A., Chehade, K., Meyer-Morse, N.*, et al.* (2004). Cathepsin cysteine proteases are effectors of invasive growth and angiogenesis during multistage tumorigenesis. *Cancer Cell* **5**, 443-453.

84. Adibekian, A., Martin, B. R., Chang, J. W., Hsu, K. L., *et al.* (2012). Confirming Target Engagement for Reversible Inhibitors in Vivo by Kinetically Tuned Activity-Based Probes. *J. Am. Chem. Soc.* **134**, 10345-10348.

85. Carlson, E. E. (2010). Natural Products as Chemical Probes. *ACS Chem. Biol.* **5**, 639-653.

86. Hegde, N. S., Sanders, D. A., Rodriguez, R. & Balasubramanian, S. (2011). The transcription factor FOXM1 is a cellular target of the natural product thiostrepton. *Nat Chem* **3**, 725-731.

87. Yee, M., Fas, S. C., Stohlmeyer, M. M., Wandless, T. J. & Cimprich, K. A. (2005). A cell-permeable, activity-based probe for protein and lipid kinases. *J. Biol. Chem.* **280**, 29053-29059.

88. Stolze, S. C., Deu, E., Kaschani, F., Li, N., *et al.* (2012). The Antimalarial Natural Product Symplostatin 4 Is a Nanomolar Inhibitor of the Food Vacuole Falcipains. *Chem. Biol.* **19**, 1546-1555.

89. Merrifield, R. B. (1963). Solid Phase Peptide Synthesis .1. Synthesis of a Tetrapeptide. *J. Am. Chem. Soc.* **85**, 2149-2154.

90. Stevenson, C. L. (2009). Advances in Peptide Pharmaceuticals. *Curr Pharm Biotechno* **10**, 122-137.

91. Sewald, N., Jakubke, H.-D., Ed. (2009). Peptides: Chemistry and Biology. 2nd Edition edit. Weinheim: WILEY-VCH Verlag GmbH & Co. KGaA.

92. Montalbetti, C. A. G. N. & Falque, V. (2005). Amide bond formation and peptide coupling. *Tetrahedron* **61**, 10827-10852.

93. Klausner, Y. S. & Bodanszk.M. (1974). Azide Method in Peptide-Synthesis - Its Scope and Limitations. *Synthesis (Stuttg.)*, 549-559.

94. Wittenberger, S. J. & McLaughlin, M. A. (1999). Preparation of endothelin antagonist ABT-627. *Tetrahedron Lett.* **40**, 7175-7178.

95. Izdebski, J. & Kunce, D. (1997). Evaluation of carbodiimides using a competition method. *J. Pept. Sci.* **3**, 141-144.

96. Carpino, L. A., Imazumi, H., Foxman, B. M., Vela, M. J., Henklein, P., El-Faham, A., Klose, J. & Bienert, M. (2000). Comparison of the effects of 5-and 6-HOAt on model peptide coupling reactions relative to the cases for the 4-and 7-isomers. *Org. Lett.* **2**, 2253-2256.

97. Carpino, L. A., Imazumi, H., El-Faham, A., Ferrer, F. J., *et al.* (2002). The uronium/guanidinium peptide coupling reagents: Finally the true uronium salts. *Angew Chem Int Edit* **41**, 442-445.

98. Chan, W. C., White, P. D., Ed. (2000). Fmoc solid phase peptide synthesis : a practical approach. New York Oxford University Press.

99. Lundt, B. F., Johansen, N. L., Volund, A. & Markussen, J. (1978). Removal of t-butyl and t-butoxycarbonyl protecting groups with trifluoroacetic acid. Mechanisms, biproduct formation and evaluation of scavengers. *Int J Pept Prot Res* **12**, 258-268.

100. Carpino, L. A. (1987). The 9-Fluorenylmethyloxycarbonyl Family of Base-Sensitive Amino-Protecting Groups. *Accounts Chem Res* **20**, 401-407.

101. Schwetlick, K., Ed. (1974). Organikum. 13 edit. Berlin: VEB Deutscher Verlag der Wissenschaften.

102. Fukuchi, N., Furihata, K., Takayama, S., Isogai, A. & Suzuki, A. (1992). Rotihibin-a, a Novel Plant-Growth Regulator, from Streptomyces Sp. *Biosci Biotech Bioch* **56**, 840-841.

103. Kusano, M., Sotoma, G., Koshino, H., Uzawa, J., Chijimatsu, M., Fujioka, S., Kawano, T. & Kimura, Y. (1998). Brevicompanines A and B: new plant growth regulators produced by the fungus, Penicillium brevicompactum. *J Chem Soc Perk T 1*, 2823-2826.

104. Kimura, Y., Sawada, A., Kuramata, M., Kusano, M., Fujioka, S., Kawano, T. & Shimada, A. (2005). Brevicompanine C, Cyclo-(D-Ile-L-Trp), and Cyclo-(D-Leu-L-Trp), plant growth regulators from Penicillium brevi-compactum. *J. Nat. Prod.* **68**, 237-239.

105. Patricelli, M. P., Szardenings, A. K., Liyanage, M., Nomanbhoy, T. K.*, et al.* (2007). Functional interrogation of the kinome using nucleotide acyl phosphates. *Biochemistry-Us* **46**, 350-358.

106. Fukuchi, N., Furikata, K., Nakayama, J., Goudo, T., Takayama, S., Isogai, A. & Suzuki, A. (1995). Rotihibins, Novel Plant-Growth Regulators from Streptomyces-Graminofaciens. *J. Antibiot. (Tokyo).* **48**, 1004-1010.

107. Raaijmakers, J. M., de Bruijn, I., Nybroe, O. & Ongena, M. (2010). Natural functions of lipopeptides from Bacillus and Pseudomonas: more than surfactants and antibiotics. *Fems Microbiol Rev* **34**, 1037-1062.

108. Peypoux, F., Bonmatin, J. M. & Wallach, J. (1999). Recent trends in the biochemistry of surfactin. *Appl. Microbiol. Biotechnol.* **51**, 553-563.

109. Steller, S., Vollenbroich, D., Leenders, F., Stein, T., Conrad, B., Hofemeister, J., Jacques, P., Thonart, P. & Vater, J. (1999). Structural and functional organization of the fengycin synthetase multienzyme system from Bacillus subtilis b213 and A1/3 (vol 6, pg 31, 1999). *Chem. Biol.* **6**, 31-41.

110. Finking, R. & Marahiel, M. A. (2004). Biosynthesis of nonribosomal peptides. *Annu. Rev. Microbiol.* **58**, 453-488.

111. Wadsworth, W. & Emmons, W. D. (1961). Utility of Phosphonate Carbanions in Olefin Synthesis. *J. Am. Chem. Soc.* **83**, 1733-1738.

112. Bisceglia, J. A. & Orelli, L. R. (2012). Recent Applications of the Horner-Wadsworth-Emmons Reaction to the Synthesis of Natural Products. *Curr. Org. Chem.* **16**, 2206-2230.

113. Still, W. C. & Gennari, C. (1983). Direct Synthesis of Z-Unsaturated Esters - a Useful Modification of the Horner-Emmons Olefination. *Tetrahedron Lett.* **24**, 4405-4408.

114. Paquet, A. (1982). Introduction of 9-Fluorenylmethyloxycarbonyl, Trichloroethoxy-carbonyl, and Benzyloxycarbonyl Amine Protecting Groups into O-Unprotected Hydroxyamino Acids Using Succinimidyl Carbonates. *Can J Chem* **60**, 976-980.

115. Cardillo, G., Gentilucci, L., Tolomelli, A. & Tomasini, C. (1999). A practical method for the synthesis of beta-amino alpha-hydroxy acids. Synthesis of enantiomerically pure hydroxyaspartic acid and isoserine. *Synlett*, 1727-1730.

116. Boger, D. L., Lee, R. J., Bounaud, P. Y. & Meier, P. (2000). Asymmetric synthesis of orthogonally protected L-threo-beta-hydroxyasparagine. *J. Org. Chem.* **65**, 6770-6772.

117. Bionda, N., Cudic, M., Barisic, L., Stawikowski, M., Stawikowska, R., Binetti, D. & Cudic, P. (2012). A practical synthesis of N-alpha-Fmoc protected L-threo-beta-hydroxyaspartic acid derivatives for coupling via alpha- or beta-carboxylic group. *Amino Acids* **42**, 285-293.

118. Guzman-Martinez, A. & VanNieuwenhze, M. S. (2007). An operationally simple and efficient synthesis of orthogonally protected L-threo-beta-hydroxyasparagine. *Synlett*, 1513-1516.

119. Herranz, E., Biller, S. A. & Sharpless, K. B. (1978). Osmium-Catalyzed Vicinal Oxyamination of Olefins by N-Chloro-N-Argentocarbamates. *J. Am. Chem. Soc.* **100**, 3596-3598.

120. Yang, H. Q. & Zubarev, R. A. (2010). Mass spectrometric analysis of asparagine deamidation and aspartate isomerization in polypeptides. *Electrophoresis* **31**, 1764-1772.

121. Wenschuh, H., Beyermann, M., Haber, H., Seydel, J. K., Krause, E., Bienert, M., Carpino, L. A., Elfaham, A. & Albericio, F. (1995). Stepwise Automated Solid-Phase Synthesis of Naturally-Occurring Peptaibols Using Fmoc Amino-Acid Fluorides. *J. Org. Chem.* **60**, 405-410.

122. Gluza, K. & Kafarski, P. (2013). *Transition State Analogues of Enzymatic Reaction as Potential Drugs*. Drug Discovery.

123. Meinke, D. W., Cherry, J. M., Dean, C., Rounsley, S. D. & Koornneef, M. (1998). Arabidopsis thaliana: A model plant for genome analysis. *Science* **282**, 662-682.

124. Beemster, G. T. S. & Baskin, T. I. (1998). Analysis of cell division and elongation underlying the developmental acceleration of root growth in Arabidopsis thaliana. *Plant Physiol.* **116**, 1515-1526.

125. Sharma, A. K. (1999). Synchronization in plant cells – an introduction. *Methods in Cell Science* **21**, 73-78.

126. Jefferson, R. A., Kavanagh, T. A. & Bevan, M. W. (1987). Gus Fusions - Beta-Glucuronidase as a Sensitive and Versatile Gene Fusion Marker in Higher-Plants. *Embo J* **6**, 3901-3907.

127. Malamy, J. E. & Benfey, P. N. (1997). Organization and cell differentiation in lateral roots of Arabidopsis thaliana. *Development* **124**, 33-44.

128. Fletcher, J. C. (2002). Shoot and floral meristem maintenance in arabidopsis. *Annu. Rev. Plant Biol.* **53**, 45-66.

129. Tanimoto, E. (2005). Regulation of root growth by plant hormones - Roles for auxin and gibberellin. *Crit Rev Plant Sci* **24**, 249-265.

130. Werner, T. & Schmulling, T. (2009). Cytokinin action in plant development. *Curr. Opin. Plant Biol.* **12**, 527-538.

131. Ruiz-Sanchis, P., Savina, S. A., Albericio, F. & Alvarez, M. (2011). Structure, Bioactivity and Synthesis of Natural Products with Hexahydropyrrolo[2,3-b]indole. *Chem. Eur. J.* **17**, 1388-1408.

132. Takase, S., Kawai, Y., Uchida, I., Tanaka, H. & Aoki, H. (1985). Structure of Amauromine, a New Hypotensive Vasodilator Produced by Amauroascus Sp. *Tetrahedron* **41**, 3037-3048.

133. Arai, K., Kimura, K., Mushiroda, T. & Yamamoto, Y. (1989). Structures of Fructigenine-a and Fructigenines-B, New Alkaloids Isolated from Penicillium-Fructigenum Takeuchi. *Chem. Pharm. Bull.* **37**, 2937-2939.

134. Carle, J. S. & Christophersen, C. (1981). Marine Alkaloids .3. Bromo-Substituted Alkaloids from the Marine Bryozoan Flustra-Foliacea, Flustramine-C and Flustraminol-a and Flustraminol-B. *J. Org. Chem.* **46**, 3440-3443.

135. Matsumura, K. & Kitahara, T. (2001). Synthesis of brevicompanines, plant growth regulators. *Heterocycles* **54**, 727-733.

136. Marsden, S. P., Depew, K. M. & Danishefsky, S. J. (1994). Stereoselective Total Syntheses of Amauromine and 5-N-Acetylardeemin - a Concise Route to Tile Family of Reverse-Prenylated Hexahydropyrroloindole Alkaloids. *J. Am. Chem. Soc.* **116**, 11143-11144.

137. Depew, K. M., Marsden, S. P., Zatorska, D., Zatorski, A., Bornmann, W. G. & Danishefsky, S. J. (1999). Total synthesis of 5-N-acetylardeemin and amauromine: Practical routes to potential MDR reversal agents. *J. Am. Chem. Soc.* **121**, 11953-11963.

138. Feller, U., Anders, I. & Mae, T. (2008). Rubiscolytics: fate of Rubisco after its enzymatic function in a cell is terminated. *J. Exp. Bot.* **59**, 1615-1624.

139. Romeis, T. (2001). Protein kinases in the plant defence response. *Curr. Opin. Plant Biol.* **4**, 407-414.

140. Stone, J. M. & Walker, J. C. (1995). Plant Protein-Kinase Families and Signal-Transduction. *Plant Physiol.* **108**, 451-457.

141. Carrera, A. C., Alexandrov, K. & Roberts, T. M. (1993). The Conserved Lysine of the Catalytic Domain of Protein-Kinases Is Actively Involved in the Phosphotransfer Reaction and Not Required for Anchoring Atp. *Proc. Natl. Acad. Sci. USA* **90**, 442-446.

142. Kovalevsky, A. Y., Johnson, H., Hanson, B. L., Waltman, M. J., Fisher, S. Z., Taylor, S. & Langan, P. (2012). Low- and room-temperature X-ray structures of protein kinase A ternary complexes shed new light on its activity. *Acta Crystallogr D* **68**, 854-860.

143. Villamor, J. G., Kaschani, F., Colby, T., Oeljeklaus, J., Zhao, D., Kaiser, M., Patricelli, M. P. & van der Hoorn, R. A. (2013). Profiling protein kinases and other ATP bindingproteins in Arabidopsis using acyl-ATP probes. *Molecular & cellular proteomics : MCP*. **12**(9), 2481-2496.

144. (1984). IUPAC-IUB Joint Commission on Biochemical Nomenclature (JCBN). Nomenclature and symbolism for amino acids and peptides. Recommendations 1983. *European journal of biochemistry / FEBS* **138**, 9-37.

9. APPENDIX

9.1 Abbreviations

The amino acids were abbreviated according to the 1-letter or 3-letter code recommended by the IUPAC-IUB joint commission on biochemical nomenclature.[144]

AA	asymmetric aminohydroxylation
Å	Ångström
A. thaliana	*Arabidopsis thaliana*
aa	amino acid(s)
ABP	activity-based probe
ABPP	activity-based protein profiling
Ac	acyl-
AcOH	acetic acid
ACN	acetonitrile
ADP	adenosine diphosphate
Alloc	allyloxycarbonyl-
AOMK	acyloxymethyl ketone
aq.	aqueous
ATP	adenosine triphosphate
atm.	standard atmosphere = 1,01325 x 10^5 Pa
b	broad signal (NMR)
BHAcATP	(+)-Biotin-Hex-Acyl-ATP
Bn	benzyl-
Boc	*tert*-butoxycarbonyl-
CH	cyclohexane
Cit	citrulline
d	doublet
Da	Dalton
Dab	diaminobutyric acid
DAG	days after germination
DCC	*N*,*N*'-dicyclohexyl carbodiimide

DCM	dichloromethane
DCU	*N*,*N*'-dicyclohexylurea
dd	doublet of doublets
DIPEA	*N*,*N*'-diisopropylethylamine
DMAP	4-dimethylamino pyridine
DMF	dimethyl formamide
DMSO	dimethyl sulfoxide
DNA	desoxyribonucleic acid
dt	doublet of triplets
E. coli	*Escherichia coli*
EDC	1-ethyl-3-(3'-dimethylaminopropyl)carbodiimide
eq.	equivalent(s)
ESI	electrospray ionization
Et	ethyl-
EtOAc	ethyl acetate
EtOH	ethanol
FA	formic acid
Fmoc	9-fluorenylmethoxy carbonyl-
GUS	*β*-glucuronidase
h	hour(s)
HATU	2-(1H-azabenzotriazole-1-yl)1,1,3,3-tetramethylaminium hexafluorophosphate
HBTU	2-(1H-benzotriazole-1-yl)1,1,3,3-tetramethylaminium hexafluorophosphate
HOBt	*N*-hydroxybenzotriazole
HOSu	*N*-hydroxysuccinimide
HPLC	high pressure liquid chromatography
HR-MS	high resolution mass spectrometry
Hz	Hertz
IBCF	*iso*butyl chloroformate
ICAT	isotope-coded affinity tags
iPr	*iso*-propyl-
J	coupling constant
k	kilo-
LC-MS	liquid chromatography mass spectrometry
LRD	lateral root density

m	multiplet
M	molar
Me	methyl
MeOH	methanol
MHz	Megahertz
min	minute(s)
ml	milliliter(s)
MS	mass spectrometry
MudPIT	multidimensional protein identification technology
N	normal
nm	nanometer
NMM	*N*-methylmorpholine
NMR	nuclear magnetic resonance
OD	optical density
o.n.	overnight
PEG	polyethylene glycole
pH	pondus Hydrogenii
PKA	Protein Kinase A
ppm	parts per million
PyBOP	benzotriazole-1-yl-oxy-tris-pyrrolidino-phosphonium hexafluorophosphate
quant.	quantitative
R_f	retention factor
rt	room temperature
RuBisCo	ribulose-1,5-bisphosphate carboxylase oxygenase
s	singlet
SAR	structure-activity relationship
SDS-PAGE	sodium dodecylsulfate polyacrylamide gel eletrophoresis
sp.	species
SPPS	solid-phase peptide synthesis
t	triplet
t_R	retention time
TMSI	trimethylsilyl iodide
TMSOTf	trimethylsilyl trifluoromethanesulfonate
TBTA	tris[(1-benzyl-1H-1,2,3-triazol-4-yl)methyl]amine

*t*Bu	*tert*-butyl
tBuOH	*tert*-butanol
TCEP	tris(2-chloroethyl)phosphate
TEA	triethylamine
Tf	triflyl-
TFA	trifluoroacetic acid
TFE	trifluoro ethanol
THF	tetrahydrofuran
TIS	triisopropyl silane
TLC	thin layer chromatography
t_R	retention time
Trt	trityl-, triphenylmethyl-
UV	ultraviolet
WT	wild type
X-Gal	5-bromo-4-chloro-3-indolyl-*β*-D-galactopyranoside
°C	degrees Celsius
δ	chemical shift
ε	extinction coefficient
µ	micro-

9.2 List of publications

1. Villamor, J. G., Kaschani, F., Colby, T., Oeljeklaus, J., Zhao, D., Kaiser, M., Patricelli, M. P. & van der Hoorn, R. A. (**2013**). Profiling protein kinases and other ATP bindingproteins in Arabidopsis using acyl-ATP probes. *Molecular & Cellular Proteomics,* **12**(9), 2481-2496

2. Oeljeklaus, J., Kaschani, F. & Kaiser, M. (**2013**). Streamlining chemical probe discovery: libraries of "fully functionalized" small molecules for phenotypic screening. *Angewandte Chemie International Edition*, **52**, 1368-70.

3. Lu, H., Wang, Z., Shabab, M., Oeljeklaus, J., Verhelst, S. H., Kaschani, F., Kaiser, M., Bogyo, M. & van der Hoorn, R. A. (**2013**). A substrate-inspired probe monitors translocation, activation, and subcellular targeting of bacterial type III effector protease AvrPphB. *Chemistry and Biology*, **20**, 168-76.

4. Weski, J., Meltzer, M., Spaan, L., Monig, T., Oeljeklaus, J., Hauske, P., Vouilleme, L., Volkmer, R., Boisguerin, P., Boyd, D., Huber, R., Kaiser, M. & Ehrmann, M. (**2012**). Chemical biology approaches reveal conserved features of a C-terminal processing PDZ protease. *Chembiochem*, **13**, 402-8.

9.3 Curriculum Vitae

CV Julian Oeljeklaus

"Der Lebenslauf ist in der Online-Version aus Gründen des Datenschutzes nicht enthalten"

Lebenslauf Julian Oeljeklaus

"Der Lebenslauf ist in der Online-Version aus Gründen des Datenschutzes nicht enthalten"

9.4 Erklärungen

Hiermit versichere ich, dass ich die vorliegende Arbeit mit dem Titel

„Development and chemical synthesis of natural product-derived and rationally designed small molecule probes for plant biology research"

selbst verfasst und keine außer den angegebenen Hilfsmitteln und Quellen benutzt habe, und dass die Arbeit in dieser oder ähnlicher Form noch bei keiner anderen Universität eingereicht wurde.

Essen, im Nov. 2013

- Julian Oeljeklaus -

Hiermit erkläre ich, gem. § 6 Abs. (2) f) der Promotionsordnung der Fakultäten für Biologie, Chemie und Mathematik zur Erlangung des Dr. rer. nat., dass ich die Dissertation von Julian Oeljeklaus mit dem Thema „Development and chemical synthesis of natural product-derived and rationally designed small molecule probes for plant biology research" betreue und die Betreuung auch im Falle eines Weggangs, wenn nicht wichtige Gründe dem entgegenstehen, weiterführen werde.

Essen, im Nov. 2013

- Prof. Dr. Markus Kaiser -

9.5 Acknowledgements/Danksagungen

Mein besonderer Dank gilt meinem Doktorvater Prof. Dr. Markus Kaiser für die gute und schöne Zusammenarbeit in den letzten vier Jahren. Ich danke ihm für die Möglichkeit, dass ich diese Arbeit in seiner Arbeitsgruppe selbständig und mit eigenen Ideen durchführen konnte sowie für sein offenes Ohr und seinen fachlichen Rat in vermeintlich chemischen Sackgassen. Ich bedanke mich auch für die tolle Zeit abseits der Arbeit – Ich werde niemals so gut Fußball spielen können wie du!!

Bei Herrn Prof. Dr. Carsten Schmuck bedanke ich mich für die bereitwillige Übernahme des Zweitgutachtens.

Ich möchte mich auch bei allen aktuellen und ehemaligen Mitgliedern der Arbeitsgruppe Kaiser bedanken:
Bei meinen Bürokollegen Timon Mö(hnesee)nig, Daniel und Jan Krahn (nicht verwandt oder verschwägert) für eine tolle Zeit und super Arbeitsatmosphäre. Bei meinen Laborkollegen Dr. Sabrina und Dr. Philipp Nickel (mittlerweile verwandt) für die tolle Zeit und das ein oder andere schwarz-gelbe Stadionerlebnis. Bei Andreas Sprengel, Marija Mamic, Yvonne Blass, Anna-Laura Schmitz, Sabrina Ninck, Dr. Barbara Saccà und Dr. Susanne Zweerink für die super Zeit auch jenseits des Laboralltages. Bei Dr. Farnusch Kaschani bedanke ich mich für die kollegiale Zusammenarbeit und die guten Ratschläge bei biologischen Fragestellungen. Ich danke auch meinen ehemaligen Kollegen Dr. Jérôme Clérc, Patrick Hauske, Dr. Sara Stolze und Dr. Zhe Ming Whang für die Hilfsbereitschaft und fachlichen Ratschläge besonders in meinen Anfängen. Und nicht zuletzt bei Svenja Kernchen, die mir bei allen verwaltungstechnischen Angelegenheiten mit Rat und Tat zur Seite stand.

Ich danke allen Mitgliedern des Chemical Genomics Centre des Max-Planck-Instituts für molekulare Physiologie in Dortmund und den Mitarbeitern der AG Ehrmann am ZMB in Essen für ihre Unterstützung und die angenehme Arbeitsatmosphäre.

Ein besonderes Dankeschön gilt auch Dr. Renier van der Hoorn und der gesamten „Plant Chemetics“ Gruppe am MPI Köln. Die Einführung in die spannende Welt der Pflanzenbiologie und die fruchtbaren Impulse in diversen Projekten haben viel zum Abschluss dieser Arbeit beigetragen.

Weiter möchte ich mich auch bei der Arbeitsgruppe um Dr. Erich Kombrink am MPI Köln bedanken. Insbesondere Dr. Markus Schlicht und Dr. Christian Meesters, die meine Substanzen (immer aufschlussreich und zeitnah) biologisch evaluiert haben.

Besonders herzlich möchte ich mich bei allen meinen Kommilitonen an der TU Dortmund bedanken, die mich während meines Studiums begleitet haben und denen ich eine wunderschöne und unvergessliche Zeit zu verdanken habe.

Ich möchte mich auch bei meiner Familie, insbesondere meinen Eltern, bedanken. Ohne deren Unterstützung und Glauben an mich, mein Studium und diese Arbeit nicht möglich gewesen wären.

Zu guter Letzt danke ich meiner Freundin, Franzsika Weßkamp, besonders dafür, dass sie immer für mich da war und ist. Du bist wie ein gutes Haarspray – gibst festen Halt ohne zu sehr zu kleben! Zusammen schaffen wir alles...